UNIVERSIDAD COMPLUTENSE DE MADRID

FACULTAD DE CIENCIAS MATEMÁTICAS

TESIS DOCTORAL

Predation

Depredación

MEMORIA PARA OPTAR AL GRADO DE DOCTOR

PRESENTADA POR

Eduardo Muñoz Hernández

DIRECTORES

Julián López-Gómez
Fabio Zanolin

Universidad Complutense de Madrid

Facultad de Ciencias Matemáticas

TESIS DOCTORAL

Predation
Depredación

Memoria para optar al grado de doctor presentada por

Eduardo Muñoz Hernández

Directores:

Julián López-Gómez y Fabio Zanolin

Universidad Complutense de Madrid

Facultad de Ciencias Matemáticas

Programa de Doctorado en Investigación Matemática

Instituto de Matemática Interdisciplinar (IMI)

TESIS DOCTORAL

Predation
Depredación

Memoria para optar al grado de doctor presentada por

Eduardo Muñoz Hernández

Directores:

Julián López-Gómez y Fabio Zanolin

A mis padres, Rosa y Francisco,
y a mi hermana, Jara.

Acknowledgements

> *–Como me quieres bien, Sancho, hablas de esa manera –dijo don Quijote–; y, como no estás experimentado en las cosas del mundo, todas las cosas que tienen algo de dificultad te parecen imposibles; pero andará el tiempo, como otra vez he dicho, y yo te contaré algunas de las que allá abajo he visto, que te harán creer las que aquí he contado, cuya verdad ni admite réplica ni disputa.*
>
> Miguel de Cervantes, *Don Quijote de la Mancha* (II, 23)

I will always be grateful to my supervisors Julián López-Gómez and Fabio Zanolin for their continuous support, patience, dedication and guidance, and for introducing me into the mathematical research. Although they are truly very different, both personally and mathematically, all their skills and abilities, often complementary, prove to be so wide that I have the feeling that these differences have been enormously rewarding for me, for as I have benefited from the best possible advisor at each stage of the preparation of this PhD Thesis. Julián has been my teacher since the third year of my bachelor and if I decided to do this thesis, it is mainly because of him. I would like to thank Julián for the infinity hours discussing and learning math at his office, for teaching me to be patient when doing research and to look problems always in a naive unprejudiced way and, ultimately, thanks for the great guidance in the course of these years. I met Fabio a few years later, as I was beginning my thesis, during a visit he made to Madrid at the invitation of Julián. All of his ideas and different points of view to address the problem we were looking at led to a very fruitful collaboration. I would also like to thank Fabio for all the time he has dedicated to me in my visits to Italy and also online, for his patience and kindness towards me and because of all the mathematics he has teached me during these years.

En segundo lugar, no puedo olvidarme de todos mis amigos matemáticos de la Complutense. Gracias a Mauro, amigo y compañero ya de toda una vida, por su incalculable amistad. Gracias a Guille por estar siempre ahí desde que comenzamos la carrera hace casi diez años. Y gracias por compartir su tiempo conmigo de forma tan variada a mis amigos Laura, Adrián, Bernardo, Aranza, Gloria, Pedro, Irene, Sofía, Mónica, Miguel, Guille G., Pelayo, David, Eric, José, Javi, Giuseppe y Cosimo.

Estaré siempre en deuda también con todos los profesores que en el camino me aportaron algo. En especial debo agradecerle a María Eugenia Jiménez Aleixandre todo lo que me enseñó y a Félix del Teso Méndez todo lo que aprendí con él.

Ha sido para mí también muy importante estos años disfrutar de mis amigos del conservatorio Nerea, Alicia, Roberto, Sofía, Marian y Álvaro, así como seguir pudiendo disfrutar de la música con todos mis compañeros de la camerata: gracias en especial a Yago por su interés y dedicación.

Quiero acordarme también de Adolfo, Ernesto y Diego, amigos de toda la vida, a los cuales es siempre un placer ver y pasar tiempo con ellos.

Gracias, en fin, a mis padres, Rosa y Francisco, y a mi hermana, Jara, por su apoyo, ayuda y cariño incondicional.

Vorrei adesso ringraziare tutte le persone che ho avuto il piacere di conoscere durante l'elaborazione della mia tesi in Italia, che ho la fortuna di poter considerare ormai una seconda casa.

Inanzitutto, grazie ai professori Alberto Boscaggin e Walter Dambrosio per avermi accolto così bene durante il mio soggiorno a Torino nel 2021, che considero sia stato uno dei periodi più belli della mia vita. Grazie anche a loro per avermi insegnato tanto e per avermi introdotto a degli argomenti davvero interessanti. Aver potuto collaborare assieme ad Alberto e Walter è stato un grande piacere e spero veramente di poter continuare a fare ricerca con loro in futuro.

Grazie ad Andrea Tellini per l'invito a partecipare nei seminari DEG1 e per aver fatto sorgere la collaborazione tra Julián e Fabio. Grazie a Guglielmo Feltrin ed Elisa Sovrano per l'invito all'Equadiff a Brno, è stata una bellissima settimana dove ho potuto conoscere altri membri del DEG1 come Alessandro Fonda, Maurizio Garrione e Paolo Gidoni che sono stati davvero simpatici con me. Grazie ancora a Elisa e Guglielmo per la sua gentilizza e la sua accoglienza quando li ho incontrati a Reggio Emilia e Udine; e grazie anche ai professori Luisa Malaguti, Valentina Taddei, Roberta Fabbri e Franco Obersnel per i loro inviti e la loro grande cortesia quando li ho visitati a Reggio Emilia, Firenze e Trieste l'anno scorso.

D'altra parte, non vorrei dimenticare i colleghi che ho conosciuto al Palazzo Campana durante il mio soggiorno a Torino. Grazie a Saverio e Andrea O. per essere stati così accoglienti e bravi con me, e per tutti i pranzi a piazza Carlo Alberto. Grazie a Lucía per le visite di sabato pomeriggio nei musei torinesi e grazie a Emanuele per le pause caffè e le chiaccherate sempre interessanti.

Vorrei anche ringraziare tutta la gente che ho conosciuto in residenza a Torino. Grazie a Tiana per la sua preziosa amicizia e per tutti i bei momenti a Torino e Madrid. E grazie anche a Elena, Greta, Noemi, Andrea F. e Anastasia che hanno fatto il mio soggiorno molto più bello e divertente.

Infine, grazie tante ai miei amici Bea, Julia e Poli – imparare l'italiano con loro è stato un grande piacere – e specialmente a Cristiana dell'Innocenti, grazie alla quale scrivo oggi queste righe.

Madrid, 14 de abril de 2023

Papers generated by this thesis

1. J. López-Gómez and Eduardo Muñoz-Hernández, Global structure of subharmonics in a class of periodic predator-prey models, *Nonlinearity*, Volume **33**, Issue 1, p. 34–71, 2020.
   https://doi.org/10.1088/1361-6544/ab49e1
2. J. López-Gómez, E. Muñoz-Hernández and F. Zanolin, On the applicability of the Poincaré–Birkhoff twist theorem to a class of planar periodic predator-prey models, *Discrete and Continuous Dynamical Systems*, Volume **40**, Issue 4, p. 2393–2419, 2020.
   https://www.aimsciences.org/article/doi/10.3934/dcds.2020119
3. J. López-Gómez and Eduardo Muñoz-Hernández, A spatially heterogeneous predator-prey model, *Discrete and Continuous Dynamical Systems, Series B*, Volume **26**, Issue 4, p. 2085–2113, 2021.
   https://www.aimsciences.org/article/doi/10.3934/dcdsb.2020081
4. J. López-Gómez, E. Muñoz-Hernández and F. Zanolin, The Poincaré–Birkhoff theorem for a class of degenerate planar Hamiltonian systems, *Advanced Nonlinear Studies*, Volume **21**, Issue 3, p. 489–499, 2021.
   https://doi.org/10.1515/ans-2021-2137
5. A. Boscaggin and E. Muñoz-Hernández. Planar Hamiltonian systems: Index theory and applications to the existence of subharmonics, *Nonlinear Analysis*, Volume **226**, 113142, 2023.
   https://doi.org/10.1016/j.na.2022.113142
6. A. Boscaggin, W. Dambrosio and E. Muñoz-Hernández, A Maupertuis-type principle in relativistic mechanics and applications, *Calculus of Variations and Partial Differential Equations*, Volume **62**, 95, 2023.
   https://doi.org/10.1007/s00526-023-02430-9
7. J. López-Gómez, E. Muñoz-Hernández and F. Zanolin, Rich dynamics in planar systems with heterogeneous nonnegative weights, *Communications on Pure and Applied Analysis*, Volume **22**, Issue 4, p. 1043–1098, 2023.
   https://www.aimsciences.org/article/doi/10.3934/cpaa.2023020
8. J. López-Gómez, E. Muñoz-Hernández and F. Zanolin, Subharmonic solutions for a class of predator-prey models with degenerate weights in periodic environments, *Submitted*. https://doi.org/10.48550/arXiv.2207.14583.
9. J. López-Gómez and E. Muñoz-Hernández, A robust multiplicity result in a generalized diffusive predator-prey model, *Submitted*. https://doi.org/10.48550/arXiv.2302.09684,

Contents

Abstract

The main purpose of this PhD Thesis is to analyze the phenomena of predation through the study of some paradigmatic periodic heterogeneous and spatially heterogeneous diffusive predator-prey models. It has been organized in two parts. Part I is devoted to the study of the Volterra periodic predator-prey models. The main findings of this part are a series of multiplicity results of subharmonics using a variety of topological techniques such as Bifurcation Theory, the Poincaré–Birkhoff Theorem, and chaotic Poincaré maps. Part II invokes a number of techniques from Nonlinear Analysis and PDEs, headed by the strong maximum principle, to analyze a generalized heterogeneous parabolic predator-prey model with saturation effects that establishes a homotopy between the classical Lotka–Volterra and Holling–Tanner models. In particular, the positive steady states of this model are constructed through local and global bifurcation techniques combined with some global continuation arguments and the fixed point index in cones. Both parts are based on the research articles [134, 137, 135, 138, 139, 140, 136] written by the candidate together with his advisors.

Part I consists of Chapters 2–5 and covers the findings related to Volterra's periodic predator-prey models. Following some ideas of Ding and Zanolin [55, 56], Chapter 2 deals with the applicability of the Poincaré–Birkhoff Theorem to a class of planar Hamiltonian systems in a non-degenerate framework and analyzes how the T-periodic solutions disappear when the weight functions in the setting of the model degenerate. Chapter 3 considers a class of planar Hamiltonian systems where the weight functions involved do degenerate. In this context, the main objective is to ascertain the minimal configuration of the weight functions in order to obtain the multiplicity of subharmonics via the Poincaré–Birkhoff Theorem. Chapter 4 establishes the existence of chaotic dynamics in a wide class of periodic Volterra models at the light of the geometric ideas of Smale [189, 190] and the ulterior refinements through the theory of topological Horseshoes developed by Zanolin and his collaborators [166, 167, 168, 152]. Finally, Chapter 5 deals with a simple, but very significant, periodic Volterra prototype introduced by López-

Gómez, Ortega and Tineo [141], for which it has been possible, by the first time in the literature, to construct a global bifurcation diagram of subharmonics bifurcating from the equilibrium solution. Surprisingly, such a simple model can present such a complex set of solutions.

As a consequence of the results packaged in Part I, it becomes evident how the seasonability through the incorporation of periodic function coefficients in the most classical autonomous non-spatial non-cooperative models, can give rise to an extremely complex and rich dynamics, or even chaos, and this even in planar systems where the coefficients are arbitrarily close to some constants, except in an arbitrarily small temporal lapses.

Part II consists of Chapters 6 and 7. It focuses on the analysis of the existence, the nonexistence, the multiplicity and the uniqueness of coexistence states for the spatially heterogeneous predator-prey hybrid system mentioned above. In Chapter 6, after the models introduced by Blat and Brown [15, 16] and Dancer [43, 44] and the sharp analysis carried out by López-Gómez and Pardo [142, 143, 144] and Casal, Eilbeck and López-Gómez [34], a hybrid model with saturation effects that establishes a homotopy between the classical Lotka–Volterra and Holling–Tanner models is introduced and studied. Then, its regions of existence and nonexistence of coexistence states are estimated in terms of the linearized stabilities of the semitrivial positive solutions, and the uniqueness of its coexistence state is established in the one-dimensional model for sufficiently small saturation effects. In strong contrast, when the amplitude of the saturation term is sufficiently large, a rather robust completely novel multiplicity result is proved in Chapter 7, establishing the existence of, at least, two coexistence states, regardless the behavior of all the other coefficients involved in the model, in the region where the attractivity character of the semitrivial positive solutions differs.

Some further results not related directly with the predator-prey models have been obtained by the candidate during the preparation of the PhD Thesis together with Boscaggin, Dambrosio, López-Gómez and Zanolin [21, 18, 139].

Resumen

El objetivo principal de esta tesis doctoral es el análisis de la depredación a través del estudio de algunos modelos paradigmáticos de presa y depredador con heterogeneidades periódicas y de algunos sistemas difusivos de presa y depredador con heterogeneidades espaciales. Por consiguiente, esta tesis doctoral se ha estructurado en dos partes. La primera parte trata los modelos periódicos de presa y depredador de Volterra. En ella, se presta particular atención a la obtención de resultados de multiplicidad de soluciones subarmónicas a través del uso de diferentes técnicas topológicas tales como la teoría de la bifurcación, el teorema de Poincaré–Birkhoff o las aplicaciones de Poincaré caóticas. En la segunda parte, mediante la aplicación de diversas técnicas de análisis no lineal y EDPs, basadas en el principio del máximo fuerte, se analizará un modelo general heterogéneo parabólico de presa y depredador con efectos de saturación que establece una homotopía entre los modelos clásicos de Lotka–Volterra y de Holling–Tanner. En concreto, se construirán los estados de coexistencia a través de técnicas de bifurcación local y global junto con algunos argumentos de continuación global y el índice de punto fijo en conos. Ambas partes de la tesis están basadas en los artículos de investigación [134, 137, 135, 138, 139, 140, 136] realizados por el candidato junto a sus directores.

La parte I consta de los capítulos 2, 3, 4 y 5, en los cuales se analizan los resultados relacionados con los modelos periódicos de presa y depredador de Volterra. Partiendo de las ideas de Ding y Zanolin [55, 56], el capítulo 2 versa sobre la aplicación del teorema de Poincaré–Birkhoff a sistemas planos hamiltonianos no degenerados y de cómo las soluciones T-periódicas se pueden llegar a perder cuando los pesos del sistema degeneran. Por otro lado, en el capítulo 3, se analiza cuál es la configuración minimal que deben satisfacer los pesos de un sistema plano hamiltoniano degenerado para obtener resultados de multiplicidad de soluciones subarmónicas mediante el teorema de Poincaré–Birkhoff. En el capítulo 4 se demuestra la existencia de dinámicas caóticas para toda una amplia clase de sistemas planos hamiltonianos periódicos de acuerdo con la síntesis geométrica de Smale [189, 190]

y los refinamientos ulteriores desarrollados mediante la teoría de herraduras topológicas por Zanolin y sus colaboradores [166, 167, 168, 152]. Por último, el capítulo 5 estudia un prototipo periódico de presa y depredador de tipo Volterra, aunque muy simple, extraordinariamente significativo, introducido por Ortega, López-Gómez y Tineo [141], para el cual se ha construido por primera vez en la literatura el diagrama global de bifurcación de todos los subarmónicos que bifurcan desde el equilibrio del sistema.

Como consecuencia de los resultados de la primera parte, es evidente que la estacionalidad mediante la incorporación de coeficientes periódicos en los modelos autónomos, no espaciales y no cooperativos más clásicos, puede dar lugar a una gran complejidad dinámica y también al caos, incluso en sistemas planos donde los coeficientes están arbitrariamente próximos a ser constantes excepto en un lapso temporal arbitrariamente pequeño.

La parte II está compuesta por los capítulos 6 y 7. En ellos el análisis se centra en la existencia, no existencia, multiplicidad y unicidad de los estados de coexistencia de un modelo híbrido espacialmente heterogéneo de presa y depredador. En el capítulo 6, basándonos en los modelos introducidos por Blat y Brown [15, 16] y Dancer [43, 44], posteriormente analizados en profundidad por López-Gómez y Pardo [142, 143, 144] y Casal, Eilbeck y López-Gómez [34], se presenta y estudia un modelo híbrido espacial de presa y depredador con saturación que establece una homotopía entre el sistema clásico de Lotka–Volterra y el modelo de Holling–Tanner. Tras ello, se determinan cuáles son las regiones de existencia y no existencia de estados de coexistencia en términos de la estabilidad de las linealizaciones de las soluciones semitriviales positivas, y se establece la unicidad de estados de coexistencia en el modelo unidimensional cuando los efectos de saturación son suficientemente pequeños. Por el contrario, cuando la amplitud del término de saturación es suficientemente grande, se prueba en el capítulo 7 un resultado robusto de multiplicidad, completamente nuevo. Dicho resultado establece la existencia de, al menos, dos estados de coexistencia en la región en la que la atractividad local de las soluciones semitriviales positivas difiere, con independencia de los valores del resto de coeficientes involucrados en el sistema.

Algunos resultados adicionales que no están relacionados directamente con los modelos de presa y depredador estudiados han sido obtenidos durante la elaboración de la tesis doctoral del candidato junto con Boscaggin, Dambrosio, López-Gómez y Zanolin [21, 18, 139].

Chapter 1

Introduction

> *La legge naturale non dà il diritto alla felicità, ma anzi prescrive la miseria e il dolore. Quando viene esposto il commestibile, vi accorrono da tutte le parte i parassiti e, se mancano, s'affrettano di nascere. Presto la preda basta appena, e subito dopo non basta più perché la natura non fa calcoli, ma esperienze. Quando non basta più, ecco che i consumatori devono diminuire a forza di morte preceduta dal dolore e così l'equilibrio, per un istante, viene ristabilito. Perché lagnarsi? Eppure tutti si lagnano.*
>
> ITALO SVEVO, *La coscienza di Zeno*[*]

Umberto D'Ancona was born in 1896 at the historic Adriatic Sea town of Fiume. In those days, Fiume belonged to the Austro-Hungarian Empire and, hence, it is not strange that, after secondary school, he first attended the Faculty of Natural Sciences at the University of Budapest. However, he moved afterwards to the University of Rome, where he completed his studies in 1920 with a thesis about the digestive tube of the eel. It was in those years as a university student, serving simultaneously as an artillery officer in the World War I in the Carso, when D'Ancona collected, probably under the high influence of Darwin's theory on struggle for existence, different statistics about the number of captures of predator and prey fish species in the Northern Adriatic Sea. In particular, in the fish markets of Fiume, Trieste

[*]Natural law does not entitle us to happiness, but rather it prescribes wretchedness and sorrow. When something edible is left exposed, from all directions parasites come running, and if there are no parasites, they are quickly generated. Soon the prey is barely sufficient, and immediately afterwards it no longer suffices at all, for nature doesn't do sums, she experiments. When food no longer suffices, then consumers must diminish through death preceded by pain; thus equilibrium, for a moment, is reestablished. Why complain? And yet everyone does complain. (Italo Svevo, *Zeno's conscience.* Translated by William Weaver).

and Venice. Darwin's theories highly influenced also the literature of this period, as in the citation opening this Introduction, in which Zeno Cosini meditates about predators and preys as a sociological metaphor during one of his walks around Trieste. D'Ancona observed, after the data collected, a considerable growth in the selachians fished during and just after the war, while, paradoxically, in spite of the reduction of the fishery of the common small prey fishes during the war years, the number of the selachians prey's had decreased. D'Ancona was student of the famous physician and zoologist Giovanni Battista Grassi at Rome, which was the first one, together with Ronald Ross, in detecting the life cycle and transmission of malarial parasite. Under the supervision of Grassi, D'Ancona pursued the study of the morphology and sexuality of eels and began various histological studies on the nervous system of crustaceans. It was in this direction that D'Ancona, following the suggestion of Grassi, applied for a fellowship from the Rockefeller Foundation for a research stay in the "Instituto Cajal de Madrid" in 1924 under the supervision of the medicine Nobel recipient Santiago Ramón y Cajal. At that time the Institute was located nearby the Atocha's train station, in the current National Anthropological Museum.

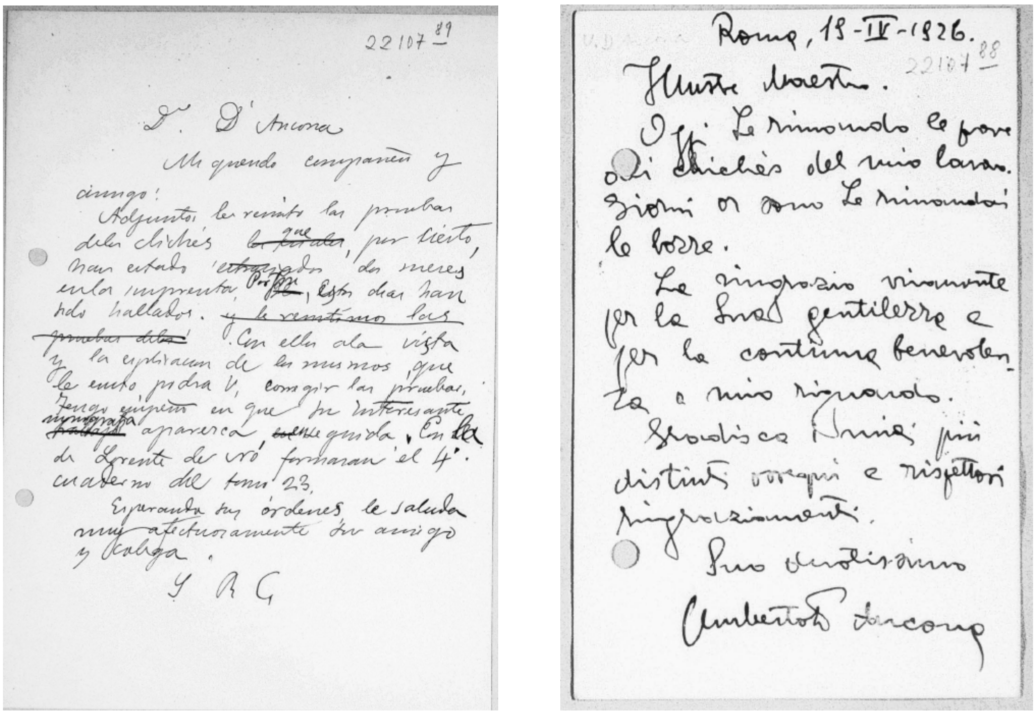

22107 89

Dr. D'Ancona

Mi querido compañero y amigo:

Adjuntos le remito las pruebas de los clichés ~~los cuales~~ que, por cierto, han estado extraviados dos meses en la imprenta. Por fin, estos días han sido hallados. ~~y le remitimos las pruebas de ellos~~. Con ellos a la vista y la explicación de los mismos, que le envío, podrá V. corregir las pruebas. Tengo empeño en que su interesante monografía aparezca en seguida. En la de Lorente de Nó formarán el 4º cuaderno del tomo 23.

Esperando sus órdenes le saluda muy afectuosamente su amigo y colega.

S. R. C.

Roma, 19-IV-1926.

22107 88

Illustre Maestro.

Oggi Le rimando le prove di clichés del mio lavoro. Giorni or sono Le rimandai le bozze.

La ringrazio vivamente per la Sua gentilezza e per la continua benevolenza a mio riguardo.

Gradisca i miei più distinti ossequi e rispettosi ringraziamenti.

Suo devotissimo

Umberto D'Ancona

Figure 1.1: A letter from Ramón y Cajal to D'Ancona about the proofs of his paper [48] (left figure) and the answer from D'Ancona to Ramón y Cajal (right figure). BNE: MSS_22107_87-89

The stay took place from September to December 1924 and there he learned the techniques of Ramón y Cajal and Pío del Río Hortega at the Histology Laboratory of the "Junta de Ampliación de Estudios", located at the "Residencia de Estudiantes", a very important educational institution where intellectuals of such a standing as Albert Einstein, Marie Curie or Igor Stravinski delivered conferences, and where D'Ancona might probably coincided with Spanish artists like Federico García Lorca, Luis Buñuel and Salvador Dalí, that resided there in that period. His stay gave later rise to the paper *Per la miglior conoscenza delle terminazioni nervose nei muscoli somatici dei crostacei decapodi* published in 1926 by Ramón y Cajal in the journal *Trabajos del Laboratorio de Investigaciones Biológicas de la Universidad de Madrid*, [48]. The interesting correspondence crossed between Ramón y Cajal and D'Ancona before and after his stay in Madrid can be read in the manuscripts of the National Library of Spain (MSS_22106_51-59, MSS_22107_87-89 and MSS_22109_73-81)[†].

Back in Italy in 1925, D'Ancona returned to the fishing fluctuations topic while courting his future wife, Luisa Volterra, the eldest daughter of Vito Volterra. This topic had already captured the attention of Volterra, who was lead to formulate his first predator-prey model in his celebrated papers of 1926 [203, 202]. By the time he wrote these publications, Volterra was 66 years old and was considered to be one of the greatest mathematicians of his generation, together with Henri Poincaré and David Hilbert, for his contributions in functional analysis, integration theory, integro-differential equations and mathematical physics. Volterra had also been interested for

[†]Transcription of the letters of Figure 1.1.
Left one (from Ramón y Cajal to D'Ancona):
D. D'Ancona,
Mi querido compañero y amigo:
Adjunto le remito las pruebas de los clichés que, por cierto, han estado extraviados dos meses en la imprenta. Por fin, estos días han sido hallados y le remitimos las pruebas. Con ellos a la vista y la explicación de los mismos que le envío podrá V. corregir las pruebas. Tengo empeño en que su interesante monografía aparezca enseguida. Con la de Lorente de Nó formarán el 4º cuaderno del tomo 23.
Esperando sus órdenes le saluda muy afectuosamente su amigo y colega,
S R C
Right one (from D'Ancona to Ramón y Cajal):
Roma, 19-IV-1926
Illustre Maestro,
Oggi Le rimando le prove dei clichés del mio lavoro. Giorni or sono Le rimandai le bozze. La ringrazio vivamente per la Sua gentilezza e per la continua benevolezza a mio riguardo. Gradisca i miei più distinti ossequi e rispettosi ringraziamenti.
Suo devotissimo,
Umberto D'Ancona

Figure 1.2: Volterra's family around year 1930. In the center Vito Volterra and on the right Umberto D'Ancona with his wife, Luisa, and their daughter Silvia. Caltech Archives

many years in the applications of Mathematics to Biology. An example of this is the title of his inaugural lecture of the academic year 1901 at the University of Rome: *Sui tentativi di applicazione delle matematiche alle scienze biologiche e sociali*. Another one, that he was the founder, in 1908, of the scientific organization *Comitato talassografico italiano*, where also D'Ancona worked, whose goal was the *studio fisico-chimico e biologico dei mari italiani, prevalentemente in rapporto alla industria della navigazione e della pesca e per l'esplorazione dell'alta atmosfera nei riguardi della navigazione aerea*. He also studied the Verhulst, or logistic, equation, incorporating it to the biological models in his monograph of 1927 [204] and in his celebrated series of lectures at the Henri Poincaré Institute [205], where he was invited by Émile Borel. The big influence of Darwin's theory is also noted in Volterra when he writes in [204], citing Charles Darwin's essay *Origin of Species by Means of Natural Selection* [51]:

"Una intuizione dei fenomeni connessi alla legge della perturbazione delle medie l'ebbe Carlo Darwin quando, parlando della lotta per l'esistenza, disse: «The amount of food for each species of course gives the extreme limit to which each can increase; but very frequently it is not the obtaining food, but the serving as prey to other animals which determines the average numbers of a species. Thus, there seems to be little doubt that the stock of partridges, grouses and hares on any large estate depends chiefly on the destruction of vermin. If not one head of game were shot during the next twenty years in England, and, at the same time, if no vermin were destroyed, there would, in all probability, be less game than at present, although hundreds of thousands of game animals are now annually shot.»"

Simultaneously, D'Ancona published in 1926 a paper diffusing the statistics elaborated by him in [47] and, some years later, the book entitled *La lotta per l'esistenza* [49]. This book, published after the death of his father-in-law in 1940, was an homage and a recognition to Volterra, who in 1931 had been expelled out from the University and all his academic positions because he refused to rend loyalty to the fascist regime of Mussolini. It turns out that he was one of the twelve Italian professors in all of Italy refusing to sign this loyalty oath. Now, it makes full sense the meaning of the words of Vito Volterra in 1931 under one of his most famous photographs: *Muoiono gli imperi, ma i teoremi d'Euclide conservano eterna giovinezza*.

Figure 1.3: Volterra's photo with the cited handwritten phrase

Focusing attention on the mathematical findings of this PhD Thesis, we have distributed them in two parts. Part I analyzes a series of models having the same structure of the original one proposed by Volterra but incorporating non-autonomous periodic coefficients instead of constant coefficients. Naturally, incorporating periodic coefficients in these models enrich substantially the dynamics with respect to the autonomous original Volterra models, and this is the main core of the Thesis. Part II deals with some more sophisticated diffusive counterparts incorporating some effects of saturation of predators in abundance of preys in the presence of spatial heterogeneities.

Part I: Periodic Volterra models

The analysis of subharmonic solutions to differential systems with periodic coefficients is a classical research topic which has been widely investigated also with respect to its relevant significance in several applications, including the study of differential equations models arising from Celestial Mechanics and Engineering. Given a first-order differential system

$$z' = F(t, z), \tag{1.1}$$

for $z = (z_1, \dots, z_d) \in \Omega$, where Ω is an open domain of $\mathbb{R}^d$ and $F \colon \mathbb{R} \times \Omega \to \mathbb{R}^d$ is a sufficiently regular vector field which is T-periodic in the t-variable, by a *subharmonic solution of order* $n \geq 2$, we mean a nT-periodic solution of system (1.1) which is not kT-periodic for $k \in \{1, \dots, n-1\}$. As pointed out by P. H. Rabinowitz in [178]:

"This latter quest is complicated by the fact that any T-periodic solution is a fortiori kT-periodic. Thus an additional argument is required to show that any subharmonics are indeed distinct."

In particular, it will also be important to check whether a subharmonic solution of order n has indeed nT as its minimal period. This is a difficult task that nevertheless can be overcome in some circumstances thanks to the special structure of the vector field F. Some sufficient conditions have been already proposed in the literature (see, e.g., Michalek and Tarantello [153]).

The general aim of Part I is to investigate, as deeply as possible, the subharmonics to a class of Lotka–Volterra systems under seasonal effects. Precisely, the model is a planar Hamiltonian system of the form

$$\begin{cases} x' = -\lambda \alpha(t) f(y), \\ y' = \lambda \beta(t) f(x), \end{cases} \tag{1.2}$$

where $f \colon \mathbb{R} \to \mathbb{R}$ is a locally Lipschitz continuous function with $f(0) = 0$ and $f(s)s > 0$ for $s \neq 0$ such that f is bounded on $(-\infty, 0]$ and has a superlinear growth at $+\infty$. The assumptions on f are motivated by the paradigmatic case

$$f(s) = e^s - 1, \tag{1.3}$$

coming from the original Volterra's equations.

In 1926, Vito Volterra in [203] proposed a mathematical model for the predator-prey interactions as an answer to the statistics on the fishing data in Northern Adriatic sea, provided by the biologist Umberto D'Ancona. His model, extraordinarily famous today, since it is discussed in most of textbooks on Ordinary Differential Equations and Ecology, has shown to be a milestone for the development of more realistic predator-prey models in Environmental Sciences and Population Dynamics (see, e.g., Begon, Harper and Townsend [11]). It can be formulated as follows

$$\begin{cases} N_1' = N_1(a - bN_2), \\ N_2' = N_2(-c + dN_1), \end{cases} \tag{1.4}$$

where $N_1(t) > 0$ and $N_2(t) > 0$ represent, respectively, the density of the prey and the predator populations at time t. In (1.4), the coefficients, a, b, c and d, are assumed to be positive (see Braun [23]). The same system had been already introduced few years before by Alfred J. Lotka from a hypothetical chemical reaction exhibiting periodic behavior in the chemical concentrations (see Murray [157, §3.1]), which reveals how the same models can mimic a variety of phenomenologies of a different nature. After these pioneering contributions, differential equations involving the interaction of two or more species are usually named as Lotka–Volterra systems and are represented in the general form

$$N_i' = N_i\Big(a_i - \sum_{j=1}^{N} b_{ij}N_j\Big), \quad i = 1, \dots, n, \tag{1.5}$$

though in this paper we will focus attention on those satisfying $b_{ii} = 0$. The choice of the sign of the coefficients a_i and b_{ij} allows describing different kinds of interactions, as competition, cooperation, or parasitism.

Although Volterra [205] and Lotka [146] considered the possibility of some varying in time coefficients, an extensive study of the Lotka–Volterra systems with periodic coefficients has not been carried out until more recently (see, e.g., Butler and Freedman [27], Cushing [39, 40] and Rosenblat [180], for some early works in this direction). However, in the past four decades, the researches in this area have originated a great number of contributions, also in connection with the study of periodically perturbed Hamiltonian systems and Reaction-Diffusion systems arising in genetics and population dynamics, beginning with the influential monograph of P. Hess [92] and the refinements of López-Gómez [120], where a general class of spatially heterogeneous diffusive Lotka–Volterra systems with periodic coefficients was studied. To understand the role played by the spatial heterogeneities in these models the reader is sent to the early works of López-Gómez [122] and Hutson et al. [97], as well as to the monographs [124, 127]. Further models covering more general spatial interactions, a bit outside the Lotka–Volterra World, were introduced by López-Gómez and Molina-Meyer [131, 130].

Although the assumption that the coefficients of the model are periodic with a common period might seem restrictive, it is based on the natural assumption that the species are affected by identical seasonal effects, which is rather natural as they interact in the same environment. Precisely, the interest of this paper focuses into the following periodic counterpart of the autonomous system (1.4)

$$\begin{cases} N_1' = N_1(a(t) - b(t)N_2) \\ N_2' = N_2(-c(t) + d(t)N_1) \end{cases} \tag{1.6}$$

where, typically, a, b, c, $d : \mathbb{R} \to \mathbb{R}$ are T-periodic functions such that

$$b(t) \gneq 0, \qquad d(t) \gneq 0, \qquad \int_0^T a(t)\, dt > 0, \qquad \int_0^T c(t)\, dt > 0.$$

In this case, by Theorem 2.3.1, the system (1.6) has a component-wise positive T-periodic solution, $(\tilde{N}_1(t), \tilde{N}_2(t))$, and the change of variables

$$N_1(t) = u(t)\tilde{N}_1(t), \quad N_2(t) = v(t)\tilde{N}_2(t),$$

leads to the equivalent system

$$\begin{cases} u' = \lambda\alpha(t)u(1 - v) \\ v' = \lambda\beta(t)v(-1 + u) \end{cases} \tag{1.7}$$

where $(\tilde{N}_1(t), \tilde{N}_2(t))$ becomes $(1, 1)$ (see the Appendix 2.3 for further details if necessary). In (1.7), $\lambda > 0$ is regarded as a parameter, while $\alpha(t) \gneq 0$ and $\beta(t) \gneq 0$ are T-periodic function coefficients, where $T > 0$ is their minimal period. The component-wise *positive* periodic solutions of (1.7) are called (periodic) *coexistence states* and, obviously, are relevant in population dynamics, as they represent states where none of the interacting species is driven to extinction by the other. Thus, they are states of *permanence* for both species.

Among the periodic coexistence states, the subharmonics are of particular interest. Focussing attention into the simplest prototype model with constant coefficients (1.4), it is folklore since Volterra [205] that all its positive solutions are periodic and oscillate around the equilibrium $P_0 \equiv (c/d, a/b)$ in the counterclockwise sense, lying on the "energy levels"

$$E(N_1, N_2) := dN_1 - c\log N_1 + bN_2 - a\log N_2 = \text{constant} = k,$$

for $k \in (k_0, +\infty)$, where

$$k_0 := E(P_0) = c\left(1 - \log\tfrac{c}{d}\right) + a\left(1 - \log\tfrac{a}{b}\right).$$

Therefore, P_0 is a global center in the open first quadrant. The fact that the period of the orbit at the level k, $\tau(k)$, is an increasing function of k is a more recent finding of Rothe [181], Shaaf [185] and Waldvogel [206], where it was also shown that

$$\lim_{k \downarrow k_0} \tau(k) = \frac{2\pi}{\sqrt{ac}} =: \tau_0 \quad \text{and} \quad \lim_{k \uparrow \infty} \tau(k) = +\infty.$$

Thus, for every $T \in (0, \tau_0)$, the equilibrium point P_0 is the unique T-periodic coexistence state (harmonic solution), though there are infinitely many non-trivial subharmonic coexistence states corresponding to the energy levels k for which $\tau(k) = mT$ for sufficiently large $m \geq 2$. This classical example also illustrates how subharmonics can be packaged in equivalence classes (two subharmonics are equivalent when they are a time-shift of the other). This also holds for *nonautonomous systems*. Indeed, if $z(t)$ is a nT-periodic solution of (1.1), then $z(t + jT)$ is also a nT-periodic solution for every $j = 0, 1, \ldots, n-1$. Michalek and Tarantello [153] referred to the set

$$\Theta(z) = \{z(\cdot + jT) : j = 0, 1, \ldots, n-1\}$$

as the *$\mathbb{Z}_n$-orbit of z*. Hence, searching subharmonics in *nonautonomous* systems is a task fraught with a number of difficulties. Then, the main goals of Part I are the following:

- finding out nT-periodic solutions having nT as *minimal period*, namely *subharmonics of order n*;
- among the subharmonics having the same order, ascertaining whether, or not, they belong to the same periodicity class.

Previous results on the existence and multiplicity of harmonic and subharmonic solutions in periodically perturbed predator-prey systems have been obtained by Hausrath [88] and Liu [117], as a consequence of the Moser twist theorem, and by Hausrath and Manásevich [89], Ding and Zanolin [55, 56] and Boscaggin [17] from the Poincaré–Birkhoff fixed point theorem. The latest results have been recently extended by Fonda and Toader [77] to systems in $\mathbb{R}^{2n}$ by means of a (previous) higher-dimensional version of the Poincaré–Birkhoff theorem due to Fonda and Ureña [78]. More recently, in [21] (see appendix 3.4) have also analyzed the subharmonic solutions in a class of planar Hamiltonian systems including (1.7).

López-Gómez, Ortega and Tineo [141] and López-Gómez [123, §5] carried out a thorough investigation of the positive coexistence states for the generalized Lotka–Volterra system with periodic coefficients

$$\begin{cases} N_1' = N_1(a_1(t) - c_1(t)N_1 - b_1(t)N_2), \\ N_2' = N_2(a_2(t) + b_2(t)N_1 - c_2(t)N_2), \end{cases} \tag{1.8}$$

which includes the presence of logistic terms incorporating to the model setting some interspecific competition effects. This model has, in addition, semi-trivial coexistence states of the form $(\hat{N}_1(t), 0)$ and $(0, \hat{N}_2(t))$, where $\hat{N}_i$ stands for the (unique) positive T-periodic solution of the logistic equation

$$N_i' = N_i(a_i(t) - c_i(t)N_i), \qquad i = 1, 2.$$

As in the periodic-parabolic counterpart of (1.8), already analyzed by Hess [92] and López-Gómez [120], the local character of the semitrivial positive solutions plays a crucial role in determining the dynamics of (1.8), being a challenging task to ascertain the stability, or instability, of the coexistence states.

López-Gómez, Ortega and Tineo [141] made the crucial observation that, for the special choice

$$\alpha(t) \equiv 0, \quad \text{for } \ t \in [T/2, T], \qquad \beta(t) \equiv 0, \quad \text{for } \ t \in [0, T/2], \tag{1.9}$$

(1.7) has a (unique) linearly unstable coexistence state, though the system can admit two coexistence states (see [141, Rem. 7.5]). This, in strong contrast with the previous one-dimensional uniqueness results found for the diffusive counterparts of these models by López-Gómez and Pardo [143, 144] and Dancer, López-Gómez and Ortega [46] (see the detailed discussion of [123]). Actually, this prototype model has shown to be rather paradigmatic for analyzing the local character and the multiplicity of harmonic and subharmonic coexistence states. Indeed, setting

$$A := \int_0^T \alpha(t)\, dt, \qquad B := \int_0^T \beta(t)\, dt, \tag{1.10}$$

it follows from [141, Pr. 7.1] that $P_0 \equiv (1, 1)$ is linearly unstable if

$$\lambda > \frac{2}{\sqrt{AB}}. \tag{1.11}$$

Moreover, by [123, Th. 5.3], the instability of P_0 guarantees the existence of three coexistence states for (1.8) within the appropriate ranges of values of its function coefficients. It turns out that, besides the unique (harmonic) coexistence state P_0, there are, at least, two additional $2T$-periodic coexistence states if (1.11) holds. After two decades, López-Gómez and Muñoz-Hernández [134] (see Chapter 5) were able to construct nT-periodic solutions for every $n \geq 2$, providing simultaneously with a sharp estimate of their minimal cardinals. Figure 1.4 shows the (minimal) global bifurcation diagram of subharmonics of (1.7) found in [134] (see Section 5.5) for an arbitrary choice of $\alpha(t)$ and $\beta(t)$ satisfying the *orthogonality condition* (1.9).

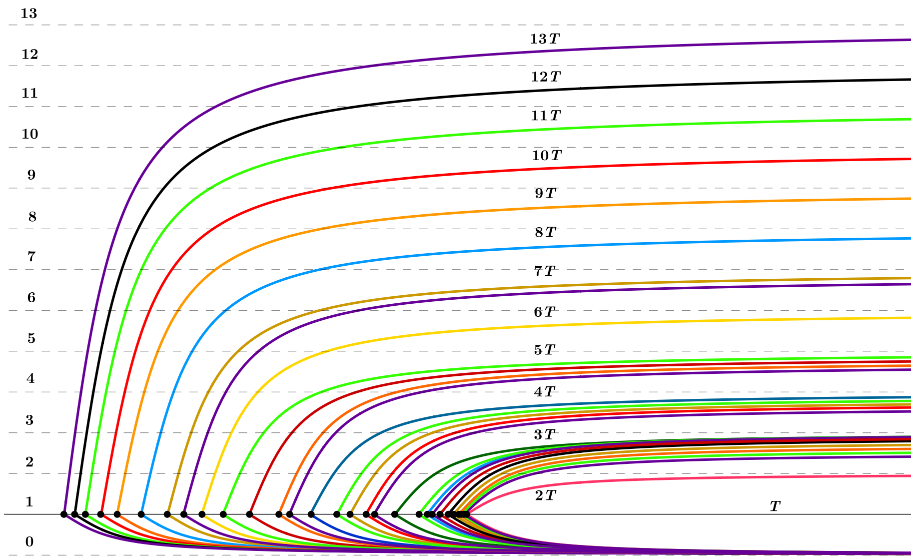

Figure 1.4: Admissible global bifurcation diagram under (1.9), after [134].

These findings should be also true, at least, when $\alpha(t)$ and $\beta(t)$ are *nearly orthogonal*, in the sense that the product $\alpha\beta$ is sufficiently small in $[0, T]$, and actually they might be also true for very general classes of weight functions $\alpha(t)$ and $\beta(t)$ far from satisfying (1.9). Thus, it is rather natural to investigate the structure of the set of subharmonics of (1.7) for more general configurations of $\alpha(t)$ and $\beta(t)$ than those satisfying (1.9). Besides its intrinsic interest, this analysis might reveal some new important features, based, e.g., on the shapes of $\alpha(t)$ and $\beta(t)$, that might be significative in population dynamics. Indeed, as it will be discussed in Appendix 2.3, when $\beta \equiv 0$, one is considering a seasonal time-interval where predator is still aggressive with respect to the prey but does not take advantage of the harvest, which may simulate the difference between the hunting and the gathering period. Analog interpretations may be given for the time-intervals when $\alpha \equiv 0$.

From the mathematical analysis of (1.7), it becomes apparent that its dynamics might vary according to the measure of the intersection of the supports of α and β. To differentiate the two extreme cases, we will name as *degenerate* the case when $|\operatorname{supp}\alpha \cap \operatorname{supp}\beta| = 0$, while the case when

$$|\operatorname{supp}\alpha \cap \operatorname{supp}\beta| > 0.$$

will be referred to as the *non-degenerate* case.

As a sharp analysis of (1.7) seems imperative to classify all the possible dynamics associated to a general predator-prey system with periodic coefficients, throughout Part I we will focus our attention into the simplest prototype model (1.7), with special emphasis towards the problem of analyzing its subharmonic solutions depending on whether, or not, the chosen configuration of $\alpha(t)$ and $\beta(t)$ is degenerate.

Among the various existing approaches in finding out subharmonics in Hamiltonian systems, the most successful ones are the following:

- variational methods (critical point theory),
- Kolmogorov–Arnold–Moser (KAM) theory, Moser twist theorem, and Poincaré–Birkhoff theorem,
- symbolic dynamics associated to Smale's horseshoe-type structures, and
- reduction via symmetry and bifurcation theory.

As we are going to invoke the last three in this paper, we will shortly revisit them in the next few paragraphs. But first, we will briefly discuss the variational method approach and introduce, in this direction, the results obtained in [18] for the so-called relativistic Kepler problem.

Variational methods (critical point theory): In this framework, a number of different arguments have been given to show that the periodic solutions that are critical points of the associated functional are indeed subharmonics of large period. For instance, Rabinowitz [178] achieves it by analyzing the critical levels of the functional (see also Fonda and Lazer [75] and Serra, Tarallo and Terracini [186]), whereas Michalek and Tarantello [153] apply a combination of estimates on critical levels and $\mathbb{Z}_p$-index theory. Assuming an additional non-degeneracy condition on the solutions, Conley and Zhender [36] can get subharmonics through their Morse indices (see also Abbondandolo [2] and the references therein).

Regarding a concrete case of study, Boscaggin, Dambrosio and Muñoz–Hernández [18] have analyzed the existence of periodic solutions with prescribed energy for the gradient like differential equation

$$\frac{\mathrm{d}}{\mathrm{d}t}\left(\frac{m\dot{x}}{\sqrt{1-|\dot{x}|^2/c^2}}\right) = \nabla V(x), \qquad x \in \Omega \subset \mathbb{R}^n, \tag{1.12}$$

where $m, c > 0$ and $V : \Omega \to \mathbb{R}$ is a function of class C^1. Thanks to the Lagrange structure of (1.12), the corresponding Hamiltonian associated to (1.12) is a constant of motion. Thus, it can be proved that, for every solution $x(t)$ of (1.12) there exists $E \in \mathbb{R}$ such that

$$\frac{mc^2}{\sqrt{1-|\dot{x}(t)|^2/c^2}} - V(x(t)) \equiv E = h + mc^2, \tag{1.13}$$

where h the difference between the relativistic energy and the particle rest energy. Note that the solutions of (1.12) are confined in the Hill's region

$$\Omega_h := \{x \in \Omega \ : \ V(x) + h > 0\}.$$

The first aim of [18] was to introduce a Maupertuis-type functional whose critical points are solutions of (1.12) with prescribed energy. This can be done the same ideas as in the non-relativistic case, relating the action, length, energy and Maupertuis functionals. Namely, the Maupertuis functional associated to problem (1.12) is defined as

$$\mathcal{M}_h(q) = \int_0^1 |\dot{q}(\sigma)|^2 \, d\sigma \int_0^1 \left(2mV(q) + \frac{1}{c^2}\left(V(q)+h\right)^2 + 2hm\right) d\sigma,$$

in the set

$$\Lambda_h' := \{q \in H^1([0,1]) : \ q(0) = q(1), \ q(\sigma) \in \Omega_h, \ \forall\, \sigma \in [0,1]\}.$$

In this setting, it is shown in [18, Prop. 2.2] that associated to any non-constant critical point $q \in \Lambda_h'$ of $\mathcal{M}_h(q)$ it corresponds, for some $T > 0$, a non-constant T-periodic solution x of (1.12) satisfying the energy law (1.13).

Once established this Maupertuis principle, an application for an N-center problem in the plane is provided by taking $\Omega = \mathbb{R}^2 \setminus \{\sigma_1, \dots, \sigma_N\}$ and

$$V(x) = \sum_{i=1}^{N} \frac{\kappa_i}{\alpha |x - \sigma_i|^\alpha} + W(x),$$

where $\alpha > 1$, $\sigma_1, \dots, \sigma_N$ are N different points of $\mathbb{R}^2$, $\kappa_i > 0$ for $i = 1, \dots, N$, and $W : \mathbb{R}^2 \to \mathbb{R}$ is a function of class C^1 satisfying the following:

(W1) there exists $M > 0$ such that $0 < W(x) \leq M$ for every $x \in \mathbb{R}^2$,

(W2) $\nabla W(x) \to 0$ for $|x| \to +\infty$.

In this context, [18, Th. 3.1] ensures that, for any given $h > 0$ and any non-trivial homotopy class $[\gamma] \in \pi_1(\mathbb{R}^2 \setminus \{\sigma_1, \ldots, \sigma_N\})$, there exists a non-collision periodic solution of equation (1.12) with energy $E = h + mc^2$ in the homotopy class $[\gamma]$. In order to prove this result several variational techniques are used such as the Ekeland variational principle (for any further details see [18, Secs. 2 & 3] if necessary)

The Poincaré–Birkhoff approach: In this setting, as well as in KAM theory when applying the Moser twist theorem, a typical approach consists in constructing an annular region enclosed by two curves, Γ_{int} and Γ_{out}, which are invariant by the Poincaré map associated to the given planar system. Recall that the Poincaré map is the homeomorphism $\Phi = \Phi_0^T$ transforming an initial point z_0 to $\zeta(T; 0, z_0)$, where $\zeta(\cdot; 0, z_0)$ stands for the solution of (1.1) with $z(0) = z_0$. The associated flow is area-preserving when $\text{div}_z F(t, z) \equiv 0$, a condition which is always satisfied by Hamiltonian systems. Then, introducing a suitable *rotation number*, $\text{rot}([0, nT], z_0)$, the Poincaré–Birkhoff fixed point theorem guarantees the existence of at least two fixed points for Φ^n in the interior of the annulus as soon as the following *twist condition*

$$\text{rot}([0, nT], z_0) \begin{cases} < j \ [\text{resp} > j] & \text{for all } \ z_0 \in \Gamma_{\text{int}} \\ > j \ [\text{resp} < j] & \text{for all } \ z_0 \in \Gamma_{\text{out}} \end{cases} \tag{1.14}$$

holds for some integer j. In such situation, the fixed points of Φ^n have j as an associated rotation number. This actually entails the existence of subharmonics of order n if n and j are co-prime integers. Theorems 2.1 and 3.1 of Neumann [159] give some sufficient conditions so that these subharmonic solutions belong to different periodicity classes.

A typical definition of rotation number can be given by passing to polar coordinates and counting the number of turns (counterclockwise, or clockwise) that the solution $\zeta(t; 0, z_0)$ makes around the origin in a given time-interval. The choice of the origin as a "pivotal point" is merely conventional, but it fits well for systems like (1.2), where $F(t, 0) \equiv 0$. Adopting this methodology, for any given interval $[t_0, t_1]$, we will set

$$\text{rot}([t_0, t_1], z_0) := \delta \frac{1}{2\pi} \int_{t_0}^{t_1} \frac{F(t, \zeta(t; t_0, z_0)) \wedge \zeta(t; t_0, z_0)}{||\zeta(t; t_0, z_0)||^2} \, dt \tag{1.15}$$

where $\delta = \pm 1$. In Boscaggin [17] and Boscaggin and Muñoz–Hernández [21] they are given some other equivalent notions (see also [20] and [82]).

Ding [57], Fonda and Ureña [78], Frank [80], Qian and Torres [173] and Rebelo [179] have found some refinements of the Poincaré–Birkhoff fixed point theorem adapted to more general settings where the boundary invariance of the underlying annular region is lost. Dalbono and Rebelo [41] and more recently Fonda, Sabatini and Zanolin [76] have reviewed a series of results on the applicability of the Poincaré–Birkhoff theorem in non-invariant annuli.

According to [21] (see Appendix 3.4), there is a link between the variational approach discussed in the previous paragraph and the rotation number estimates necessary to apply the Poincaré–Birkhoff theorem based on the Conley–Zehnder–Maslov index (see Abbondandolo [2] and Long [119]).

Nevertheless, establishing the existence of the invariant curves is a hard task that typically requires to invoke the KAM theory or some of its variants (see Laederich and Levi [111]), like, e.g., the Moser twist theorem [155], as in Dieckerhoff and Zehnder [54] and Levi [112] for the scalar second order differential equation

$$x'' + V_x(x,t) = 0,$$

or as in Hausrath [88] and Liu [117] for the more sophisticated predator-prey system.

Chaotic dynamics: In connection with the previous discussion, subharmonics can be also detected by applying to the Poincaré map and its iterates various methods coming from the theory of dynamical systems, the most paradigmatic being the celebrated Smale's horseshoe (see Smale [188, 189], Moser [156, Ch. III] and Wiggins [210]). Essentially, it consists of a toy-diffeomorphism stretching and bending, recursively, a square onto a horseshoe-type domain.

In Chapter 4, we will work in a slightly weaker setting entering into the theory of *topological horseshoes* as developed, adapting different perspectives, by Carbinatto, Kwapisz and Mischaikow [33], Mischaikow and Mrozek [154], Srzednicki [193], Srzednicki and Wójcik [194], Wójcik and Zgliczyński [211], Zgliczyński [214] and Zgliczyński and Gidea [215], just to quote some of the most illustrative contributions among a vast literature on this topic. The theory of topological horseshoes, as discussed by Burns and Weiss [25] and Kennedy and Yorke [101], consists of a series of methods introduced to extend the classical geometry of the Smale horseshoe to more general dynamical situations involving topological crossings and, crucially, avoiding any hyperbolicity assumptions on the diffeomorphism, as it might be a challenge to verify them in applications.

In particular, in Chapter 4 we will benefit of a topological approach developed by Papini and Zanolin [166, 167] and Pascoletti, Pireddu and Zanolin [168] leading to the following notion of *chaos in the coin-tossing sense*.

Definition 1.0.1. *Let X be a metric space and $\Phi : \mathcal{Q} \to X$ be a homeomorphism. It is said that Φ has a topological horseshoe in the set $\mathcal{Q}$ if there are $\ell \geq 2$ non-empty pairwise disjoint compact sets $\mathcal{H}_0, \ldots, \mathcal{H}_{\ell-1} \subset \mathcal{Q}$ such that, for every two-sided sequence of ℓ symbols,*

$$\boldsymbol{s} = (s_i)_{i\in\mathbb{Z}} \in \Sigma_\ell := \{0, \ldots, \ell-1\}^{\mathbb{Z}},$$

there exists $z \in \mathcal{Q}$ such that $z_i := \Phi^i(z) \in \mathcal{H}_{s_i}$ for all $i \in \mathbb{Z}$ and, whenever $(s_i)_i$ is a n-periodic sequence, then z can be chosen so that the sequence of iterates $(z_i)_i$ is as well n-periodic. In this case, it is also said that Φ induces chaotic dynamics on ℓ symbols in $\mathcal{Q}$.

Definition 1.0.1 is inspired in the concept of chaotic dynamics as a situation where a deterministic map can reproduce, along its iterates, all the possible outcomes of a coin-flipping experiment, as discussed by Smale [190] (see also Kirchgraber and Stoffer [102]). According to Medio, Pireddu and Zanolin [152], any map Φ inducing chaotic dynamics on ℓ symbols in $\mathcal{Q}$ is *semi-conjugate* to the Bernoulli shift automorphism

$$\sigma : \Sigma_\ell \to \Sigma_\ell, \qquad \sigma((s_i)_i) := (s_{i+1})_i \quad \text{for all } \ i \in \mathbb{Z},$$

in the sense that there exist a compact subset, $\Lambda \subset \bigcup_{i=0,\ldots\ell-1} \mathcal{H}_i \subset \mathcal{Q}$, invariant for Φ, whose set of periodic points, $\operatorname{Per}\Phi$, is dense in Λ, and a *continuous and surjective map* $g : \Lambda \to \Sigma_\ell$ such that:

i) $g \circ \Phi = \sigma \circ g$, and

ii) for every periodic sequence $\mathbf{s} \in \Sigma_\ell$, the set $g^{-1}(\mathbf{s})$ contains a periodic point of Φ with the same period.

Property ii) corresponds to the one introduced by Zgliczyński in [214, Th. 4.1]. Thus, adopting Definition 1.0.1 we are entering into a genuine classical definition of chaotic dynamics of Block–Coppel type, as discussed by Aulbach and Kieninger [9]. Hence, according to Adler, Konheim and McAndrew [3], Φ has a positive topological entropy. The semi-conjugation property provides a weaker form of chaos with respect to the original Smale's horseshoe, where $g : \Lambda \to \Sigma_\ell$ is assumed to be a homeomorphism and, so, $\Phi|_\Lambda$ is *conjugate* to the Bernoulli shift. The conjugation property provides us with a stronger type of chaotic dynamics as, in such case, Φ inherits on the invariant set Λ all the properties of the automorphism σ. Therefore, all the existing notions of chaos, such as those introduced by Devaney [53], Li and Yorke [115], Aulbach and Kieninger [9] and Kirchgraber and Stoffer [102] hold simultaneously. Although there are series of results ensuring the conjugation, as, e.g., the celebrated Melnikov theorem, which requires the delicate task of analyzing perturbations of homoclinic, or heteroclinic, configurations, or the theory of linked twist maps developed by Devaney [52] and Sturman, Ottino and Wiggins [195], except in concrete special examples, it is a challenge to make sure that these sufficient conditions hold. For a survey in the several notions of chaos and some applications obtained considering the approach of [167, 166, 168] see Sovrano [191, 192].

Clearly, for any map Φ satisfying the requirements of Definition 1.0.1, one can infer the existence of periodic points of arbitrary minimal period, and hence subharmonics if Φ is the Poincaré map of an ODE with periodic coefficients. For instance, if $\ell = 2$, given any periodic sequence in $\{0, 1\}$ of minimal period n, there is also a periodic point of Φ in $\mathcal{Q}$ with minimal period n. Similar notions of "chaos" can be given by means of a number of topological methods, based on the Conley index, fixed point theories, or topological degree (see, e.g., Carbinatto, Kwapisz and Mischaikow [33], Mischaikow and Mrozek [154], Srzednicki [193], Srzednicki and Wójcik [194], Wójcik and Zgliczyński [211], Zgliczyński [214] and Zgliczyński and Gidea [215]). Typically, in any setting entailing Definition 1.0.1, it is possible to detect a larger number of subharmonics than merely applying the Poincaré–Birkhoff theorem (see Feltrin [67, Rem. 4.1]).

Among the main advantages of using the theory of topological horseshoes, instead of the methods discussed in the two previous items, it is worth-mentioning that, besides the system is not required to inherit any Hamiltonian structure, there are not constraints on the dimension.

The method of *stretching along the paths* (SAP) introduced by Papini and Zanolin in [166, 167], was already used by these authors not only to prove the existence of chaotic dynamics but to analyze the existence of nodal solutions for a second order differential equation with indefinite sign. In this direction, in the second part of López-Gómez, Muñoz-Hernández and Zanolin [139], by the use of the SAP method it has been done a comprehensive analysis of the nodal solutions of the one-dimensional quasilinear equation of ϕ-laplacian type

$$-(\phi(u'))' = \lambda u + a(t)g(u), \qquad \lambda \in \mathbb{R}, \ \ t \in [0, L],$$

where $L > 0$ and $a(t)$ is a stepwise non-negative function. More precisely, it has been determined the existence and multiplicity of nodal solutions of the generalized Sturm-Liouville boundary value problem

$$\begin{cases} x' = h(y), \\ y' = -\lambda x - a(t)g(x), \\ x(0) \in r_0, \ \ x(L) \in r_L, \end{cases} \tag{1.16}$$

where $h = \phi^{-1}$, and r_0 and r_L are two general curves included in some quadrant of the phase plane with the property of connecting the inner with the outer boundary of a suitable annulus of periodic solutions. The basic idea to analyze (1.16) is to study separately the cases when $a \equiv 0$ ((1.16) is linear in the second component) and $a(t) \equiv \mu > 0$ ((1.16) is fully nonlinear), and, then, gluing them together appropriately. If $\lambda \geq 0$ the multiplicity results follow under rather mild assumptions while in the case $\lambda > 0$ some further hypothesis should be assumed.

A bifurcation approach: Another successful approach for solving a huge variety of nonlinear differential equations, both ODEs and PDEs, relies on the topological degree through local and global bifurcation theory. Essentially, in the context of bifurcation theory, the continuation methods in parametric models do substitute the Implicit Function Theorem in the presence of degenerate solutions, provided that a change of degree occurs as the parameter, λ, crosses some critical value, λ_0. The relevance of bifurcation theory in studying nonlinear differential equations was first understood by Krasnosel'skii [108], who was able to show that any eigenvalue of the linearization at a given state with an odd (classical) algebraic multiplicity is a nonlinear eigenvalue. By a nonlinear eigenvalue we mean a bifurcation value from the given state, regardless the nature of the nonlinear terms of the differential equation. In other words, nonlinear eigenvalues are those for which the fact that bifurcation occurs is *based on the linear part*, as discussed by Chow and Hale [35]. Some years later, Rabinowitz [175, 177] established his celebrated global alternative within the setting of the Krasnosel'skii's theorem founding Global Bifurcation Theory. According to the Rabinowitz's global alternative, the global connected component, $\mathfrak{C}$, bifurcating from the given state at an eigenvalue with an odd (classical) algebraic multiplicity must be either unbounded, or it bifurcates from the given state at, at least, two different values of λ. The relevant fact that if $\mathfrak{C}$ is bounded, then the number of bifurcation points from the given state with an odd algebraic multiplicity must be even was observed by Nirenberg [162].

However, the precise role played by the classical spectral theory in the context of the emerging bifurcation theory remained a real mystery for two decades. That was a mystery is confirmed by the astonishing circumstance that the extremely popular transversality condition of Crandall and Rabinowitz [37, 38] for bifurcation from simple eigenvalues was not known to entail a change of the Leray–Schauder degree until Theorem 5.6.2 of López-Gómez [124] could be derived through the generalized algebraic multiplicity, χ, of Esquinas and López-Gómez [66, 65, 124]. The multiplicity χ is far more general that the one introduced in [37, 38] for algebraically simple eigenvalues and it was used, e.g., by López-Gómez and Mora Corral [133], to characterize the existence of the Smith canonical form. According to [124, Ch.4], the oddity of χ characterizes whether, or not, λ_0 is a nonlinear eigenvalue of the problem, and this occurs if, and only if, the local degree changes as λ crosses λ_0. And this regardless if we are dealing with the Leray–Schauder degree, or with degree for Fredholm operators of Fitzpatrick, Pejsachowicz and Rabier [72, 73], or Benevieri and Furi [12, 13], which are almost equivalent. Therefore, by Corollary 2.5 of López-Gómez and Mora-Corral [132], the local theorem of Crandall and Rabinowitz [37] is actually global. This important feature was later *rediscovered* by Shi and Wang [187] in a much less general context.

As a rather direct application of this theory, in the first part of [139], we could construct the bifurcation diagrams of the set of solutions of the one dimensional semilinear problem

$$\begin{cases} -u'' = \lambda u + a(t)|u|^{p-1}u & \text{in } (0, L), \\ u(0) = u(L) = 0, \end{cases} \tag{1.17}$$

where $L > 0$, $\lambda \in \mathbb{R}$, $p > 0$ and $a(t) \gneq 0$ a non-negative continuous function. If $p = 1$, then problem (1.17) is linear and vertical bifurcating components arise when $\lambda \in \sigma(D^2 - a(t))$. In the so-called superlinear case when $p > 1$, the above cited references can be used in order to prove the existence of local bifurcations components from the trivial curve, while in the sublinear case $0 < p < 1$ it is applied the local theorem in bifurcation from infinity by Rabinowitz [176]. The global bifurcation results should be complemented with the existence of a priori bounds for the solutions, which adapts the methodology of Amann and López-Gómez [7]. This imply that all the components bifurcating from the values of the generalized spectrum $\sigma_n = (n\pi/L)^2$, with $n \geq 1$, are not bounded in λ, as shown in Figure 1.5.

Some more specific important information in the context of dynamical bifurcation theory and singularity theory can be found in the textbooks of Guckenheimer and Holmes [85] and Golubitsky and Shaeffer [84]. Essentially, singularity theory tries to classify canonically all the possible local structures at the bifurcation values, while dynamical bifurcation theory focuses attention in bifurcation phenomena not involving only equilibria.

These abstract developments have tremendously facilitated the mathematical analysis of a huge variety of nonlinear bvp's related to a huge variety of nonlinear differential equations and systems (see, e.g., the monographs of López-Gómez [124, 127], Cantrell and Cosner [31] and Ni [160], as well as their abundant lists of references). However, the underlying mathematical analysis is more involved when dealing with periodic conditions, instead of

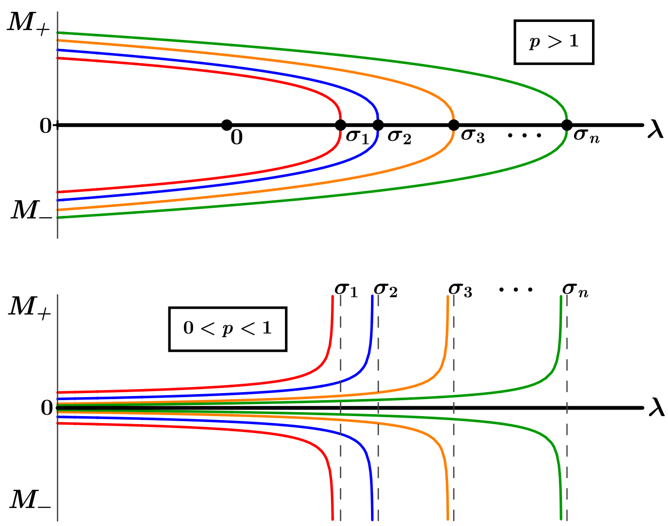

Figure 1.5: Global bifurcation diagrams of (1.17).

mixed boundary conditions, especially when searching for branches of subharmonic solutions bifurcating from a given state. Indeed, although the pioneering strategy for constructing coexistence states as bifurcating from the semitrivial solution branches in Reaction-Diffusion systems of Lotka–Volterra type was developed by Cushing [39, 40] for their classical periodic counterparts, rather astonishingly, except for certain technicalities inherent to Nonlinear PDEs, the level of difficulty in establishing the existence of the coexistence states in the diffusive prototype models inherits the same order of magnitude as getting them in their classical periodic counterparts. Not to talk about finding out infinitely many subharmonics of large order. Although some additional contributions in this direction were done by Táboas [196], the analysis of the periodic-parabolic counterparts of these classical models, extraordinarily facilitated by the pioneering results of Cushing [39, 40] for the non-spatial models, was already ready to be developed by Hess [92] and López-Gómez [120].

Nevertheless, in spite of the huge amount of literature on bifurcation for Reaction-Diffusion Systems in population dynamics, almost no reference is available about harmonic and subharmonic solutions for predator-prey systems of Volterra type, except for those already discussed in this section, beginning with [141] and [123], and continuing, after two decades, with [134], where the weight functions $\alpha(t)$ and $\beta(t)$ were assumed to have nonoverlapping supports so that the underlying Poincaré map associated with (1.7) could take a special form to allow solving the periodic problem via a one-dimensional reduction.

As already told above, the main goal of Part I is to analyze the existence, multiplicity and structure of subharmonic solutions to planar systems, including the periodic Volterra's predator-prey model (1.7). Naturally, as the underlying Poincaré maps play a crucial role in this analysis, we will benefit of a number of methods and tools among those already described in the previous paragraphs. As a consequence of our analysis, the richness of the dynamics of (1.7) will become apparent even for the simplest configurations of $\alpha(t)$ and $\beta(t)$. Some recent applications of the Poincaré–Birkhoff fixed point theorem to equations directly related to (1.7) have been given by Boscaggin [17], Ding and Zanolin [55, 56], Fonda and Toader [77], Hausrath and Manásevich [89] and Rebelo [179]. Essentially, Part I presents the research program done in [134, 137, 138, 140] trying to understand how the relative position of the supports of the weight functions $\alpha(t)$ and $\beta(t)$ might influence the dynamics of (1.7) and the global structure of the set of its subharmonics.

As a byproduct of our mathematical analysis it becomes apparent how the evolution in seasonal environments where predator-prey interaction plays a role might be random. Note that, actually, the harmonics and subharmonics of (1.7) are the non-spatial periodic harmonic and subharmonic solutions of the following reaction-diffusion periodic-parabolic problem

$$\begin{cases} \frac{\partial u}{\partial t} - d_1 \Delta u = \lambda \alpha(t) u(1-v) & \text{in } \Omega \times (0, +\infty), \\ \frac{\partial v}{\partial t} - d_2 \Delta v = \lambda \beta(t) v(-1+u) & \text{in } \Omega \times (0, +\infty), \\ \frac{\partial u}{\partial n_x} = \frac{\partial v}{\partial n_x} = 0 & \text{on } \partial\Omega \times (0, +\infty), \end{cases} \tag{1.18}$$

where Ω stands for a $\mathcal{C}^2$ bounded domain of $\mathbb{R}^N$, $N \geq 1$, n_x stands for the outward normal vector-field to Ω on its boundary, d_1 and d_2 are two positive constants, and Δ stands for the Laplace's operator in $\mathbb{R}^N$. As a consequence of our analysis, non-cooperative systems in periodic environments can provoke chaotic dynamics. This cannot occur in cooperative and quasi-cooperative dynamics, as a consequence of the ordering imposed by the maximum principle. Therefore, it is just the lack of a maximum principle for the predator-prey models the main mechanism provoking chaos in these models, though this sharper analysis will be accomplished in a forthcoming study.

As commented before, Volterra also considered the Verhulst (logistic) equation as the description of the evolution of the population of a single species. This equation was introduced by the mathematician Pierre-François

Verhulst in 1838 [201] after the famous ideas of Thomas R. Malthus in his essay on the *Principle of Population* [147] of 1798, that had been taken up again by Adolphe Quetelet in 1835 [174]. These ideas also influenced hugely Charles Darwin in his celebrated essay [51], where it can be read:

"A struggle for existence inevitably follows from the high rate at which all organic beings tend to increase. Every being, which during its natural lifetime produces several eggs or seeds, must suffer destruction during some period of its life, and during some season or occasional year, otherwise, on the principle of geometrical increase, its numbers would quickly become so inordinately great that no country could support the product. Hence, as more individuals are produced than can possibly survive, there must in every case be a struggle for existence, either one individual with another of the same species, or with the individuals of distinct species, or with the physical conditions of life. It is the doctrine of Malthus applied with manifold force to the whole animal and vegetable kingdoms; for in this case there can be no articial increase of food, and no prudential restraint from marriage. Although some species may be now increasing, more or less rapidly, in numbers, all cannot do so, for the world would not hold them."

Basically, the logistic equation substitutes the equation

$$p'(t) = mp(t)$$

for the growth of a population p, in order to reflect the obstacle of such a population to grow indefinitely. Namely, the logistic equation introduced by Verhulst reads as follows:

$$p'(t) = mp(t) - np^2(t).$$

Unfortunately, the research of Verhulst about the logistic equation was forgotten for almost 80 years until the biologists Raymond Pearl and Lowell J. Reed rediscovered it experimentally in 1920 [169]. It was, by the way, Volterra himself who called as *Verhulst–Pearl effect* the behavior of the logistic curve. This is not surprising at the light of the fruitful correspondence about Mathematical Biology crossed by Volterra and Pearl during the thirties (see [98]). It was the Russian mathematician Andrei N. Kolmogorov, one of the finest mathematicians of the XX$^{\text{th}}$ century, who took forwards the next crucial step. Very interested as well in different aspects of Mathematical Biology, Kolmogorov had already published in 1936 the paper *Sulla teoria di Volterra della lotta per l'esistenza* [106], where he had introduced the more general model

$$\begin{cases} N_1'(t) = K_1(N_1, N_2)N_1, \\ N_2'(t) = K_2(N_1, N_2)N_2, \end{cases}$$

named, after him, as Kolmogorov-type systems. It is the next year, in 1937, when, together with Ivan G. Petrovski and Nikolai S. Piskunov [107], he introduced the reaction diffusion equation

$$\frac{\partial p}{\partial t} - d\Delta p = mp - np^2,$$

to model the growth of a single species. Independently, this equation was also introduced in genetics by Ronald A. Fisher [71]. Unfortunately, the World War II delayed the development of the necessary topological tools to attack this kind of nonlinear parabolic problems. It was not until the seventies, with the influential monograph of Amann [?] and the seminal paper of Cushing [39], and the eighties with the seminal papers of Dancer [43, 44] and Blat and Brown [15, 16], when topological techniques were incorporated for analyzing the existence of coexistence states in semilinear elliptic systems, constructing global components of coexistence states as bifurcating from the semitrivial positive solutions of the system. Actually, Amann, Dancer, Blat and Brown were the first ones to introduce a systematic use of topological techniques for studying nonlinear parabolic systems. In the next paragraph, we will present the reaction-diffusion prototypes that we will study in this PhD Thesis.

Part II: Parabolic predator-prey models

According to the diffusive logistic equation introduced by Kolmogorov, Petrovski, Piskunov and Fisher the simplest parabolic predator-prey model is

$$\begin{cases} \frac{\partial u}{\partial t} - d_1\Delta u = \lambda u - au^2 - buv, \\ \frac{\partial v}{\partial t} - d_2\Delta v = \mu v - dv^2 + cuv, \end{cases}$$

where $u(x,t)$ and $v(x,t)$ are functions depending on t and on the spatial variable $x \in \Omega$, which is a bounded region of $\mathbb{R}^N$, the inhabiting territory by the species, and a, b, c, d, d_1 and d_2 are positive constants. In this model $u(x,t)$ and $v(x,t)$ measure the density of the preys and the predators, respectively, at every location x of the habitat Ω after time t. Completing this system of equations with boundary and initial conditions, we are lead to the following prototype analyzed by Blat and Brown in [15]

$$\begin{cases} \frac{\partial u}{\partial t} - d_1\Delta u = \lambda u - au^2 - buv & \text{in } \Omega \times (0,+\infty), \\ \frac{\partial v}{\partial t} - d_2\Delta v = \mu v - dv^2 + cuv & \text{in } \Omega \times (0,+\infty), \\ u = v = 0 & \text{on } \partial\Omega \times (0,+\infty), \\ u(\cdot,0) = u_0 \geq 0, \quad v(\cdot,0) = v_0 \geq 0, & \text{in } \Omega. \end{cases} \tag{1.19}$$

The dynamics of (1.19) are governed by the non-negative steady states of the problem, which satisfy the following elliptic boundary value problem

$$\begin{cases} -d_1\Delta u = \lambda u - au^2 - buv & \text{in } \ \Omega, \\ -d_2\Delta v = \mu v - dv^2 + cuv & \text{in } \ \Omega, \\ u = v = 0 & \text{on } \ \partial\Omega. \end{cases} \tag{1.20}$$

Blat and Brown [15], adapting the same methodology of Cushing for the ODE periodic system [39], used the local bifurcation theorem of Crandall and Rabinowitz [37] and the global theorem of Rabinowitz [176] to give some sufficient conditions for the existence of coexistence states of the system. By a coexistence state we mean a component-wise positive solution. Almost simultaneously, Dancer [43, 44] used the fixed point index in cones introduced by Amann [6] and elaborated by himself [42] to characterize the existence of coexistence states in terms of the spectral radius of some artificial resolvent operators associated with the system, regarding as the main continuation parameters of the model the diffusion coefficient d_2 and the interaction coefficients b and c. Some years later, López-Gómez and Pardo [142] adopted the terminology of Blat and Brown [15] and used the fixed point index to characterize the existence of coexistence states in terms of the linearized stability of the semitrivial positive solutions. Namely, they prove in [142] that (1.20) admits a coexistence state if, and only if, both semitrivial positive solutions are linearly unstable. Moreover, they constructed for the first time in the (λ, μ)-plane the optimal wedges for the existence and non-existence of coexistence states. Later, they gave in [143, 144], first in the setting of (1.20) and then in a general framework involving general elliptic operators and mixed-type boundary conditions, the unique existing global uniqueness result for diffusive predator-prey models. It establishes, under no further conditions, that the one dimensional counterpart of (1.20), had at most one coexistence state, regardless the values of λ and μ. Almost simultaneously, the importance of the role of the spatial heterogeneities in spatial ecology, was revealed by the works of Cantrell and Cosner [29, 30].

Even though (1.20) might be regarded as the most natural predator-prey model according to our previous historical discussion, the interaction between predators and preys is far from respecting the experimental data. Indeed, for a fixed population of predators, v,

$$\lim_{u\to+\infty} (buv) = +\infty,$$

meaning that predators should be capable of consuming prey at an infinitely great rate. However, as observed by the biologists Crawford S. Holling [93, 94] and James T. Tanner [199], saturation effects on the predator can appear in presence of an abundant number of preys. This is why, in the same framework of (1.19), Blat and Brown analyzed in [16] the following parabolic Holling-Tanner model

$$\begin{cases} \frac{\partial u}{\partial t} - d_1 \Delta u = \lambda u - a u^2 - b\frac{uv}{1+mu} & \text{in } \ \Omega \times (0, +\infty), \\ \frac{\partial v}{\partial t} - d_2 \Delta v = \mu v - d v^2 + c\frac{uv}{1+mu} & \text{in } \ \Omega \times (0, +\infty), \\ u = v = 0 & \text{on } \ \partial\Omega \times (0, +\infty), \\ u(\cdot, 0) = u_0 \geq 0, \ \ v(\cdot, 0) = v_0 \geq 0, & \text{in } \ \Omega, \end{cases} \tag{1.21}$$

where m is a positive constant measuring the saturation effects of the predator. Hence, in this case, for a fixed v,

$$\lim_{u \to +\infty} \left(b\frac{uv}{1+mu} \right) = b\frac{v}{m},$$

which is far more realistic. Naturally, the dynamics of the parabolic problem are given by the positive steady-states of the following elliptic boundary value problem

$$\begin{cases} -d_1 \Delta u = \lambda u - a u^2 - b\frac{uv}{1+mu} & \text{in } \ \Omega, \\ -d_2 \Delta v = \mu v - d v^2 + c\frac{uv}{1+mu} & \text{in } \ \Omega, \\ u = v = 0 & \text{on } \ \partial\Omega. \end{cases} \tag{1.22}$$

Using the same technical devices as in their previous paper [15], Blat and Brown [16] proved some necessary and sufficient conditions for the existence of coexistence states of (1.22). Few years later, Casal, Eilbeck and López-Gómez in [34] built optimal regions of coexistence in the parameter (λ, μ). In strong contrast with the behavior of the classical Lotka–Volterra model (1.20), in the Holling–Tanner model (1.22) they can arise coexistence states in a region where the semitrivial positive solution $(0, v)$ is linearly stable, while $(u, 0)$, $u > 0$, is linearly unstable. Moreover, in this case there is a limitation on the parameter μ for the existence of coexistence states, contrarily to what happens in the classical case. Further, in [34], some numerical experiments were implemented, revealing the existence of an S-shaped component of coexistence states, i.e., there is a range on the parameter λ where (1.22) admits, at least, three coexistence states. A rigorous proof of the existence of that S-shaped component was formalized, some time later, under very restrictive conditions on the several coefficients involved in the setting of the model by Du and Lou in [60, 61]. Adopting the uniqueness theorem of López-Gómez and Pardo [143], Casal et al. [34] established a uniqueness result of coexistence states of (1.22) in the one-dimensional prototype for sufficiently small m positive.

Part II deals with the following generalized heterogeneous counterpart of (1.22),

$$\begin{cases} \mathfrak{L}_1 u = \lambda u - a(x)u^2 - b(x)\frac{uv}{1+m(x)u} & \text{in } \Omega, \\ \mathfrak{L}_2 v = \mu v - d(x)v^2 + c(x)\frac{uv}{1+m(x)u} & \text{in } \Omega, \\ \mathfrak{B}_1 u = \mathfrak{B}_2 v = 0 & \text{on } \partial\Omega, \end{cases} \tag{1.23}$$

where $\mathfrak{L}_1$ and $\mathfrak{L}_2$ are arbitrary second order uniformly elliptic operators in Ω, $\mathfrak{B}_1$ and $\mathfrak{B}_2$ are general boundary operators of mixed type, in a sense to be described in Chapter 6, and $b(x)$, $d(x)$ and $m(x)$ can degenerate, i.e., they can vanish in some open subdomain of Ω, making the problem far more realistic. This model establishes an homotopy between the classical Lotka–Volterra model (1.20) and the Holling–Tanner prototype (1.22) by varying the support of the saturation term $m(x)$. Based on the techniques of Casal et al. [34], in this PhD Thesis we will analyze the existence, the nonexistence, the multiplicity and the uniqueness of coexistence states in the model (1.22).

To close this introductory chapter, we now collect in a compact way the main findings overall this PhD Thesis.

- **Part I: Periodic Volterra models**

  (i) Systematic construction of chaotic dynamics in a class of non-autonomous planar Hamiltonian systems including the periodic Volterra predator-prey model. As the chaotic dynamics are provoked by the periodicity of the coefficients of the model, we can conclude that seasonality effects cause complex dynamics and chaos in Population Dynamics.

  (ii) Constructing the global bifurcation diagram of the subharmonics solutions bifurcating from the equilibrium, in a degenerate periodic Volterra predator-prey model, which is the unique available example where such a construction has been accomplished. Actually, this might be also the structure for more general planar Hamiltonian systems.

  (iii) Analyzing the applicability of the Poincaré–Birkhoff theorem in general classes of degenerate and non-degenerate non-autonomous planar Hamiltonian systems including the periodic Volterra predator-prey model.

- **Part II: Parabolic predator-prey models**

  (i) Constructing the coexistence states regions of (1.23) by means of local and global bifurcation techniques and analyzing their dependence with respect to the saturation function coefficient $m(x)$.

  (ii) Getting uniqueness of coexistence states for the one dimensional counterpart of (1.23) for sufficiently small m positive.

  (iii) Establishing the existence of, at least, two coexistence states for sufficiently large $m(x)$ when one of the semitrivial positive solutions is linearly stable and the other is linearly unstable, regardless the size and the geometry of the support of the saturation function $m(x)$, which is a phenomenology observed by the first time in the literature.

To avoid unnecessary repetitions, throughout Part I we will assume that $\alpha, \beta : \mathbb{R} \to \mathbb{R}^+ := [0, +\infty)$ are continuous and T-periodic functions, though our results are easily extended to the Carathéodory setting with measurable coefficients in $L^1([0,T], \mathbb{R}^+)$. In particular, bounded and piecewise-continuous α, β fall within our functional setting. Thus, piecewise-constant coefficients are admissible in Chapter 4.

Some further results obtained by the candidate together with Boscaggin, Dambrosio, López-Gómez and Zanolin [21, 18, 139], not related directly with the analysis of the predator-prey models dealt with in this PhD Thesis, have been also obtained during its preparation. Regarding [18, 139], a brief discussion about has been already carried out in a number of parts of the Introduction. For a summary of the main ideas and results of [21], the reader is sent Appendix 3.4.

Part I

Periodic Volterra models

Chapter 2

The Poincaré–Birkhoff approach: non-degenerate models

This chapter studies the non-autonomous Volterra predator-prey model

$$\begin{cases} u' = \lambda\alpha(t)u(1-v) \\ v' = \lambda\beta(t)v(-1+u) \end{cases} \tag{2.1}$$

where $\lambda > 0$ and $\alpha(t) \gneq 0$, $\beta(t) \gneq 0$ are T-periodic continuous functions satisfying $\alpha(t)\beta(t) \gneq 0$. Let us notice that model (2.1) can be derived from a general Volterra model under a rather weak assumption. Indeed, a general Volterra predator-prey system with periodic coefficients takes the form

$$\begin{cases} x' = x(a(t) - b(t)y) \\ y' = y(-c(t) + d(t)x) \end{cases} \tag{2.2}$$

with $a, b, c, d : \mathbb{R} \to \mathbb{R}$ T-periodic functions and $b(t) \gneq 0$, $d(t) \gneq 0$. If we are able to find a T-periodic coexistence state $\tilde{z}(t) := (\tilde{x}(t), \tilde{y}(t))$ of (2.2), namely, a positive componentwise T-periodic solution of the system, then the change of variables

$$x(t) = u(t)\tilde{x}(t), \quad y(t) = v(t)\tilde{y}(t),$$

transforms (2.2) into the equivalent system

$$\begin{cases} u' = b(t)\tilde{y}(t)u(1-v) \\ v' = d(t)\tilde{x}(t)v(-1+u) \end{cases} \tag{2.3}$$

which is of the same form as (2.1). In the Appendix of this chapter (Section 7.3), it will be shown that (2.2) admits a coexistence state if and only if

$$\int_0^T a(t)\,dt > 0 \quad \text{and} \quad \int_0^T c(t)\,dt > 0.$$

For system (2.3) as well as for (2.1), the constant solution $(1,1)$ is considered as a trivial coexistence state and thus we are interested in finding nontrivial componentwise positive mT-periodic solutions, which, from a geometrical point of view, would be trajectories in the interior of the first quadrant winding around the equilibrium point. Sometimes, instead of studying (2.1) (or (2.3)), it may be convenient to perform a further change of variables, moving the equilibrium point to the origin. For instance, a typical transformation is given by

$$x = \log u, \quad y = \log v,$$

yielding to the equivalent Hamiltonian planar system

$$\begin{cases} x' = -\lambda\alpha(t)(e^y - 1) \\ y' = \lambda\beta(t)(e^x - 1) \end{cases} \tag{2.4}$$

and now we just look for nontrivial mT-periodic solutions of (2.4). Due to the Hamiltonian structure of the new system, a powerful tool to prove the existence of nontrivial periodic solutions is the Poincaré–Birkhoff twist fixed point theorem. Applications of this method to Volterra predator-prey systems can be found in [89], [55], [56], [179], [17], as well as in the recent ones [77] and [58]. A typical strategy of proof consists in showing that there is a sufficiently large gap in the rotation numbers between the small solutions and the large solutions of (2.4), which, in turns, guarantees a suitable twist property for the associated Poincaré map. In this context, increasing the value of the parameter $\lambda > 0$ in (2.1) may play the role of enlarging the gap in the rotation numbers. If we try to apply the above quoted results [17, 55, 56, 58, 77, 89, 179] to (2.1), we find that at least one of the two coefficients $\alpha(t), \beta(t)$ should be assumed to be always strictly positive and this prevents the applications to models where the kinetics may vanish in some time interval. On the other hand, for the special choice

$$\operatorname{supp}\alpha \subseteq [0, T/2] \quad \text{and} \quad \operatorname{supp}\beta \subseteq [T/2, T], \tag{2.5}$$

the results of Chapter 5 establish that (2.1) does not admit a nontrivial T-periodic coexistence state, independently of the value of λ, and therefore it becomes apparent that the Poincaré–Birkhoff theorem cannot be applied to

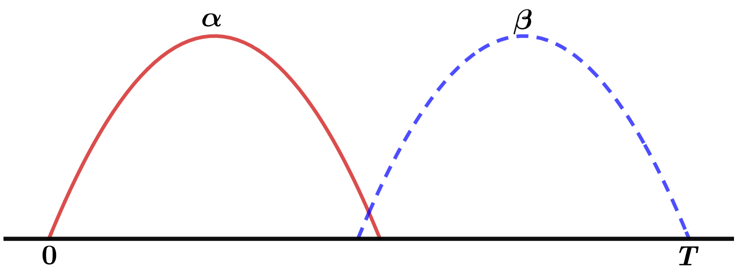

Figure 2.1: Two weights such that $\alpha\beta \gneq 0$.

(2.1) for some specific coefficients in a certain period time. Otherwise, (2.1) should admit a pair of nontrivial T-periodic solutions for sufficiently large λ.

Astonishingly, when the support of the product function $\alpha(t)\beta(t)$ is non-empty, as illustrated in Figure 2.1, then, according to our results in Section 2.1, the Poincaré–Birkhoff theorem establishes that, for every $m \geq 1$, (2.1) possesses at least two mT-periodic coexistence states for sufficiently large λ. Moreover, the number of these periodic solutions increases with λ. And this regardless the length of the support of $\alpha\beta$!

Thus, a rather natural question arises. What's going on with the (nontrivial) T-periodic coexistence states of (2.1) when $\alpha(t)\beta(t)$ does approximate zero? In Section 2.2 we analyze what happens for the configuration (2.5) of $\alpha(t)$ and $\beta(t)$ and the perturbed problem

$$\begin{cases} u' = \lambda\alpha_\varepsilon(t)u(1-v) \\ v' = \lambda\beta(t)v(-1+u) \end{cases} \tag{2.6}$$

where

$$\alpha_\varepsilon(t) := \begin{cases} \alpha(t) & t \in [0, T/2] \\ \varepsilon\varphi(t) & t \in (T/2, T] \end{cases}$$

for some function φ, as plotted in Figure 2.2.

By the results of Section 2.1, based on the Poincaré–Birkhoff theorem, for every $\varepsilon > 0$ and $m \geq 1$, there exists $\lambda_m(\varepsilon) > 0$ such that (2.6) admits at least two mT-coexistence states for each $\lambda > \lambda_m(\varepsilon)$. Our main result in Section 2.2 establishes that, setting

$$\lambda_1^*(\varepsilon) := \inf\{\lambda > 0 \ : \ (2.6) \text{ has at least one } T\text{-periodic coexistence state}\},$$

either

$$\lim_{\varepsilon \downarrow 0} \lambda_1^*(\varepsilon) = \infty,$$

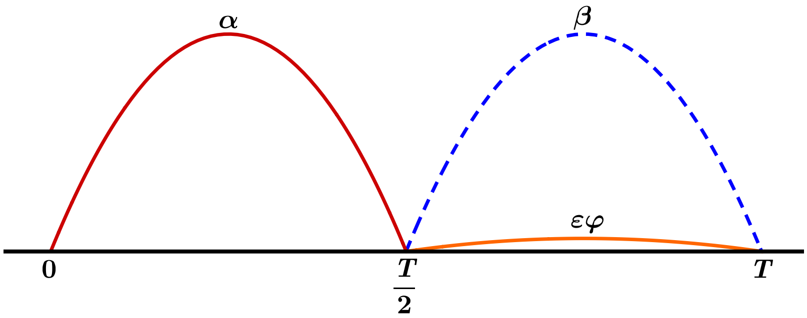

Figure 2.2: The weight functions $\alpha_\varepsilon(t)$ and $\beta(t)$.

or the v-component of any T-periodic coexistence state of problem (2.6), $(u(t,\varepsilon), v(t,\varepsilon))$, blows-up in $[T/2, T]$ as $\varepsilon \downarrow 0$, which explains why the degenerate problem for the choice (2.5) cannot admit any nontrivial T-periodic coexistence state.

2.1 An application of the Poincaré–Birkhoff theorem

In this section we consider the non-autonomous planar Hamiltonian system

$$\begin{cases} x' = -\lambda\alpha(t) f(y) \\ y' = \lambda\beta(t) g(x) \end{cases} \tag{2.7}$$

where $\lambda > 0$ and $\alpha \gneq 0$ and $\beta \gneq 0$ are T-periodic continuous functions such that

$$\alpha(t_0)\beta(t_0) > 0 \quad \text{for some } \; t_0 \in [0, T]. \tag{2.8}$$

In model (2.7), λ is regarded as a real parameter, and $f, g \in \mathcal{C}(\mathbb{R})$ are locally Lipschitz functions such that $f, g \in \mathcal{C}^1$ on a neighborhood of the origin and

$$\begin{cases} f(0) = 0, & f(y)y > 0 \;\text{ for all }\; y \neq 0, \\ g(0) = 0, & g(x)x > 0 \;\text{ for all }\; x \neq 0, \\ f'(0) > 0, & g'(0) > 0. \end{cases} \tag{2.9}$$

Moreover, either f, or g, satisfies, at least, one of the following conditions:

$$\begin{array}{llll} (f_-) & f \;\text{ is bounded in }\; \mathbb{R}^-, & (f_+) & f \;\text{ is bounded in }\; \mathbb{R}^+, \\ (g_-) & g \;\text{ is bounded in }\; \mathbb{R}^-, & (g_+) & g \;\text{ is bounded in }\; \mathbb{R}^+. \end{array} \tag{2.10}$$

Under these conditions, $(x, y) = (0, 0)$ provides us with a steady-state solution of (2.7). Throughout this chapter, we will denote by D_R the disc of radius R centered at the origin, $(x, y) = (0, 0)$. Although the next result is a direct consequence of the Lipschitz dependence of the solutions of (2.7) with respect to the initial conditions, we will provide with a short self-contained proof of it.

Proposition 2.1.1. *For every integer $m \geq 1$ and $\lambda, \varepsilon > 0$, there exists $\delta = \delta(m, \varepsilon, \lambda) > 0$ such that if $(x_0, y_0) \in D_\delta$, then the unique solution of (2.7), $(x(t), y(t))$, with $(x(0), y(0)) = (x_0, y_0)$, satisfies $(x(t), y(t)) \in D_\varepsilon$ for all $t \in [0, mT]$.*

Since $\delta(m, \varepsilon, \lambda) \downarrow 0$ as $m \uparrow \infty$ cannot be excluded, $(0, 0)$ is not necessarily stable in the sense of Lyapunov towards the right.

Proof. Let us fix $K > \max\{f'(0), g'(0)\}$ and take $\delta_1 > 0$ such that

$$\frac{g(x)}{x} < K \text{ if } 0 < |x| < \delta_1, \text{ and } \frac{f(y)}{y} < K \text{ if } 0 < |y| < \delta_1.$$

Without loss of generality, we suppose that $(x(0), y(0)) \neq (0, 0)$ and hence $(x(t), y(t))$ is a nontrivial solution. Introducing polar coordinates, we have that

$$\rho^2(t) = x^2(t) + y^2(t), \qquad t \geq 0.$$

Thus, differentiating with respect to t, it follows from (2.7) that

$$\rho(t)\rho'(t) = x(t)x'(t) + y(t)y'(t) = -\lambda\alpha(t)x(t)f(y(t)) + \lambda\beta(t)y(t)g(x(t))$$

for all $t \geq 0$ for which the solution is defined, say $t \in I := [0, T_{\max})$. Hence,

$$|\rho(t)\rho'(t)| = \lambda \left| x(t)y(t) \left[\beta(t)\frac{g(x(t))}{x(t)} - \alpha(t)\frac{f(y(t))}{y(t)} \right] \right|.$$

Then, considering the T-periodic function

$$\gamma(t) := K[\beta(t) + \alpha(t)], \qquad t \in \mathbb{R},$$

it is apparent that, for every $t \in I$ such that $(x(s), y(s)) \in D_{\delta_1}$ for all $s \in [0, t]$, the following holds:

$$|\rho(s)\rho'(s)| \leq \lambda|x(s)y(s)||\gamma(s)| \leq \frac{\lambda}{2}(x^2(s) + y^2(s))|\gamma(s)| = \frac{\lambda}{2}\rho^2(s)|\gamma(s)|$$

for all $s \in [0, t]$. This, in turn, implies

$$|\rho'(s)| \leq \frac{\lambda}{2}\rho(s)|\gamma(s)|, \quad \forall\, s \in [0, t].$$

Therefore, as long as $(x(s), y(s)) \in D_{\delta_1}$ for all $s \in [0, t]$ with $t \in I$, we find that

$$\rho(s) \leq e^{\frac{\lambda}{2}\int_0^s |\gamma(\xi)|\, d\xi}\rho(0).$$

Lastly, set

$$E := e^{\frac{\lambda}{2}\int_0^T |\gamma(\xi)|\, d\xi} = e^{\frac{\lambda}{2}\int_{kT}^{(k+1)T} |\gamma(\xi)|\, d\xi}, \qquad k \geq 1,$$

and choose $\rho_0 := \rho(0)$ such that

$$\rho_0 < E^{-m} \min\{\varepsilon, \delta_1\} =: \delta(m, \varepsilon, \lambda).$$

Then,

$$\rho(t) < \min\{\varepsilon, \delta_1\} \leq \varepsilon$$

for all $t \in [0, mT]$, which ends the proof. $\square$

Remark 2.1.2. We observe that condition (2.9), together with $\alpha, \beta \gneq 0$, imply that if $(x(t), y(t))$ is a solution of (2.7) which is not globally defined in the future, then for its maximal interval of existence $[0, T_{\max})$, it happens that $x^2(t) + y^2(t) \to +\infty$ as $t \to T_{\max}^-$ and both $x(t)$ and $y(t)$ have infinitely many zeros accumulating at $T_{\max}$. Indeed, assume, for instance that $x(t) > 0$ and $y(t) > 0$ for all $t \in [t_0, T_{\max})$, for some $t_0 < T_{\max}$. Then, from the first equation in (2.7) we have that $x(t)$ is non-increasing and therefore $0 < x(t) \leq x(t_0)$. Hence $x(t)$ is bounded and then from the second equation in (2.7) y' is bounded and hence $y(t)$ is bounded as well. Since we have find that both $x(t)$ and $y(t)$ are bounded on $[t_0, T_{\max})$, this gives a contradiction. From the above argument, we can infer that any solution entering the first quadrant must leave it and enter the second one. With a similar proof we can see that it is impossible for a blow-up solution to stay in the second quadrant and hence, it must enter the third one after some time. Repeating this process it becomes apparent that any blowing-up solution of (2.7) must perform infinitely many turns around the origin as $t \to T_{\max}^-$.

As we will see in the second part of the proof of Theorem 2.1.5, such a situation about solutions presenting blow-up with infinitely many rotations is not possible by condition (2.10). Therefore, all the solutions of (2.7) are globally defined in the future (and also in the past).

Our main existence result in this section, that is Theorem 2.1.5, is a direct consequence of the Poincaré–Birkhoff theorem as presented in [41], [76] and [179] (see also [22, Remark 1] for a short discussion about this topic). It establishes the existence of, at least, two mT-periodic solutions of (2.7) for every $m \geq 1$ provided λ is sufficiently large.

To be more specific, to any nontrivial solution $(x(t), y(t))$ of (2.7) with $(x(0), y(0)) = z_0 \neq (0,0)$ we associate an angular polar coordinate $\theta(t)$ and, for a given interval $[0, mT]$, we define a rotation number

$$\mathrm{rot}(z_0; [0, mT]) := \frac{\theta(mT) - \theta(0)}{2\pi}. \tag{2.11}$$

The rotation number is an algebraic counter of the counterclockwise turns of the solution $(x(t), y(t))$ around the origin during the time-interval $[0, mT]$. The version of the Poincaré–Birkhoff fixed point theorem that we use in this section is the following one.

Theorem 2.1.3. *Assume there are $0 < r_0 < R_0$ and a positive integer k such that the twist condition*

$$\mathrm{rot}(z_0; [0, mT]) > k \ \ \textit{if} \ \ ||z_0|| = r_0 \quad \textit{and} \quad \mathrm{rot}(z_0; [0, mT]) < k \ \ \textit{if} \ \ ||z_0|| = R_0$$

holds. Then, system (2.7) has at least 2 nontrivial mT-periodic solutions belonging to different periodicity classes and having k as a rotation number.

This is essentially an application of W.Y. Ding version of the twist theorem for planar annuli (see [57]), as presented also in [148, Theorem A] (see also [22] for an application of the same version of the theorem). As observed in [56, §3] once that for some $m \geq 2$ we have a mT-periodic solution (x, y), then, for each $j = 1, 2, \ldots, m-1$, also (x_j, y_j) is a mT-periodic solution of the same system, for

$$x_j(t) := x(t + jT), \quad y_j(t) := y(t + jT).$$

We consider all these solutions as equivalent and we say they belong to the same periodicity class.

Remark 2.1.4. The information about the rotation number provided by Theorem 2.1.3 is crucial for different reasons. First we notice that solutions with different associated rotation numbers are essentially different since as paths in $\mathbb{R}^2 \setminus \{(0,0)\}$ are not homotopically equivalent. Moreover, the number k is useful in order to prove the minimality of the period of the solutions. More precisely, if k is relatively prime with m, then, as consequence, the mT-periodic solutions $(x(t), y(t))$ that we find cannot be ℓT-periodic for some integer $\ell < m$. Indeed, if, by contradiction, we suppose that $(x(t), y(t))$ is ℓT-periodic for some $\ell = 1, \ldots, m-1$, then the rotation number associated to the solution in the interval $[0, \ell T]$ must be an integer, say k_1. Then, by the obvious additivity property of the rotation numbers, we obtain, for $z_0 = (x(0), y(0))$,

$$\mathrm{rot}(z_0; [0, m\ell T]) = \ell k = k_1 m$$

which contradicts the fact that $\gcd(k, m) = 1$. This also shows that, in particular, for $k = 1$ we have a periodic solution of minimal period mT.

Theorem 2.1.5. *For every integers $k \geq 1$ and $m \geq 1$, there exists a constant $\lambda_m^k > 0$ such that (2.7) admits, at least, two mT-periodic solutions of rotation number k, for each $\lambda > \lambda_m^k$.*

Proof. In order to apply the version of the Poincaré–Birkhoff theorem given in Theorem 2.1.3 we should show that, near the origin, the solutions have a *rotation number* greater than k, while, far from the origin, the solutions cannot complete one turn.

First, we will focus our attention on small solutions. By (2.9), there exists a constant $\eta > 0$ such that

$$\min\{f'(0), g'(0)\} > \eta.$$

By the limit definition, we claim that, for sufficiently small $\zeta \sim 0$, say for $|\zeta| \leq \varepsilon$,

$$f(\zeta)\zeta \geq \eta\zeta^2, \qquad g(\zeta)\zeta \geq \eta\zeta^2. \tag{2.12}$$

Let $m \geq 1$ be an integer that we fix from now to the end of the proof. Given ε as above, for any $\lambda > 0$ we can apply Proposition 2.1.1 and find a constant $\delta_\lambda = \delta(m, \varepsilon, \lambda) > 0$ such that if $(x(t), y(t))$ is any solution of (2.7) with initial point in D_{δ_λ}, then $(x(t), y(t)) \in D_\varepsilon$ for all $t \in [0, mT]$. For these solutions with initial value in $D_{\delta_\lambda} \setminus \{(0, 0)\}$ we introduce the angular polar coordinate $\theta(t)$. Since, locally and up to an additive constant,

$$\theta(t) = \arctan \frac{y(t)}{x(t)}, \quad \text{or} \quad \theta(t) = -\arctan \frac{x(t)}{y(t)},$$

differentiating with respect to time and using (2.7) yields

$$\theta'(t) = \frac{y'(t)x(t) - x'(t)y(t)}{x^2(t) + y^2(t)} = \frac{\lambda\beta(t)g(x(t))x(t) + \lambda\alpha(t)f(y(t))y(t)}{x^2(t) + y^2(t)}$$

for all $t \in [0, mT]$. Hence, owing to (2.12), it is apparent that

$$\theta'(t) \geq \frac{\lambda\eta[\beta(t)x^2(t) + \alpha(t)y^2(t)]}{x^2(t) + y^2(t)} \geq 0, \qquad t \in [0, mT]. \tag{2.13}$$

On the other hand, by the continuity of α, β in t_0, it follows from (2.8) that there exist $\omega > 0$ and $\tau > 0$ such that

$$\min\{\beta(t), \alpha(t)\} \geq \omega > 0 \quad \text{for all} \;\; t \in J := [t_0 - \tau, t_0 + \tau].$$

Thus, for every $t \in J + iT$, with $i = 0, 1, \ldots, m-1$, (2.13) implies that $\theta'(t) \geq \lambda\eta\omega$. Hence, we have that

$$\theta(mT) - \theta(0) = \int_0^{mT} \theta'(s)\,ds \geq m \int_{t_0-\tau}^{t_0+\tau} \theta'(s)\,ds \geq m\lambda\eta\omega 2\tau =: m\lambda\nu.$$

Therefore,

$$\theta(mT) - \theta(0) \geq m\lambda\nu > 2\pi k \quad \text{if } \lambda > \frac{2\pi k}{m\nu} =: \lambda_m^k. \tag{2.14}$$

At this point, we take an arbitrary (but fixed) $\lambda > \lambda_m^k$. Then there exists $r_0 > 0$ with $r_0 < \delta(m, \varepsilon, \lambda)$ such that, for every $z_0 = (x(0), y(0))$ with $||z_0|| = r_0$, one has that

$$(x(t), y(t)) \in D_\varepsilon \quad \text{for all } t \in [0, mT]$$

and hence,

$$\operatorname{rot}(z_0; [0, mT]) > k. \tag{2.15}$$

Now, besides the integers m and k, also the constant $\lambda > 0$ is fixed and we proceed by showing that the rotation number for large solutions is less than one.

In order to prove that the solutions of (2.7) with sufficiently large initial data, (x_0, y_0), cannot complete a rotation in the interval $[0, mT]$, we argue as follows. Suppose that (2.10) holds with g satisfying (g_-). We shall consider only this situation as the other ones are completely symmetric.

Clearly, a solution making at least one turn around the origin must cross completely the second or the third quadrant. Indeed, if the initial point z_0 is in the first or in the fourth quadrant and $\operatorname{rot}(z_0; [0, mT]) \geq 1$, then $(x(t), y(t))$ must cross completely both the second and the third quadrants; if z_0 is in the second (respectively third) quadrant, then the trajectory must cross completely the third (respectively the second) one. We shall show that these cases are prevented for large solutions, by finding some general bounds for a generic solution $(x(t), y(t))$ on the third or the second quadrant.

As a first case, we suppose that $(x(t), y(t))$ is a nontrivial solution which crosses entirely the third quadrant. Then, there exists an interval $[t_1, t_2] \subset [0, mT]$ such that $y(t_1) = 0 = x(t_2)$ and $x(t) < 0$, $y(t) < 0$ for all $t \in (t_1, t_2)$. Recalling also the sign condition for $g(x)$ given in (2.10), there exists a constant, $M > 0$, such that

$$\sup_{x \leq 0} |g(x)| \leq M.$$

Then it is clear that, for every $t \in [t_1, t_2]$, we have that

$$|y(t)| = |\lambda \int_{t_1}^{t} \beta(s) g(x(s)) ds| \leq \lambda M \int_{t_1}^{t_2} \beta \leq \lambda M \int_0^{mT} \beta = \lambda M m \int_0^T \beta.$$

Thus, setting

$$N := \max \left\{ |f(y)| \ : \ |y| \leq \lambda M m \int_0^T \beta \right\},$$

we also find that

$$|x(t)| = |\lambda \int_{t}^{t_2} \alpha(s) f(y(s)) ds| \leq \lambda N \int_0^{mT} \alpha = \lambda N m \int_0^T \alpha.$$

Hence, denoting

$$A := \int_0^T \alpha > 0, \qquad B := \int_0^T \beta > 0, \tag{2.16}$$

and

$$R^2 := \lambda^2 m^2 (M^2 B^2 + N^2 A^2),$$

we conclude that if $(x(t), y(t))$ is any solution of (2.7) such that $x^2(\hat{t}) + y^2(\hat{t}) > R^2$ for some $\hat{t} \in [0, mT]$, with $(x(\hat{t}), y(\hat{t}))$ in the third quadrant, then such a solution cannot cross entirely the third quadrant during a time interval containing $\hat{t}$. Analogous estimates allow to find exactly the same constants such that the same non-crossing property holds with respect to the second quadrant where $x \leq 0$ as well.

To complete our analysis, we now look at what happens in the other quadrants.

So, let s_0 be such that $x(s_0) = 0$ and $0 < y(s_0) \leq R$. Let also $[s_1, s_0] \subseteq [0, s_0]$ be a maximal interval such that $x(t) \geq 0$ and $y(t) \geq 0$ for all $t \in [s_1, s_0]$. From (2.7) we know that x is non-increasing and y is non-decreasing on $[s_1, s_0]$. Therefore, $0 \leq y(t) \leq R$ for all $t \in [s_1, s_0]$. Hence

$$|f(y(t))| \leq N_1 := \max\{f(y) : 0 \leq y \leq R\}$$

for all t in the same interval. Integrating the first equation on $[t, s_0] \subseteq [s_1, s_0]$ yields to an upper bound for $x(t)$, namely $|x(t)| \leq \lambda N_1 m A$. Now, taking R_1 as

$$R_1^2 := \lambda^2 m^2 (M^2 B^2 + N^2 A^2 + N_1^2 A^2),$$

we conclude that if $(x(t), y(t))$ is any solution of (2.7) such that $x^2(\hat{t}) + y^2(\hat{t}) > R_1^2$ for some $\hat{t} \in [0, mT]$, with $(x(\hat{t}), y(\hat{t}))$ in the first quadrant, then such a solution cannot cross entirely the second or the third quadrant.

As a final case, let us suppose now there exists s_2 such that $y(s_2) = 0$ and $0 < x(s_2) \leq R_1$. Let also $[s_3, s_2] \subseteq [0, s_2]$ be a maximal interval such that $x(t) \geq 0$ and $y(t) \leq 0$ for all $t \in [s_3, s_2]$. Arguing as above (and using the fact that now both x and y are non-decreasing on $[s_3, s_2]$), we define

$$M_1 := \max\{g(x) : 0 \leq x \leq R_1\}.$$

In this manner, $|g(x(t))| \leq M_1$ for all $t \in [s_3, s_2]$ and thus we obtain a constant

$$R_2^2 := \lambda^2 m^2 (M^2 B^2 + N^2 A^2 + N_1^2 A^2 + M_1^2 B^2)$$

such that if $(x(t), y(t))$ is any solution of (2.7) with $x^2(\hat{t}) + y^2(\hat{t}) > R_2^2$ for some $\hat{t} \in [0, mT]$, with $(x(\hat{t}), y(\hat{t}))$ in the fourth quadrant, then such a solution cannot cross entirely the second or the third quadrant.

Therefore, the solutions of (2.7) with $x_0^2 + y_0^2 = R_0^2 > R_2^2$, satisfy

$$\operatorname{rot}(z_0; [0, mT]) < 1. \tag{2.17}$$

Notice that the above proof also ensures that all the solutions are globally defined, as anticipated in Remark 2.1.2.

By (2.15) and (2.17) the twist condition holds and hence, according to Theorem 2.1.3, the system (2.7) has, at least, two mT-periodic solutions with rotation number k, for each $\lambda > \lambda_m^k$. This ends the proof. □

Remark 2.1.6. Theorem 2.1.5 when applied for $m = 1$, guarantees the existence of $2k$ geometrically distinct T-periodic solutions when $\lambda > \lambda_1^k$. Indeed it provides at least two (nontrivial) T-periodic solutions with rotation number j for each integer $j = 1, 2, \ldots, k$. In view of the analysis performed in [123], [134], the condition (2.8) is optimal (see the next section for a detailed discussion). System (2.7) can be obtained from a Volterra predator-prey equation via a change of variables. In this case $g(x) = e^x - 1$ and $f(y) = e^y - 1$ and therefore both (f_-) and (g_-) are satisfied. This simplifies the second part of the above proof.

We stress that Theorem 2.1.5 considers a situation which is not covered in the previous works dealing with periodic solutions of non-autonomous Volterra equations [89], [56], [179], [77]. For instance, we do not assume monotonicity of $\alpha(t)f(\cdot)$ or $\beta(t)g(\cdot)$ *for all* t; indeed such functions can identically vanish on some time intervals.

Remark 2.1.7. As a final observation, we should mention the fact, without any significant change in the proof, a slightly more general version of Theorem 2.1.5 could be proved, by assuming f, g only continuous (and not locally

Lipschitz) and replacing the condition on the derivatives in (2.9) with the following one

$$0 < \liminf_{|y|\to 0} \frac{f(y)}{y} \leq \limsup_{|y|\to 0} \frac{f(y)}{y} < \infty, \quad 0 < \liminf_{|x|\to 0} \frac{g(x)}{x} \leq \limsup_{|x|\to 0} \frac{g(x)}{x} < \infty.$$

To this aim, instead of Theorem 2.1.3, one can apply a generalized version of the Poincaré–Birkhoff theorem due to Fonda and Ureña [78] for Hamiltonian systems where the uniqueness of the solutions of the initial value problems is not required (see also [74, Theorem 10.6.1] for the precise statement). Since in our application to the Volterra system, f and g are smooth functions, we preferred to state our theorem in this case, instead of considering the most general situation.

2.2 Limiting behaviour of the T-periodic solutions

In this section we analyze the perturbed model

$$\begin{cases} u' = \lambda\alpha_\varepsilon(t)u(1-v) \\ v' = \lambda\beta(t)v(-1+u), \end{cases} \tag{2.18}$$

where $\lambda > 0$ and $\alpha(t)$, $\beta(t)$ satisfy (2.5), and, for sufficiently small $\varepsilon > 0$,

$$\alpha_\varepsilon(t) := \alpha(t) + \varepsilon\varphi(t), \qquad t \in \mathbb{R},$$

where φ is a T-periodic function such that

$$\varphi(t) < 1 \ \text{ for each } \ t \in \operatorname{supp}\varphi = [\tfrac{T}{2}, T]. \tag{2.19}$$

By technical reasons, β and φ are assumed to be differentiable functions in $[\frac{T}{2}, T]$ such that

$$\beta(t) > 0, \quad \varphi(t) > 0, \qquad \text{for all } \ t \in (\tfrac{T}{2}, T)$$

and

$$\beta'(\tfrac{T}{2}) > 0, \quad \beta'(T) < 0, \quad \varphi'(\tfrac{T}{2}) > 0, \quad \varphi'(T) < 0. \tag{2.20}$$

Under these assumptions, (2.18) fits within the abstract setting of Section 2.1 by performing the change of variables

$$x = \log u, \quad y = \log v.$$

Indeed, under this transformation, (2.18) becomes into

$$\begin{cases} x' = -\lambda\alpha_\varepsilon(t)(e^y - 1) \\ y' = \lambda\beta(t)(e^x - 1) \end{cases} \tag{2.21}$$

and, since

$$\alpha_\varepsilon(t)\beta(t) > 0 \quad \text{for all} \;\; t \in (\tfrac{T}{2}, T),$$

the problem (2.21) fits into the setting of Section 2.1 for the special choices

$$f(y) = e^y - 1, \quad g(x) = e^x - 1.$$

Therefore, by Theorem 2.1.5, for every $\varepsilon > 0$, there exists $\lambda_1 = \lambda_1(\varepsilon) > 0$ (see (2.14) for the definition of λ_1^1, with $m = 1$ and $k = 1$) such that (2.21) possesses, at least, two T-periodic solutions for each $\lambda > \lambda_1$. However, by (2.5), at the particular value of the parameter $\varepsilon = 0$, (2.21) does not admit a nontrivial T-periodic solution (see (5.13) for a explicit formula). Thus, a natural question is to ascertain what's going on with the T-periodic solutions of (2.18) as $\varepsilon \downarrow 0$. This analysis should explain why the T-periodic solutions of (2.18) do disappear as $\varepsilon \downarrow 0$. Subsequently, for any given $\varepsilon > 0$, we will denote by $(u(t,\varepsilon), v(t,\varepsilon))$ any T-periodic solution of (2.18). Naturally, in such case, we set

$$u_0(\varepsilon) := u(0,\varepsilon), \quad v_0(\varepsilon) := v(0,\varepsilon).$$

To state the main result of this section we need to introduce the next auxiliary constant

$$\lambda_1^*(\varepsilon) := \inf\{\lambda > 0 \;:\; (2.21) \;\text{ has at least one nontrivial } T\text{-periodic solution}\}$$

Notice that $\lambda_1^*(\varepsilon)$ is also the infimum of the positive λ's such that (2.18) has, at least, one nontrivial T-periodic coexistence state. By definition,

$$\lambda_1^*(\varepsilon) \le \lambda_1(\varepsilon), \quad \text{for every} \quad \varepsilon > 0.$$

Then, the main result of this section can be stated as follows.

Theorem 2.2.1. *One of the following two excluding options holds:*

(a) *Either $\lambda_1^*(\varepsilon) \uparrow \infty$ as $\varepsilon \downarrow 0$, or*

(b) *there exist $\varepsilon_0 > 0$ and a fixed $\lambda > 0$, such that, for every $0 < \varepsilon < \varepsilon_0$, (2.18) admits, at least, one (nontrivial) T-periodic coexistence state. Moreover, in such case, any nontrivial T-periodic coexistence state of (2.18) blows up in $(T/2, T)$ as $\varepsilon \downarrow 0$.*

The proof of this theorem will follow after a series of lemmas of technical nature. Suppose $t \in [0, T/2]$. Then, as $\beta = 0$ in $[0, T/2]$, $v' = 0$ and hence

$$\begin{cases} v(t,\varepsilon) = v_0(\varepsilon), \\ u(t,\varepsilon) = u_0(\varepsilon)e^{\lambda(1-v_0(\varepsilon))\int_0^t \alpha(s)ds}. \end{cases} \tag{2.22}$$

Consequently, for every $t \in [T/2, T]$, we have that

$$\begin{cases} u(t,\varepsilon) & = u(\frac{T}{2})e^{\lambda\varepsilon\int_{T/2}^t \varphi(s)(1-v(s,\varepsilon))ds} \\ & = u_0(\varepsilon)e^{\lambda A(1-v_0(\varepsilon))+\lambda\varepsilon\int_{T/2}^t \varphi(s)(1-v(s,\varepsilon))ds}, \\ v(t,\varepsilon) & = v(\frac{T}{2})e^{\lambda\int_{T/2}^t \beta(s)(-1+u(s,\varepsilon))ds} = v_0(\varepsilon)e^{\lambda\int_{T/2}^t \beta(s)(-1+u(s,\varepsilon))ds}. \end{cases} \tag{2.23}$$

A solution of (2.18) is a T-periodic coexistence state if $u_0, v_0 > 0$ and

$$\mathcal{P}_1(u_0, v_0) = (u_0, v_0)$$

where $\mathcal{P}_1$ is the Poincaré map at time T, i.e., by (2.23), if

$$\begin{cases} A(1 - v_0(\varepsilon)) + \varepsilon\int_{T/2}^T \varphi(s)(1 - v(s,\varepsilon))ds = 0, \\ \int_{T/2}^T \beta(s)(-1 + u(s,\varepsilon))ds = 0, \end{cases} \tag{2.24}$$

which is equivalent to

$$\int_0^T \alpha_\varepsilon(s)(1 - v(s,\varepsilon))ds = 0, \quad \int_0^T \beta(s)(-1 + u(s,\varepsilon))ds = 0.$$

In particular, by the positivity of α_ε and β, the components of any (nontrivial) T-periodic solution of (2.18) cross the constant curve 1. The next result provides us with some sharper properties of these crossings.

Lemma 2.2.2. *Let $\varepsilon > 0$ be such that (2.18) has a (nontrivial) T-periodic coexistence state,*

$$(u(t), v(t)) \equiv (u(t,\varepsilon), v(t,\varepsilon)).$$

Then, the next properties hold in the interval $(T/2, T)$:

(a) *The zeroes of $1 - v$ and $1 - u$ are simple.*

(b) *There exists a bijection between the critical points of v (resp. u) and the zeroes of $1 - u$ (resp. $1 - v$).*

(c) *None of the functions $1 - v$ and $1 - u$ can admit a critical point which is also an inflection point.*

(d) *Between each two consecutive zeros of* $1-v$ *(resp.* $1-u$*) there is an odd number of critical points of* v *(resp.* u*).*

(e) *The curvature of* v *at* $\frac{T}{2}$ *is given through*

$$v''(\tfrac{T}{2},\varepsilon) = \lambda\beta'(\tfrac{T}{2})v_0(\varepsilon)\left[-1+u(\tfrac{T}{2},\varepsilon)\right].$$

Proof. By the assumptions, $(u,v)\neq(1,1)$. Suppose that $v(t_0)=1$ for some $t_0\in(T/2,T)$. Then, by the uniqueness of the solutions for the Cauchy problem associated to (2.18), we have that $u(t_0)\neq 1$ and hence,

$$v'(t_0) = \lambda\beta(t_0)v(t_0)(-1+u(t_0))\neq 0.$$

Similarly, if $u(t_0)=1$, then

$$u'(t_0) = \lambda\varepsilon\varphi(t_0)u(t_0)(1-v(t_0))\neq 0.$$

This ends the proof of Part (a).

To prove Part (b), suppose that $v'(t_0)=0$ for some $t_0\in(T/2,T)$. Then,

$$0 = v'(t_0) = \lambda\beta(t_0)v(t_0)(-1+u(t_0))$$

and hence, $u(t_0)=1$. Similarly, if $u'(t_0)=0$, then

$$0 = u'(t_0) = \lambda\varepsilon\varphi(t_0)u(t_0)(1-v(t_0)).$$

So, $v(t_0)=1$, which ends the proof of Part (b).

To prove Part (c), suppose that $v'(t_0)=0$ for some $t_0\in(T/2,T)$. Then, by Part (b), $u(t_0)=1$. Thus, by Part (a), $u'(t_0)\neq 0$. Hence, differentiating the v-equation of (2.18) yields

$$\begin{aligned} v''(t_0) &= \lambda\beta'(t_0)v(t_0)(-1+u(t_0)) + \lambda\beta(t_0)[v'(t_0)(-1+u(t_0)) + v(t_0)u'(t_0)] \\ &= \lambda\beta(t_0)v(t_0)u'(t_0)\neq 0. \end{aligned}$$

Similarly, $u'(t_0)=0$ implies that

$$\begin{aligned} u''(t_0) &= \lambda\varepsilon\varphi'(t_0)u(t_0)(1-v(t_0)) + \lambda\varepsilon\varphi(t_0)[u'(t_0)(1-v(t_0)) - u(t_0)v'(t_0)] \\ &= -\lambda\varepsilon\varphi(t_0)u(t_0)v'(t_0)\neq 0. \end{aligned}$$

Therefore, any critical point of v, or u, is a quadratic maximum, or minimum, which ends the proof of Part (c). Part (d) is a byproduct of this property.

Finally, since $\beta\equiv 0$ on the interval $[0,T/2]$, by (2.22) it becomes apparent that

$$\begin{aligned} v''(\tfrac{T}{2}) &= \lambda\beta'(\tfrac{T}{2})v(\tfrac{T}{2})(-1+u(\tfrac{T}{2})) + \lambda\beta(\tfrac{T}{2})[v'(\tfrac{T}{2})(-1+u(\tfrac{T}{2})) + v(\tfrac{T}{2})u'(\tfrac{T}{2})] \\ &= \lambda\beta'(\tfrac{T}{2})v(\tfrac{T}{2})(-1+u(\tfrac{T}{2})) = \lambda\beta'(\tfrac{T}{2})v_0(-1+u(\tfrac{T}{2})), \end{aligned}$$

which shows Part (e) and ends the proof of the lemma. □

The next result provides us with the non-degeneration of the T-periodic solutions with respect to the equilibrium $(1,1)$.

Lemma 2.2.3. *There exist $\eta > 0$ and $\varepsilon_0 > 0$ such that, for every nontrivial T-periodic family of solutions, $(u(t,\varepsilon), v(t,\varepsilon))$, $0 < \varepsilon < \varepsilon_0$, the following estimate holds*

$$\inf_{t\in[0,T]} \{|u(t,\varepsilon) - 1| + |v(t,\varepsilon) - 1|\} > \eta.$$

Proof. Throughout this proof, we will use the fact that the fixed points of the Poincaré map $\mathcal{P}_1$ are the zeroes of the function

$$\begin{aligned}
&\Phi(u_0, v_0, \varepsilon) = (f_1, f_2) := \mathcal{P}_1(u_0, v_0, \varepsilon) - (u_0, v_0)\\
&= (u_0 e^{\lambda A(1-v_0)+\lambda\varepsilon \int_{T/2}^T \varphi(s)(1-v(s,\varepsilon))ds} - u_0, v_0 e^{\lambda \int_{T/2}^T \beta(s)(-1+u(s,\varepsilon))ds} - v_0),
\end{aligned}$$

where

$$(u_0, v_0) := (u(0,\varepsilon), v(0,\varepsilon)), \qquad \varepsilon \in (0, \varepsilon_0).$$

We claim that the matrix $D_{(u_0,v_0)}\Phi(1,1,0)$ is invertible. Indeed, by differentiating with respect to u_0 and v_0 yields

$$\begin{aligned}
\frac{\partial f_1}{\partial u_0} &= e^{\lambda A(1-v_0)+\lambda\varepsilon \int_{T/2}^T \varphi(s)(1-v(s,\varepsilon))ds}\\
&\quad + u_0 \lambda\varepsilon \frac{\partial}{\partial u_0}\left(\int_{T/2}^T \varphi(s)(1-v(s,\varepsilon))ds\right) e^{\lambda A(1-v_0)+\lambda\varepsilon \int_{T/2}^T \varphi(s)(1-v(s,\varepsilon))ds} - 1,
\end{aligned}$$

$$\begin{aligned}
\frac{\partial f_1}{\partial v_0} &= u_0 \frac{\partial}{\partial v_0}\Bigg(\lambda A(1-v_0)\\
&\quad + \lambda\varepsilon \int_{T/2}^T \varphi(s)(1-v(s,\varepsilon))ds\Bigg) e^{\lambda A(1-v_0)+\lambda\varepsilon \int_{T/2}^T \varphi(s)(1-v(s,\varepsilon))ds}\\
&= u_0\left(-\lambda A + \lambda\varepsilon \frac{\partial}{\partial v_0}\int_{T/2}^T \varphi(s)(1-v(s,\varepsilon))ds\right) e^{\lambda A(1-v_0)+\lambda\varepsilon \int_{T/2}^T \varphi(s)(1-v(s,\varepsilon))ds},
\end{aligned}$$

$$\begin{aligned}
\frac{\partial f_2}{\partial u_0} &= v_0 \lambda \frac{\partial}{\partial u_0}\left(\int_{T/2}^T \beta(s)(-1+u(s,\varepsilon))ds\right) e^{\lambda \int_{T/2}^T \beta(s)(-1+u(s,\varepsilon))ds}\\
&= v_0\lambda \left[\int_{T/2}^T \beta(s) \frac{\partial}{\partial u_0}\left(f_1(u_0,v_0,\varepsilon) + u_0\right) ds\right] e^{\lambda \int_{T/2}^T \beta(s)(-1+u(s,\varepsilon))ds}\\
&= v_0\lambda \left[\int_{T/2}^T \beta(s)\left(\frac{\partial f_1}{\partial u_0}(u_0,v_0,\varepsilon) + 1\right) ds\right] e^{\lambda \int_{T/2}^T \beta(s)(-1+u_0+f_1(u_0,v_0,\varepsilon))ds}.
\end{aligned}$$

Thus, since

$$\frac{\partial f_1}{\partial u_0}(1,1,0) = 0, \quad \frac{\partial f_1}{\partial v_0}(1,1,0) = -\lambda A,$$

it is easily seen that

$$\frac{\partial f_2}{\partial u_0}(1,1,0) = \lambda B.$$

Therefore,

$$D_{(u_0,v_0)}\Phi(1,1,0) = \begin{pmatrix} 0 & -\lambda A \\ \lambda B & \frac{\partial f_2}{\partial v_0} \end{pmatrix}$$

and, hence,

$$\det D_{(u_0,v_0)}\Phi(1,1,0) = \lambda^2 AB > 0,$$

which shows the claim above. Consequently, by the Implicit Function Theorem, since

$$\Phi(1,1,\varepsilon) = 0, \;\; \text{for all } \; \varepsilon \geq 0,$$

there exist $R > 0$ and $\varepsilon_0 > 0$ such that (1,1) is the unique T-periodic solution of (2.18) in the ball $B_R(1,1)$ of $\mathcal{C}_T(\mathbb{R}) \times \mathcal{C}_T(\mathbb{R})$ for all $\varepsilon \in [0,\varepsilon_0]$. Therefore, by the uniqueness provided by the implicit function theorem, if (u,v) is a T-periodic solution of (2.18) for some $\varepsilon \in [0,\varepsilon_0]$ such that

$$||u(\cdot,\varepsilon) - 1||_{\mathcal{C}_T(\mathbb{R})} + ||v(\cdot,\varepsilon) - 1||_{\mathcal{C}_T(\mathbb{R})} \leq R, \tag{2.25}$$

then $u \equiv 1$ and $v \equiv 1$.

It remains to show that there exists $\eta > 0$ such that, whenever

$$|u(t_0,\varepsilon) - 1| + |v(t_0,\varepsilon) - 1| \leq \eta$$

for some $t_0 \in [0,T]$ and $\varepsilon \in [0,\varepsilon_0]$, then the condition (2.25) holds. Indeed, by the Lipschitz dependence of the solutions of (2.18) with respect to the initial data, there exists a constant L such that

$$|u(t,\varepsilon) - 1| \leq L|u(t_0,\varepsilon) - 1|, \qquad |v(t,\varepsilon) - 1| \leq L|v(t_0,\varepsilon) - 1|,$$

for all $t \in [0,T]$ and $\varepsilon \in [0,\varepsilon_0]$. Thus,

$$|u(t,\varepsilon) - 1| + |v(t,\varepsilon) - 1| \leq L(|u(t_0,\varepsilon) - 1| + |v(t_0,\varepsilon) - 1|) \leq L\eta < R$$

if, and only if, $\eta < R/L$. Therefore,

$$\inf_{t\in[0,T]} \{|u(t,\varepsilon) - 1| + |v(t,\varepsilon) - 1|\} \leq \eta,$$

implies $u \equiv 1$ and $v \equiv 1$, which ends the proof. □

The next result provides us with the behavior of $v(s,\varepsilon)$ when $v_0(s,\varepsilon)>1$.

Lemma 2.2.4. *For any sequence $\{\varepsilon_n\}_{n\geq 1}$ such that $\lim_{n\to\infty}\varepsilon_n=0$ and $v_0(\varepsilon_n)>1$ for all $n\geq 1$, the following holds*

$$\lim_{n\to\infty} v_0(\varepsilon_n)=1.$$

Moreover, there exists a subsequence, $\{\varepsilon_{n_m}\}_{m\geq 1}$, such that

$$\lim_{m\to\infty} u(t,\varepsilon_{n_m})=u_0(0)$$

for all $t\in[0,T/2]$, where $u_0(0)$ is a suitable positive constant.

Proof. For any $A>0$, the first equation of (2.24) can be expressed as

$$A=\frac{\varepsilon_n}{v_0(\varepsilon_n)-1}\int_{\frac{T}{2}}^{T}\varphi(s)(1-v(s,\varepsilon_n))ds.$$

Thus, since $(u(t,\varepsilon_n),v(t,\varepsilon_n))$ is a coexistence state, i.e. a componentwise positive solution, the next estimate holds

$$A=\frac{\varepsilon_n}{v_0(\varepsilon_n)-1}\int_{\frac{T}{2}}^{T}\varphi(s)(1-v(s,\varepsilon_n))ds<\frac{T\varepsilon_n}{2(v_0(\varepsilon_n)-1)} \tag{2.26}$$

for all $n\geq 1$. Hence, since $\lim_{n\to\infty}\varepsilon_n=0$, (2.26) entails that

$$\lim_{n\to\infty} v_0(\varepsilon_n)=1.$$

The last assertion follows readily from the second identities of (2.22) and (2.24). This ends the proof. □

We are ready to prove the main theorem of this section.

Proof of Theorem 2.2.1: Suppose that Alternative (a) does not occur. In this case, there exists $\lambda>0$ such that there are coexistence states of (2.18), for sufficiently small $\varepsilon>0$. Accordingly, let $(u(t,\varepsilon),v(t,\varepsilon))$ denote a family of coexistence states of (2.18) (for a fixed $\lambda>0$), for $\varepsilon>0$ small ($0<\varepsilon<\varepsilon_0$). We must prove that $v(t,\varepsilon)$ blows-up in a finite time as $\varepsilon\downarrow 0$. To accomplish the proof we will distinguish between several different cases.

Case 1: There exists a sequence $\{\varepsilon_n\}_{n\geq 1}$ such that $\lim_{n\to\infty}\varepsilon_n=0$ and $v_0(\varepsilon_n)>1$ for all $n\geq 1$. Then, by Lemma 2.2.4,

$$\lim_{n\to\infty} v_0(\varepsilon_n)=1.$$

Subcase 1.A: Suppose, in addition, that $u_0(\varepsilon_n) > 1$ for all $n \geq 1$. Then, by Lemma 2.2.3, there exists $n_0 \in \mathbb{N}$ and $\rho > 0$ such that $u(t, \varepsilon_n) \geq 1 + \rho > 1$ for all $n \geq n_0$ and $t \in [0, T/2]$. By our assumptions in this special case, we can infer from (2.22) that

$$v(t, \varepsilon_n) = v(0, \varepsilon_n) = v_0(\varepsilon_n) > 1$$

for all $t \in [0, T/2]$ and $n \geq 1$. Thus, by (2.18), $u'(t, \varepsilon_n) < 0$ for every $t \in [0, T/2]$. Let $r(\varepsilon_n)$ be the first zero, or node, of $1 - u(\cdot, \varepsilon_n)$ in $[0, T]$. As illustrated in Figure 2.3, for small n, $r(\varepsilon_n)$ might lye in $(0, \frac{T}{2})$.

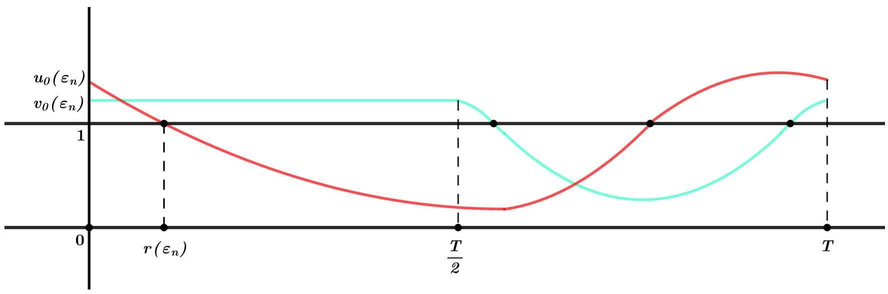

Figure 2.3: Behavior of $u(t, \varepsilon_n)$ and $v(t, \varepsilon_n)$ in Case 1.A for small n.

Nevertheless, without lost of generality, choosing an appropriate subsequence if necessary, we can assume that

$$T > \lim_{n\to\infty} r(\varepsilon_n) = r_{\max} > \frac{T}{2},$$

because, thanks to Lemma 2.2.3, $r_{\max} \leq T/2$ cannot occur and, by periodicity, we cannot have $r_{\max} \geq T$. Thus, there exists an integer n_0 such that $r(\varepsilon_n) > T/2$ for every $n \geq n_0$. This is the situation illustrated in Figure 2.4. Consequently, $u(\frac{T}{2}, \varepsilon_n) > 1$ for sufficiently large n, which implies, by Lemma 2.2.2 (e), that $v''(\frac{T}{2}) > 0$ as illustrated by Figure 2.4. So, according to the properties established by Lemma 2.2.2, in Case 1.A the graphs of $u(t, \varepsilon_n)$ and $v(t, \varepsilon_n)$ for sufficiently large n should be like sketched in Figure 2.4, where the number of nodes of $1 - u$ and $1 - v$ have been represented in a situation of minimal complexity.

On the other hand, due to (2.20), the l'Hôpital rule yields

$$\lim_{t\to\frac{T}{2}} \frac{\beta(t)}{\varphi(t)} = \lim_{t\to\frac{T}{2}} \frac{\beta'(t)}{\varphi'(t)} = \frac{\beta'(\frac{T}{2})}{\varphi'(\frac{T}{2})} > 0, \quad \lim_{t\to T} \frac{\beta(t)}{\varphi(t)} = \lim_{t\to T} \frac{\beta'(t)}{\varphi'(t)} = \frac{\beta'(T)}{\varphi'(T)} > 0.$$

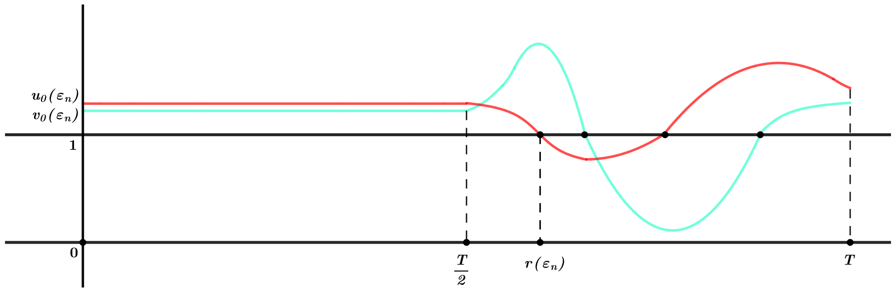

Figure 2.4: Behavior of $u(t,\varepsilon_n)$ and $v(t,\varepsilon_n)$ in Case 1.A for large n. Notice that v is constant on $[0,T/2]$ while, on the same interval, u is near to a constant for large n.

Thus, the next estimate holds

$$\frac{1}{\varepsilon}m := \frac{1}{\varepsilon}\min_{t\in[\frac{T}{2},T]}\frac{\beta(t)}{\varphi(t)} \leq \frac{1}{\varepsilon}\frac{\beta(t)}{\varphi(t)} \leq \frac{1}{\varepsilon}\max_{t\in[\frac{T}{2},T]}\frac{\beta(t)}{\varphi(t)} =: \frac{1}{\varepsilon}M. \tag{2.27}$$

Moreover, according to (2.18), the next identity holds

$$\frac{u'(t,\varepsilon_n)(-1+u(t,\varepsilon_n))}{u(t,\varepsilon_n)}\frac{\beta(t)}{\varepsilon_n\varphi(t)} = \frac{v'(t,\varepsilon_n)(1-v(t,\varepsilon_n))}{v(t,\varepsilon_n)} \tag{2.28}$$

for all $t\in[T/2,T]$. Using the estimate (2.27) and integrating (2.28) in $[T/2, r(\varepsilon_n)]$, we find that

$$\frac{m}{\varepsilon_n}\int_{\frac{T}{2}}^{r(\varepsilon_n)}\left(-\frac{u'(s,\varepsilon_n)}{u(s,\varepsilon_n)}+u'(s,\varepsilon_n)\right)ds \geq \int_{\frac{T}{2}}^{r(\varepsilon_n)}\left(\frac{v'(s,\varepsilon_n)}{v(s,\varepsilon_n)}-v'(s,\varepsilon_n)\right)ds.$$

We are choosing the lower estimate in (2.27) because

$$\frac{u'(t,\varepsilon_n)(-1+u(t,\varepsilon_n))}{u(t,\varepsilon_n)} < 0$$

for all $t\in(T/2, r(\varepsilon_n))$ and $n\geq n_0$. Thus, developing the above integrals, shows that

$$\begin{aligned}\frac{m}{\varepsilon_n}&\left[-\log u(r(\varepsilon_n),\varepsilon_n)+\log u(\tfrac{T}{2},\varepsilon_n)+u(r(\varepsilon_n),\varepsilon_n)-u(\tfrac{T}{2},\varepsilon_n)\right]\\ &\geq \log v(r(\varepsilon_n),\varepsilon_n)-\log v(\tfrac{T}{2},\varepsilon_n)-v(r(\varepsilon_n),\varepsilon_n)+v(\tfrac{T}{2},\varepsilon_n)\end{aligned}$$

or, equivalently, since, by definition, $u(r(\varepsilon_n),\varepsilon_n)=1$,

$$\begin{aligned}\frac{m}{\varepsilon_n}\left[\log u(\tfrac{T}{2},\varepsilon_n)+1-u(\tfrac{T}{2},\varepsilon_n)\right] \geq \log v(r(\varepsilon_n),\varepsilon_n)&-\log v_0(\varepsilon_n)\\ &-v(r(\varepsilon_n),\varepsilon_n)+v_0(\varepsilon_n).\end{aligned}$$

Consequently, for sufficiently large n, the next estimate holds

$$\left(\frac{e^{u(\frac{T}{2},\varepsilon_n)-1}}{u(\frac{T}{2},\varepsilon_n)}\right)^{\frac{m}{\varepsilon_n}} \le \frac{v_0(\varepsilon_n)e^{v(r(\varepsilon_n),\varepsilon_n)-v_0(\varepsilon_n)}}{v(r(\varepsilon_n),\varepsilon_n)}. \tag{2.29}$$

Now, we claim that there exists an integer n_1 such that

$$u(\tfrac{T}{2},\varepsilon_n) > 1+\frac{\eta}{2} > 1 \quad \text{and} \quad v(r(\varepsilon_n),\varepsilon_n) > 1+\eta > 1 \tag{2.30}$$

for all $n \ge n_1$. Indeed, by Lemma 2.2.3, we have that, for sufficiently large n,

$$|u(\tfrac{T}{2},\varepsilon_n)-1| + |v(\tfrac{T}{2},\varepsilon_n)-1| \ge \inf_{t\in[0,T]}\{|u(t,\varepsilon_n)-1|+|v(t,\varepsilon_n)-1|\} > \eta.$$

Moreover,

$$\lim_{n\to\infty} v(\tfrac{T}{2},\varepsilon_n) = 1.$$

Thus, there exists an integer n_1 such that, for every $n \ge n_1$,

$$|u(\tfrac{T}{2},\varepsilon_n)-1| > \eta - |v(\tfrac{T}{2},\varepsilon_n)-1| > \frac{\eta}{2}.$$

On the other hand, as for every $n \ge n_1$

$$|u(r(\varepsilon_n),\varepsilon_n)-1| + |v(r(\varepsilon_n),\varepsilon_n)-1| \ge \inf_{t\in[0,T]}\{|u(t,\varepsilon_n)-1|+|v(t,\varepsilon_n)-1|\} > \eta$$

and

$$u(r(\varepsilon_n),\varepsilon_n) = 1 \quad \text{for all} \quad n\in\mathbb{N},$$

it becomes apparent that

$$v(r(\varepsilon_n),\varepsilon_n) > 1+\eta > 1$$

for every $n \ge n_1$. Thus, (2.30) holds. Therefore, since function

$$x \mapsto \frac{e^{x-1}}{x}$$

is strictly increasing for all $x > 1$, the following estimate holds for every $n \ge n_1$:

$$(1+\delta)^{\frac{m}{\varepsilon_n}} = \left(\frac{e^{1+\frac{\eta}{2}-1}}{1+\frac{\eta}{2}}\right)^{\frac{m}{\varepsilon_n}} < \left(\frac{e^{u(\frac{T}{2},\varepsilon_n)-1}}{u(\frac{T}{2},\varepsilon_n)}\right)^{\frac{m}{\varepsilon_n}} \le \frac{v_0(\varepsilon_n)e^{v(r(\varepsilon_n),\varepsilon_n)-v_0(\varepsilon_n)}}{v(r(\varepsilon_n),\varepsilon_n)}, \tag{2.31}$$

where

$$\delta := \left(1 + \frac{\eta}{2}\right)^{-1} \sum_{k=2}^{\infty} \frac{(\eta/2)^k}{k!} > 0.$$

Hence, by (2.31),

$$\lim_{n\to\infty} \frac{v_0(\varepsilon_n)e^{v(r(\varepsilon_n),\varepsilon_n)-v_0(\varepsilon_n)}}{v(r(\varepsilon_n),\varepsilon_n)} = \infty$$

and, due to (2.30), we can conclude that

$$\lim_{n\to\infty} v(r(\varepsilon_n),\varepsilon_n) = \infty.$$

Therefore, the components $v(\cdot,\varepsilon_n)$ blow up at $r_{\max}$ as $n\to\infty$.

Subcase 1.B: Now, instead of $u_0(\varepsilon_n) > 1$, we suppose that $u_0(\varepsilon_n) < 1$ for all $n \geq 1$. Then, by Lemma 2.2.3, there exists $n_0 \in \mathbb{N}$ and $\rho > 0$ such that $u(t,\varepsilon_n) \leq 1-\rho < 1$ for all $n \geq n_0$ and $t \in [0,T/2]$, like illustrated by Figure 2.5. As in the previous case, (2.22) implies that

$$v(t,\varepsilon_n) = v(0,\varepsilon_n) = v_0(\varepsilon_n) > 1$$

for all $t \in [0,T/2]$ and $n \geq 1$. Thus, by (2.18), also in this case $u'(t,\varepsilon_n) < 0$ for each $t \in [0,T/2]$. Moreover $r(\varepsilon_n) > T/2$ for all $n \geq n_0$.

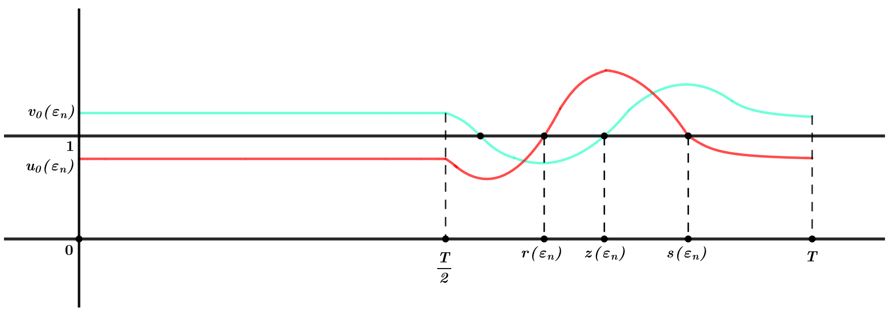

Figure 2.5: Admissible $u(t,\varepsilon_n)$ and $v(t,\varepsilon_n)$ in Subcase 1.B for large n. As in Figure 2.4, v is constant on $[0,T/2]$ while, on the same interval, u is near to a constant for large n.

According to Lemma 2.2.2 (e), since

$$u(\tfrac{T}{2},\varepsilon_n) \leq 1-\rho < 1,$$

it is apparent that $v''(\frac{T}{2},\varepsilon_n) < 0$, as illustrated in Figure 2.5.

By the properties established by Lemma 2.2.2, the graphs of $u(t,\varepsilon_n)$ and $v(t,\varepsilon_n)$ for sufficiently large n look like shows Figure 2.5. As in the previous cases, the number of nodes of $1-u$ and $1-v$ have been represented in a situation of minimal complexity to be T-periodic. Let $s(\varepsilon_n)$ be the very last node of $u(\cdot,\varepsilon_n)-1$ in $[0,T]$. Since $r(\varepsilon_n)<s(\varepsilon_n)$, it is clear that $s(\varepsilon_n)\in(T/2,T)$ for sufficiently large n. Finally, let $z(\varepsilon_n)$ denote the very last node of $v(t,\varepsilon_n)-1$ (see Figure 2.5).

Taking into account that, for every $t\in(z(\varepsilon_n),s(\varepsilon_n))$,

$$\frac{u'(t,\varepsilon_n)(-1+u(t,\varepsilon_n))}{u(t,\varepsilon_n)}<0, \qquad n\geq n_0,$$

integrating (2.28) in the interval $(z(\varepsilon_n),s(\varepsilon_n))$ and using (2.27) yields

$$\frac{m}{\varepsilon_n}\int_{z(\varepsilon_n)}^{s(\varepsilon_n)}\left(-\frac{u'(\sigma,\varepsilon_n)}{u(\sigma,\varepsilon_n)}+u'(\sigma,\varepsilon_n)\right)d\sigma\geq\int_{z(\varepsilon_n)}^{s(\varepsilon_n)}\left(\frac{v'(\sigma,\varepsilon_n)}{v(\sigma,\varepsilon_n)}-v'(\sigma,\varepsilon_n)\right)d\sigma.$$

Thus, since

$$v(z(\varepsilon_n),\varepsilon_n)=1 \quad\text{and}\quad u(s(\varepsilon_n),\varepsilon_n)=1,$$

the next estimate holds for sufficiently large n

$$\left(\frac{e^{u(z(\varepsilon_n),\varepsilon_n)-1}}{u(z(\varepsilon_n),\varepsilon_n)}\right)^{\frac{m}{\varepsilon_n}}\leq\frac{e^{v(s(\varepsilon_n),\varepsilon_n)-1}}{v(s(\varepsilon_n),\varepsilon_n)}. \tag{2.32}$$

Without lost of generality, choosing a subsequence if necessary, one can assume that

$$\lim_{n\to\infty}z(\varepsilon_n)=z\in(T/2,T), \qquad \lim_{n\to\infty}s(\varepsilon_n)=s_{\max}\in(T/2,T).$$

We claim that there exists $\eta>0$ such that, for sufficiently large n,

$$u(z(\varepsilon_n),\varepsilon_n)>1+\eta>1 \quad\text{and}\quad v(s(\varepsilon_n),\varepsilon_n)>1+\eta>1. \tag{2.33}$$

Indeed, by Lemma 2.2.3, there exists an integer n_0 such that, for every $n\geq n_0$,

$$|u(z(\varepsilon_n),\varepsilon_n)-1|+|v(z(\varepsilon_n),\varepsilon_n)-1|\geq\inf_{t\in[0,T]}\{|u(t,\varepsilon_n)-1|+|v(t,\varepsilon_n)-1|\}>\eta.$$

Thus, the first estimate of (2.33) holds. Similarly, since for every $n\geq n_0$

$$|u(s(\varepsilon_n),\varepsilon_n)-1|+|v(s(\varepsilon_n),\varepsilon_n)-1|\geq\inf_{t\in[0,T]}\{|u(t,\varepsilon_n)-1|+|v(t,\varepsilon_n)-1|\}>\eta,$$

the second estimate of (2.33) also holds. Consequently, arguing as in the previous case, the estimate (2.32) provides us with the next one

$$(1+\delta)^{\frac{m}{\varepsilon_n}}=\left(\frac{e^{1+\eta-1}}{1+\eta}\right)^{\frac{m}{\varepsilon_n}}<\left(\frac{e^{u(z(\varepsilon_n),\varepsilon_n)-1}}{u(z(\varepsilon_n),\varepsilon_n)}\right)^{\frac{m}{\varepsilon_n}}\leq\frac{e^{v(s(\varepsilon_n),\varepsilon_n)-1}}{v(s(\varepsilon_n),\varepsilon_n)},$$

where

$$\delta := (1+\eta)^{-1} \sum_{k=2}^{\infty} \frac{\eta^k}{k!} > 0.$$

Therefore,

$$\lim_{n\to\infty} v(s(\varepsilon_n), \varepsilon_n) = \infty.$$

In other words, the components $v(\cdot, \varepsilon_n)$ blow up at $s_{\max}$.

Case 2: There is a sequence $\{\varepsilon_n\}_{n\geq 1}$, such that $\lim_{n\to\infty} \varepsilon_n = 0$, $v_0(\varepsilon_n) < 1$ for all $n \geq 1$, and $\lim_{n\to\infty} v_0(\varepsilon_n) = 1$.

When, in addition, $u_0(\varepsilon_n) > 1$ for all $n \geq 1$, arguing as in the Subcase 1.A, it is easily seen that $v(t, \varepsilon_n)$ blows-up as $n \to \infty$. Figure 2.6 shows the minimal complexity of T-periodic components in this case; $a(\varepsilon_n)$ stands for the first node of $v(\cdot, \varepsilon_n) - 1$.

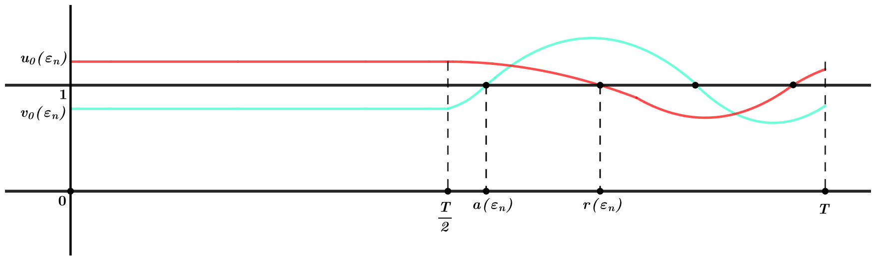

Figure 2.6: Admissible $u(t, \varepsilon_n)$ and $v(t, \varepsilon_n)$ in Case 2 for large n.

If instead of $u_n(\varepsilon_n) < 1$, we assume that $u_0(\varepsilon_n) < 1$ for all $n \geq 1$, then adapting the proof of the Subcase 1.B, it is apparent that $v(t, \varepsilon_n)$ blows-up as $n \to \infty$. Figure 2.7 shows the minimal complexity of T-periodic components in this particular case.

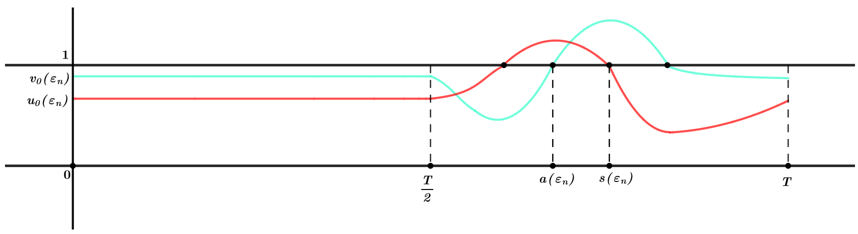

Figure 2.7: Admissible $u(t, \varepsilon_n)$ and $v(t, \varepsilon_n)$ in Case 2 for large n.

Case 3: There is a sequence $\{\varepsilon_n\}_{n\geq 1}$ such that $\lim_{n\to\infty} \varepsilon_n = 0$ and, for some

$\rho > 0$, $v_0(\varepsilon_n) < 1 - \rho$ for all $n \geq 1$. Then, according to (2.24),

$$0 < \frac{A}{\varepsilon_n} = \frac{-1}{1 - v_0(\varepsilon_n)} \int_{T/2}^{T} \varphi(s)(1 - v(s, \varepsilon_n))ds$$
$$= \frac{1}{1 - v_0(\varepsilon_n)} \int_{T/2}^{T} \varphi(s)(v(s, \varepsilon_n) - 1)ds.$$

As $v_0(\varepsilon_n) < 1 - \rho$, it is clear that $\rho < 1 - v_0(\varepsilon_n)$ for every $n \geq 1$. Thus,

$$\frac{A}{\varepsilon_n} = \frac{1}{1 - v_0(\varepsilon_n)} \int_{T/2}^{T} \varphi(s)(v(s, \varepsilon_n) - 1)ds < \frac{1}{\rho} \int_{T/2}^{T} \varphi(s)(v(s, \varepsilon_n) - 1)ds$$
$$\leq \frac{1}{\rho} \int_{T/2}^{T} \varphi(s)\, ds \left(\|v(\cdot, \varepsilon_n)\|_{\mathcal{C}[\frac{T}{2}, T]} - 1 \right).$$

Therefore,

$$\lim_{n \to \infty} \max_{x \in [T/2, T]} v(x, \varepsilon_n) = \infty$$

and the proof is also completed in this case.

Case 4: There is a sequence $\{\varepsilon_n\}_{n \geq 1}$ such that $\lim_{n \to \infty} \varepsilon_n = 0$ and $v_0(\varepsilon_n) = 1$ for all $n \geq 1$. Then, due to (2.22), we have that $v(t, \varepsilon_n) = 1$ for all $t \in [0, T/2]$ and $n \geq 1$, like illustrated in Figure 2.8.

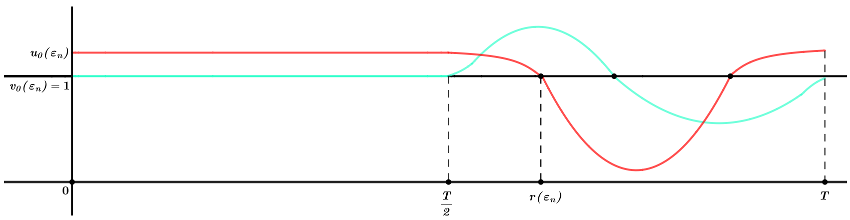

Figure 2.8: Admissible components with $u_0(\varepsilon_n) > 1$ for sufficiently large $n \geq 1$.

Subcase 4.A: Suppose, in addition, that $u_0(\varepsilon_n) > 1$ for each $n \geq 1$, like in Figure 2.8. According to Lemma 2.2.2, $1 - v(\cdot, \varepsilon_n)$ has finitely many zeroes in the interval $(T/2, T)$. Figure 2.8 shows a case with exactly one zero. Necessarily, the number of zeroes of $1 - v(\cdot, \varepsilon_n)$ is odd. Indeed, if it would be even, $1 - v(\cdot, \varepsilon_n)$ would have an odd number of critical points, which entails the existence of an odd number of zeroes of the function $1 - u(\cdot, \varepsilon_n)$ in the interval $(T/2, T)$. But this would contradict the periodicity of u. Therefore, $1 - v(\cdot, \varepsilon_n)$ has an odd number of zeroes. Now, adapting the argument of the Subcase 1.A, it readily follows that v blows-up as $n \to \infty$.

Subcase 4.B: Now, suppose that, in addition, that $u_0(\varepsilon_n) < 1$ for all $n \geq 1$. then, the same argument of the previous case shows that $1 - v(\cdot, \varepsilon_n)$ has an odd number of zeroes in the interval $(T/2, T)$, like shown in Figure 2.9. The blow-up of $v(\cdot, \varepsilon_n)$ as $n \to \infty$ can be shown by adapting the argument of the Subcase 1.B. This ends the proof. $\square$

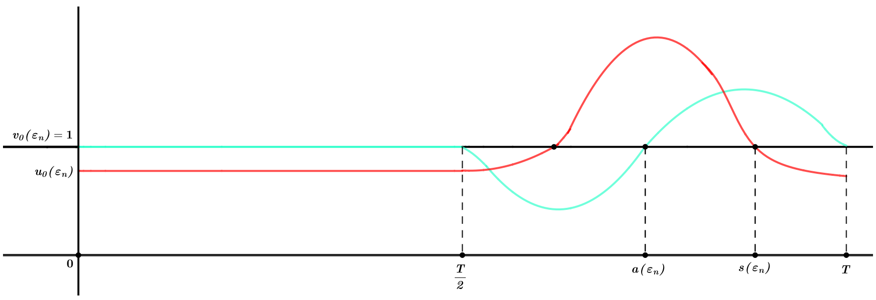

Figure 2.9: Admissible components in the Subcase 4.B for sufficiently large n.

2.3 Appendix: On the periodic Volterra model

The classical predator-prey model is a planar system of the form

$$x' = x(a - by), \qquad y' = y(-c + dx). \tag{A1}$$

The main assumptions of the model involve the fact that *all* the coefficients a, b, c, d are positive. In this manner, in the absence of predators, the prey population $x(t)$ is supposed to grow in a Malthusian way, exponentially, while, in absence of the prey, the predator population decays exponentially. According to [157],

"the term xy can be thought of as representing the conversion of energy from one source to another: bxy is taken from the prey and dxy accrues to the predators".

A natural, more realistic, extension of $(A1)$ considers the fact that all the dynamics occurs in the frame of a periodic (seasonally varying) environment. Incorporating seasonal effects to the prototype model $(A1)$, one is naturally lead to

$$\begin{cases} x' = x(a(t) - b(t)y), \\ y' = y(-c(t) + d(t)x), \end{cases} \tag{A2}$$

where $a, b, c, d : \mathbb{R} \to \mathbb{R}$ are periodic coefficients of a common period $T > 0$. Although the intrinsic growth rates and the decay coefficients may change during the time interval $[0,T]$, to be consistent with the original hypotheses in the Volterra model, one has to assume the positivity of the averages of these coefficients. Similarly, to be consistent with the fact that $x(t)$ and $y(t)$ represent, respectively, the prey and the predators, requires to impose that

$$b(t) \gneq 0, \qquad d(t) \gneq 0. \tag{$A3$}$$

The fact that $b(t)$ and $d(t)$ may vanish on a subinterval of $[0,T]$ mimics the (real) possibility that, seasonally, the predation/hunting is absent. The existence of periodic solutions for predator-prey systems with periodic coefficients was established by Cushing in [39] and Butler and Freedman [27] using bifurcation techniques. The next result provides a general existence principle for coexistence states of $(A2)$ under a minimal set of assumptions. In this result, we restrict ourselves to consider the case of continuous coefficients, in the same vein as in the previous sections, though the same result holds for general T-periodic coefficients in $L^1(0,T)$.

Theorem 2.3.1. *Assume* $(A3)$. *Then, the system* $(A2)$ *has a* T*-periodic solution* $(\tilde{x}(t), \tilde{y}(t))$ *with* $\tilde{x}(t) > 0$ *and* $\tilde{y}(t) > 0$ *for all* $t \in [0,T]$*, if and only if*

$$\int_0^T a(t)\,dt > 0 \quad \textit{and} \quad \int_0^T c(t)\,dt > 0. \tag{$A4$}$$

Proof. Suppose that $(A2)$ has a componentwise positive T-periodic solution, $(\tilde{x}(t), \tilde{y}(t))$. Then, by the uniqueness of the associated Cauchy problem, $\tilde{x}(t) > 0$ and $\tilde{y}(t) > 0$ for all $t \in [0,T]$ and hence, for every $t \in [0,T]$,

$$\frac{\tilde{x}'(t)}{\tilde{x}(t)} = a(t) - b(t)\tilde{y}(t), \qquad -\frac{\tilde{y}'(t)}{\tilde{y}(t)} = c(t) - d(t)\tilde{x}(t).$$

Therefore, integrating on $[0,T]$ establishes the necessity of $(A4)$ for the existence of a coexistence state.

Conversely, let us assume $(A4)$ and re-write the system $(A2)$ in the form

$$x' = xP(t,y), \qquad y' = yQ(t,x), \tag{$A5$}$$

with

$$P(t,y) := a(t) - b(t)y \quad \text{and} \quad Q(t,x) := -c(t) + d(t)x.$$

Let $M > 0$ be a sufficiently large constant such that

$$\max\left\{ \frac{\int_0^T a(t)\,dt}{\int_0^T b(t)\,dt}, \frac{\int_0^T c(t)\,dt}{\int_0^T d(t)\,dt} \right\} < M$$

and set

$$P_\infty(t) := a(t) - Mb(t), \qquad Q_\infty(t) := -c(t) + Md(t).$$

Using the fact that $P(t,y)$ is non-increasing in y and $Q(t,x)$ is non-decreasing in x, it becomes apparent that

$$\limsup_{s\to+\infty} P(t,s) \le P_\infty(t), \qquad \liminf_{s\to+\infty} Q(t,s) \ge Q_\infty(t),$$

uniformly in $t \in [0,T]$. Thus, we have entered in the setting of [56, Th. 3], which implies the existence of, at least, one T-periodic solution of $(A5)$, and hence of $(A2)$, because the next conditions

$$\int_0^T P(t,0)\,dt = \int_0^T a(t)\,dt > 0 > \int_0^T a(t)\,dt - M\int_0^T b(t)\,dt = \int_0^T P_\infty(t)\,dt$$

$$\int_0^T Q(t,0)\,dt = -\int_0^T c(t)\,dt < 0 < -\int_0^T c(t)\,dt + M\int_0^T d(t)\,dt = \int_0^T Q_\infty(t)\,dt$$

are satisfied. Although the second part of [56, Th. 3], the one discussing the existence of subharmonics, requires the strict monotonicity of either $P(t,\cdot)$ or $Q(t,\cdot)$ for all $t \in [0,T]$, its first part, not requiring any strict monotonicity, can be applied here. □

Clearly, Theorem A.1 justifies the passage from the system (2.2) to the system (2.3), an hence our motivation in studying (2.1).

We conclude this Appendix with a brief additional discussion on our model, which is a prototype that allows $\alpha(t)\beta(t)$ not only vanishing on a subinterval of $[0,T]$ but also the possibility that the supports of $\alpha(t)$ and $\beta(t)$ do not coincide. Although from the point of view of its applications in Population Dynamics, there is a strong debate concerning the validity of the classical predator-prey model of Lotka–Volterra type, which is (2.1) with $\alpha(t)$ and $\beta(t)$ positive constants, the basic features of this model still conform the basis upon which the mathematical theory of predation is built. According to ecologists, predation is essentially consumption of one organism (the prey) by another one (the predator), in which the prey is alive when the predator first attacks it, [11]. Incorporating to the simplest prototype models saturation effects for the predators does not really change the most basic features of these models, though might make them more realistic, of course.

In nature, there are many examples in which a predator, or a prey, maintains a fairly constant density in spite of the fluctuations of its prey. In general, the hunting-collecting processes adapt to these dynamics. While within a certain period of the year the predators damage the prey population by hunting their individuals and collecting them on their stocks, in another period they stop hunting the preys and simply consume the ones collected, the prey being unaffected by the action of the predators during these periods. Naturally, these periods can overlap or not, which is reflected by the length of the support of the product function $\alpha(t)\beta(t)$ in model (2.1).

A very concrete example which fits very well within the setting of the model (2.1) takes place in the Mediterranean pine woods, where the *Thaumetopoea pityocampa*, commonly refereed to as the pine processionary, defoliates the pines before being ready to pupate. Indeed, while attacking the pines and becoming pupates, the pine processionary density stays constant, whereas the pine density fluctuates. Moreover, depending on the impact of the defoliation, the new generation of caterpillars can increase or decrease before the beginning of a new cycle. Naturally, a very severe defoliation of one generation might seriously damage the individuals of the next one. The model (2.1) is the simplest prototype model mimicking those real situations which are far from understood yet.

Chapter 3

The Poincaré–Birkhoff approach: degenerate models

This chapter considers again, as in Section 2.1 of Chapter 2, the non autonomous planar Hamiltonian system

$$\begin{cases} x' = & -\lambda\alpha(t)f(y), \\ y' = & \lambda\beta(t)g(x), \end{cases} \tag{3.1}$$

where $\lambda > 0$ is a real parameter, and, given a real number $T > 0$, α and β are nonnegative T-periodic continuous functions such that $\alpha(t) \gneq 0$ and $\beta(t) \gneq 0$. Now, instead of assuming $\alpha(t)\beta(t) \gneq 0$ as in Chapter 2, we consider that

$$\alpha(t)\beta(t) = 0 \quad \text{for all } \ t \in [0, T]. \tag{3.2}$$

This is why the model (3.1) is said to be *degenerate* in this case. Moreover, the functions f and g of (3.1) will satisfy the same assumptions as in Chapter 2 (cf. (2.9), (2.10) and their discussion).

The aim of this chapter is to analyze, for any integer $n \geq 1$, the existence of nT-periodic solutions of model (3.1) when the degenracy condition (3.2) holds. Recall that, those with $n \geq 2$ (and n minimal) are also referred to as subharmonics of order n.

Besides condition (3.2), through this chapter we assume that, given two positive integers $k, \ell \geq 1$ such that $|k - \ell| \leq 1$, there exist $k + \ell$ continuous functions in the interval $[0, T]$, $\alpha_i \gneq 0$, $1 \leq i \leq k$, and $\beta_j \gneq 0$, $1 \leq j \leq \ell$, such that

$$\alpha = \alpha_1 + \alpha_2 + \cdots + \alpha_k, \qquad \beta = \beta_1 + \beta_2 + \cdots + \beta_\ell,$$

with

$$\operatorname{supp} \alpha_i \subseteq [t_0^i, t_1^i] \ \text{ and } \ \operatorname{supp} \beta_j \subseteq [t_2^j, t_3^j], \tag{3.3}$$

for some partition of $[0,T]$

$$0 \leq t_0^1 < t_1^1 \leq t_2^1 < t_3^1 \leq t_0^2 < t_1^2 \leq t_2^2 < t_3^2 \leq \cdots \leq t_0^k < t_1^k \leq t_2^k < t_3^k \leq T$$

if $k = \ell$, or

$$0 \leq t_0^1 < t_1^1 \leq t_2^1 < t_3^1 \leq t_0^2 < t_1^2 \leq t_2^2 < t_3^2 \leq \cdots \leq t_0^k < t_1^k \leq T$$

if $k = \ell + 1$. Similarly, we also consider the case when, instead of (3.3),

$$\operatorname{supp} \beta_j \subseteq [t_0^j, t_1^j] \quad \text{and} \quad \operatorname{supp} \alpha_i \subseteq [t_2^i, t_3^i], \tag{3.4}$$

for some partition of $[0,T]$

$$0 \leq t_0^1 < t_1^1 \leq t_2^1 < t_3^1 \leq t_0^2 < t_1^2 \leq t_2^2 < t_3^2 \leq \cdots \leq t_0^\ell < t_1^\ell \leq t_2^\ell < t_3^\ell \leq T$$

if $\ell = k$, or

$$0 \leq t_0^1 < t_1^1 \leq t_2^1 < t_3^1 \leq t_0^2 < t_1^2 \leq t_2^2 < t_3^2 \leq \cdots \leq t_0^\ell < t_1^\ell \leq T$$

if $\ell = k + 1$.

Moreover, we refer to an *α-interval* (resp. *β-interval*) as the maximal interval where $\beta \equiv 0$ (resp. $\alpha \equiv 0$). So, the total number of α-intervals and β-intervals in $[0,T]$ is $k + \ell$. However, ascertaining the total number of α and β-intervals in $[0,nT]$ when $n \geq 2$ is slightly more subtle, as it depends on whether $k = \ell$, or $|k - \ell| = 1$. If $k = \ell$, it is apparent that the number of α-intervals is nk whereas the number of β-intervals is $n\ell$. Thus, the total number of α and β-intervals in this case equals

$$n(k + \ell) = 2nk. \tag{3.5}$$

Now, assume that $|k - \ell| = 1$. Then, in case $k = \ell + 1$, there are $n\ell + 1$ α-intervals and $n\ell$ β-intervals in $[0,nT]$. Indeed, as for every $i \in \{0, 1, \ldots, n-2\}$ the last α-interval of $[iT, (i+1)T]$ and the first one of $[(i+1)T, (i+2)T]$ produce a unique α-interval in $[0,nT]$, the total number of α-intervals in $[0,nT]$ is given by

$$n(\ell + 1) - (n - 1) = n\ell + 1.$$

Obviously, the number of β-intervals in $[0,nT]$ is $n\ell$. Thus, the total number of α and β-intervals equals

$$n\ell + 1 + n\ell = 2n\ell + 1.$$

Similarly, in case $\ell = k + 1$, the total number of α and β-intervals in $[0,nT]$ is

$$nk + 1 + nk = 2nk + 1.$$

Therefore, setting $m := \min\{k,\ell\}$, the total number of α and β-intervals in $[0,nT]$ in case $|k-\ell| = 1$ is

$$2nm + 1 \tag{3.6}$$

Figure 3.1 shows a series of examples satisfying the previous requirements. Note that the support of the α_i's and the β_j's on each of the intervals $[t_r^i, t_{r+1}^i]$, $1 \leq i \leq k$, and $[t_r^j, t_{r+1}^j]$, $1 \leq j \leq \ell$, might not be connected.

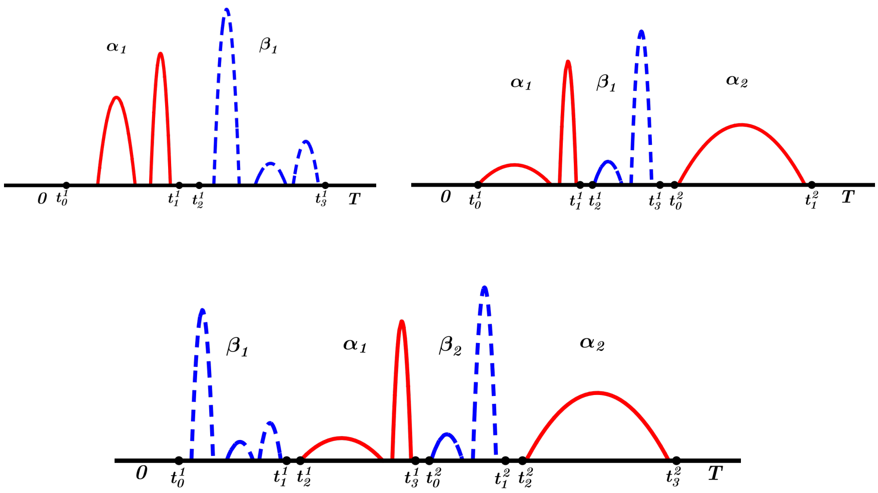

Figure 3.1: Some admissible distributions of α and β.

On each of the intervals $[t_r^s, t_{r+1}^s]$, $s \in \{i,j\}$, $r \in \{0,2\}$, the structure of the support of α_i, or β_j, might be rather involved topologically, as illustrated by Figure 3.2, where we have plotted a sketch of the graph of a function α_i, or β_j, vanishing on the tertiary Cantor set of the interval $[t_r^s, t_{r+1}^s]$, and being positive on the interior of its complement.

Note that the cases when $k+\ell \neq 2$, or $k+\ell = 2$ under condition (3.4), were not dealt with in any previous references. In particular, they stay outside the general scope of [141, 123, 134]. The main result of this chapter can be stated as follows. (Subsequently, for every $r \in \mathbb{R}$, we are denoting by $[r]$ the integer part of r).

Theorem 3.0.1. *Assume $nm \geq 3$ for some integer $n = 3h + i$, with $i \in \{0,1,2\}$, where $m := \min\{k,\ell\}$. Then, there exists $\lambda_n > 0$ such that, for*

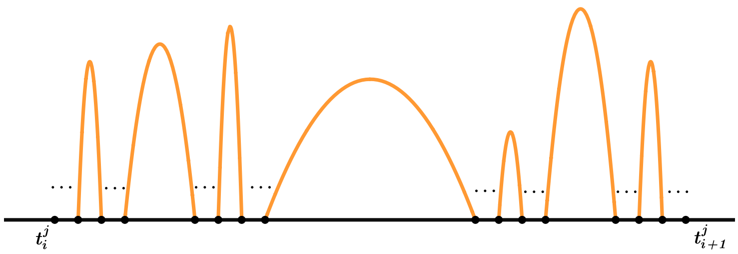

Figure 3.2: The internal complexity of the weights on each of their support intervals.

every $\lambda > \lambda_n$, (3.1) *possesses, at least,*

$$\sigma(n) := 2\left(hm + \left[\tfrac{im}{3}\right]\right)$$

periodic solutions with period nT. *Moreover, setting*

$$\gamma(n) := \min\left\{\gamma \geq 0 \ : \ \gcd\left(n, \tfrac{\sigma(n)}{2} - \gamma\right) = 1\right\},$$

it turns out that, for every $\lambda > \lambda_n$, (3.1) *has, at least,* $\sigma(n) - 2\gamma(n)$ *periodic solutions with minimal period* nT.

The main technical device to prove Theorem 3.0.1 is the Poincaré–Birkhoff *twist* theorem collected in Theorem 3.1.1. Theorem 3.0.1 deals with a degenerate case in the context of Hamiltonian systems not previously studied in the literature, because neither the monotonicity of $\alpha(t)f(y)$, or $\beta(t)g(x)$, *for all* t, nor the non-degeneration of $\alpha(t)$ and $\beta(t)$, are required (see [89, 56, 179, 77], and [137, §1]).

In Section 3.1 we state the version of the Poincaré–Birkhoff theorem invoked in the proof of Theorem 3.0.1 and make sure that it can be applied to deal with the degenerate model (3.1). Then, in Section 3.2, the proof of Theorem 3.0.1 is delivered. Finally, in Section 3.3, an application to a class of periodic predator-prey models is provided.

3.1 The Poincaré–Birkhoff theorem in a degenerate setting

In this section we adapt the Poincaré–Birkhoff theorem to deal with the problem (3.1) in the *degenerate* case when $\alpha(t)\beta(t) \equiv 0$ (see (3.2), if necessary).

The Poincaré–Birkhoff theorem has been applied, very successfully, to study some *non-degenerate* Volterra predator-prey models of the type (3.1) (see, e.g., [89, 55, 56, 179, 17, 77, 58] and also Chapter 2).

According to Theorem 2.1.5, as soon as there exists $t_0 \in [0, T]$ such that $\alpha(t_0)\beta(t_0) > 0$, the system (3.1) possesses, at least, two nT-periodic solutions for every integer $n \geq 1$ and sufficiently large $\lambda > 0$. The main result of this section, Theorem 3.1.2, provides with some general sufficient conditions on the coefficients $\alpha(t)$ and $\beta(t)$ for the validity of the same result in the case $\alpha(t)\beta(t) \equiv 0$.

As presented in Chapter 2, for any given non-trivial solution $(x(t), y(t))$ with initial data

$$z_0 := (x(0), y(0)) \neq (0, 0),$$

we denote by $\theta(t)$ the angular polar coordinate, so that on any interval $[0, nT]$, the rotation number of the solution can be defined through

$$\mathrm{rot}(z_0; [0, nT]) := \frac{\theta(nT) - \theta(0)}{2\pi}.$$

To obtain the main result of this section, we need again the version of the Poincaré–Birkhoff twist theorem stated in Theorem 2.1.3. For the sake of simplicity with the notation, we restate this theorem:

Theorem 3.1.1. *Assume that, for some* $0 < r_0 < R_0$ *and an integer* $\omega \geq 1$, *the next twist condition holds*

$$\begin{cases} \mathrm{rot}(z_0; [0, nT]) > \omega & \textit{if } \ ||z_0|| = r_0 \\ \mathrm{rot}(z_0; [0, nT]) < \omega & \textit{if } \ ||z_0|| = R_0. \end{cases} \tag{3.7}$$

Then, the system (3.1) *has, at least,* 2 *nontrivial* nT*-periodic solutions belonging to different periodicity classes with rotation number* ω.

According to (3.5) and (3.6) and recalling that $m = \min\{k, \ell\}$, we will assume that $2nm \geq 6$ if $k = \ell$, and $2nm + 1 \geq 7$ if $|k - \ell| = 1$. Thus, unifying both conditions, throughout the rest of this chapter, we will actually assume that

$$nm \geq 3. \tag{3.8}$$

This condition entail, essentially, at least five alternations between the components of the supports of $\alpha(t)$ and $\beta(t)$, as illustrated in Figure 3.3.

The main result of this section reads as follows.

Theorem 3.1.2. *Assume* $nm \geq 3$. *Then, there exists* $\lambda_n > 0$ *such that, for every* $\lambda > \lambda_n$, *the twist condition* (3.7) *in model* (3.1) *holds for* $\omega \geq 1$.

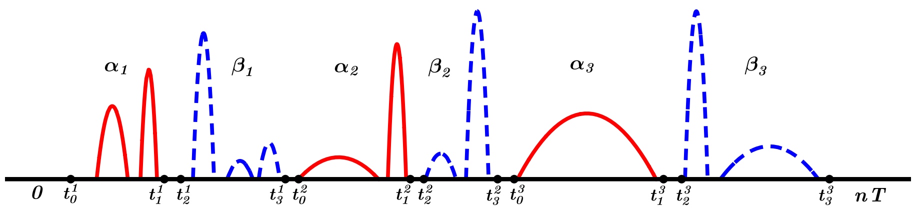

Figure 3.3: An example of five alternations between the supports of α and β.

This theorem analyzes a degenerate case for Hamiltonian systems of the form of (3.1), through the Poincaré–Birkhoff *twist* theorem, which had not been previously studied in this context, for as neither the monotonicity of $\alpha(t)f(y)$, or $\beta(t)g(x)$, *for all* t, nor the non-degeneration of $\alpha(t)$ and $\beta(t)$, are required (see [89, 56, 179, 77], and [137, §1]).

The technical details of the proof will be given in the special case when α and β satisfy (3.3), as the case when (3.4) holds follows similarly. By (2.9),

$$\min\{f'(0), g'(0)\} > \eta$$

for some constant $\eta > 0$. Thus, for sufficiently small $|\zeta| \leq \varepsilon$,

$$f(\zeta)\zeta \geq \eta\zeta^2, \qquad g(\zeta)\zeta \geq \eta\zeta^2. \tag{3.9}$$

Hence, since up to an additive constant,

$$\theta(t) = \arctan\frac{y(t)}{x(t)},$$

differentiating with respect to t and using the fact that $(x(t), y(t))$ solves (3.1) yields

$$\theta'(t) = \frac{y'(t)x(t) - x'(t)y(t)}{x^2(t) + y^2(t)} = \frac{\lambda\beta(t)g(x(t))x(t) + \lambda\alpha(t)f(y(t))y(t)}{x^2(t) + y^2(t)}$$

for every $t \in [0, nT]$. So, owing to (3.9), we have that

$$\begin{aligned} \theta'(t) &\geq \lambda\eta\left[\beta(t)\frac{x^2(t)}{x^2(t)+y^2(t)} + \alpha(t)\frac{y^2(t)}{x^2(t)+y^2(t)}\right] \\ &= \lambda\eta\left[\beta(t)\cos^2\theta(t) + \alpha(t)\sin^2\theta(t)\right] \geq 0 \end{aligned} \tag{3.10}$$

for every $t \in [0, nT]$. In particular, $\theta(t)$ is non-decreasing. Moreover, by Proposition 2.1.1, for every integer $n \geq 1$, there exists $\delta > 0$ such that $(x(t), y(t)) \in D_\varepsilon$ for all $t \in [0, nT]$ if

$$(x_0, y_0) := (x(0), y(0)) \in D_\delta.$$

This condition will be kept throughout the next lemmas and the proof of Theorem 3.1.2 in order to guarantee that the solution cannot escape from D_ε. Naturally, the bigger is λ the smaller δ.

Based on (3.10) and Proposition 2.1.1, the next result holds. Essentially, it establishes that each of the components of the support of the α_i's pushes the solutions of (3.1) from the first quadrant towards the second one, as well as from the third towards the fourth.

Lemma 3.1.3. *Assume that there exists* $(\rho_0, \rho_1) \subsetneq \operatorname{supp} \alpha$ *such that* $\theta(\rho_0) \in [\omega_0, \pi - \omega_0]$ *for some* $\omega_0 \in (0, \frac{\pi}{2})$. *Then, there exists* $\lambda_1 > 0$ *such that* $\theta(\rho_1) > \pi - \omega_0$ *for all* $\lambda > \lambda_1$. *Similarly, if* $\theta(\rho_0) \in [\pi + \zeta_0, 2\pi - \zeta_0]$ *for some* $\zeta_0 \in (0, \frac{\pi}{2})$, *then* $\theta(\rho_1) > 2\pi - \zeta_0$ *for sufficiently large* λ.

Proof. Since we are dealing with small solutions, it is apparent from (3.10) that

$$\theta(\rho_1) = \theta(\rho_0) + \int_{\rho_0}^{\rho_1} \theta'(s)ds \geq \theta(\rho_0) + \lambda\eta \int_{\rho_0}^{\rho_1} \alpha(s) \frac{y^2(\rho_0)}{x^2(s) + y^2(\rho_0)} ds$$

because $\beta = 0$ on (ρ_0, ρ_1) and, hence, $y(s) \equiv y(\rho_0)$ there in. Thus, setting

$$\nu := \frac{\eta y^2(\rho_0)}{\varepsilon^2} \int_{\rho_0}^{\rho_1} \alpha(s)ds$$

and taking into account that

$$(x(s), y(s)) = (x(s), y(\rho_0)) \in D_\varepsilon \quad \text{for all } \; s \in (\rho_0, \rho_1),$$

it follows that

$$\theta(\rho_1) \geq \theta(\rho_0) + \lambda\nu \geq \omega_0 + \lambda\nu > \pi - \omega_0$$

provided

$$\lambda > \frac{\pi - 2\omega_0}{\nu} =: \lambda_1.$$

Note that the bound λ_1 remains invariant if either $\theta(\rho_0)$, or $y^2(\rho_0)$, increases. Moreover, $\theta(\rho_1)$ increases with λ for any given (fixed) $\theta(\rho_0)$ and $y^2(\rho_0)$. Similarly, $\theta(\rho_1) > 2\pi - \zeta_0$ for sufficiently large λ if $\theta(\rho_0) \in [\pi + \zeta_0, 2\pi - \zeta_0]$ for some $\zeta_0 \in (0, \frac{\pi}{2})$. This ends the proof. $\square$

Analogously, the next result establishes that each of the components of the support of the β_i's pushes the solutions of (3.1) from the fourth quadrant towards the first, while it moves them from the second towards the third one.

Lemma 3.1.4. *Assume that there exists* $(\sigma_0, \sigma_1) \subsetneq \operatorname{supp}\beta$ *such that* $\theta(\sigma_0) \in [-\frac{\pi}{2}+\tau_0, \frac{\pi}{2}-\tau_0]$ *for some* $\tau_0 \in (0, \frac{\pi}{2})$. *Then, there exists* μ_1 *such that* $\theta(\sigma_1) > \frac{\pi}{2} - \tau_0$ *for all* $\lambda > \mu_1$. *Similarly,* $\theta(\sigma_1) > \frac{3\pi}{2} - \xi_0$ *for sufficiently large* λ *if* $\theta(\sigma_0) \in [\frac{\pi}{2} + \xi_0, \frac{3\pi}{2} - \xi_0]$ *for some* $\xi_0 \in (0, \frac{\pi}{2})$.

Proof. As in Lemma 3.1.3, from (3.10) it follows that

$$\theta(\sigma_1) = \theta(\sigma_0) + \int_{\sigma_0}^{\sigma_1} \theta'(s)ds \geq \theta(\sigma_0) + \int_{\sigma_0}^{\sigma_1} \beta(s)\frac{x^2(\sigma_0)}{x^2(\sigma_0)+y^2(s)}ds$$

because $\alpha = 0$ on (σ_0, σ_1) and, hence, $x(s) \equiv x(\sigma_0)$ there in. Thus, denoting

$$\varsigma := \frac{\eta x^2(\sigma_0)}{\varepsilon^2}\int_{\sigma_0}^{\sigma_1}\beta(s)ds,$$

and arguing as in Lemma 3.1.3, it is apparent that

$$\theta(\sigma_1) \geq \theta(\sigma_0) + \lambda\varsigma \geq \tau_0 + \lambda\varsigma > \frac{\pi}{2} - \tau_0$$

provided

$$\lambda > \frac{\pi - 4\tau_0}{2\varsigma} =: \mu_1.$$

As highlighted in the proof of Lemma 3.1.3, the value of μ_1 does not vary if either $\theta(\sigma_0)$, or $x^2(\sigma_0)$, increases. Similarly, $\theta(\sigma_1)$ increases with λ, and the second assertion of the lemma holds. This ends the proof. □

Now, we are ready to prove Theorem 3.1.2.

Proof of Theorem 3.1.2: The proof is based on the version of the Poincaré–Birkhoff theorem collected in Theorem 3.1.1. First, we will prove that all small solutions in the disc D_ε, where ε is chosen sufficiently small so that (3.9) holds, have a rotation number greater than one. To prove this feature, we will distinguish between three different cases according to the precise location of their initial values, (x_0, y_0).

Case 1: Assume that $x_0y_0 > 0$. Then, (x_0, y_0) lies either in the first or in the third quadrant. Being both cases similar, we will pay attention only to the case when $x_0 > 0$ and $y_0 > 0$. Then, $\theta(t_0^1) \in \left(0, \frac{\pi}{2}\right)$. Thus, by Lemma 3.1.3, there exists $\lambda_1 > 0$ such that

$$\theta(t_1^1) > \pi - \theta(t_0^1)$$

for all $\lambda > \lambda_1$. Since $\alpha = \beta = 0$ in $[t_1^1, t_2^1]$, this implies that

$$\theta(t_2^1) = \theta(t_1^1) > \pi - \theta(t_0^1).$$

Thus, by Lemma 3.1.4, there exists $\lambda_2 > 0$ such that

$$\theta(t_3^1) > \pi + \theta(t_0^1)$$

as soon as $\lambda > \max\{\lambda_1, \lambda_2\}$. Also by Lemma 3.1.3, there exists $\lambda_3 > 0$ such that $\theta(t_1^2) > 2\pi - \theta(t_0^1)$ for every $\lambda > \max\{\lambda_1, \lambda_2, \lambda_3\}$, and, due to Lemma 3.1.4, there is $\lambda_4 > 0$ such that $\theta(t_3^2) > 2\pi + \theta(t_0^1)$ for all $\lambda > \max\{\lambda_1, \lambda_2, \lambda_3, \lambda_4\}$. Therefore, the solution with initial values (x_0, y_0) completes an entire turn in the interval $[0, t_3^2]$ for every

$$\lambda > \max\{\lambda_1, \lambda_2, \lambda_3, \lambda_4\}.$$

In order to apply Theorem 3.1.1, it remains to show the existence of a uniform bound, $\Lambda_1 > 0$, such that, the solutions with initial data in the sector of the circumference of radius r_0 within the first quadrant,

$$S_1 := \{z = (x, y) \in \mathbb{R}^2 \ : \ \|z\| = r_0 \ \text{ and } \ x > 0, \ y > 0\},$$

have a rotation number greater than one for all $\lambda > \Lambda_1$ if $0 < r_0 < \varepsilon$. To prove it, we consider an angle $\tilde{\omega}_0 \in (0, \frac{\pi}{2})$ and the sectors of S_1 defined by

$$\begin{aligned} S_{1,\tilde{\omega}_0}^{+} &:= \{z = (x, y) \in \mathbb{R}^2 \ : \ \|z\| = r_0, \ r_0 \cos\tilde{\omega}_0 \geq x > 0, \ y > 0\}, \\ S_{1,\tilde{\omega}_0}^{-} &:= S_1 \setminus S_{1,\tilde{\omega}_0}^{+}. \end{aligned}$$

Using recursively the Lemmas 3.1.3 and 3.1.4 as above it becomes apparent that there exists $M_1 > 0$ such that the solutions with initial data in $S_{1,\tilde{\omega}_0}^{+}$ complete an entire turn in the interval $[0, t_3^2]$ for every $\lambda > M_1$. For every $t > 0$, let denote by Φ_t the Poincaré map at time t of the system (3.1), if defined. Then, by Lemma 3.1.4, there exists $\omega_1 > 0$ such that

$$\Phi_{t_3^1}(S_{1,\tilde{\omega}_0}^{-}) \subset \left\{(r, \theta) \ : \ 0 < r \leq \varepsilon, \ 0 < \omega_1 \leq \theta < \tfrac{3\pi}{2}\right\}.$$

Therefore, arguing as for $S_{1,\tilde{\omega}_0}^{+}$, there is M_2 such that $S_{1,\tilde{\omega}_0}^{-}$ completes one turn in $[0, t_3^3]$ for all $\lambda > \max\{M_1, M_2\}$.

Adapting the previous argument, it readily follows the existence of $\tilde{M}_1 > 0$ and $\tilde{M}_2 > 0$ such that the solutions of (3.1) with initial data in

$$S_3 := \{z = (x, y) \in \mathbb{R}^2 \ : \ \|z\| = r_0 \ \text{ and } \ x < 0, \ y < 0\}$$

have a rotation number greater than one for all $\lambda > \max\{\tilde{M}_1, \tilde{M}_2\}$. Consequently, for every $z_0 \in S_1 \cup S_3$, it is apparent that

$$\operatorname{rot}(z_0; [0, nT]) > 1$$

for all $\lambda > \Lambda_1 := \max\{M_1, M_2, \tilde{M}_1, \tilde{M}_2\}$.

Case 2: Assume that $x_0 y_0 < 0$. Most of the attention will be focused to the special case when $x_0 < 0$ and $y_0 > 0$, as the case $x_0 > 0$ and $y_0 < 0$ is analogous. Obviously, in this case, $\theta(t_0^1) \in \left(\frac{\pi}{2}, \pi\right)$. As in Case 1, it should be proved the existence of a uniform bound, Λ_2, such that the solutions with initial data in the quadrant sector

$$S_2 := \{z = (x, y) \in \mathbb{R}^2 \ : \ \|z\| = r_0 \ \text{ and } \ x < 0, \ y > 0\},$$

have rotation number greater than one for all $\lambda > \Lambda_2$ if $0 < r_0 < \varepsilon$. By Lemma 3.1.3, there exists $\omega_2 > \frac{\pi}{2}$ such that

$$\Phi_{t_1^1}(S_2) \subset \left\{(r, \theta) \ : \ 0 < r \leq \varepsilon, \ \tfrac{\pi}{2} < \omega_2 \leq \theta < \pi\right\}.$$

Thus, as in Case 1 we have already proven that, once the solution reaches the second quadrant, being separated away from $\frac{\pi}{2}$, it must have a rotation number greater than one for sufficiently large λ (which was a direct consequence from Lemmas 3.1.3 and 3.1.4), there exists $\Lambda_2 > 0$ such that the solution with

$$\theta(t_1^1) = \omega_2 > \frac{\pi}{2}$$

completes one turn for all $\lambda > \Lambda_2$. Moreover, by the monotonicity properties of Lemmas 3.1.3 and 3.1.4, the solutions with initial data in S_2 have rotation number greater than one for all $\lambda > \Lambda_2$. Since the previous argument can be easily adapted to deal with

$$S_4 := \{z = (x, y) \in \mathbb{R}^2 \ : \ \|z\| = r_0 \ \text{ and } \ x > 0, \ y < 0\},$$

it becomes apparent that, for every $z_0 \in S_2 \cup S_4$,

$$\operatorname{rot}(z_0; [0, nT]) > 1$$

for all $\lambda > \Lambda_2$.

Case 3: Assume $x_0 y_0 = 0$, i.e., (x_0, y_0) lies on some coordinate axis. Without lost of generality, we can assume that $x_0 > 0$ and $y_0 = 0$, as the remaining cases can be treated similarly. Then, since $y_0 = 0$ and $\beta = 0$ on $[t_0^1, t_1^1]$, integrating (3.1) yields

$$\theta(t_0^1) = \theta(t_2^1) = 0.$$

Thus, by Lemma 3.1.4, for every $\omega \in (0, \frac{\pi}{2})$, there exists $\mu_1 := \mu_1(\omega)$ such that $\theta(t_3^1) > \omega$ for all $\lambda > \mu_1$. Thus, much like in Case 1, owing to Lemmas 3.1.3 and 3.1.4, there exist $\mu_2, \mu_3, \mu_4, \mu_5 > 0$, depending on ω, such that

$$\begin{aligned}
\theta(t_1^2) &> \pi - \omega && \text{if } \lambda > \max\{\mu_1, \mu_2\},\\
\theta(t_3^2) &> \pi + \omega && \text{if } \lambda > \max\{\mu_1, \mu_2, \mu_3\},\\
\theta(t_1^3) &> 2\pi - \omega && \text{if } \lambda > \max\{\mu_1, \mu_2, \mu_3, \mu_4\},\\
\theta(t_3^3) &> 2\pi && \text{if } \lambda > \max\{\mu_1, \mu_2, \mu_3, \mu_4, \mu_5\} =: \Lambda_{3,1}.
\end{aligned}$$

Therefore, the solution completes one turn in the time interval $[0, t_3^3]$ for all $\lambda > \Lambda_{3,1}$. Similarly, it can be easily shown that the solutions complete a turn in each of the remaining three cases when $x_0 = 0$ and $y_0 > 0$, $x_0 < 0$ and $y_0 = 0$, or $x_0 = 0$ and $y_0 < 0$, for $\lambda > \Lambda_{3,2}$, $\lambda > \Lambda_{3,3}$ and $\lambda > \Lambda_{3,4}$, respectively. Thus, taking

$$\Lambda_3 := \max\{\Lambda_{3,1}, \Lambda_{3,2}, \Lambda_{3,3}, \Lambda_{3,4}\},$$

it becomes apparent that

$$\mathrm{rot}(z_0; [0, nT]) > 1$$

provided $\lambda > \Lambda_3$ and

$$z_0 \in S_0 := \{z = (x, y) \in \mathbb{R}^2 \ : \ \|z\| = r_0 \ \text{ and } \ xy = 0\}.$$

Subsequently, we set

$$\lambda_n := \max\{\Lambda_1, \Lambda_2, \Lambda_3\}.$$

By Proposition 2.1.1 and the analysis already done in the proof of the theorem, it is apparent that, for every $\lambda > \lambda_n$, there exists $0 < r_0 < \delta(n, \lambda, \varepsilon)$ such that, for every $z_0 = (x_0, y_0)$ with $\|z_0\| = r_0$,

$$(x(t), y(t)) \in D_\varepsilon \ \text{ for all } \ t \in [0, nT]$$

and

$$\mathrm{rot}(z_0; [0, nT]) > 1. \tag{3.11}$$

In order to apply Theorem 3.1.1, it remains to prove that, for sufficiently large $\lambda > 0$, the large solutions do not rotate. As the proof of this feature follows the general scheme of the proof of [137, Th. 2.1.], we will simply sketch it here. Being analogous the remaining cases, we will deliver the proof in the special case when condition (g_-) holds in (2.10).

We proceed by contradiction assuming that, regardless the size of the initial data, (x_0, y_0), the solution, $(x(t), y(t))$, completes at least one turn for sufficiently large λ. Thus, without lost of generality, changing the initial data if necessary, we can assume that $(x(t), y(t))$ goes across the entire third quadrant. In such case, there is an interval $[s_0, s_1] \subset [0, nT]$ such that $y(s_0) = 0 = x(s_1)$ and $x(t) < 0$, $y(t) < 0$ for every $t \in (s_0, s_1)$. Thus, by (g_-), it becomes apparent that, setting $B := \int_0^T \beta(s)\, ds$,

$$|y(t)| = \lambda |\int_{s_0}^{t} \beta(s) g(x(s))\, ds| \leq \lambda M \int_0^{nT} \beta(s)\, ds = \lambda M n B$$

for every $t \in [s_0, s_1]$. Hence, defining

$$N := \max \{|f(y)| \ : \ |y| \leq \lambda M n B\},$$

it follows that, for every $t \in [s_0, s_1]$,

$$|x(t)| = |\lambda \int_{t}^{s_1} \alpha(s) f(y(s))\, ds| \leq \lambda N \int_0^{nT} \alpha(s)\, ds = \lambda N n A,$$

where $A := \int_0^T \alpha(s)\, ds$. Suppose that, for some $\tilde{t} \in [0, nT]$,

$$x^2(\tilde{t}) + y^2(\tilde{t}) > \lambda^2 n^2 (M^2 B^2 + N^2 A^2) \equiv R^2$$

with $x(\tilde{t}) < 0$ and $y(\tilde{t}) < 0$. Then, the solution $(x(t), y(t))$ cannot cross entirely the third quadrant. At this stage, the proof follows almost *mutatis mutandis* the steps of the proof of [137, Th. 2.1.], where the reader is sent for any further details. According to it, there exists a radius $R_0 \geq R$ such that, for every solution with $z_0 = x_0^2 + y_0^2 \geq R_0$,

$$\mathrm{rot}(z_0; [0, nT]) < 1. \tag{3.12}$$

By (3.11) and (3.12) the twist condition holds and, hence, by Theorem 3.1.1, the system (3.1) admits at least 2 nontrivial nT-periodic solutions belonging to different periodicity classes with rotation number $\omega \leq n$ for sufficiently large λ. This concludes the proof. □

In order to apply Theorem 3.1.1, the distribution of the weight functions settled by (3.8) is *optimal*. Indeed, if $\alpha_i = 0$, or $\beta_i = 0$, for some $i \in \{1, 2, 3\}$, then each of the points $(-r_0, 0)$ and $(r_0, 0)$, for sufficiently small $r_0 > 0$, have rotation number less than one in the interval $[0, T]$.

Remark 3.1.5. As already observed in [137, Rem. 3], without any significant change in the proof, a slightly more general version of Theorem 3.1.1 can be proven by assuming f, g only continuous (and not locally Lipschitz) and replacing the condition on the derivatives in (2.9) with the following one

$$0 < \liminf_{|y|\to 0} \frac{f(y)}{y} \le \limsup_{|y|\to 0} \frac{f(y)}{y} < \infty, \quad 0 < \liminf_{|x|\to 0} \frac{g(x)}{x} \le \limsup_{|x|\to 0} \frac{g(x)}{x} < \infty.$$

To this aim, instead of Theorem 3.1.1, one can apply the generalized version of the Poincaré–Birkhoff theorem due to Fonda and Ureña [78] for Hamiltonian systems where the uniqueness of the solutions of the initial value problems is not required (see also [74, Theorem 10.6.1] for the precise statement).

3.2 Counting T-periodic solutions and subharmonics

This section applies Theorem 3.1.2 to the model (3.1) when condition (3.8) holds. Recall that either $k = \ell$, or $|k - \ell| = 1$ and $m = \min\{k, \ell\}$. Based on Theorem 3.1.2, the next result holds.

Theorem 3.2.1. *Assume that $nm \ge 3$ for some integer $n \ge 1$. Then, there exists $\lambda_n > 0$ such that, for every $\lambda > \lambda_n$, (3.1) possesses, at least, $\sigma(n)$ periodic solutions with period nT, where*

$$\sigma(n) := \begin{cases} 2hm & \text{if } n = 3h, \\ 2\left(hm + \left[\frac{m}{3}\right]\right) & \text{if } n = 3h+1, \\ 2\left(hm + \left[\frac{2m}{3}\right]\right) & \text{if } n = 3h+2. \end{cases} \tag{3.13}$$

Moreover, setting

$$\gamma(n) := \mathrm{card}\left(\left\{1 \le j \le \frac{\sigma(n)}{2} \ : \ \gcd(j, n) = 1\right\}\right), \tag{3.14}$$

it turns out that, for every $\lambda > \lambda_n$, (3.1) has, at least, $2\gamma(n)$ periodic solutions with minimal period nT.

Proof. Suppose $k = \ell$. Then, $m = k = \ell$. Hence, according to (3.5) the total number of α and β-intervals in $[0, nT]$ equals

$$2nk = 2nm. \tag{3.15}$$

Thus, if $n = 3h$ for some integer $h \geq 1$, then, the sum of α-intervals and β-intervals in $[0, nT]$ is $6hk$. Hence, by Theorem 3.1.2, there exists $\lambda_n > 0$ such that, for every $\lambda > \lambda_n$, the solutions of (3.1) with sufficiently small $z_0 = (x_0, y_0)$ complete hk turns, whereas the solutions with sufficiently large z_0 cannot complete any. Therefore, by Theorem 3.1.1, (3.1) has, at least, two nT-periodic coexistence states with rotation number $j \in \{1, 2, \dots, hk\}$. Consequently, (3.1) possesses, at least, $2hk = \sigma(n)$ coexistence states with period nT.

Now, assume that $n = 3h + 1$ for some integer $h \geq 0$. Then, there are a total of

$$2mn = 2k(3h + 1) = 6hk + 2k = 6\left(hk + \tfrac{k}{3}\right)$$

α and β-intervals in $[0, nT]$. Thus, by Theorem 3.1.2, there exists $\lambda_n > 0$ such that, for every $\lambda > \lambda_n$, the solutions of (3.1) with sufficiently small z_0 complete $hk + \left[\frac{k}{3}\right]$ turns, while the solutions with large initial data cannot rotate. Therefore, thanks to Theorem 3.1.1, (3.1) possesses, at least,

$$2(hk + \left[\tfrac{k}{3}\right]) = \sigma(n)$$

periodic coexistence states of period nT.

Similarly, according to Theorems 3.1.1 and 3.1.2, when $n = 3h + 2$ for some integer $h \geq 0$, there exists $\lambda_n > 0$ such that, for every $\lambda > \lambda_n$, (3.1) possesses, at least,

$$2(hk + \left[\tfrac{2k}{3}\right]) = \sigma(n)$$

coexistence states with period nT.

The last assertion of the theorem will be derived from the fact that, owing to Remark 2.1.4, any nT-periodic coexistence state of (3.1) such that, for some $0 < r_0 < R_0$, satisfies

$$\begin{cases} \operatorname{rot}(z_0; [0, nT]) > \omega & \text{if } \|z_0\| = r_0, \\ \operatorname{rot}(z_0; [0, nT]) < \omega & \text{if } \|z_0\| = R_0, \end{cases} \tag{3.16}$$

has minimal period nT if $\gcd(n, \omega) = 1$. In all the cases covered by Theorem 3.2.1, we have actually proven the existence of $0 < r_0 < R_0$ such that

$$\begin{cases} \operatorname{rot}(z_0; [0, nT]) > \frac{\sigma(n)}{2} & \text{if } \|z_0\| = r_0, \\ \operatorname{rot}(z_0; [0, nT]) < 1 & \text{if } \|z_0\| = R_0, \end{cases}$$

by the definition of $\sigma(n)$. Thus, (3.16) holds for the choice $\omega = \frac{\sigma(n)}{2}$. Hence, taking $\gamma(n)$ as defined in (3.14), by Remark 2.1.4, the problem (3.1) possesses, at least, $2\gamma(n)$ coexistence states with minimal period nT. This concludes the proof. $\square$

3.3 An application to a class of predator-prey models

The non-autonomous planar Hamiltonian system (3.1) cover a large number of mathematical models of physical and biological nature. In particular, for the special choice

$$f(y) = e^y - 1 \quad \text{and} \quad g(x) = e^x - 1,$$

system (3.1) can be written, trough the change of variables

$$x = \log u \quad \text{and} \quad y = \log v,$$

as

$$\begin{cases} u' = \lambda\alpha(t)u(1-v), \\ v' = \lambda\beta(t)v(-1+u), \end{cases} \tag{3.17}$$

which is a non-autonomous T-periodic predator-prey model of Volterra type. As shown in [17, Section 5] and in [137, Introduction], system (3.17) can be obtained from the Volterra system with periodic coefficients

$$\begin{cases} p' = \lambda p\Big(a(t)p - b(t)q\Big), \\ q' = \lambda q\Big(-c(t) + d(t)p\Big), \end{cases}$$

after a suitable change of variables. It is clear that the (nontrivial) nT-periodic solutions of (3.1) are the nT-periodic coexistence states of (3.17). By a coexistence state it is meant a component-wise positive solution pair. This model was introduced in a degenerate setting in [141] and [123], and it will be deeply analyzed for all possible degenerate configurations in Section 5.6 of Chapter 5. Since the functions

$$f(y) = e^y - 1, \qquad g(x) = e^x - 1,$$

satisfy (2.9) and (2.10), according to Theorems 3.1.1, 3.1.2 and 3.2.1, the system (3.17) has, at least, $\sigma(n)$ coexistence states with period nT provided $n(k+\ell) \geq 6$; among them, $2\gamma(n)$ with minimal period nT.

3.4 Appendix: Index theory for planar Hamiltonian systems

In this appendix, we present a brief summary of the main results obtained in [21] in an abstract setting containing all planar systems analyzed in Part

I. Namely, we deal with planar Hamiltonian systems of the type

$$Jz' = \nabla_z H(t,z), \qquad z \in \mathbb{R}^2, \tag{3.18}$$

where

$$J = \begin{pmatrix} 0 & -1 \\ 1 & 0 \end{pmatrix}$$

is the standard symplectic matrix and the Hamiltonian function $H : \mathbb{R}\times\mathbb{R}^2 \to \mathbb{R}$ is continuous, T-periodic in the t-variable and differentiable in z with $\nabla_z H$ continuous with respect to (t,z). Moreover, we always assume that the uniqueness for the solutions of the Cauchy problems associated with system (3.18) is guaranteed. More precisely, we are concerned with the case in which system (3.18) can be linearized at zero and at infinity, meaning that

$$\nabla_z H(t,z) = S_0(t)z + o(|z|), \qquad z \to 0, \;\; \text{uniformly in } t \in [0,T],$$

and

$$\nabla_z H(t,z) = S_\infty(t)z + o(|z|), \qquad |z| \to +\infty, \;\; \text{uniformly in } t \in [0,T],$$

with $S_0(t)$ and $S_\infty(t)$ continuous paths of T-periodic symmetric matrices.

As carefully discussed in the pioneering paper [148], a powerful tool to be applied in this situation in order to investigate the T-periodic solvability of the system is represented by the celebrated Poincaré–Birkhoff fixed point theorem. Indeed, taking into account that the Hamiltonian structure of system (3.18) yields the area-preservation property of the associated Poincaré map, a planar annulus can be naturally constructed for the application of the fixed point theorem. More precisely, one can consider an annulus centered at the origin, and having a sufficiently small inner radius and a sufficiently large outer radius: in this way, the usual boundary twist condition of the Poincaré–Birkhoff theorem is implied by the existence of a sufficiently large gap for the winding numbers around the origin of the solutions of system (3.18) departing, respectively, from the inner and on the outer radius. The fact that these radii are chosen small and large enough ensures that the solutions departing from them differ not too much from the solutions of the linear systems $Jz' = S_0(t)z$ and $Jz' = S_\infty(t)z$, respectively: as a consequence, the existence of T-periodic solutions to the nonlinear system (3.18) can be ensured by imposing suitable conditions on (the winding number of the solutions of) the systems linearizing (3.18) at zero and at infinity.

As a consequence of the key [148, Lemma 4], the winding number

$$\eta_T(\omega) = \frac{\theta(T;\omega) - \omega}{2\pi}$$

of the solution (having $\theta(T;\omega)$ as angular component and starting at $e^{-i\omega}$) of a (non-resonant) linear planar Hamiltonian system can be completely characterized in terms of its so-called Conley–Zehnder index[*], i_T, a topological index of symplectic nature which has a crucial role when investigating periodic solutions of Hamiltonian systems (also in higher dimension) via variational methods, see [2].

First in [21], it is provided a recap of the index theory for linear planar Hamiltonian systems with periodic coefficients, with special emphasis on the relation between the Conley–Zehnder index and the winding number of the solutions. Even if we essentially rely on the results already given in [148], our point of view is slightly different. Indeed, we move from an a priori classification for the angular behavior of the solutions of a (possibly resonant) linear Hamiltonian system: in such a way, we are naturally led to a definition of the Conley–Zehnder index for resonant systems, which differs from the classical one but seems to be more appropriate from the point of view of the rotational behavior of the solutions (and, in turn, for the application of the Poincaré–Birkhoff theorem to nonlinear systems). Moreover, for such a classification, it is also crucial the study performed in [19, Appendix C] about the winding number η_T, which allow us to prove which are all the possible behaviors for η_T. As a by-product of the analysis, the relation with the stability of the system is also presented. Hence, denoting by μ_1 and μ_2 the eigenvalues of the monodromy matrix associated to a planar linear Hamiltonian system and given $\ell \in \mathbb{Z}$, the next tables hold true. The resonant cases are the ones in which the eigenvalues μ_1 and μ_2 equal one.

Case 1: $\ell - 1/2 < \eta_T^- \leq \ell \leq \eta_T^+ < \ell + 1/2$			
η_T	i_T	Eigenvalues	Stability
$\ell - 1/2 < \eta_T^- < \ell < \eta_T^+ < \ell + 1/2$	2ℓ	$\mu_1 = 1/\mu_2 \in \mathbb{R}^+_*$	Unstable
$\ell - 1/2 < \eta_T^- < \eta_T^+ = \ell$	2ℓ	$\mu_1 = \mu_2 = 1$	Unstable
$\ell = \eta_T^- < \eta_T^+ < \ell + 1/2$	2ℓ	$\mu_1 = \mu_2 = 1$	Unstable
$\ell = \eta_T^- = \eta_T^+$	2ℓ	$\mu_1 = \mu_2 = 1$	Stable

[*]In [2, 148] the name Maslov index is used. Actually, the Maslov index is a more general object, defined as an intersection index for a pair of paths in the Lagrangian Grassmanian: it turns out that the Conley–Zehnder index (of a linear Hamiltonian system with periodic coefficients) can be obtained as a particular case of this general setting, cf. [32]. Nowadays, the name Conley–Zehnder index is typically preferred.

Case 2: $\ell < \eta_T^- \leq \eta_T^+ < \ell+1$			
η_T	i_T	Eigenvalues	Stability
$\ell < \eta_T^- < \ell+1/2 < \eta_T^+ < \ell+1$	$2\ell+1$	$\mu_1 = 1/\mu_2 \in \mathbb{R}_*^-$	Unstable
$\ell < \eta_T^- < \eta_T^+ = \ell+1/2$	$2\ell+1$	$\mu_1 = \mu_2 = -1$	Unstable
$\ell+1/2 = \eta_T^- < \eta_T^+ < \ell+1$	$2\ell+1$	$\mu_1 = \mu_2 = -1$	Unstable
$\ell+1/2 = \eta_T^- = \eta_T^+$	$2\ell+1$	$\mu_1 = \mu_2 = -1$	Stable
$\ell < \eta_T^- \leq \eta_T^+ < \ell+1/2$	$2\ell+1$	$\mu_1 = \bar{\mu}_2 \in \mathbb{S}_*^1$	Strong Stable
$\ell+1/2 < \eta_T^- \leq \eta_T^+ < \ell+1$	$2\ell+1$	$\mu_1 = \bar{\mu}_2 \in \mathbb{S}_*^1$	Strong Stable

Further, in [21, Sec.3] we deal again with linear planar Hamiltonian systems, focusing our attention on two asymptotic indices which turn out to be the crucial ones when dealing with the problem of subharmonics. Such indices are known as *mean Conley-Zehnder index* and *rotation number* and they are defined, respectively, as

$$m = \lim_{k\to+\infty} \frac{i_{kT}}{k} \qquad \text{and} \qquad \rho = \lim_{k\to+\infty} \frac{\theta(kT;\omega)-\omega}{2\pi k}.$$

Once defined these two asymptotic indices, the following relations hold:

Case 1: $\ell-1/2 < \eta_T^- \leq \ell \leq \eta_T^+ < \ell+1/2$			
η_T	ρ	i_T	m
$\ell-1/2 < \eta_T^- < \ell < \eta_T^+ < \ell+1/2$	ℓ	2ℓ	2ℓ
$\ell-1/2 < \eta_T^- < \eta_T^+ = \ell$	ℓ	2ℓ	2ℓ
$\ell = \eta_T^- < \eta_T^+ < \ell+1/2$	ℓ	2ℓ	2ℓ
$\ell = \eta_T^- = \eta_T^+$	ℓ	2ℓ	2ℓ

Case 2: $\ell < \eta_T^- \leq \eta_T^+ < \ell+1$			
η_T	ρ	i_T	m
$\ell < \eta_T^- < \ell+1/2 < \eta_T^+ < \ell+1$	$\ell+1/2$	$2\ell+1$	$2\ell+1$
$\ell < \eta_T^- < \eta_T^+ = \ell+1/2$	$\ell+1/2$	$2\ell+1$	$2\ell+1$
$\ell+1/2 = \eta_T^- < \eta_T^+ < \ell+1$	$\ell+1/2$	$2\ell+1$	$2\ell+1$
$\ell+1/2 = \eta_T^- = \eta_T^+$	$\ell+1/2$	$2\ell+1$	$2\ell+1$
$\ell < \eta_T^- \leq \eta_T^+ < \ell+1/2$	$\ell+\tau$	$2\ell+1$	$2(\ell+\tau)$
$\ell+1/2 < \eta_T^- \leq \eta_T^+ < \ell+1$	$\ell+\tau$	$2\ell+1$	$2(\ell+\tau)$

Finally, in [21, Sec.4], we investigate, via the Poincaré-Birkhoff theorem, the existence of subharmonic solutions to the nonlinear system (3.18). Our main result, which unifies and extends the ones obtained in [1, 208], provides the existence of large-order subharmonic solutions whenever the rotation numbers of the linearizations of system (3.18) are different and reads as follows.

Theorem 3.4.1. *Denoting by ρ_0 and ρ_∞ the rotation numbers of the linear systems $Jz' = S_0(t)z$ and $Jz' = S_\infty(t)z$, respectively, suppose that*

$$\rho_0 \neq \rho_\infty.$$

Then, there exists an integer $k^* \geq 1$ such that system (3.18) possesses subharmonic solutions of order k, for every $k \geq k^*$. More precisely, for every $k \geq k^*$ system (3.18) possesses at least two subharmonic solutions of order k making j turns around the origin in the interval $[0, kT]$, for every integer $j \neq 0$ coprime with k and such that

$$\frac{j}{k} \in (\min\{\rho_0, \rho_\infty\}, \max\{\rho_0, \rho_\infty\}) \,. \tag{3.19}$$

Let us notice that in principle it could be quite unclear if there are integers j coprime with k and satisfying (3.19); however, by an elementary prime number argument it can be shown that, on growing of k, more and more integers j with these properties can be found: hence from Theorem 3.4.1 we can infer that *the number of subharmonic solutions of order k goes to infinity as $k \to +\infty$.*

As a direct consequence of Theorem 3.4.1, there exists k^* such that the Volterra predator-prey model

$$\begin{cases} u' = \lambda\alpha(t)u(1-v), \\ v' = \lambda\beta(t)v(-1+u), \end{cases}$$

already presented in (3.17), has subharmonics of order k for every $k \geq k^*$ if $\alpha(t) \gneq 0$ and $\beta(t) \gneq 0$, which can be seen as a dual result of the ones obtained in Theorem 2.1.5 and Section 3.3.

Chapter 4

Chaotic dynamics

It is the aim of this chapter to show a simple mechanism producing chaotic dynamics for system

$$\begin{cases} x' = -\lambda\alpha(t)f(y), \\ y' = \lambda\beta(t)g(x), \end{cases} \tag{4.1}$$

where $f, g : \mathbb{R} \to \mathbb{R}$ satisfy again conditions (2.9) and (2.10) as presented in Chapter 2. To be more specific and just to fix a possible case, we will suppose that f is bounded on $(-\infty, 0]$. In order to prove chaotic dynamics in system (4.1), it will be initially assumed that the coefficient $\alpha(t)$ vanishes on some interval and the coefficient $\beta(t)$ satisfies some integral assumption. Then, other related cases will be also analyzed.

As already seen in Chapters 2 and 3, a possible application of system (4.1) is the Volterra predator-prey model just assuming

$$f(s) = g(s) = e^s - 1,$$

that is, considering the system

$$\begin{cases} x' = -\lambda\alpha(t)(e^y - 1), \\ y' = \lambda\beta(t)(e^x - 1). \end{cases} \tag{4.2}$$

The existence of complex dynamics for predator-prey equations has been studied since the Eighties, mostly from a numerical point of view (see Takeuchi and Adachi [197]). Evidence of chaos has been detected in numerical simulations for three-dimensional (or higher-dimensional) autonomous systems, for instance for the interaction of one predator with two preys or the case of a prey, a predator and a top predator, as well as introducing as a third variable a nutrient.

For the two-dimensional case results have been obtained for discrete models of Holling type, as, e.g., those of Agiza et al. [4], which are in line with the classical works of May [151] and Li and Yorke [115], when proving chaos for discrete single species logistic-type equations. Other examples of chaos for two-dimensional systems have been numerically produced by adding some delay effects in the equations, as in Nakaoka, Saito and Takeuchi [158].

But less results are available in the literature concerning chaotic-like solutions to planar predator-prey systems with periodic coefficients (see, for instance, Baek and Do [10], Broer et al. [24], Kuznetsov, Muratori and Rinaldi [109] and Volterra [200]). Typical features of these models is to add logistic and/or Holling growth effects on the prey population and assume that the intraspecific growth rate takes the form $r(1+\varepsilon\sin(\omega t))$. The special choice of the periodic coefficient allows to study numerically the bifurcation diagrams to give evidence of complex dynamics for some choices of the parameters.

Up to the best of our knowledge, only very few results provide a complete analytic proof of the presence of chaotic dynamics, without the need of numeric support, for the classical Volterra predator-prey system with periodic coefficients. In Pireddu and Zanolin [171] the Volterra original system with harvesting effects was considered and it was proved that chaos may arise under special forms of a periodic harvesting; these authors also considered a case of intermittency in the predation in [172, pp.221-225]. Also in Ruiz-Herrera [182], a rigorous analysis of chaos for periodically perturbed planar systems, was performed for a case in which the Volterra system switches periodically to new system with logistic effects and no predation.

The introduction of the parameter $\lambda > 0$ in (4.1) is not relevant from the mathematical point of view. For us it is convenient in order to make a comparison to the result about subharmonic solutions obtained in the chapters of Part I. The main theorem of this section is the following one.

Theorem 4.0.1. *Assume that there exists $T_0 \in (0,T)$ such that:*

(c_1) $\alpha \gneq 0$, $\beta \gneq 0$ *on* $[0,T_0]$ *and there exists* $\hat{t} \in [0,T_0]$ *with* $\alpha(\hat{t})\beta(\hat{t}) > 0$;

(c_2) $\alpha \equiv 0$ *and* $\beta \gneq 0$ *on* $[T_0,T]$.

Then, for every $\ell \geq 2$, there exists $\lambda^* = \lambda^*_\ell$ such that, for each $\lambda > \lambda^*$, there exists a constant K_λ such that, if

$$\int_{T_0}^{T} \beta(t)\,dt > K_\lambda, \tag{4.3}$$

then, the Poincaré map associated with (4.1) induces chaotic dynamics on ℓ-symbols on some compact subset, $\mathcal{Q}$, of the first quadrant.

The proof of Theorem 4.0.1 is postponed to a next subsection. From the proof, it will become apparent how to determine the constants λ^* and K_λ.

As far as we know, this is the most general result available for complex dynamics to the predator-prey equations with periodic coefficients. In fact, the previous theorems of Pireddu and Zanolin [171, 172] and Ruiz-Herrera [182] required very specific structural assumptions on the coefficients, which were assumed to be stepwise, in order to transform Volterra equation to a switched system. Nevertheless, we will also present a less general version of Theorem 4.0.1 where β = constant > 0, α is a piecewise constant function vanishing on $[T_0, T]$, according to (c_2), and $f(s) = g(s) = e^s - 1$. This more elementary and special case is introduced in the following subsection in order to better explain the geometry and the dynamics associated to our system. Actually, for expository reasons, this chapter has been split into three parts. In Section 4.1, we perform a detailed analysis of the equation with a stepwise coefficient. Then, we show in Section 4.2 how the same geometrical ideas can be adapted to prove Theorem 4.0.1 and some related cases. Finally, in Section 4.3, we will recall some of the main features of the Smale's horseshoe, adapted to our situation here, in order to discuss a possible further improvement of our results from a numerical point of view.

4.1 The simplest model with chaotic dynamics

In this section we consider a special case of Theorem 4.0.1 that already exhibits all the significant geometrical features of the main result. Precisely, for a given $T_0 \in (0, T)$, we will consider the T-periodic functions $\alpha(t)$ and $\beta(t)$ defined by

$$\alpha(t) := \begin{cases} \alpha > 0 & \text{if } t \in [0, T_0), \\ 0 & \text{if } t \in [T_0, T), \end{cases} \qquad \beta(t) := \begin{cases} \beta_0 > 0 & \text{if } t \in [0, T_0), \\ \beta_1 > 0 & \text{if } t \in [T_0, T), \end{cases} \tag{4.4}$$

where the positive constants α and β_0, β_1 and the exact values of T_0 and T are going to be made precise later. Also, we will set $T_1 := T - T_0$. Thus, the dynamics of (4.2) on each of the intervals $[0, T_0]$ and $[T_0, T]$ are those of the associated autonomous Volterra predator-prey systems in the intervals $[0, T_0]$ and $[0, T_1]$, respectively.

Although the function $\alpha(t)$, and possibly $\beta(t)$, has a jump at $t = T_0$, for any given $z := (x_0, y_0) \in \mathbb{R}^2$, the Poincaré map associated to the system (4.2) in the interval $[0, T]$ is a diffeomorphism defined as

$$\begin{aligned} \Phi : \mathbb{R}^2 &\to \mathbb{R}^2 \\ z &\mapsto \Phi(z) := (x(T; z), y(T; z)), \end{aligned}$$

where $(x(t; z), y(t; z))$ stands for the unique solution of (4.2) such that

$$(x(0; z), y(0; z)) = z.$$

Under the assumption (4.4), the action of system (4.2) can be regarded as a composition of the actions of the systems

$$\text{(I)} \quad \begin{cases} x' = \alpha(1 - e^y) \\ y' = -\beta_0(1 - e^x) \end{cases} \qquad\qquad \text{(II)} \quad \begin{cases} x' = 0 \\ y' = -\beta_1(1 - e^x) \end{cases} \tag{4.5}$$

on each of the intervals $[0, T_0]$ and $[T_0, T]$, respectively. In this manner, system (4.2) turns out to be a *switched system* with a T-periodic *switching signal* and with (4.5)-(I) and (4.5)-(II) as *active subsystems*, according to the terminology adopted by Liberzon [116]. In other words, the Poincaré map Φ is the composition of the two Poincaré maps associated to each of these systems,

$$\Phi := \Phi_{T_1} \circ \Phi_{T_0},$$

where Φ_{T_0} and Φ_{T_1} stand for the Poincaré maps associated to the first and second systems of (4.5) on the intervals $[0, T_0]$ and $[0, T_1]$, respectively.

Subsequently, we denote by $\theta(t, z)$ the angular polar coordinate at time $t \geq 0$ of the solution $(x(t; z), y(t; z))$ for system (4.5)-(I). Then, for any given $\varrho > 0$, the rotation number of the solution in the interval $[0, \varrho]$ is defined through

$$\operatorname{rot}([0, \varrho], z) := \frac{\theta(\varrho, z) - \theta(0, z)}{2\pi}.$$

It is an algebraic counter, modulo 2π, of the winding number of the solution around the origin. It can be equivalently expressed using (1.14) on the first subsystem.

Dynamics of (4.2) in the interval $[0, T_0]$

We begin by analyzing the dynamics of (4.2) on $[0, T_0]$ under the action of Φ_{T_0}, i.e., the dynamics of (4.5)-(I). It is folklore that the phase-portrait of the (autonomous) system is a global nonlinear center around the origin, i.e., every solution different from the equilibrium $(0, 0)$ is periodic and determines a closed curve around the origin; the *first integral*, or *energy function*, of the system being

$$\mathcal{E}(x,y) = \alpha(e^y - y) + \beta_0(e^x - x). \tag{4.6}$$

Thus, setting

$$\omega := \mathcal{E}(0,0) = \alpha + \beta_0 = \min_{\mathbb{R}^2} \mathcal{E},$$

for every $\ell > \omega$, the corresponding level line of the first integral, $\Gamma(\ell) = \mathcal{E}^{-1}(\ell)$, is a closed orbit of a periodic solution. Moreover, by simply having a glance at the system, it is easily realized that the solutions run counter-clockwise around the origin.

Subsequently, for every $\ell > \omega$, we will denote by $\tau(\ell)$ the (minimal) period of the orbit $\Gamma(\ell)$. Thanks to a result of Waldvogel [206], the fundamental period map $\tau : (\omega, +\infty) \to \mathbb{R}$ is increasing and it satisfies

$$\lim_{\ell \downarrow \omega} \tau(\ell) = \frac{2\pi}{\sqrt{\alpha\beta_0}}, \qquad \lim_{\ell \uparrow +\infty} \tau(\ell) = +\infty.$$

For the rest of this section, we fix $\ell_1 > \omega$ and choose

$$T_0 := 2\tau(\ell_1). \tag{4.7}$$

If a solution of the system (4.5)-(I) crosses entirely the third quadrant, then, there exists an interval $[t_0, t_1] \subseteq [0, T_0]$, with $x(t_0) < 0$, $y(t_0) = 0$, $x(t_1) = 0$ and $y(t_1) < 0$, such that $x(t) < 0$ and $y(t) < 0$ for all $t \in (t_0, t_1)$. Thus, for every $t \in [t_0, t_1]$, we have that

$$|y(t)| = |\int_{t_0}^{t} \beta_0(e^{x(s)} - 1)\, ds| \le \int_{t_0}^{t_1} \beta_0\, ds \le \beta_0 T_0 =: M,$$
$$|x(t)| = |\int_{t}^{t_1} \alpha(1 - e^{y(s)})\, ds| \le \int_{t_0}^{t_1} \alpha\, ds \le \alpha T_0 =: N.$$

Hence, if there exists a $\tilde{t} \in [0, T_0]$ such that

$$x(\tilde{t}) < 0, \quad y(\tilde{t}) < 0, \quad x^2(\tilde{t}) + y^2(\tilde{t}) > M^2 + N^2,$$

then the solution cannot cross entirely the third quadrant in $[0, T_0]$, though, as all the solutions are periodic around the origin, all must cross the third quadrant in a sufficiently large time. Therefore, given (x_2, y_2) such that

$$x_2 < 0, \quad y_2 < 0, \quad x_2^2 + y_2^2 > M^2 + N^2$$

and setting $\ell_2 := \mathcal{E}(x_2, y_2)$ (and, without loss of generality, with $\ell_2 > \ell_1$), it becomes apparent that, if $z = (0, y_0) \in \Gamma(\ell_2)$ with $y_0 > 0$, then

$$\theta(t, z) \in [\pi/2, 3\pi/2) \quad \text{for all } 0 \le t \le T_0,$$

because the orbit through (x_2, y_2), $\Gamma(\ell_2)$, cannot cross the entire third quadrant in the time interval $[0, T_0]$. Consequently, by (4.7), we find that

$$\begin{cases} \operatorname{rot}([0, T_0], z) = 2 & \text{if } z \in \Gamma(\ell_1), \\ \operatorname{rot}([0, T_0], z) < 1/2 & \text{if } z = (0, y_0) \in \Gamma(\ell_2),\ y_0 > 0. \end{cases} \tag{4.8}$$

Subsequently, in order to analyze the Poincaré map Φ_{T_0}, we will focus attention into the annular region, $\mathcal{A}$, of the phase-plane enclosed by the orbits $\Gamma(\ell_1)$ and $\Gamma(\ell_2)$, where (4.8) holds, which has been represented in Figure 4.1, i.e.,

$$\mathcal{A} := \left\{(x, y) \in \mathbb{R}^2 \, : \, \ell_1 \le \mathcal{E}(x, y) \le \ell_2\right\} = \bigcup_{\ell_1 \le \ell \le \ell_2} \Gamma(\ell).$$

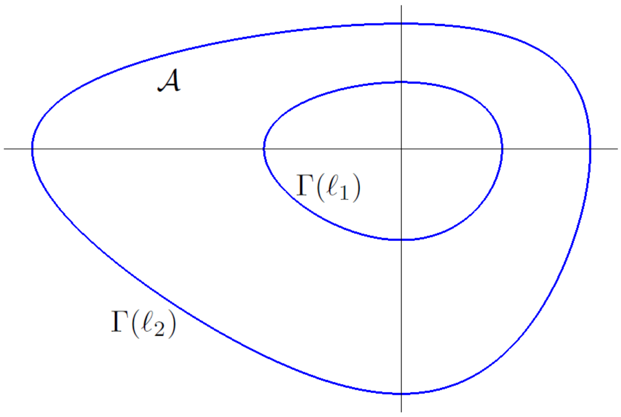

Figure 4.1: The region $\mathcal{A}$ enclosed by curves $\Gamma(\ell_1)$ and $\Gamma(\ell_2)$ with $\omega < \ell_1 < \ell_2$.

For graphical purposes, the aspect ratios in Figure 4.1 have been slightly modified. By the dynamical properties of (4.5)-(I), the Poincaré map Φ_{T_0} transforms the portion of $\mathcal{A}$ on the positive y-axis, i.e., the segment

$$\sigma_0 := \mathcal{A} \cap \{(0, y) \in \mathbb{R}^2 \, : \, y > 0\} = \{(0, y) \in \mathbb{R} \times (0, \infty) \, : \, \ell_1 \le \mathcal{E}(0, y) \le \ell_2\}$$

into the spiraling line plotted in Figure 4.2 (a). The unique $(0, y_1)$ such that $\mathcal{E}(0, y_1) = \ell_1$ remains invariant by Φ_{T_0} because $T_0 = 2\tau(\ell_1)$. Thus, $(0, y_1)$ gives two rounds around the orbit $\Gamma(\ell_1)$ as $t \in [0, T_0]$. Since the period map $\tau(\ell)$ is increasing with respect to ℓ, the points $(0, y) \in \sigma_0$ with $y > y_1$ close to y_1 cannot complete two rounds around the origin, though close to get it. The bigger is taken $y > y_1$, the bigger is the gap $\frac{\pi}{2} + 4\pi - \theta(T_0, (0, y))$, until y approximates y_2, the unique value of y such that $\mathcal{E}(0, y_2) = \ell_2$, where, according to the choice of $\Gamma(\ell_2)$, we already know that $\theta(T_0, (0, y)) < 3\pi/2$.

Similarly, defining $(x_+(\ell_1), 0)$ as the intersection of $\Gamma(\ell_1)$ with the positive x-axis, Figure 4.2 (b) shows a plot of the parallel (vertical) segment

$$\begin{aligned}\sigma_1 &:= \mathcal{A} \cap (\{x_+(\ell_1)\} \times [0, \infty)) \\ &= \{(x_+(\ell_1), y) \in \mathbb{R} \times [0, \infty) \,:\, \ell_1 \leq \mathcal{E}(x_+(\ell_1), y) \leq \ell_2\}.\end{aligned} \tag{4.9}$$

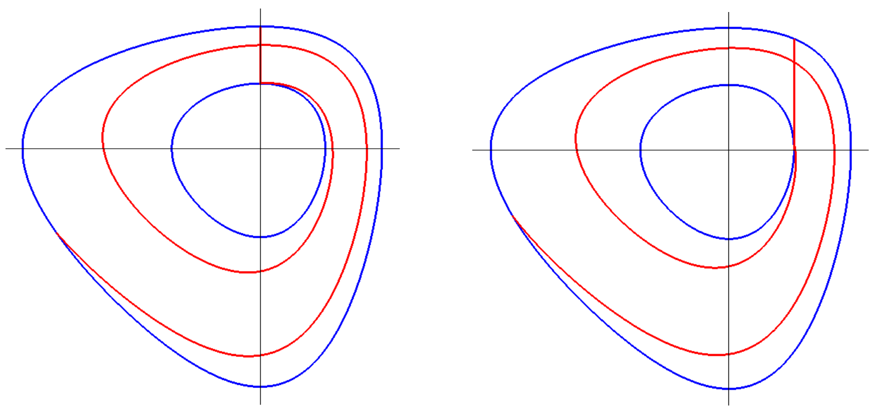

Figure 4.2: The segments σ_i and the curves $\Phi_{T_0}(\sigma_i)$ for $i = 0$ (left) and $i = 1$ (right).

The curves $\Phi_{T_0}(\sigma_i)$ look like sort of logarithmic spirals with the angular polar coordinate increasing along their trajectories. As illustrated by Figure 4.2 (b), $\Phi_{T_0}(\sigma_1)$ is a curve looking like $\Phi_{T_0}(\sigma_0)$.

Throughout the rest of this section, we consider the topological square, $\mathcal{Q}$, enclosed by the segments σ_0 and σ_1 in $\mathcal{A}$, i.e.,

$$\mathcal{Q} := \{(x, y) \in \mathcal{A} \,:\, 0 \leq x \leq x_+(\ell_1),\, y > 0\}.$$

The plot of Figure 4.3 shows $\Phi_{T_0}(\mathcal{Q})$, which is the spiral-like region enclosed in the annuls $\mathcal{A}$ and bounded by the curves $\Phi_{T_0}(\sigma_0)$ and $\Phi_{T_0}(\sigma_1)$. Subsequently, we will also consider the topological square

$$\mathcal{R} := \{(x, y) \in \mathcal{A} \,:\, 0 \leq x \leq x_+(\ell_1),\, y < 0\},$$

which has been also represented in Figure 4.3, where $\Phi_{T_0}(\mathcal{Q}) \cap \mathcal{R}$ consists of two smaller rectangular regions which have been named as $\mathcal{R}_0$ and $\mathcal{R}_1$.

Remark 4.1.1. For convenience in the exposition, we have chosen ℓ_1 and T_0 to satisfy (4.8). But one can adjust the parameters to have $T_0 \geq j\tau(\ell_1)$ for some integer $j \geq 2$, of course. In this case, we should modify the choice of ℓ_2 in order to get the second condition of (4.8). Now, we will have $\mathrm{rot}([0, T_0], z) \geq j$ if $z \in \Gamma(\ell_1)$ as first condition. Indeed, the intersection of $\Phi_{T_0}(\mathcal{Q})$ with $\mathcal{R}$ consists of $j \geq 2$ rectangular regions.

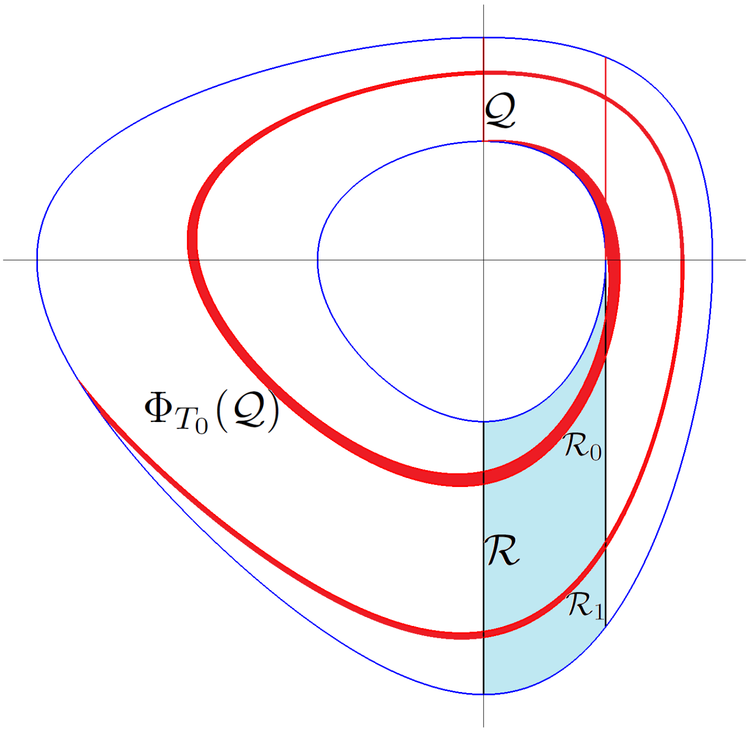

Figure 4.3: The regions $\mathcal{Q}$, $\mathcal{R}$, $\Phi_{T_0}(\mathcal{Q})$, $\mathcal{R}_0$ and $\mathcal{R}_1$.

Dynamics of (4.2) in the interval $[T_0, T] \equiv [0, T_1]$.

Throughout this paragraph we recall that $T_1 := T - T_0$ and consider the Poincaré map Φ_{T_1}. Choosing $\alpha = 0$ in the interval $[T_0, T]$ our main goal in this section is to show that, for sufficiently large $\beta_1 T_1 = \int_{T_0}^{T} \beta(t)\, dt > 0$, the region $\mathcal{R}$ is mapped across $\mathcal{Q}$ by the Poincaré map Φ_{T_1}. Actually we have that $\Phi_{T_1}(\mathcal{R})$ intersects transversally $\mathcal{Q}$. Such transversality entails a complex behavior reminiscent of Smale's horseshoe.

Since $\alpha(t) = 0$ and $\beta(t) = \beta_1$ for all $t \in [0, T_1]$ in (4.5)-(II), we have that

$$x'(t) = 0 \ \text{ and } \ x(t) = x_0 \ \text{ for all } \ t \in [0, T_1]. \tag{4.10}$$

Thus,

$$y(T_1) - y(0) = \int_0^{T_1} \beta_1(e^{x_0} - 1)dt = \beta_1(e^{x_0} - 1)T_1. \tag{4.11}$$

By (4.10) and (4.11), we find that $\Phi_{T_1}(z) = z$ if $z = (0, y_0) \in \mathcal{R}$, and, hence,

$$\Phi_{T_1}(\{(x, y) \in \mathcal{R} \,:\, x = 0\}) = \{(x, y) \in \mathcal{R} \,:\, x = 0\}.$$

In other words, the left side of $\mathcal{R}$ consists of fixed points of Φ_{T_1}.

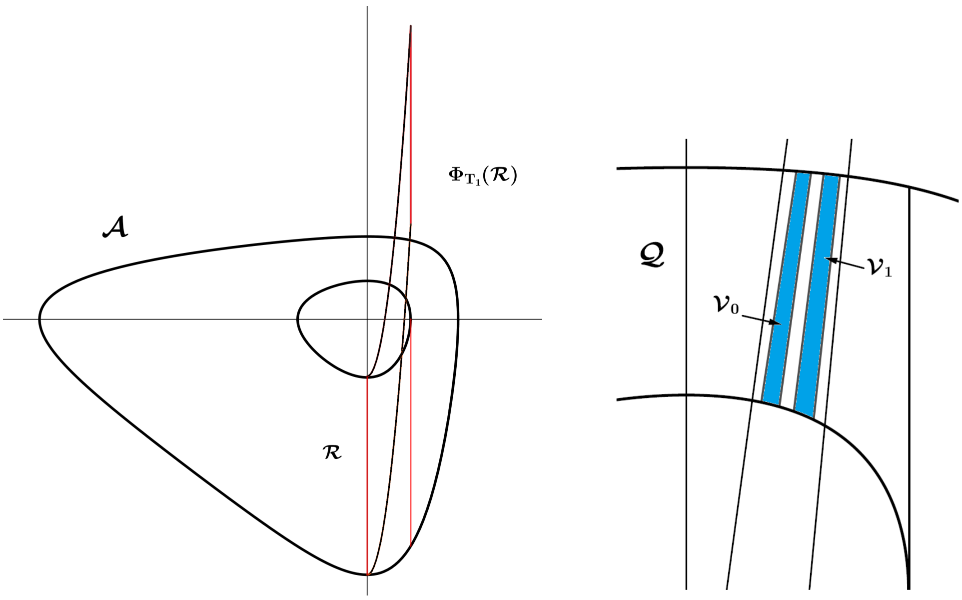

Figure 4.4: The topological squares $\mathcal{R}$ and $\Phi_{T_1}(\mathcal{R})$ (left panel), as well as the squares $\mathcal{V}_0 := \Phi_{T_1}(\mathcal{R}_0) \cap \mathcal{Q}$ and $\mathcal{V}_1 := \Phi_{T_1}(\mathcal{R}_1) \cap \mathcal{Q}$ (right panel).

On the other hand, by (4.10), for every $z = (x_1, y) \in \mathcal{R}$, with $0 < x_1 \leq x_+(\ell_1)$, we have that $x(t) = x_1$ for all $t \in [0, T_1]$, and hence

$$y(T_1) - y(0) = \int_0^{T_1} \beta_1(e^{x_1} - 1)dt = \beta_1(e^{x_1} - 1)T_1.$$

Consequently, if we denote by $y_2^- < 0$ and $y_2^+ > 0$ the unique values of y such that $\mathcal{E}(0, y_2^\pm) = \ell_2$, then, setting $M^* = M^*(\ell_2) := \max\{|y_2^-|, |y_2^+|\}$ and choosing T_1 satisfying

$$T_1 > \frac{2M^*}{\beta_1(e^{x_+} - 1)}, \quad \text{for } x_+ := x_+(\ell_1), \tag{4.12}$$

it becomes apparent that $y(T_1) - y(0) > 2M^*$. So,

$$\Phi_{T_1}(\{(x, y) \in \mathcal{R} : x = x_+\}) \subsetneq \{x_+\} \times (y_2^+, \infty).$$

Therefore, for $i = 1, 2$, the topological rectangle $\mathcal{V}_i := \Phi_{T_1}(\mathcal{R}_i) \cap \mathcal{Q}$ crosses $\mathcal{Q}$, transversally, as represented in the second picture of Figure 4.4. As (4.12) holds for sufficiently large $\beta_1 > 0$, regardless the size of T_1, as a rather direct consequence of the abstract theory of Papini and Zanolin [166, 167], it becomes apparent that, for every $T_0 \in (0, T)$, the problem (4.1), with the special choice (4.4), exhibits complex dynamics for sufficiently large $\beta_1 > 0$.

Actually, the geometry of the problem is very similar to the one considered by Pascoletti, Pireddu and Zanolin [168, Figs. 6, 7, 8] and Labouriau and Sovrano [110, Def. 3.3], consisting of a twist map acting in an annular region, composed with a shift map on a strip. The type of chaotic dynamics which occurs is that stated in Definition 1.0.1 with the semi-conjugation to the Bernoulli shift on two symbols. Actually, we can produce a semi-conjugation with respect to a larger set of ℓ symbols by suitably adapting the parameters $(\alpha, \beta_0, \beta_1)$ as well as T_0 and T_1, as already sketched in Remark 4.1.1. This concludes the proof of Theorem 4.0.1 for stepwise constant coefficients.

We omit the technical details regarding the application of the results from Papini and Zanolin [166, 167] for the special choice (4.4), since we will present this approach in a more thoroughly manner along the proof of Theorem 4.0.1. On the other hand, the case of stepwise constant coefficients in (4.4) and (4.5)-(I)&(II) suggests that, at least from a numerical point of view, we are in a situation where a stronger result about chaotic dynamics can be obtained, namely the *conjugation* to the Bernoulli automorphism, due to the presence of a Smale horseshoe. Indeed, the geometry that we have described above suggests a rather elementary mechanism to generate complex dynamics, by adopting the original methodology of Smale [188], as illustrated in the Conley–Moser approach in [156, Ch. III]. In the next subsection, we will prove Theorem 4.0.1 in its more general form, using the theory of topological horseshoes. Then, we will end this chapter by discussing some possible sharper results in the frame of the original horseshoe geometry, by assuming (4.1) with the special choice of coefficients in (4.4).

4.2 Proof of Theorem 4.0.1

As already discussed in Section 4.1, in order to prove the presence of chaotic dynamics according to Definition 1.0.1 there are various different approaches of topological nature, though these results provide a weaker form of chaos with respect to classical Smale's horseshoe, because they guarantee the semi-conjugation to the Bernoulli shift automorphism, instead of the conjugation. However, the approaches based on the the so-called theory of topological horseshoes, guarantee a broader range of applications. Here we briefly recall some basic facts from the "stretching along the path method", by specializing our presentation to planar homeomorphisms.

Let $\Phi : \mathbb{R}^2 \to \mathbb{R}^2$ be a planar homeomorphism and let $\mathcal{M}$ be a compact set of the plane which is homeomorphic to the unit square. We select two disjoint compact arcs on the boundary of $\mathcal{M}$ that we conventionally denote $\mathcal{M}^-_{\mathrm{left}}$ and $\mathcal{M}^-_{\mathrm{right}}$ and call the left and right sides of $\mathcal{M}$. Then, setting $\mathcal{M}^- :=$

$\mathcal{M}^-_{\text{left}} \cup \mathcal{M}^-_{\text{right}}$, the pair $\widehat{\mathcal{M}} := (\mathcal{M}, \mathcal{M}^-)$ is called an oriented rectangle. Given two oriented rectangles $\widehat{\mathcal{M}}$ and $\widehat{\mathcal{N}}$ and a compact set $\mathcal{H} \subset \mathcal{M}$, we write

$$(\mathcal{H}, \Phi) : \widehat{\mathcal{M}} \Bumpeq\!\!\!\!\!\!\!\!\longrightarrow \widehat{\mathcal{N}}$$

if the following property holds:

> for every path $\gamma_0 : [0,1] \to \mathcal{M}$ with $\gamma_0(0)$ and $\gamma_0(1)$ belonging to different components of $\mathcal{M}^-$, there exists a sub-path $\gamma_1 := \gamma_0|_{[s_0,s_1]}$ such that $\gamma_1(t) \in \mathcal{H}$ for all $t \in [s_0, s_1]$ and $\Phi(\gamma_1(t)) \in \mathcal{N}$ with $\Phi(\gamma_1(s_0))$ and $\Phi(\gamma_1(s_1))$ belonging to different components of $\mathcal{N}^-$.

If $\mathcal{H} = \mathcal{M}$, we just write $\Phi : \widehat{\mathcal{M}} \Bumpeq\!\!\!\!\!\!\!\!\longrightarrow \widehat{\mathcal{N}}$. Moreover, for any integer $\ell \geq 2$, we will use the notation

$$\Phi : \widehat{\mathcal{M}} \Bumpeq\!\!\!\!\!\!\!\!\longrightarrow^{\ell} \widehat{\mathcal{N}},$$

if there are ℓ pairwise disjoint (nonempty) compact sets $\mathcal{H}_0, \dots, \mathcal{H}_{\ell-1}$ in $\mathcal{M}$, such that

$$(\mathcal{H}_i, \Phi) : \widehat{\mathcal{M}} \Bumpeq\!\!\!\!\!\!\!\!\longrightarrow \widehat{\mathcal{N}} \quad \text{for all } \ i = 0, \dots, \ell - 1.$$

In the proof of Theorem 4.0.1 the following result, adapted from Pascoletti, Pireddu and Zanolin [168]) will be used.

Lemma 4.2.1. *Assume that $\Phi = \Phi_2 \circ \Phi_1$ and let $\widehat{\mathcal{Q}}$ and $\widehat{\mathcal{R}}$ be two oriented rectangles such that*

i) $\Phi_1 : \widehat{\mathcal{Q}} \Bumpeq\!\!\!\!\!\!\!\!\longrightarrow^{\ell} \widehat{\mathcal{R}}$ *for some $\ell \geq 2$,*

ii) $\Phi_2 : \widehat{\mathcal{R}} \Bumpeq\!\!\!\!\!\!\!\!\longrightarrow \widehat{\mathcal{Q}}$.

Then, Φ induces chaotic dynamics on ℓ symbols in the set $\mathcal{Q}$.

We are in position now to prove Theorem 4.0.1, with Φ_1 and Φ_2 the Poincaré maps associated to the system (4.1) in the intervals $[0, T_0]$ and $[T_0, T]$, respectively. Clearly, $\Phi = \Phi_2 \circ \Phi_1$ is the Poincaré map on the interval $[0, T]$ and its n-periodic points corresponds to the nT-periodic solutions to the differential system.

For the sake of simplicity in the exposition, we restrict ourselves to the case of $\ell = 2$ symbols, conventionally $\{0, 1\}$. The case of an arbitrary $\ell \geq 2$ can be easily proved via a simple modification of our argument.

As a first step, we focus our attention in the time-interval $[0, T_0]$ where the supports of α and β intersect nontrivially on a set containing a non-degenerate interval, J, where, without loss of generality, we can suppose that

$$\min_{t \in J} \{\alpha(t), \beta(t)\} \geq \varsigma_0 > 0.$$

In $[0, T_0]$ we are precisely in the same situation as in Section 2.1. Accordingly, for the sake of simplicity, we just recall some main facts from Section 2.1 which are needed for our proof. For a fixed $\eta > 0$ with $\min\{f'(0), g'(0)\} > \eta$, we can find a (small) radius $r_0 > 0$ such that

$$\theta(T_0, z_0) - \theta(0, z_0) \geq \lambda\eta\varsigma_0|J| \quad \text{for all} \;\; z_0 \;\; \text{with} \;\; \|z_0\| = r_0$$

(see formula (2.14)). Here, as in Section 4.1, we are denoting by $\theta(t, z_0)$ the angular coordinate associated with the solution of (4.1) with $z_0 \neq 0$ as initial point. Then, for

$$\lambda > \lambda^* := \frac{7\pi}{2\eta\varsigma_0|J|}, \tag{4.13}$$

we have that

$$\theta(T_0, z_0) > 4\pi \quad \text{if} \quad 0 \leq \theta(0, z_0) \leq \pi/2 \;\; \text{with} \;\; \|z_0\| = r_0. \tag{4.14}$$

On the other hand, following the same argument as in the previous steps (4.7)-(4.8) (see also the second part of the proof of Theorem 2.1.5), we can find a (large) radius $R_0 > r_0$ such that the solutions departing from the first quadrant outside the disc of radius R_0 cannot cross the third quadrant, that is

$$\theta(T_0, z_0) < \frac{3\pi}{2} \quad \text{if} \quad 0 \leq \theta(0, z_0) \leq \pi/2 \;\; \text{with} \;\; \|z_0\| = R_0. \tag{4.15}$$

Suppose now that $\lambda > \lambda^*$ is fixed. By the continuous dependence of the solutions from initial data (see Proposition 2.1.1) there are two radii r_λ and R_λ with

$$0 < r_\lambda \leq r_0 < R_0 \leq R_\lambda$$

such that any solution $\zeta(t; z_0)$ of (4.1) with z_0 in the first quadrant and $r_0 \leq \|z_0\| \leq R_0$ satisfies $r_\lambda \leq \|\zeta(t; z_0)\| \leq R_\lambda$ for all $t \in [0, T_0]$.

Subsequently, we introduce the sets

$$\mathcal{Q} := \{z = (x, y) \in \mathbb{R}^2 : 0 \leq x \leq r_0, \, y \geq 0, \, r_0 \leq \|z\| \leq R_0\},$$

and

$$\mathcal{Q}^-_{\text{left}} := \mathcal{Q} \cap C_{r_0}, \qquad \mathcal{Q}^-_{\text{right}} := \mathcal{Q} \cap C_{R_0},$$

where C_ρ denotes the circumference of center at the origin and radius $\rho > 0$, and

$$\mathcal{R} := \{z = (x, y) \in \mathbb{R}^2 : 0 \leq x \leq r_\lambda, \, y \leq 0, \, r_\lambda \leq \|z\| \leq R_\lambda\},$$

$$\mathcal{R}^-_{\text{left}} := \mathcal{R} \cap \{(x, y) : x = 0\}, \qquad \mathcal{R}^-_{\text{right}} := \mathcal{R} \cap \{(x, y) : x = r_\lambda\}.$$

So that the oriented rectangles $\widehat{Q}$ and $\widehat{R}$ are defined, too. It is obvious that both $\mathcal{Q}$ and $\mathcal{R}$ are homeomorphic to the unit square. For instance, the map

$$(u,v) \mapsto \Big(ur_0, (\varrho(v)^2 - u^2r_0^2)^{1/2}\Big),$$

with $\varrho(v) = r_0 + v(R_0 - r_0)$, provides a homeomorphism from the unit square $[0,1]^2$ onto $\mathcal{Q}$, mapping $v = 0$ to $\mathcal{Q}^-_{\text{left}}$ and $v = 1$ to $\mathcal{Q}^-_{\text{right}}$ and, similarly, the map

$$(u,v) \mapsto \Big(ur_\lambda, -(\varrho_\lambda(v)^2 - u^2r_\lambda^2)^{1/2}\Big),$$

with $\varrho_\lambda(v) = r_\lambda + v(R_\lambda - r_\lambda)$, provides a homeomorphism from the unit square onto $\mathcal{R}$, mapping $u = 0$ to $\mathcal{R}^-_{\text{left}}$ and $u = 1$ to $\mathcal{R}^-_{\text{right}}$. Thus, the definition of oriented rectangles is well posed.

We also introduce the pairwise disjoint compact (nonempty) subsets of $\mathcal{Q}$

$$\mathcal{H}_{1-j} := \{z \in \mathcal{Q} : \Phi_1(z) \in \mathcal{R},\, 3\pi/2+2j\pi \le \theta(T_0,z) \le 2\pi+2j\pi\} \quad \text{for } j = 0,1.$$

By definition,

$$\mathcal{H}_0 \sqcup \mathcal{H}_1 \subset \mathcal{Q} \cap \Phi_1^{-1}(\mathcal{R}).$$

Figure 4.5 shows a possible hierarchy of the sets $\mathcal{H}_0$ and $\mathcal{H}_1$ within $\mathcal{Q}$.

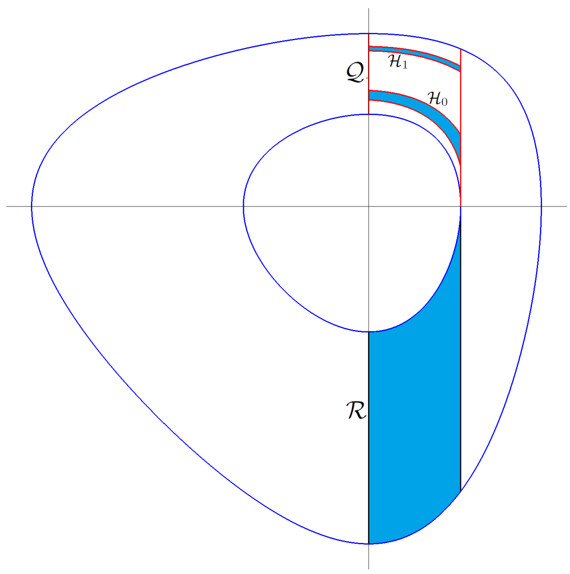

Figure 4.5: The sets $\mathcal{H}_0$ and $\mathcal{H}_1$, as well as $\mathcal{Q}$ and $\mathcal{R}$, for the stepwise constant coefficients studied in Section 3.1. Although in this special situation $\mathcal{H}_0 \sqcup \mathcal{H}_1 = \mathcal{Q} \cap \Phi_1^{-1}(\mathcal{R})$, by the choice of T_0, in general, $\mathcal{Q} \cap \Phi_1^{-1}(\mathcal{R})$ might contain more components.

Let $\gamma : [0,1] \to \mathcal{Q}$ be a continuous map such that $\gamma(0) \in \mathcal{Q}^-_{\text{left}}$ and $\gamma(1) \in \mathcal{Q}^-_{\text{right}}$ and let us consider the evolution of $\gamma(s)$ through the first Poincaré map Φ_1. The angular coordinate $\theta(T_0, \gamma(s))$ as a function of the parameter $s \in [0,1]$ is a continuous map which, according to (4.14) and (4.15) satisfies

$$\theta(T_0, \gamma(0)) > 4\pi, \quad \theta(T_0, \gamma(1)) \le 3\pi/2.$$

Hence, the path $s \mapsto \theta(T_0, \gamma(s))$ crosses at least twice the portion of the fourth quadrant between C_{r_λ} and C_{R_λ} and therefore it also crosses (at least twice) the region $\mathcal{R}$ from $x = 0$ to $x = r_\lambda$.

By an elementary continuity argument, there are two subintervals, $[s_0, s_1]$ and $[s_3, s_4]$, with $0 < s_0 < s_1 < s_3 < s_4 < 1$, such that, for every $s \in [s_0, s_1]$,

$$\theta(T_0, \gamma(s_0)) = 4\pi, \quad \theta(T_0, \gamma(s_1)) = \frac{3\pi}{2} + 2\pi, \quad \frac{3\pi}{2} + 2\pi \le \theta(T_0, \gamma(s)) \le 4\pi,$$

and, for all $s \in [s_3, s_4]$,

$$\theta(T_0, \gamma(s_3)) = 2\pi, \quad \theta(T_0, \gamma(s_4)) = \frac{3\pi}{2}, \quad \frac{3\pi}{2} \le \theta(T_0, \gamma(s)) \le 2\pi.$$

Thus, the path $[s_0, s_1] \ni s \mapsto \theta(T_0, \gamma(s))$ crosses the fourth quadrant and hence there is a subinterval $[s_0', s_1'] \subset [s_0, s_1]$ such that $\Phi_1(\gamma(s)) \in \mathcal{R}$ for all $s \in [s_0', s_1']$ with $\Phi_1(\gamma(s_0')) \in \mathcal{R}^-_{\text{right}}$ and $\Phi_1(\gamma(s_1')) \in \mathcal{R}^-_{\text{left}}$. By the definition of $\mathcal{H}_0$, we have that $\gamma(s) \in \mathcal{H}_0$ for all $s \in [s_0', s_1']$. Therefore, we have proved that $(\mathcal{H}_0, \Phi_1) : \widehat{Q} \Leftarrow\!\!\!\Rightarrow \widehat{R}$. In the same manner, we can find a subinterval $[s_3', s_4'] \subset [s_3, s_4]$ such that $\Phi_1(\gamma(s)) \in \mathcal{R}$ for all $s \in [s_3', s_4']$, with $\Phi_1(\gamma(s_3')) \in \mathcal{R}^-_{\text{right}}$ and $\Phi_1(\gamma(s_4')) \in \mathcal{R}^-_{\text{left}}$. Therefore, by the definition of $\mathcal{H}_1$ we have that $\gamma(s) \in \mathcal{H}_1$ for all $s \in [s_3', s_4']$, thus proving that $(\mathcal{H}_1, \Phi_1) : \widehat{Q} \Leftarrow\!\!\!\Rightarrow \widehat{R}$. This ends the proof of Lemma 4.2.1 (i) for $\ell = 2$.

To have the result for an arbitrary $\ell \ge 2$, we have just to modify the choice of λ^* in (4.13) to $\lambda > \lambda^* := (4\ell - 1)\pi/(2\eta\varsigma_0|J|)$ and introduce corresponding subsets $\mathcal{H}_0, \dots, \mathcal{H}_{\ell-1}$ of $\mathcal{Q} \cap \Phi_1^{-1}(\mathcal{R})$.

Now, we consider the map Φ_2 by studying the equation (4.1) in the interval $[T_0, T]$, where $\alpha \equiv 0$ and hence

$$\Phi_2(x_0, y_0) = \Big(x_0, y_0 + \lambda g(x_0) \int_{T_0}^{T} \beta(t)\, dt\Big).$$

Thus, the dynamics is the same as that of (4.2) in the interval $[T_0, T]$ considered in Section 3.1, modulo a minor change in the parameters involved. It is clear that the points on $\mathcal{R}^-_{\text{left}}$ remain stationary, while those of $\mathcal{R}^-_{\text{right}}$ move upward at the new position

$$y_0 + \lambda g(x_\lambda) \int_{T_0}^{T} \beta(t)\, dt \geq -R_\lambda + \lambda g(x_\lambda) \int_{T_0}^{T} \beta(t)\, dt.$$

Therefore, if

$$\int_{T_0}^{T} \beta(t)\, dt > K_\lambda := \frac{2R_\lambda}{\lambda g(x_\lambda)}, \tag{4.16}$$

then Lemma 4.2.1 (ii) holds. Indeed, any path in $\mathcal{R}$ linking the two sides of $\mathcal{R}^-$ is stretched to a path crossing entirely the set $\mathcal{Q}$ (from $\mathcal{Q}^-_{\text{left}}$ to $\mathcal{Q}^-_{\text{right}}$) and remaining inside the strip $[0, r_\lambda] \times \mathbb{R}$. This concludes the proof of Theorem 4.0.1. □

Remark 4.2.2. The chaotic dynamics associated with the Poincaré map $\Phi = \Phi_2 \circ \Phi_1$ comes from the composition of a twist rotation (due to Φ_1) with a shearing parallel to the y-axis (due to Φ_2). Clearly, if we consider the Poincaré map of initial time T_0, we will obtain $\Phi_1 \circ \Phi_2$ and, by a similar argument, through a symmetric counterpart of Lemma 4.2.1 where the order of the two maps is commuted, we may prove the existence of a horseshoe type structure inside the set $\mathcal{R}$. Moreover, using the fact that the shear map moves downward the points with $x < 0$ (in fact, $g(x) < 0$ for $x < 0$), we can also start from a set

$$\mathcal{Q} := \{z = (x, y) \in \mathbb{R}^2 : 0 \leq -r_0 \leq x \leq 0,\ y \leq 0,\ r_0 \leq \|z\| \leq R_0\}$$

and a target set

$$\mathcal{R} := \{z = (x, y) \in \mathbb{R}^2 : r_\lambda \leq x \leq 0,\ y \geq 0,\ r_\lambda \leq \|z\| \leq R_\lambda\},$$

again reversing the roles of $\mathcal{Q}$ and $\mathcal{R}$ by commuting Φ_1 with Φ_2.

Furthermore, we can obtain a variant of Theorem 4.0.1 by keeping condition (c_1) and modifying condition (c_2) to

(c_2') $\alpha \gneqq 0$ and $\beta \equiv 0$ on $[T_0, T]$.

In this situation, the assumption (4.3) should be replaced by a similar hypothesis involving $\int_{T_0}^{T} \alpha$. Under conditions $(c_1) - (c_2')$, the Poincaré maps produce a dynamics where a twist rotation is composed with a shearing parallel to the x-axis.

Remark 4.2.3. Hénon proposed in [90], as a model problem, the mapping given by the quadratic equations

$$x_1 = x \cos \alpha - (y - x^2) \sin \alpha, \qquad y_1 = x \sin \alpha + (y - x^2) \cos \alpha,$$

as a simple example of an area-preserving mapping which exhibits chaotic dynamics. The mapping in Hénon's model splits into a product of a shearing parallel to the y-axis and a rotation. It is interesting that the typical numerical features observed in the experiments in [90] appear also in Volterra's equations for the setting of Theorem 4.0.1, as shown in Figure 4.6.

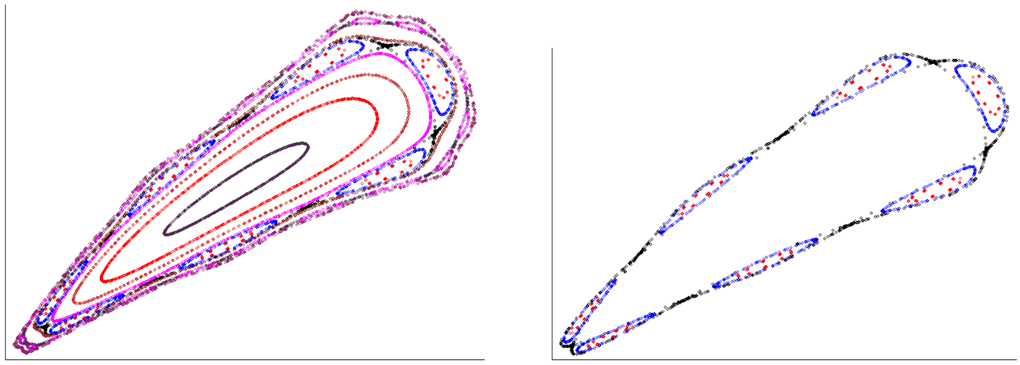

Figure 4.6: Some numerical experiments for a periodic Volterra system.

The left picture of Figure 4.6 shows the first 800 iterations of the Poincaré map for a Volterra system

$$\begin{cases} u' = \lambda\alpha(t)u(1-v), \\ v' = -\lambda\beta(t)v(1-u), \end{cases}$$

under the general assumptions of Theorem 4.0.1, starting from different initial points. The numerical experiments reveal the presence of stability regions (invariant curves around the constant coexistence state $(1, 1)$, according to Liu [117]), as well as some more complicated discrete orbits of "chaotic type". The right figure highlights some special orbits, in particular, seven-fold island chains (according to Arrowsmith and Place [8, p.262]) separated away by heteroclinic connections and including higher order subharmonics. See also Hénon [90, Figs. 4, 5].

Chaotic dynamics in the degenerate case for system (4.1)

To conclude our analysis, we show now how to adapt the proof of Theorem 4.0.1 to deal with degenerate weights in system (4.1). This will be achieved by applying the estimates previously obtained by the authors in Chapter 3, where results about the existence of periodic solutions for (4.1) were found when the functions α and β have a common support of zero measure.

To fix ideas, we suppose that in the interval $[0, T_0]$ there are ℓ positive humps of α separated away by $k = \ell$ positive humps of β, as in (3.3), with the corresponding support intervals intersecting on sets of zero measure. The symmetric case when, instead of (3.3), the condition (3.4) holds, can be treated similarly by interchanging the roles of α and β and modifying the choice of the initial set $\mathcal{Q}$ and the target set $\mathcal{R}$, as it will explained in Remark 4.2.5 below. Then the following result holds.

Theorem 4.2.4. *Assume that there exists $T_0 \in (0, T)$ such that:*

(c_1') $\ell = k \geq 4$, *with ℓ, k even integers;*

(c_2) $\alpha \equiv 0$ *and* $\beta \gneqq 0$ *on* $[T_0, T]$.

Then, there exists $\lambda^* = \lambda^*_\ell$ such that, for every $\lambda > \lambda^*$, there exists a constant K_λ for which, whenever

$$\int_{T_0}^{T} \beta(t)\, dt > K_\lambda, \tag{4.17}$$

the Poincaré map associated with (4.1) induces chaotic dynamics on $\ell/2$ symbols on some compact set $\mathcal{Q}$ contained in the first quadrant.

Proof. For simplicity in the exposition in the proof, we will focus attention in the case $\ell = k = 4$, where, starting on the region $\mathcal{Q}$ we obtain two crossings of the region $\mathcal{R}$ and, as a consequence, a complex dynamics on two symbols.

We will follow the same argument as in the proof of Theorem 4.0.1, just emphasizing the necessary modifications. As a first step, we will focus our attention in the time-interval $[0, T_0]$.

As the supports of α and β do not overlap, the associated dynamics is a composition of shear maps of the following form. If $\alpha \gneqq 0$, $\beta \equiv 0$ and $y > 0$ (resp. $y < 0$), the points are moved parallel to the x-axis from right to left (resp. from left to right). Similarly, when $\alpha \equiv 0$, $\beta \gneqq 0$ and $x < 0$ (resp. $x > 0$), then the points are moved parallel to the y-axis in a decreasing (resp. increasing) sense. Once passed two positive humps of α and an intermediate positive hump of β, the points in the first quadrant with $y_0 \geq \delta_0$ end in the fourth quadrant for sufficiently large $\lambda > 0$. Thus, after another interval where $\beta \gneqq 0$, we come back to the first quadrant and can repeat the process, as described in detail in Chapter 3. Since the points on the x-axis (resp. the y-axis) do not move when $\beta \equiv 0$ (resp. when $\alpha \equiv 0$), in the proof of this theorem it is convenient to slightly modify the choice of $\mathcal{Q}$ and $\mathcal{R}$ as follows

$$\mathcal{Q} := \{z = (x, y) \in \mathbb{R}^2 : 0 \leq x \leq r_1,\, y \geq 0,\, r_0 \leq \|z\| \leq R_0\},$$

for $0 < r_1 < r_0$, and

$$\mathcal{Q}^{-}_{\text{left}} := \mathcal{Q} \cap C_{r_0}, \qquad \mathcal{Q}^{-}_{\text{right}} := \mathcal{Q} \cap C_{R_0}.$$

In this manner, there is $\hat{y}_0 := (r_0^2 - r_1^2)^{1/2} > 0$ such that $y \geq \hat{y}_0$ for all $(x, y) \in \mathcal{Q}$. According to Lemmas 3.1.3, 3.1.4 and Theorem 3.1.2, for that choice, there exists λ^* such that the condition (4.14) is reestablished for every (fixed) $\lambda > \lambda^*$, i.e.,

$$\theta(T_0, z_0) > 4\pi \quad \text{if} \quad z_0 \in \mathcal{Q} \cup C_{r_0}. \tag{4.18}$$

On the other hand, exactly as explained above, for sufficiently large $R_0 > r_0$, the solutions departing from the first quadrant outside the disc of radius R_0 cannot cross the third quadrant, that is

$$\theta(T_0, z_0) < \frac{3\pi}{2} \quad \text{if} \quad z_0 \in \mathcal{Q} \cup C_{R_0}. \tag{4.19}$$

By continuous dependence, once fixed a $\lambda > \lambda^*$, one can find two radii r_λ and R_λ, with

$$0 < r_\lambda \leq r_1 < R_0 \leq R_\lambda,$$

such that any solution $\zeta(t; z_0)$ of (4.1) with $z_0 \in \mathcal{Q}$ lies in the set

$$\mathcal{R} := \{z = (x, y) \in \mathbb{R}^2 : 0 \leq x \leq r_\lambda,\, y \leq 0,\, r_\lambda \leq \|z\| \leq R_\lambda\},$$

for all $t \in [0, T_0]$.
Thus, much like in the proof of Theorem 4.0.1, we can also define

$$\mathcal{R}^{-}_{\text{left}} := \mathcal{R} \cap \{(x, y) : x = 0\}, \qquad \mathcal{R}^{-}_{\text{right}} := \mathcal{R} \cap \{(x, y) : x = r_\lambda\}.$$

From now on, we have just to repeat the proof of Theorem 4.0.1 without any significant change in order to show that $\Phi_1 : \widehat{\mathcal{Q}} \Bumpeq\!\!\!\!\longrightarrow^{2} \widehat{\mathcal{R}}$. The verification that $\Phi_2 : \widehat{\mathcal{R}} \Bumpeq\!\!\!\!\longrightarrow \widehat{\mathcal{Q}}$ proceeds exactly as before. Therefore, according to Lemma 4.2.1, we get the chaotic dynamics for $\Phi = \Phi_2 \circ \Phi_1$ on two symbols.

Note that, in order to produce a semi-conjugation on m-symbols, we need to make at least m-turns around origin, starting at $\mathcal{Q}$, in the time-interval $[0, T_0]$. This can be achieved, for sufficiently large λ, if both α and β are assumed to have, at least, $2m$ positive humps. The proof is complete. $\square$

Remark 4.2.5. If, instead of (3.3), the condition (3.4) holds, then we can assume (c_2'), instead of (c_2), and take $\mathcal{Q}$ and $\mathcal{R}$ to be *adjacent to the x-axis and opposite with respect to the y-axis.*

Chaotic dynamics when $\alpha(t)\beta(t) > 0$ for all $t \in [0, T]$.

So far, in this section we have studied the system (4.1) by assuming that either $\alpha \equiv 0$ and $\beta \gneq 0$, or $\beta \equiv 0$ and $\alpha \gneq 0$, on some time-interval. In both these cases, the dynamics is spanned by the superposition of a twist rotation with a shear map. In this section, we would like to stress the fact that a rich dynamics can be also produced, through a different mechanism, when α and β are throughout positive and appropriately separated away from each other, in a sense to be specified below. To analyze the simplest geometry, we restrict ourselves to consider the system (4.2) with stepwise constant function coefficients, $\alpha(t)$ and $\beta(t)$, as in Section 4.1. More precisely, we assume that $T = T_0 + T_1$ and

$$\beta(t) := \begin{cases} \beta_0 > 0 & \text{if } t \in [0, T_0), \\ \beta_1 > 0 & \text{if } t \in [T_0, T), \end{cases} \qquad \alpha(t) := \begin{cases} \alpha_0 > 0 & \text{if } t \in [0, T_0), \\ \alpha_1 > 0 & \text{if } t \in [T_0, T), \end{cases}$$

where the positive constants α_0, α_1, β_0, β_1 and the exact values of T_0 and T_1 will be made precise later. In this case, the dynamical behaviors of (4.2) on each of the intervals $[0, T_0]$ and $[T_0, T] \equiv [0, T_1]$ are those of the associated autonomous Volterra-type systems

$$\text{(I)} \quad \begin{cases} x' = \alpha_0(1 - e^y) \\ y' = -\beta_0(1 - e^x) \end{cases} \qquad \text{(II)} \quad \begin{cases} x' = \alpha_1(1 - e^y) \\ y' = -\beta_1(1 - e^x) \end{cases} \tag{4.20}$$

respectively. Note that the systems (4.20)-(I) and (4.20)-(II) have the same equilibrium point (the origin), and both describe a global center. However, for different choices of the pairs (α_0, β_0) and (α_1, β_1) the shape of the level lines of the Hamiltonian may change. Geometrically, this situation is reminiscent to that already studied by Takeuchi et al. in [198], where a predator-prey model with randomly varying coefficients was considered.

Now, making a choice so that

$$\frac{\beta_1}{\alpha_1} > \frac{\beta_0}{\alpha_0}, \tag{4.21}$$

or the converse inequality, it is possible to find level lines of the two systems crossing to each other.

From this, we can construct two annular domains $\mathcal{A}_0$ and $\mathcal{A}_1$, filled by periodic orbits of (4.20)-(I) and (4.20)-(II), respectively, in such a manner that the annuli intersect into four rectangular regions, as illustrated in Figure 4.7, where the annulus $\mathcal{A}_0$ is obtained for $\alpha_0 = \beta_0 = 1$ and the level lines passing through the initial points $(0, 0.8)$ and $(0, 1.5)$, whereas $\mathcal{A}_2$ is obtained for $\alpha_1 = 0.1, \beta_1 = 5$ and the level lines passing through the initial points $(0, 1.7)$ and $(0, 2.5)$. From a numerical point of view, the larger is the gap in condition (4.21), the wider are the linked annuli which can be constructed.

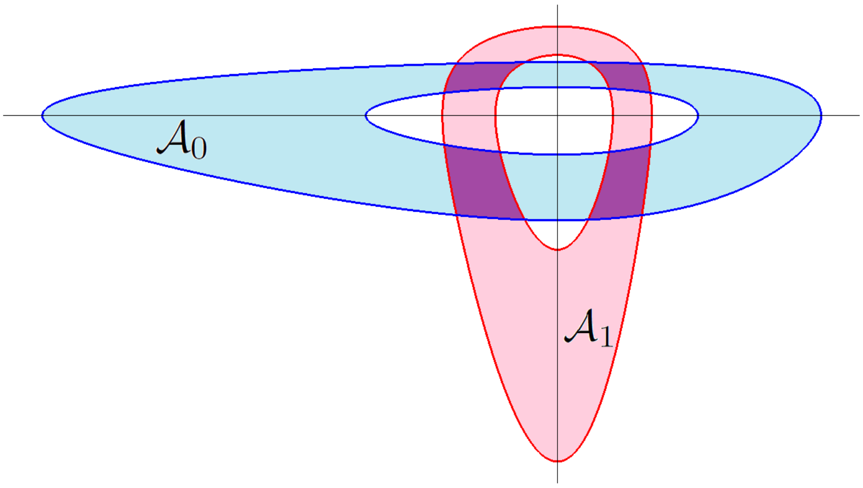

Figure 4.7: Two linked annuli $\mathcal{A}_0$ and $\mathcal{A}_1$ filled in by the periodic orbits of (4.20)-(I) and (4.20)-(II), respectively, and crossing to each other into four rectangular regions.

In general, to describe in a precise manner the construction of the two linked annuli, we denote by $\mathcal{E}_i$ the energy functions for the pair (α_i, β_i) $(i = 0, 1)$, so that

$$\mathcal{A}_i := \{(x, y) \in \mathbb{R}^2 : c_i \leq \mathcal{E}_i(x, y) \leq d_i\},$$

for

$$d_i > c_i > \min \mathcal{E}_i = \mathcal{E}_i(0, 0) = \alpha_i + \beta_i.$$

We also denote by $x_i^-(\ell) < 0 < x_i^+(\ell)$ the abscissas of the intersection points of the level line $\mathcal{E}_i = \ell \in [c_i, d_i]$ with the x-axis and, symmetrically, by $y_i^-(\ell) < 0 < y_i^+(\ell)$ the ordinates of the intersection points of the level line $\mathcal{E}_i = \ell \in [c_i, d_i]$ with the y-axis. Then $\mathcal{A}_0$ and $\mathcal{A}_1$ are *linked* provided that

$$x_0^-(c_0) < x_1^-(d_1), \;\; x_1^+(d_1) < x_0^+(c_0); \quad y_1^-(c_1) < y_0^-(d_0), \;\; y_0^+(d_0) < y_1^+(c_1).$$

This definition corresponds to that considered by Margheri, Rebelo and Zanolin [149] (see also Papini, Villari and Zanolin [165, Def. 3.2]). The regions obtained as intersections of the two annuli, are the four components of

$$\{(x, y) \in \mathbb{R}^2 : c_0 \leq \mathcal{E}_0(x, y) \leq d_0 \, \wedge \, c_1 \leq \mathcal{E}_1(x, y) \leq d_1\},$$

each one lying in a different quadrant. They are all homeomorphic to the unit square. Now, if we denote by $\mathcal{Q}$ and $\mathcal{R}$ any pair chosen among these four intersections, we define the following orientations

$$\mathcal{Q}^- := \{(x, y) \in \mathcal{Q} : \mathcal{E}_0(x, y) = c_0\} \cup \{(x, y) \in \mathcal{Q} : \mathcal{E}_0(x, y) = d_0\},$$

$$\mathcal{R}^- := \{(x,y) \in \mathcal{R} : \mathcal{E}_1(x,y) = c_1\} \cup \{(x,y) \in \mathcal{R} : \mathcal{E}_1(x,y) = d_1\},$$

not being relevant the order in which the names “left” and “right” in these components of $[\cdot]^-$ are assigned. Finally, if we denote by Φ_1 and Φ_2 the Poincaré maps associated with (4.20)-(I) and (4.20)-(II), respectively, by the monotonicity of the period map (already exploited as, for instance, in Remark 4.1.1), we can prove that $\Phi_1(\mathcal{Q})$ crosses ℓ-times $\mathcal{R}$ or, more precisely, $\Phi_1 : \widehat{\mathcal{Q}} \Leftrightarrow\!\!\!\rightarrow^{\ell} \widehat{\mathcal{R}}$, provided that T_0 is sufficiently large. Similarly, one can prove that $\Phi_2 : \widehat{\mathcal{R}} \Leftrightarrow\!\!\!\rightarrow^{m} \widehat{\mathcal{Q}}$, for sufficiently large T_1. Thus, a chaotic dynamics on $\ell \times m$ symbols is produced for the map Φ in the set $\mathcal{Q}$. Equivalently, instead of taking sufficiently large T_0 and T_1, one can put a parameter λ in front of α and β, with T_0 and T_1 fixed, to obtain complex dynamics on $\ell \times m$ symbols for all $\lambda > \lambda^*$, where λ^* depends on (ℓ, m), as well as on the several coefficients of the equation.

Here the geometrical configuration is the same as that considered by Burra and Zanolin [26], and later generalized by Margheri, Rebelo and Zanolin [149] and Papini, Villari and Zanolin [165]. The reader is sent to these references for any further technical details.

4.3 Ideal horseshoe dynamics

In this section, we will perform a schematic construction of the Smale’s horseshoe inspired on the numerical simulations of model (4.2) with an stepwise configuration of α and β as in (4.4). These simulations show that there is *transversal intersection* between the sets $\mathcal{H}_0, \mathcal{H}_1$ and $\Phi(\mathcal{H}_0), \Phi(\mathcal{H}_1)$ in the sense that, for $i, j \in \{1, 2\}$, the intersection

$$\mathcal{H}_i \cap \Phi(\mathcal{H}_j)$$

is a unique connected set. Assuming that this is the behavior for all forward and backward iterates of the Poincaré map Φ, implies that Φ is not only semi-conjugated to the Bernouilli shift, as proved in the previous subsections (also for the general case of Theorem 4.0.1), but also conjugated. Figures 4.12-4.13-4.14 give evidence of these facts.

We will assume that there are two disjoint proper *horizontal* topological squares, $\mathcal{H}_0$, $\mathcal{H}_1 \subsetneq \mathcal{Q}$, such that

$$\Phi(\mathcal{H}_i) := \mathcal{V}_i \quad \text{for } \; i \in \{0, 1\}. \tag{4.22}$$

By *horizontal*, we mean that the lateral sides of $\mathcal{H}_0$ and $\mathcal{H}_1$ lie on the lateral sides of the square $\mathcal{Q}$, as sketched in Figure 4.8. In this figure, as in the remaining figures of this section, we will represent any topological square as an homeomorphic square quadrangle. In order to have (4.22), it is assumed that

$$\Phi_{T_0}(\mathcal{Q}) \cap \mathcal{R} = \mathcal{R}_0 \cup \mathcal{R}_1$$

and, setting

$$\mathcal{V}_i := \Phi_{T_1}(\mathcal{R}_i) \cap \mathcal{Q}, \qquad i \in \{0,1\},$$

it follows that

$$\Phi_{T_1}(\Phi_{T_0}(\mathcal{Q}) \cap \mathcal{R}) \cap \mathcal{Q} = \Phi_{T_1}(\mathcal{R}_0 \cup \mathcal{R}_1) \cap \mathcal{Q} = \mathcal{V}_0 \cup \mathcal{V}_1.$$

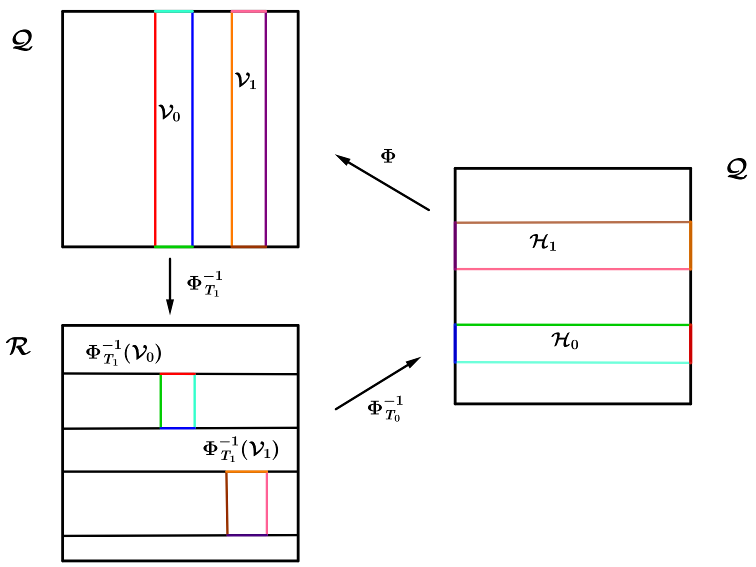

Figure 4.8: Φ establishes an homeomorphism between $\mathcal{H}_i$ and $\mathcal{V}_i$, $i \in \{0,1\}$.

By simply having a look at Figure 4.8, it is easily realized that, for every $i \in \{0,1\}$, $\mathcal{S}_i := \Phi_{T_1}^{-1}(\mathcal{V}_i)$ is a *vertical* sub-square of $\mathcal{R}_i$; vertical in the sense that it is a portion of $\mathcal{R}_i$ linking the upper and lower sides of $\mathcal{R}_i$. It turns out that Φ_{T_0} sends $\mathcal{R}_i \setminus \mathcal{S}_i$ outside $\mathcal{Q}$. Since

$$\mathcal{H}_i := \Phi_{T_0}^{-1}(\mathcal{S}_i) = \Phi_{T_0}^{-1}(\Phi_{T_1}^{-1}(\mathcal{V}_i)) = \Phi^{-1}(\mathcal{V}_i), \qquad i \in \{0,1\},$$

it is apparent that, for every $i \in \{0,1\}$, Φ establishes an homeomorphism between $\mathcal{H}_i$ and $\mathcal{V}_i$. In particular,

$$\Phi(\mathcal{H}_i) = \mathcal{V}_i \ \text{ and } \ \Phi^{-1}(\mathcal{V}_i) = \mathcal{H}_i \ \text{ for each } \ i \in \{0,1\}.$$

This feature is pivotal in the next construction. The intersection (in $\mathcal{Q}$) of the *vertical squares* $\mathcal{V}_i$ with the *horizontal squares* $\mathcal{H}_j$, $i, j \in \{0, 1\}$, generates $2^2 = 4$ topological squares in $\mathcal{Q}$, namely

$$\mathcal{Q}_{(i,j)} := \mathcal{V}_i \cap \mathcal{H}_j, \qquad i, j \in \{0, 1\},$$

which have been represented in Figure 4.9.

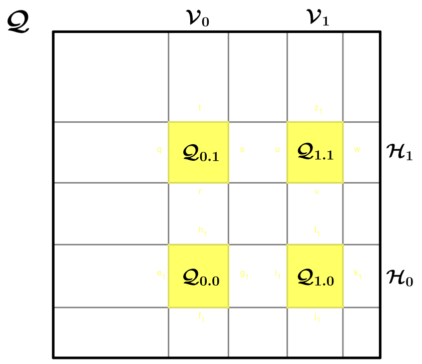

Figure 4.9: The invariant squares $\mathcal{Q}_{(i,j)}$, $i, j \in \{0, 1\}$.

Subsequently, we will denote Φ^0 the identity map. By construction, for every $s_{-1}, s_0 \in \{0, 1\}$ and

$$z \in \mathcal{Q}_{(s_{-1},s_0)} = \mathcal{V}_{s_{-1}} \cap \mathcal{H}_{s_0},$$

we have that

$$\Phi^0(z) = z \in \mathcal{H}_{s_0} \;\text{ and }\; \Phi^{-1}(z) \in \Phi^{-1}(\mathcal{V}_{s_{-1}}) = \mathcal{H}_{s_{-1}}. \tag{4.23}$$

In other words,

$$\Phi^0(\mathcal{Q}_{(s_{-1},s_0)}) = \mathcal{Q}_{(s_{-1},s_0)} \subset \mathcal{H}_{s_0}, \quad \Phi^{-1}(\mathcal{Q}_{(s_{-1},s_0)}) \subset \mathcal{H}_{s_{-1}}. \tag{4.24}$$

Naturally, the previous *duplication process* can be repeated for each of the topological squares $\mathcal{V}_i$, $i \in \{0, 1\}$. Much like $\mathcal{Q}$, for each $i \in \{0, 1\}$, the upper and lower sides of $\mathcal{V}_i$ consist of two arcs of trajectory of $\Gamma(\ell_2)$ and $\Gamma(\ell_1)$, respectively. Thus, replacing $\mathcal{Q}$ by $\mathcal{V}_i$ we can generate the four vertical topological squares

$$\mathcal{V}_{(i,j)} := \Phi(\mathcal{V}_i) \cap \mathcal{V}_j, \qquad i, j \in \{0, 1\}. \tag{4.25}$$

Then, as in $\mathcal{Q}$, $\mathcal{V}_0$ and $\mathcal{V}_1$, for every $i,j \in \{0,1\}$, $\mathcal{V}_{(i,j)}$ provides us with a vertical topological square linking $\Gamma(\ell_1)$ to $\Gamma(\ell_2)$; vertical in the sense that their upper and lower sides consist of certain arcs of trajectory of $\Gamma(\ell_2)$ and $\Gamma(\ell_1)$, respectively. According to (4.25), it becomes apparent that, for every $i,j \in \{0,1\}$,

$$\begin{aligned} \Phi^{-1}(\mathcal{V}_{(i,j)}) &= \Phi^{-1}(\Phi(\mathcal{V}_i) \cap \mathcal{V}_j) \subsetneq \Phi^{-1}(\mathcal{V}_j) = \mathcal{H}_j, \\ \Phi^{-2}(\mathcal{V}_{(i,j)}) &= \Phi^{-2}(\Phi(\mathcal{V}_i) \cap \mathcal{V}_j) \subsetneq \Phi^{-2}(\Phi(\mathcal{V}_i)) = \Phi^{-1}(\mathcal{V}_i) = \mathcal{H}_i. \end{aligned} \tag{4.26}$$

Similarly, we can duplicate the horizontal squares by setting

$$\mathcal{H}_{(i,j)} := \Phi^{-1}(\mathcal{H}_j) \cap \mathcal{H}_i, \qquad i,j \in \{0,1\}. \tag{4.27}$$

By construction, for every $i,j \in \{0,1\}$, $\mathcal{H}_{(i,j)}$ is an horizontal topological square connecting the lateral sides of $\mathcal{Q}$, i.e., linking $\{(x,y) \in \mathcal{Q} : x = 0\}$ to $\{(x,y) \in \mathcal{Q} : x = x_1\}$. By (4.27), we have that, for every $i,j \in \{0,1\}$,

$$\begin{aligned} \Phi^0(\mathcal{H}_{(i,j)}) &= \mathcal{H}_{(i,j)} = \Phi^{-1}(\mathcal{H}_j) \cap \mathcal{H}_i \subsetneq \mathcal{H}_i, \\ \Phi(\mathcal{H}_{(i,j)}) &= \Phi(\Phi^{-1}(\mathcal{H}_j) \cap \mathcal{H}_i) \subsetneq \Phi(\Phi^{-1}(\mathcal{H}_j)) = \mathcal{H}_j. \end{aligned} \tag{4.28}$$

Therefore, we can consider the $2^4 = 16$ topological squares in $\mathcal{Q}$ defined as

$$\mathcal{Q}_{(s_{-2},s_{-1},s_0,s_1)} := \mathcal{V}_{(s_{-2},s_{-1})} \cap \mathcal{H}_{(s_0,s_1)}, \qquad s_{-2}, s_{-1}, s_0, s_1 \in \{0,1\}. \tag{4.29}$$

We claim that, for every $s_{-2}, s_{-1}, s_0, s_1 \in \{0,1\}$,

$$\Phi^\kappa(\mathcal{Q}_{(s_{-2},s_{-1},s_0,s_1)}) \subsetneq \mathcal{H}_{s_\kappa}, \qquad \kappa \in \{-2,-1,0,1\}. \tag{4.30}$$

Indeed, by (4.29) and (4.28), we have that

$$\Phi(\mathcal{Q}_{(s_{-2},s_{-1},s_0,s_1)}) \subsetneq \Phi(\mathcal{H}_{(s_0,s_1)}) \subsetneq \mathcal{H}_{s_1}.$$

Thus, (4.30) holds for $\kappa = 1$. Moreover, by (4.29) and (4.27),

$$\Phi^0(\mathcal{Q}_{(s_{-2},s_{-1},s_0,s_1)}) = \mathcal{Q}_{(s_{-2},s_{-1},s_0,s_1)} \subset \mathcal{H}_{(s_0,s_{-1})} \subset \mathcal{H}_{s_0},$$

which establishes (4.30) for $\kappa = 0$. Similarly, according to (4.29) and (4.26)

$$\Phi^{-1}(\mathcal{Q}_{(s_{-2},s_{-1},s_0,s_1)}) \subsetneq \Phi^{-1}(\mathcal{V}_{(s_{-2},s_{-1})}) \subsetneq \mathcal{H}_{s_{-1}},$$

and

$$\Phi^{-2}(\mathcal{Q}_{(s_{-2},s_{-1},s_0,s_1)}) \subsetneq \Phi^{-2}(\mathcal{V}_{(s_{-2},s_{-1})}) \subsetneq \mathcal{H}_{s_{-2}},$$

which shows (4.30) for $\kappa = -1, -2$, which ends the proof of (4.30).

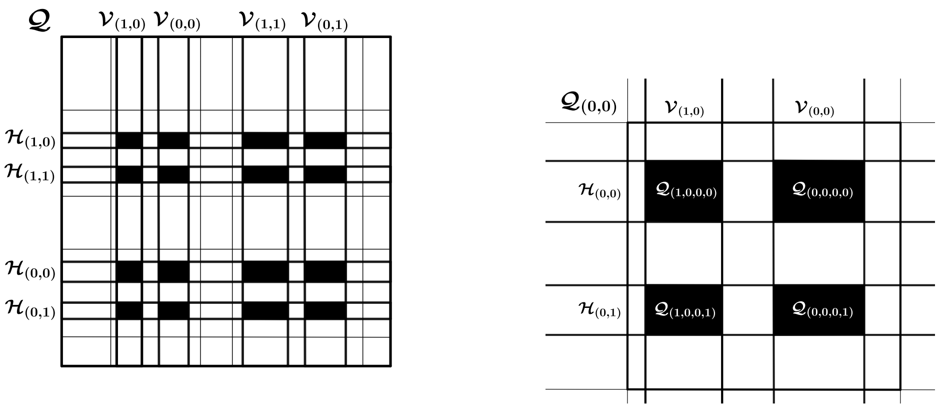

Figure 4.10: The squares $\mathcal{Q}_{(s_{-2},s_{-1},s_0,s_1)}$ (left), and a zoom of $\mathcal{Q}_{(0,0)}$ (right).

The first picture of Figure 4.10 represents the sixteen topological squares $\mathcal{Q}_{(s_{-2},s_{-1},s_0,s_1)}$, $s_i \in \{0,1\}$, $i \in \{-2,-1,0,1\}$, as defined by (4.29), while the second one provides a magnification of $\mathcal{Q}_{(0,0)}$ where the dyadic fractal behavior of this process can be appreciated.

Iterating m times the previous process, it turns out that we can generate 2^m vertical rectangles. Namely, for $v_m := (s_{-m},\dots,s_{-2},s_{-1}) \in \{0,1\}^m$,

$$\mathcal{V}_{v_m} := \Phi(\mathcal{V}_{(s_{-m},\dots,s_{-2})}) \cap \mathcal{V}_{s_{-1}} = \Phi(\overset{m}{\cdots} (\Phi(\mathcal{V}_{s_{-m}}) \cap \mathcal{V}_{s_{-m+1}}) \cdots) \cap \mathcal{V}_{-2}) \cap \mathcal{V}_{-1}.$$

Thus, by definition, for $\kappa \in \{-1,-2,\dots,-m\}$,

$$\Phi^{\kappa}(\mathcal{V}_{v_m}) \subsetneq \Phi^{-1}(\mathcal{V}_{s_\kappa}) = \mathcal{H}_{s_\kappa}. \tag{4.31}$$

Similarly, there exists 2^m horizontal rectangles such that for

$$h_m = (s_0, s_1, \dots, s_{m-1}) \in \{0,1\}^m,$$

it follows that

$$\mathcal{H}_{h_m} := \Phi(\mathcal{H}_{(s_1,\dots,s_{m-1})}) \cap \mathcal{H}_{s_0} = \Phi^{-1}(\overset{m-1}{\cdots} (\Phi^{-1}(\mathcal{H}_{s_{m-1}}) \cap \mathcal{H}_{s_{m-2}}) \cdots) \cap \mathcal{H}_{s_1}) \cap \mathcal{H}_{s_0}.$$

and, hence, for $\kappa \in \{0,1,\dots,m-1\}$,

$$\Phi^{\kappa}(\mathcal{H}_{h_m}) \subsetneq \mathcal{H}_{s_\kappa}. \tag{4.32}$$

Figure 4.11 shows the steps $m = 2$ and $m = 3$ of this process for both the vertical and horizontal squares.

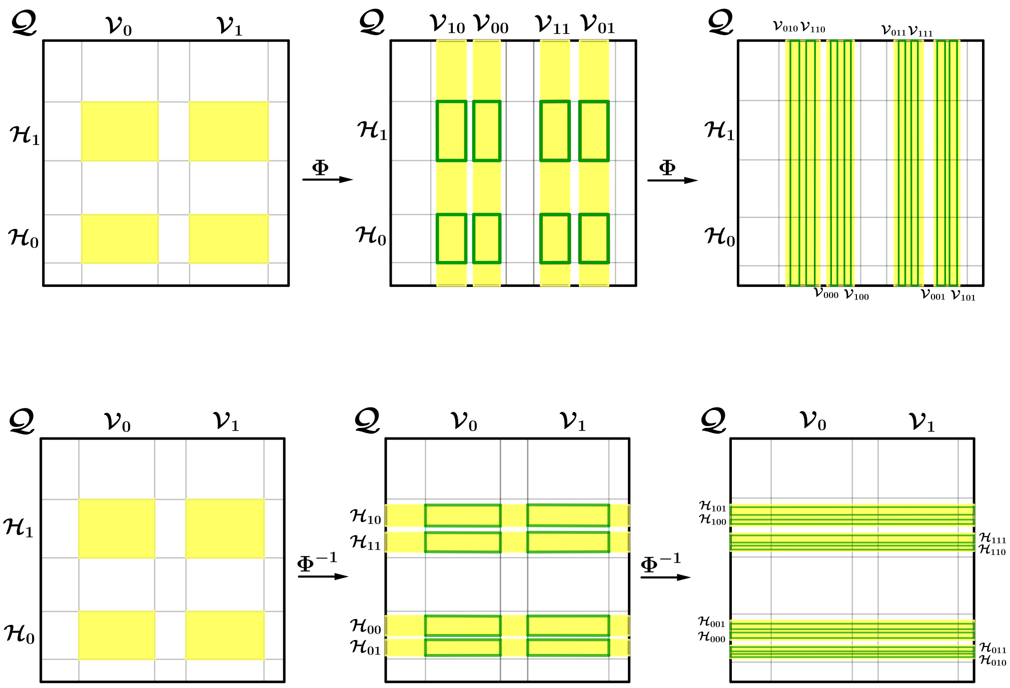

Figure 4.11: Dyadic fragmentation in horizontal and vertical lines.

Then, setting

$$\mathcal{Q}_{\Sigma_m} := \mathcal{V}_{v_m} \cap \mathcal{H}_{h_m},$$

where

$$\Sigma_m := (v_m, h_m) = (s_{-m}, \dots, s_{-1}, s_0, \dots, s_{m-1}) \in \{0,1\}^{2m},$$

it becomes apparent that, by (4.31) and (4.32), for every integer $\kappa \in [-m, m-1]$,

$$\Phi^{\kappa}(\mathcal{Q}_{\Sigma_m}) \subset \mathcal{H}_{s_\kappa}.$$

As we have constructed two sequences of nonempty compact, connected nested topological squares, $\mathcal{V}_{v_m}$, $\mathcal{H}_{h_m}$, by the Cantor principle,

$$\mathcal{V}_{s_v} := \lim_{m \to +\infty} \mathcal{V}_{v_m} \quad \text{and} \quad \mathcal{H}_{s_h} := \lim_{m \to +\infty} \mathcal{H}_{h_m}$$

are two nonempty continua with

$$s_v = (\dots, s_{-2}, s_{-1}) \in \{0,1\}^{\mathbb{N}}, \quad s_h = (s_0, s_1, \dots) \in \{0,1\}^{\mathbb{N}}.$$

Moreover, by the transversality assumptions, the intersection $\mathcal{V}_{s_v} \cap \mathcal{H}_{s_h}$ is a point and $(s_v, s_h) \in \{0,1\}^{\mathbb{Z}}$. Furthermore,

$$\Lambda := \bigcup_{s_v, s_h \in \{0,1\}^{\mathbb{N}}} \mathcal{V}_{s_v} \cap \mathcal{H}_{s_h}$$

is the invariant set of Φ. Therefore, thanks to the choice of the labels s_v and s_h that we have done, it becomes apparent that Φ is conjugated to the Bernoulli full shift in two symbols.

We conclude this section with some geometrical and numerical schemes illustrating the actual occurrence of the theoretical horseshoe framework described above. To simplify the exposition, we consider the case of an annular region under the effect of the composition of a twist map with a vertical shear map. Even if the geometry of the level lines associated with the predator-prey system does not consist of circumferences, nonetheless this can be assumed as a reasonable approximation if we consider small orbits around the equilibrium point (as in [117]) or we suppose to have performed an action-angle transformation leading to an equivalent planar system where the radial component is constant.

The following pictures describe the geometric effect of the composition of a twist map Φ_{T_0} and a vertical shear map Φ_{T_1} on a domain in the first quadrant which is defined like the set $\mathcal{Q}$ in Section 4.1, and denoted again by $\mathcal{Q}$. Actually, we describe the effect of the maps and their composition $\Phi = \Phi_{T_1} \circ \Phi_{T_0}$, with respect to the homeomorphic unit square $[0,1]^2$, considered as a reference domain, where we can transfer the geometry. Figure 4.12 shows $\mathcal{Q}$, its image through a twist map (with a sufficiently large twist, corresponding to a sufficiently large time T_0) and the effect on the unit square. More precisely, if we denote by $\eta = (\eta_1, \eta_2)$ the homeomorphism from the unit square to $\mathcal{Q}$, the two bands in the third panel of Figure 4.12 represent the sets $[0,1]^2 \cap (\hat{\eta}^{-1} \circ \Phi_{T_0} \circ \eta)^{-1}([0,1]^2)$ where $\hat{\eta} = (\eta_1, -\eta_2)$ is the homeomorphism from the unit square to $\mathcal{R}$, which is the target set in the fourth quadrant symmetric to $\mathcal{Q}$. As a next step, Figure 4.13 shows the effect on the vertical shear mapping on the set $\mathcal{R}$ and we also show the set of points in the unit square which are mapped into $\mathcal{Q}$, that is $[0,1]^2 \cap (\eta^{-1} \circ \Phi_{T_1} \circ \hat{\eta})^{-1}([0,1]^2)$.

Finally, Figure 4.14 puts in evidence the set of points of $\mathcal{Q}$, represented in the unit square, which come back to $\mathcal{Q}$ after $\Phi = \Phi_{T_1} \circ \Phi_{T_0}$, that is $[0,1]^2 \cap (\eta^{-1} \circ \Phi \circ \eta)^{-1}([0,1]^2)$. Obviously, this is a subset of the two bands domain appearing in the third panel of Figure 4.12.

If we consider the inverse homeomorphism $\Phi^{-1} = \Phi_{T_0}^{-1} \circ \Phi_{T_1}^{-1}$ and look for the sets of points of $\mathcal{Q}$ which remain in the domain after the first iteration, we can repeat, symmetrically the same argument as before. As a first step, passing to the unit square, we will consider the set of the points $w \in [0,1]^2$

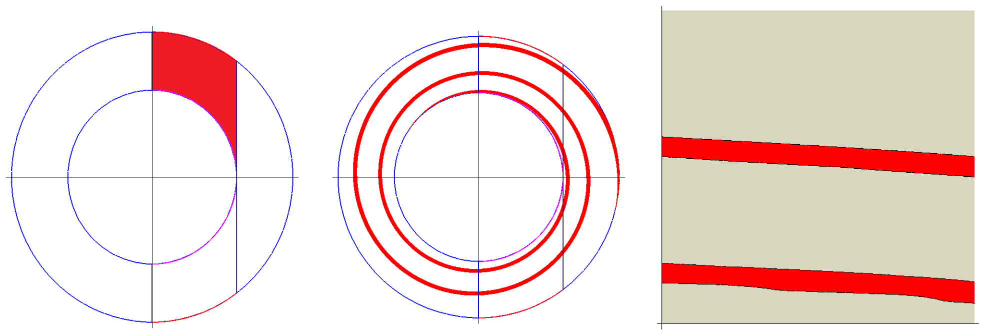

Figure 4.12: Example of an annular region under the action of a twist map. From left to right: a rectangular domain $\mathcal{Q}$ in the first quadrant, its evolution by a twist map, the part of the unit square (homeomorphic to $\mathcal{Q}$) which is mapped to the region in the fourth quadrant which is symmetric to $\mathcal{Q}$.

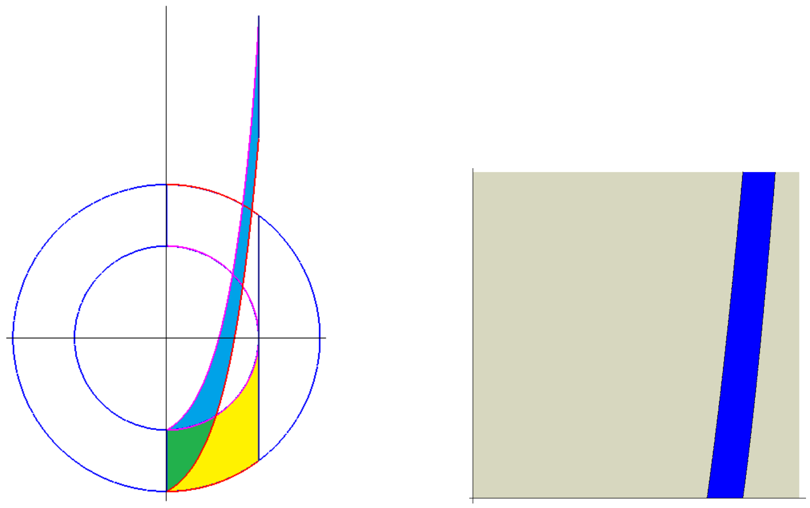

Figure 4.13: The region in the fourth quadrant (symmetric to $\mathcal{Q}$) and its transformation by a vertical shear map as in Section 4.1 (left panel). The right panel put in evidence, with respect to the homeomorphic unit square, the part of the region which arrives to $\mathcal{Q}$.

such that $(\hat{\eta}^{-1} \circ \Phi_{T_1}^{-1} \circ \eta)(w) \in [0,1]^2$, which clearly equals $[0,1]^2 \cap (\eta^{-1} \circ \Phi_{T_1} \circ \hat{\eta})^{-1}([0,1]^2)$, that is, the blue set appearing in the second panel of Figure 4.13. Next we will consider the set of points of $\mathcal{R}$ which belong to $\mathcal{Q}$ after the action of the inverse twist $\Phi_{T_0}^{-1}$, which transferred to the unit square is $[0,1]^2 \cap (\eta^{-1} \circ \Phi_{T_0}^{-1} \circ \hat{\eta})^{-1}([0,1]^2)$. This is exactly the set described in the third panel of Figure 4.12. At the end, the set $[0,1]^2 \cap (\eta^{-1} \circ \Phi^{-1} \circ \eta)^{-1}([0,1]^2)$ will be made by two narrow bands inside the rectangular region in the second panel of Figure 4.13.

From these numerical outcomes it is apparent that the "real dynamics" follows precisely the abstract scheme of the Smale's horseshoe map.

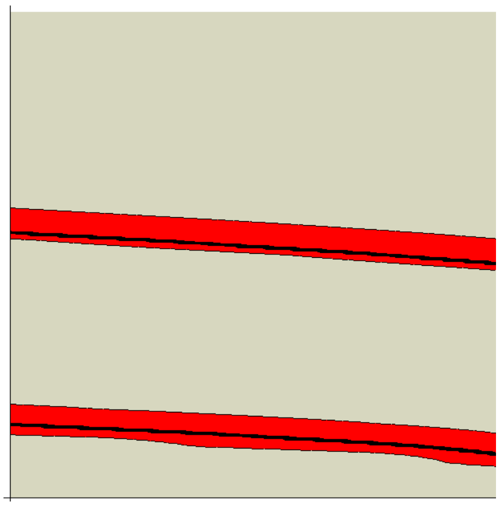

Figure 4.14: The final effect of the twist map and the vertical shear map, as viewed from the unit square. The larger horizontal bands represent the set of points in $\mathcal{Q}$ which are moved to $\mathcal{R}$ under the action of the twist map. The narrow darker bands represent the set of points which come back to $\mathcal{Q}$ after the application of the vertical shear map.

Chapter 5

The bifurcation approach

Once proved in the past chapters the existence of subharmonics and chaotic dynamics for a general class of planar Hamiltonian systems via the Poincaré–Birkhoff theorem and the "SAP" method, now it we will be established the global structure of the set of subharmonics for the specific predator-prey model

$$\begin{cases} u' = \alpha(t)u(1-v) \\ v' = \beta(t)v(-1+u). \end{cases} \tag{5.1}$$

Here, $\alpha(t)$ and $\beta(t)$ are real continuous T-periodic functions such that

$$\alpha = 0 \quad \text{on} \quad [\tfrac{T}{2}, T], \qquad \beta = 0 \quad \text{on} \quad [0, \tfrac{T}{2}], \tag{5.2}$$

$\alpha(t) > 0$ if $t \in (0, \frac{T}{2})$, and $\beta(t) > 0$ if $t \in (\frac{T}{2}, T)$, which entail $\alpha\beta = 0$. This model was introduced by J. López-Gómez, R. Ortega and A. Tineo [141] as a simple example of a predator-prey model with an unstable coexistence state. Later, it was shown in [123] that it actually admits at least two $2T$-periodic non-degenerate nontrivial coexistence states if

$$\int_0^T \alpha(t)\,dt \int_0^T \beta(t)\,dt > 4,$$

while it cannot have any non-trivial T-periodic coexistence state; the equilibrium $(1,1)$ is considered to be a trivial T-periodic coexistence state.

The main goal of this chapter is to construct the set of all subharmonics of (5.1) in the special, but extremely interesting case, when

$$A := \int_0^T \alpha(t)\,dt = \int_0^T \beta(t)\,dt > 0. \tag{5.3}$$

Precisely, it will be shown that, under assumption (5.3), the model (5.1) admits subharmonics of any order for the appropriate range of values of $A >$

0, which will be regarded as a bifurcation parameter throughout this chapter. Actually, our analysis establishes the existence of an integer $m^*(A) \geq 1$ such that (5.1) possesses, at least, *two* subharmonic solutions of order m for all $m \geq m^*(A)$. Moreover, as a direct consequence of our analysis,

$$\lim_{A\downarrow 0} m^*(A) = +\infty, \quad \text{whereas } \; m^*(A) = 2 \; \text{ if } \; A > 2. \tag{5.4}$$

Figure 5.1 summarizes, at a glance, the main findings of this chapter. It is an sketch of the global bifurcation diagram of subharmonics, where we are plotting the value of A in abscisas versus the value of $x = u_0 = v_0$ in ordinates. Naturally,

$$(u_0, v_0) = (u(0), v(0))$$

stands for the initial condition of (5.1). Each of the curves plotted in Figure

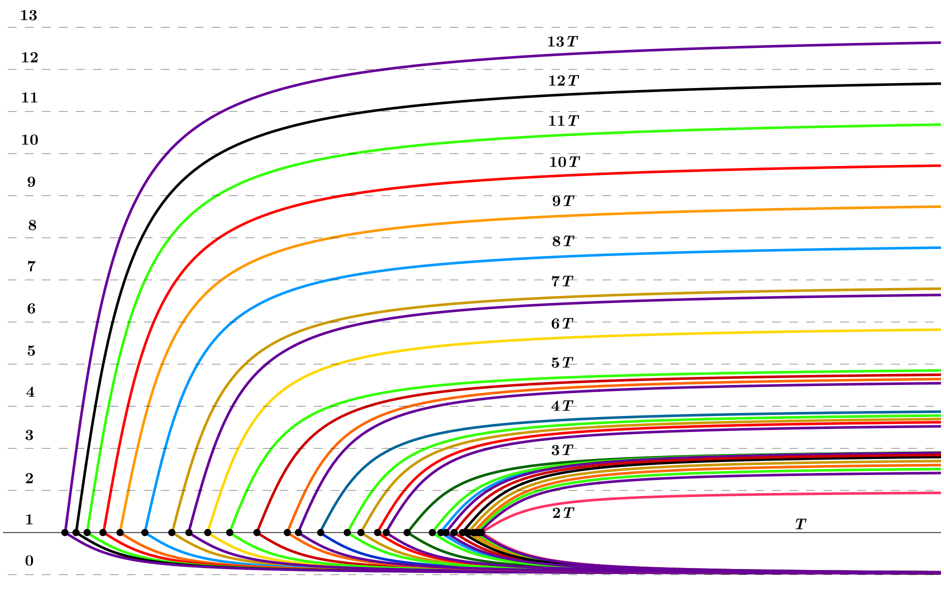

Figure 5.1: Subharmonics of (5.1) under condition (5.3) with $x = u_0 = v_0$.

5.1 represents a component of nT-periodic coexistence states of (5.1) for each integer $n \geq 1$. By a component it is meant a closed and connected subset of the solution set of (5.1) which is maximal for the inclusion. Each point on the corresponding line, (A, x), provides us with a value of A for which (5.1) admits a nT-periodic solution with $u_0 = v_0 = x$. By the intrinsic nature of (5.1), it turns out that all these components are separated from each other. By some existing results of topological nature in global bifurcation theory, all of them have an unbounded A-projection. However, except for the first three, whose local bifurcation diagrams are described by Theorem 5.5.1, the nature of their local bifurcations from $(A, 1)$ is not known yet, being possibly random. The problem of ascertaining weather, or not, this occurs, seems extremely challenging. Note that

$$(A, u, v) = (A, 1, 1)$$

solves (5.1) for all $A > 0$. More precisely, Figure 5.1 shows all the components of subharmonics of order n of (5.1) emanating from the straight line $(A, 1)$ for $1 \leq n \leq 13$. It contains the plots of:

- 1 component of subharmonics of order 1;
- 1 component of subharmonics of order 2;
- 1 component of subharmonics of order 3;
- 2 components of subharmonics of order 4; one of them is actually the component of subharmonics of order 2;
- 2 components of subharmonics of order 5;
- 3 components of subharmonics of order 6; one of them is actually the component of subharmonics of order 2 and another must be the component of order 3;
- 3 components of subharmonics of order 7;
- 4 components of subharmonics of order 8; one of them must be the component of order 2 and another one is a component of subharmonics with minimal order 4;

and so on... The fact that the number of components of subharmonics of order $n \geq 1$ grows to $+\infty$ as $n \uparrow +\infty$ is rather intriguing and it seems inherent to the non-cooperative character of (5.1) and attributable to the T-periodicity of $\alpha(t)$ and $\beta(t)$. The emergence of secondary bifurcations in any of these components cannot be a priori excluded, however no higher order bifurcations have been represented in Figure 5.1.

Thanks to Theorems 5.3.8 and Theorem 5.5.1, for every $n \geq 1$, the bifurcation points from $(A, 1)$ to the nT-periodic coexistence states of (5.1) are given by the positive roots of the polynomial

$$p_n(A) := [2 - (-1)^n A]p_{n-1}(A) - p_{n-2}(A), \qquad n \geq 3, \tag{5.5}$$

where

$$p_1(A) := 1, \qquad p_2(A) := 2 - A.$$

Although, according to Theorem 5.4.2, for every $n \geq 2$, the positive roots of $p_{2n}(A)$ are separated by the positive roots of $p_{2n-1}(A)$, the positive roots of $p_{2n+1}(A)$ are separated by those of $p_{2n}(A)$ less than 2, and, for every $n \geq 1$, the (even) polynomials $\frac{p_{2n}(A)}{2-A}$ and $p_{2n-1}(A)$ have (exactly) $n-1$ positive roots, which are real and algebraically simple, the problem of ascertaining the sharp ordering structure, if any, of the set of all these positive roots, which is a numerable subset of $(0, 2]$, remains an open problem in this chapter. Although there are some serious evidences that this set should be dense in the interval $[0, 2]$, a rigorous proof of this feature is not available yet.

The fact that the positive roots of $p_n(A)$ are algebraically simple allows us to apply the main theorem of M. G. Crandall and P. H. Rabinowitz [37] to prove that each of the components of subharmonics in Figure 5.1 must be a real analytic curve about their bifurcation points from $(A, 1)$.

Besides the general scheme of [141] and [123] adapts to show that the non-degenerate nT-periodic solutions of (5.1) provide us with nT-periodic solutions

$$\begin{cases} u' = \lambda(t)u - a(t)u^2 - b(t)uv, \\ v' = -\mu(t)v + c(t)uv - d(t)v^2, \end{cases}$$

which is a model which has attracted a considerable attention in Population Dynamics, the analysis carried out in this chapter provides us with the set of all the subharmonics of the Volterra model (5.1) in the special case when $A = B$. From the point of view of the applications, the construction of all these subharmonics is essential to ascertain the dynamics of (5.1). The stable subharmonics describe the asymptotic profiles of a wide class of solutions of the Cauchy problem associated to (5.1). The existence of subharmonics of arbitrary order is expected to entail the existence of initial conditions for which the asymptotic behavior of the predator and the prey is unpredictable. But this analysis will be accomplished elsewhere.

The mathematical analysis carried out in this chapter has been tremendously facilitated by the fact that $\alpha\beta = 0$, which provides us with a rather explicit formula for the iterates, $\mathcal{P}_n$, $n \geq 2$, of the monodromy operator, $\mathcal{P}_1$. Thanks to Proposition 5.2.2, for every $n \geq 2$, the Poincaré map $\mathcal{P}_n$ can be expressed through

$$(u_n, v_n) = \mathcal{P}_n(x, x) = \left(xE_{2n-1}(x), xE_{2n}(x)\right), \tag{5.6}$$

where

$$\left\{\begin{array}{l} E_0(x) := 1, \quad E_1(x) := e^{(1-x)A}, \\ E_n(x) := \left\{\begin{array}{ll} e^{[x(E_1(x)+E_3(x)+\cdots+E_{n-1}(x))-\frac{n}{2}]A} & \text{if} \quad n \in 2\mathbb{N}, \\ e^{[\frac{n+1}{2}-x(E_0(x)+E_2(x)+\cdots+E_{n-1}(x))]A} & \text{if} \quad n \in 2\mathbb{N}+1. \end{array}\right. \end{array}\right. \tag{5.7}$$

Thanks to Theorem 5.2.3, for every $n \geq 2$, the positive fixed points of $\mathcal{P}_n$, which provide us with the nT-periodic coexistence states of (5.1), are given by the zeros of the map

$$\varphi_n(x) = \varphi_{n-1}(x) - 1 + xE_{n-1}(x), \qquad x \in [0, n]. \tag{5.8}$$

Thus,

$$\begin{aligned} \varphi_1(x) &= x - 1, \\ \varphi_2(x) &= \varphi_1(x) - 1 + xe^{(1-x)A}, \\ \varphi_3(x) &= \varphi_2(x) - 1 + xe^{(xe^{(1-x)A}-1)A}, \\ \varphi_4(x) &= \varphi_3(x) - 1 + xe^{(2-x-xe^{(xe^{(1-x)A}-1)A})A}, \\ \varphi_5(x) &= \varphi_4(x) - 1 + xe^{\left(xe^{(1-x)A}+xe^{(2-x-xe^{(xe^{(1-x)A}-1)A})A}-2\right)A}. \end{aligned}$$

In particular, the positive fixed points of $\mathcal{P}_5$ are given by the positive zeros of $\varphi_5(x)$, which consists, essentially, in the composition of 4 exponentials functions. This circumstance might provoke dramatic oscillations of $\varphi_5(x)$ between some consecutive positive zeros. For instance, choosing $A = 5$ and $x = 0.1$, it turns out that $\varphi_5(0.1) \sim 10^{30}$, which lies outside the precision range of most of personal computers. Therefore, without no further work, numerics cannot be of any help in constructing the global bifurcation diagram sketched in Figure 5.1.

Lastly, we will consider the associated perturbed T-periodic functions

$$\alpha_\varepsilon := \alpha + \varepsilon, \qquad \beta_\varepsilon = \beta + \varepsilon, \tag{5.9}$$

where $\varepsilon > 0$, as well as the associated predator-prey model

$$\left\{\begin{array}{l} u' = \alpha_\varepsilon(t)u(1-v), \\ v' = \beta_\varepsilon(t)v(-1+u). \end{array}\right. \tag{5.10}$$

Taking $\varepsilon = 0$ in (5.10) gives (5.1). Although the nT-periodic coexistence states of (5.1) might degenerate, thanks to a celebrated result of A. Sard [184], most of the subharmonics of order n of (5.1) should provide us with subarmonics of order n of (5.10) for sufficiently small $\varepsilon > 0$. Therefore, the global topological structure sketched by Figure 5.1 should be essentially preserved, at least for sufficiently small $\varepsilon > 0$.

The distribution of the chapter is the following. Section 5.1 studies the structure and multiplicity of the low order subharmonics of (5.1) in the general case when

$$0 < A := \int_0^T \alpha(t)\,dt \neq B := \int_0^T \beta(t)\,dt > 0.$$

It substantially sharpens some previous findings of [123] by establishing the exact multiplicity of the $2T$-periodic solutions of (5.1) when $AB > 4$. The rest of the chapter focuses attention into the special, but extremely important case, when $A = B$. In Section 5.2 we construct the Poincaré maps $\mathcal{P}_n$ for all $n \geq 1$. In Section 5.3 we introduce the associated polynomials

$$p_n(A) := \frac{d\varphi_n(A,1)}{dx} = \mathfrak{L}(n;A), \qquad A > 0,$$

whose positive roots provide us with the bifurcation points to subharmonics from $(A,1)$, and analyze some of their most fundamental properties. In Section 5.4 we establish some fundamental separation properties between the zeros of these polynomials and show that all their positive roots are algebraically simple. This property has important consequences from the point of view of local and global bifurcation theory. Finally, in Section 5.5 we derive and discuss the global bifurcation diagram sketched in Figure 5.1.

5.1 Structure of T and $2T$-periodic solutions

According to [123, Th. 5.1], $(u,v) = (1,1)$ provides us with the unique T-periodic solution of (5.1), and (5.1) admits, at least, two $2T$-periodic coexistence states if, and only if, $AB > 4$, where

$$A := \int_0^T \alpha(s)\,ds > 0, \qquad B := \int_0^T \beta(s)\,ds > 0. \tag{5.11}$$

The next result sharpens these findings.

Theorem 5.1.1. *Suppose $AB > 4$. Then, the problem (5.1) possesses exactly two $2T$-periodic coexistence states (with minimal period $2T$, of course).*

Proof. We proceed as in the proof [123, Th. 5.1]. Since $\alpha\beta = 0$ in $\mathbb{R}$, the system (5.1) can be solved. Actually, for every $(u_0, v_0) \in \mathbb{R}^2$, the unique solution of (5.1), (u,v), such that $(u(0), v(0)) = (u_0, v_0)$ is given by

$$u(t) = u_0 e^{(1-v_0)\int_0^t \alpha}, \qquad v(t) = v_0 e^{(u(T)-1)\int_0^t \beta}, \qquad t \in [0,T]. \tag{5.12}$$

Thus, the associated T-time and $2T$-time Poincaré maps, $\mathcal{P}_1$ and $\mathcal{P}_2$, are given by

$$(u_1, v_1) := \mathcal{P}_1(u_0, v_0), \qquad u_1 := u_0 e^{(1-v_0)A}, \qquad v_1 := v_0 e^{(u_1-1)B}, \tag{5.13}$$

and

$$\begin{aligned}(u_2, v_2) := \mathcal{P}_2(u_0, v_0) &= \mathcal{P}_1^2(u_0, v_0)\\ &= \mathcal{P}_1(u_1, v_1) = \left(u_1 e^{(1-v_1)A}, v_1 e^{(u_2-1)B}\right).\end{aligned} \tag{5.14}$$

Thus, substituting (5.13) into (5.14) yields

$$u_2 = u_0 e^{(2-v_0-v_1)A}, \qquad v_2 = v_0 e^{(u_1+u_2-2)B}. \tag{5.15}$$

A solution with initial data (u_0, v_0) provides us with a componentwise positive fixed point of $\mathcal{P}_2$ if, and only if, $u_0 > 0$, $v_0 > 0$, $v_0 + v_1 = 2$ and $u_1 + u_2 = 2$. Hence, since $u_2 = u_0$, this is equivalent to

$$u_0 > 0, \qquad v_0 > 0, \qquad v_0 + v_1 = 2, \qquad u_0 + u_1 = 2. \tag{5.16}$$

Note that, owing to (5.16),

$$0 < u_0, u_1 < 2, \qquad 0 < v_0, v_1 < 2.$$

Since $u_1 = 2 - u_0$ and $v_1 = 2 - v_0$, from (5.13) it becomes apparent that

$$2 - u_0 = u_0 e^{(1-v_0)A}, \qquad 2 - v_0 = v_0 e^{(1-u_0)B}. \tag{5.17}$$

Consequently,

$$u_0 = \frac{2}{e^{(1-v_0)A}+1}, \qquad 2 - v_0 = v_0 e^{\left(1-\frac{2}{e^{(1-v_0)A}+1}\right)B} = v_0 e^{\frac{e^{(1-v_0)A}-1}{e^{(1-v_0)A}+1}B} \tag{5.18}$$

and therefore, the $2T$-periodic coexistence states are given by the interior zeros of the map

$$\varphi(x) := x\left(e^{\frac{e^{(1-x)A}-1}{e^{(1-x)A}+1}B} + 1\right) - 2, \qquad x \in [0, 2]. \tag{5.19}$$

As this function satisfies $\varphi(0) = -2 < 0$, $\varphi(1) = 0$, $\varphi(2) > 0$ and

$$\varphi'(1) = 2 - \frac{AB}{2} < 0,$$

because we are assuming that $AB > 4$, it is easily seen that $\varphi(x)$ possesses, at least, besides 1, two zeros, $z_1 \in (0, 1)$ and $z_2 \in (1, 2)$. Note that 1 provides us with the (unique) T-periodic solution of (5.1). That these zeros are unique is based on the fact that any critical point of φ on $(0,1)$, x, must satisfy $\varphi''(x) < 0$, and hence, it is a quadratic local maximum, while $\varphi''(y) > 0$ for all critical point, y, of φ in $(1,2)$. In particular, since $\varphi(0) < 0$ and $\varphi'(1) < 0$, this entails that z_1 is simple and, actually, $\varphi'(z_1) > 0$, for as, otherwise, $\varphi(x)$ should have a local minimum in $(0,1)$, which is impossible. Similarly, $\varphi'(z_2) > 0$. In order to show the previous claim, suppose

$$\varphi'(x) = 0 \quad \text{for some } \; x \in (0,2).$$

Then,

$$\varphi'(x) = e^{\frac{e^{(1-x)A}-1}{e^{(1-x)A}+1}B}\left(1 - \frac{2ABxe^{(1-x)A}}{[e^{(1-x)A}+1]^2}\right) + 1 = 0. \tag{5.20}$$

Moreover, differentiating φ' and rearranging terms yields

$$\varphi''(x) = e^{\frac{e^{(1-x)A}-1}{e^{(1-x)A}+1}B}\left[x\left(\frac{2ABe^{(1-x)A}}{[e^{(1-x)A}+1]^2}\right)^2 - \frac{4ABe^{(1-x)A}}{[e^{(1-x)A}+1]^2} + 2A^2Bxe^{(1-x)A}\frac{1-e^{(1-x)2A}}{[e^{(1-x)A}+1]^4}\right]. \tag{5.21}$$

Now, after some straightforward manipulations, it is easily seen that (5.20) implies

$$\frac{2\left(e^{-\frac{e^{(1-x)A}-1}{e^{(1-x)A}+1}B}+1\right)}{x} = \frac{4ABe^{(1-x)A}}{[e^{(1-x)A}+1]^2}, \quad \left(\frac{e^{-\frac{e^{(1-x)A}-1}{e^{(1-x)A}+1}B}+1}{x}\right)^2 = \left(\frac{2ABe^{(1-x)A}}{[e^{(1-x)A}+1]^2}\right)^2 \tag{5.22}$$

and substituting (5.22) into (5.21) we find that

$$\begin{aligned}
\varphi''(x) &= e^{\frac{e^{(1-x)A}-1}{e^{(1-x)A}+1}B}\left[x\left(\frac{e^{-\frac{e^{(1-x)A}-1}{e^{(1-x)A}+1}B}+1}{x}\right)^2 - \frac{2\left(e^{-\frac{e^{(1-x)A}-1}{e^{(1-x)A}+1}B}+1\right)}{x}\right] \\
&\quad + e^{\frac{e^{(1-x)A}-1}{e^{(1-x)A}+1}B}\left[2A^2Bxe^{(1-x)A}\frac{1-e^{(1-x)2A}}{[e^{(1-x)A}+1]^4}\right] \\
&= e^{\frac{e^{(1-x)A}-1}{e^{(1-x)A}+1}B}\left[\frac{e^{-2\frac{e^{(1-x)A}-1}{e^{(1-x)A}+1}B}-1}{x} + 2A^2Bxe^{(1-x)A}\frac{1-e^{(1-x)2A}}{[e^{(1-x)A}+1]^4}\right].
\end{aligned}$$

Suppose $x \in (0,1)$. Then, the following holds

$$e^{-2\frac{e^{(1-x)A}-1}{e^{(1-x)A}+1}B} - 1 < 0, \qquad 1 - e^{(1-x)2A} < 0.$$

Therefore, $\varphi''(x) < 0$, as claimed above.

Suppose $x \in (1,2]$. Then,

$$e^{-2\frac{e^{(1-x)A}-1}{e^{(1-x)A}+1}B} - 1 > 0, \qquad 1 - e^{(1-x)2A} > 0,$$

and hence, $\varphi''(x) > 0$, as requested. The proof is completed. □

According to the proof of Theorem 5.1.1, if $AB > 4$ then $\varphi(x)$ has exactly three (simple) zeros in $(0,2)$, z_1, z_2, z_3, such that $z_1 \in (0,1)$, $z_2 \in (1,2)$ and $z_3 = 1$, whereas

$$\varphi'(1) = 2 - \frac{AB}{2} \geq 0 \quad \text{if} \;\; AB \leq 4,$$

and hence, 1 is the unique zero of φ in this case. Note that if $AB = 4$, then $\varphi'(1) = 0$ and

$$\varphi''(1) = \left(\frac{AB}{2}\right)^2 - AB = 4 - 4 = 0.$$

Moreover, differentiating twice yields

$$\varphi'''(x) = e^q \left(3(q')^2 + 3q'' + x\left[(q')^3 + 3q'q'' + q'''\right]\right),$$

with $q(x) := e^{\frac{e^{(1-x)A}-1}{e^{(1-x)A}+1}B}$ for $x \in [0,2]$. Thus,

$$\varphi'''(1) = \tfrac{AB(5AB+2A^2)}{8} > 0$$

and therefore, 1 is a treble zero of $\varphi(x)$ if $AB = 4$. On the other hand, the function $\varphi(x)$ can be also regarded as an analytic function of x that varies continuously with $B > 0$ and does not vanish at the ends of $[0,2]$. By Rouché's theorem, φ must have three zeros, counting orders, for every $B > 0$. As 1 is the unique real zero of $\varphi(x)$ if $AB < 4$ and $\varphi'(1) > 0$ in this range, it becomes apparent that $\varphi(x)$ possesses two complex zeros if $AB < 4$. Those complex solutions are not going to be taken into account throughout this chapter.

Subsequently, we are going to regard B as the main continuation parameter in problem (5.1). According to our previous analysis, we already know that $(1,1)$ is the unique $2T$-periodic solution of (5.1) if $B < 4/A$ (note that the minimal period of this solution is T), whereas (5.1) possesses (exactly) three $2T$-periodic solutions for every $B > 4/A$. Moreover, two of them, those with minimal period $2T$, bifurcate from $(1,1)$ as the parameter B crosses the critical value $4/A$, as it will become apparent later. Precisely, we regard the solutions of (5.1) as solutions of

$$0 = \varphi(B,x) := x\left(e^{\frac{e^{(1-x)A}-1}{e^{(1-x)A}+1}B} + 1\right) - 2, \qquad x \in [0,2], \tag{5.23}$$

for some $B > 0$. Note that $(B,x) = (B,1)$ is a solution curve of (5.23) defined for all $B > 0$. Moreover, the linearization of (5.23) at $(B,1)$ is

$$\mathfrak{L}(B) = \frac{d\varphi(B,1)}{dx} = 2 - \frac{AB}{2}$$

which establishes an isomorphism of $\mathbb{R}$, unless $B = 4/A$. Thus, this is the unique value of the parameter where bifurcation to $2T$-periodic solutions of (5.1) can occur from $(1, 1)$. Since

$$N[\mathfrak{L}(4/A)] = \mathbb{R} = \operatorname{span}[1]$$

and

$$\mathfrak{L}_1 := \frac{d\mathfrak{L}(4/A)}{dB} = -\frac{A}{2} \neq 0,$$

it becomes apparent that

$$\mathfrak{L}_1 1 \notin R[\mathfrak{L}(4/A)] = [0]. \tag{5.24}$$

Hence, by the main theorem of M. G. Crandall and P. H. Rabinowitz [37], there exist $s_0 > 0$ and two analytic maps, $x, B : (-s_0, s_0) \to \mathbb{R}$ such that $x(0) = 1$, $B(0) = 4/A$, $x(s) = 1 + s + \mathcal{O}(s^2)$ as $s \to 0$, and $\varphi(B(s), x(s)) = 0$ for every $s \in (-s_0, s_0)$. Moreover, except for $x = 1$, these are the unique solutions of $\varphi(B, x) = 0$ in a neighborhood of $(B, x) = (4/A, 1)$. As due to Theorem 5.1.1, $\varphi(B, x) = 0$ cannot admit a solution $x \neq 1$ if $B \leq 4/A$, it becomes apparent that $B(s) > 4/A$ for all $s \in (-s_0, s_0)$. Note that $x(s) > 1$ if $s \in (0, s_0)$, while $x(s) < 1$ if $s \in (-s_0, 0)$. On the other hand, it readily follows from (5.23) that $\varphi(B, x) < 0$ if $x \leq 0$ and $\varphi(B, x) > 0$ if $x \geq 2$. Thus, any solution of $\varphi(B, x) = 0$ satisfies $x \in (0, 2)$. In particular, $x(s) \in (0, 2)$ for all $s \in (-s_0, s_0)$. Thus, as owing to [123, Th. 5.2] any solution, (B, x), of $\varphi = 0$ with $B > 4/A$ is non-degenerated, by a rather standard continuation argument involving the Implicit Function Theorem the next result holds true.

Theorem 5.1.2. *The set of zeros (B, x) of $\varphi = 0$ with $x \neq 1$, consists of a (global) analytic curve, $(B(s), x(s))$, $s \in \mathbb{R}$, such that $x(s) \in (0, 2)$ for all $s \in \mathbb{R}$ and $B(\mathbb{R}) = (4/A, +\infty)$, much like illustrated by Figure 5.2. Actually, each of the two half-branches, the upper and the lower ones, can be globally parameterized by $B \in (4/A, +\infty)$.*

Since $\varphi(B, x) = 0$ can be equivalently written down as

$$\frac{2}{x} - 1 = e^{\frac{e^{(1-x)A} - 1}{e^{(1-x)A} + 1} B},$$

letting $B \to +\infty$ in this identity, it becomes apparent that

$$\lim_{B \uparrow +\infty} x = \begin{cases} 0 & \text{if } \ x \in (0, 1), \\ 2 & \text{if } \ x \in (1, 2), \end{cases}$$

which is reflected in the global bifurcation diagram of Figure 5.2.

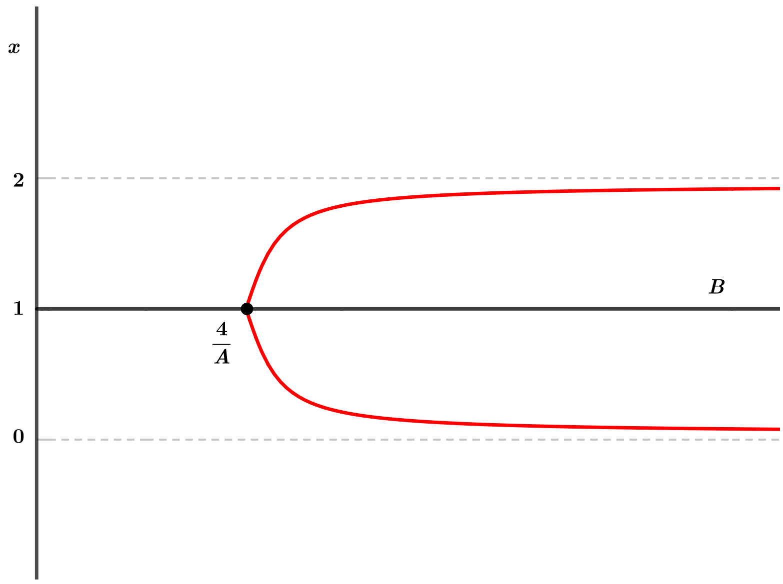

Figure 5.2: The set of $2T$-periodic solutions of (7.1).

5.2 Constructing the nT-Poincaré maps

Throughout the rest of this chapter, for every integer $n \geq 1$, we denote by $\mathcal{P}_n$ the nT-Poincaré map of (5.1), and, for every initial data (u_0, v_0), with $u_0 > 0$ and $v_0 > 0$, we set

$$(u_n, v_n) := \mathcal{P}_n(u_0, v_0) = \mathcal{P}_1^n(u_0, v_0). \tag{5.25}$$

Then, iterating (5.13) n times, it becomes apparent that

$$(u_n, v_n) = \left(u_0 e^{(n-v_0-v_1-\cdots-v_{n-1})A}, v_0 e^{(u_1+u_2+\cdots+u_n-n)B}\right), \qquad n \geq 1. \tag{5.26}$$

Consequently, the solution of (5.1) with initial data (u_0, v_0), with $u_0 > 0$ and $v_0 > 0$, provides us with a nT-periodic coexistence state of (5.1) if, and only if,

$$\begin{cases} n = u_0 + u_1 + \cdots + u_{n-1}, \\ n = v_0 + v_1 + \cdots + v_{n-1}, \end{cases} \tag{5.27}$$

where we are using that $u_n = u_0$. According to (5.26), (5.27) can be equivalently expressed as

$$\begin{cases} n = u_0 \left[1+e^{(1-v_0)A} + e^{(2-v_0-v_1)A} + \cdots + e^{(n-1-v_0-v_1-\cdots-v_{n-2})A}\right], \\ n = v_0 \left[1+e^{(u_1-1)B} + e^{(u_1+u_2-2)B} + \cdots + e^{[u_1+u_2+\cdots+u_{n-1}-(n-1)]B}\right]. \end{cases} \tag{5.28}$$

As already shown in the proof of Theorem 5.1.1, in the special case when $n = 2$, u_0 can be easily obtained as a (explicit) function of v_0, which allowed as to express the system as a single equation of the unknown $x = v_0$. As this strategy does not work when $n \geq 3$, in order to construct the set of nT-periodic solutions of (5.1) for all $n \geq 3$, throughout the rest of this chapter we will make the additional assumption that

$$x := u_0 = v_0 \quad \text{and} \quad A = B. \tag{5.29}$$

Later, we will analyze their global topological structure through the distribution of their bifurcation points from the trivial curve $x = 1$. Under these assumptions the next result holds. It is a pivotal result to express the Poincaré maps in a manageable way.

Lemma 5.2.1. *Suppose (5.27) and (5.29). Then, for every $n \geq 2$,*

$$u_h = v_{n-h} \qquad \textit{for all } \; h \in \{1, \dots, n-1\}. \tag{5.30}$$

Thus, the two equations of the system (5.28) coincide.

Proof. Fix $n \geq 2$. Then, owing to (5.26), (5.27) and (5.29), we find that

$$u_1 = u_0 e^{(1-v_0)A} = v_0 e^{(1-u_0)B} = v_0 e^{[u_1+u_2+\cdots+u_{n-1}-(n-1)]B} = v_{n-1}.$$

This relation provides us with the first identity of (5.30) ($h = 1$). In particular, it shows (5.30) when $n = 2$. More generally, suppose that $n \geq 3$ and that there exists $k \geq 1$ such that

$$u_h = v_{n-h} \qquad \text{for all } \; h \in \{1, \dots, n-k-1\}. \tag{5.31}$$

Then, thanks to (5.26), we have that

$$u_{n-k} = u_0 e^{[(n-k)-v_0-v_1-\cdots-v_{n-k-1}]A}.$$

Thus, by (5.29) and (5.31),

$$\begin{aligned} u_{n-k} &= v_0 e^{[(n-k)-u_0-u_{n-1}-\cdots-u_{k+1}]B} \\ &= v_0 e^{[(n-k)-u_0-u_{n-1}-\cdots-u_{k+1}-u_k-u_{k-1}-\cdots-u_1+k+u_1+u_2+\cdots+u_k-k]B}. \end{aligned}$$

Thus, due to (5.27), it becomes apparent that

$$u_{n-k} = v_0 e^{(u_1+\cdots+u_k-k)B} = v_k,$$

which concludes the proof of (5.30). Therefore since (5.27) is equivalent to (5.28), the two equtions of (5.28) coincide. The proof is complete. □

According to Lemma 5.2.1, under condition (5.29), to construct the fixed points of the Poincaré map $\mathcal{P}_n$, it suffices to consider any of the identities of (5.27) (or (5.28)), for instance, the first one. Thus, setting

$$\varphi_n(u_0) := u_0 + u_1(u_0) + u_2(u_0) + \cdots + u_{n-1}(u_0) - n, \qquad u_0 > 0, \tag{5.32}$$

it becomes apparent that the zeros of φ_n provide us with the positive fixed points of the Poincaré map $\mathcal{P}_n$. By (5.26)

$$\begin{aligned} u_1(u_0) &:= u_0 e^{(1-u_0)A}, \\ u_2(u_0) &:= u_0 e^{[2-u_0-v_1(u_0)]A} = u_0 e^{[2-u_0-v_0 e^{(u_1-1)A}]A} \\ &\phantom{:= u_0 e^{[2-u_0-v_1(u_0)]A}} = u_0 e^{(2-u_0-u_0 e^{[u_0 e^{(1-u_0)A}-1]A})A} \end{aligned} \tag{5.33}$$

and so on... though, in order to get a manageable expression for $\varphi_n(u_0)$, all these terms should be reorganized in a slightly tricky way by using the relationships (5.27), or (5.28), which will be described in the proof of Theorem 5.27. The next result provides us with the Poincaré maps.

Proposition 5.2.2. *Setting*

$$\begin{cases} E_0(x) := 1, \quad E_1(x) := e^{(1-x)A}, \\ E_n(x) := \begin{cases} e^{[x(E_1(x)+E_3(x)+\cdots+E_{n-1}(x))-\frac{n}{2}]A} & \text{if} \quad n \in 2\mathbb{N}, \\ e^{[\frac{n+1}{2}-x(E_0(x)+E_2(x)+\cdots+E_{n-1}(x))]A} & \text{if} \quad n \in 2\mathbb{N}+1, \end{cases} \end{cases} \tag{5.34}$$

for every $n \geq 1$ the Poincaré map is given through

$$(u_n, v_n) = \mathcal{P}_n(x, x) = (xE_{2n-1}(x), xE_{2n}(x)). \tag{5.35}$$

Proof. By (5.26) and the definition of E_1 and E_2, it is easily seen that

$$u_1 = xe^{(1-x)A} = xE_1(x) \quad \text{and} \quad v_1 = xe^{[xe^{(1-x)A}-1]A} = xE_2(x).$$

Assume, as an induction hypothesis, that, for some integer $n \geq 1$,

$$u_{n-1} = xE_{2(n-1)-1}(x) \quad \text{and} \quad v_{n-1} = xE_{2(n-1)}(x). \tag{5.36}$$

To prove (5.35)we argue as follows. According to (5.26),

$$u_n = xe^{(n-v_0-v_1-\cdots-v_{n-1})A} = u_{n-1}e^{(1-v_{n-1})A}.$$

Thus, by the induction hypothesis and (5.34),

$$\begin{aligned} u_n &= xE_{2n-3}(x)e^{(1-xE_{2n-2}(x))A} \\ &= xe^{[\frac{2n-2}{2}-x(E_0+E_2+\cdots+E_{2n-4})]A}e^{(1-xE_{2n-2})A} \\ &= xe^{[n-x(E_0+E_2+\cdots+E_{2n-4}+E_{2n-2})]A} = xE_{2n-1}(x). \end{aligned}$$

This provides us with the value of u_n in (5.35). Similarly,

$$v_n = xe^{(u_1+\cdots+u_n-n)A} = v_{n-1}e^{(u_n-1)A}.$$

Thus, by (5.36), since we already know that $u_n = xE_{2n-1}(x)$, we can infer that

$$\begin{aligned} v_n &= xE_{2n-2}(x)e^{(xE_{2n-1}(x)-1)A} \\ &= xe^{[x(E_1+E_3+\cdots+E_{2n-3})-(n-1)]A}e^{(xE_{2n-1}-1)A} \\ &= xe^{[x(E_1+E_3+\cdots+E_{2n-3}+E_{2n-1})-n]A} = xE_{2n}(x). \end{aligned}$$

This ends the proof. $\square$

As a direct consequence, from Proposition 5.2.2 one can get the auxiliary maps φ_n, $n \geq 1$, introduced in (5.32).

Theorem 5.2.3. *For every integer $n \geq 1$,*

$$\varphi_n(x) = \varphi_{n-1}(x) - 1 + xE_{n-1}(x). \tag{5.37}$$

Proof. First note that when n is an odd integer, according to Lemma 5.2.1, we have that

$$\begin{aligned} \varphi_n(x) &= u_0 + u_1 + \cdots + u_{\frac{n-1}{2}} + u_{\frac{n-1}{2}+1} + u_{\frac{n-1}{2}+2} + \cdots + u_{n-2} + u_{n-1} - n \\ &= u_0 + u_1 + \cdots + u_{\frac{n-1}{2}} + v_{\frac{n-1}{2}} + v_{\frac{n-1}{2}-1} + \cdots + v_2 + v_1 - n \\ &= u_0 + u_1 + v_1 + u_2 + v_2 + \cdots + u_{\frac{n-1}{2}-1} + v_{\frac{n-1}{2}-1} + u_{\frac{n-1}{2}} + v_{\frac{n-1}{2}} - n. \end{aligned} \tag{5.38}$$

Similarly, when n is even,

$$\begin{aligned} \varphi_n(x) &= u_0 + u_1 + \cdots + u_{\frac{n}{2}} + u_{\frac{n}{2}+1} + u_{\frac{n}{2}+2} + \cdots + u_{n-2} + u_{n-1} - n \\ &= u_0 + u_1 + \cdots + u_{\frac{n}{2}} + v_{\frac{n}{2}-1} + v_{\frac{n}{2}-2} + \cdots + v_2 + v_1 - n \\ &= u_0 + u_1 + v_1 + u_2 + v_2 + \cdots + u_{\frac{n}{2}-1} + v_{\frac{n}{2}-1} + u_{\frac{n}{2}} - n. \end{aligned} \tag{5.39}$$

To prove (5.37) a complete induction argument will be used. When $n = 1$,

$$\varphi_1(x) = x - 1.$$

When $n = 2$, by (5.26),

$$\varphi_2(x) := x + u_1 - 2 = x + xe^{(1-x)A} - 2 = \varphi_1(x) - 1 + xE_1(x).$$

As the complete induction hypothesis, suppose that, for any given $\nu \geq 2$, (5.37) holds for every $n \in \{1, 2, \ldots, 2\nu-3, 2\nu-2\}$. Then, thanks to (5.38) and (5.39),

$$\begin{aligned} \varphi_{2\nu-1}(x) &= u_0 + u_1 + v_1 + u_2 + v_2 + \cdots + u_{\nu-2} + v_{\nu-2} + u_{\nu-1} + v_{\nu-1} - 2\nu + 1, \\ \varphi_{2\nu}(x) &= u_0 + u_1 + v_1 + u_2 + v_2 + \cdots + u_{\nu-1} + v_{\nu-1} + u_\nu - 2\nu. \end{aligned}$$

Thus, thanks to (5.35),

$$\begin{aligned} \varphi_{2\nu-1}(x) = x &+ xE_1(x) + xE_2(x) + xE_3(x) + xE_4(x) + \cdots \\ &+ xE_{2\nu-5}(x) + xE_{2\nu-4}(x) + xE_{2\nu-3}(x) \\ &+ xE_{2\nu-2}(x) - 2\nu + 1. \end{aligned} \tag{5.40}$$

Similarly,

$$\begin{aligned} \varphi_{2\nu}(x) = x &+ xE_1(x) + xE_2(x) + xE_3(x) + xE_4(x) + \cdots \\ &+ xE_{2\nu-3}(x) + xE_{2\nu-2}(x) + xE_{2\nu-1}(x) - 2\nu. \end{aligned} \tag{5.41}$$

Therefore, by the induction hypothesis,

$$\varphi_{2\nu-1}(x) = \varphi_{2\nu-2}(x) - 1 + xE_{2\nu-2}(x).$$

Similarly,

$$\varphi_{2\nu}(x) = \varphi_{2\nu-1}(x) - 1 + xE_{2\nu-1}(x).$$

The proof is complete. □

Remark 5.2.4. *By (5.40) and (5.41) it becomes apparent that*

$$\varphi_n(0) = -n < 0 \quad \textit{and} \quad \varphi_n(n) > 0 \quad \textit{for all integer } n \geq 2.$$

According to Theorem 5.2.3, it is easily seen that

$$\begin{aligned} \varphi_1(x) &= x - 1, \\ \varphi_2(x) &= \varphi_1(x) - 1 + xe^{(1-x)A}, \\ \varphi_3(x) &= \varphi_2(x) - 1 + xe^{(xe^{(1-x)A}-1)A}, \\ \varphi_4(x) &= \varphi_3(x) - 1 + xe^{(2-x-xe^{(xe^{(1-x)A}-1)A})A}. \end{aligned} \tag{5.42}$$

Crucially, in the formula for $\varphi_3(x)$ given by Theorem 5.2.3 it is only required to compose two exponentials, while in (5.33) we had to nest three. Such reduction in the complexity of φ_3 is explained by the symmetries revealed by Lemma 5.2.1 which facilitated the reorganization of the terms of φ_n as to get a function with a minimal number of nested exponentials, much like in the algorithm of the proof of Theorem 5.2.3. Using this algorithm, the number of nested exponentials decreases by one when n is odd, and each of the the E_n's defined by (5.34) consists of a composition of exactly n exponentials. The relevance of this reduction will not be completely understood until the next sections, where the structure of the zeros of the φ_n's introduced in (5.32) will be analyzed. Those zeros are the positive fixed points of the nT-time Poincaré maps.

The main technical difficulty to determine the zeros of the φ_n's, even from the point of view of numerical analysis, relies on the high sensitivity of these functions to very small variations in the value of the parameter $A = B$. The higher the number of exponentials nested, the higher the sensitivity in A. As a result, when one tries to determine numerically the zeros of the map φ_4 for values of A near 4, the function $\varphi_4(x)$ takes values of order 10^{31} in a neighborhood of zero. So, there is no chance to compute the zeros of these maps assisted by the computer. When dealing with φ_5 the value of the parameter $A = B$ should not exceed the value 2.5, which is extremely unsatisfactory for our purposes here. These technical troubles inherent to the internal structure of the associated maps φ_n push us to make a direct analysis of the global structure of their zeros. In order to perform this global analysis we first need to ascertain the set of bifurcation points of $\varphi_n = 0$ from the curve $(A, 1)$. This analysis will be carried out in the next section.

5.3 A canonical chain of associated polynomials

Searching for the potential bifurcation points from the curve $(A, 1)$ to nT-periodic coexistence states, this section analyzes the spectrum of the linearized family

$$\mathfrak{L}(n; A) := \frac{d\varphi_n(A, 1)}{dx}, \quad n \in \mathbb{N},$$

i.e., its zero set as a function of the parameter A, as well as the global structure of $\mathfrak{L}(n; A)$. Note that, since $(A, 1)$ is the T-periodic coexistence state, it also provides us with a nT-periodic solution for all $n \geq 1$ and, hence, by construction, $\varphi_n(A, 1) = 0$ for all $A > 0$ and $n \geq 1$. The curve $(A, 1)$, $A > 0$, is the *trivial* curve, as it is known. It is the curve from which are going to bifurcate the nT-periodic coexistence states of (5.1) under assumption (5.29). Note also that, since every nT-periodic solution is knT-periodic for all integer $k \geq 1$,

$$\varphi_{kn}(x) = 0 \quad \text{for all} \;\; x \in \varphi_n^{-1}(0) \quad \text{and} \quad k \geq 1. \tag{5.43}$$

Throughout the rest of this chapter we will denote

$$p_n(A) := \frac{d\varphi_n(A,1)}{dx} = \mathfrak{L}(n;A), \qquad A>0. \tag{5.44}$$

Differentiating with respect to x the identity (5.37) yields

$$p_n(A) = p_{n-1}(A) + E_{n-1}(1) + E'_{n-1}(1) \qquad \text{for all } \; A>0. \tag{5.45}$$

The next result shows that $p_n \in \mathbb{Z}\,[A]$.

Lemma 5.3.1. *For every $n \in \mathbb{N}$, $p_n(A)$ is a polynomial in the variable A with integer coefficients, i.e., $p_n \in \mathbb{Z}[A]$.*

Proof. By (5.35), it becomes apparent that, since $(1,1)$ is a fixed point of $\mathcal{P}_n$,

$$(1,1) = \mathcal{P}_n(1,1) = (E_{2n-1}(1), E_{2n}(1))$$

for all integer $n \geq 1$. Thus,

$$E_n(1) = 1 \quad \text{for all } \; n \geq 0. \tag{5.46}$$

Thus, (5.45) becomes

$$p_n(A) = p_{n-1}(A) + 1 + E'_{n-1}(1) \tag{5.47}$$

for all $A>0$ and $n \geq 1$. Therefore, due to (5.42) , $p_1(A) = \frac{d\varphi_1(A,1)}{dx} = 1$ and iterating (5.47) $n-2$ times show that, for every integer $n \geq 2$,

$$p_n(A) = n + E'_1(1) + E'_2(1) + \cdots + E'_{n-1}(1). \tag{5.48}$$

Consequently, to complete the proof it suffices to show that $E'_n(1) \in \mathbb{Z}[A]$ for all $n \geq 1$. Indeed, by (5.34), $E'_0(1) = 0$, $E'_1(1) = -A$ and

$$E'_n(1) = \begin{cases} A \displaystyle\sum_{\substack{j=1 \\ j\in 2\mathbb{N}+1}}^{n-1} \Big[E_j(1) + E'_j(1)\Big] & \text{if } n \in 2\mathbb{N}, \\ -A \displaystyle\sum_{\substack{j=0 \\ j\in 2\mathbb{N}}}^{n-1} \Big[E_j(1) + E'_j(1)\Big] & \text{if } n \in 2\mathbb{N}+1. \end{cases} \tag{5.49}$$

Thus, by a complete induction argument it becomes apparent that $E'_n(1) \in \mathbb{Z}[A]$ for all $n \in \mathbb{N}$. This concludes the proof. $\square$

Remark 5.3.2. In Section 5 we will prove that all the roots of the polynomial $p_n(A)$ are simple. In other words,

$$p_n'(r) = \frac{d\mathfrak{L}}{dA}(n;r) \neq 0$$

for all $r \in p_n^{-1}(0)$. Thus, the transversality condition of M. G. Crandall and P. H. Rabinowitz [37] holds true. Therefore, by the main theorem of [37], at every positive root of $p_n(A)$, r, an analytic curve of nT-periodic coexistence states of (5.1) bifurcates from $(A,1)$ at r. This feature explains our interest here in analyzing the nature and the distribution of the positive roots of the polynomials $p_n(A)$, $n \in \mathbb{N}$.

Remark 5.3.3. Occasionally, we will make explicit the dependence of the function $\varphi_n(x)$ on the parameter A by setting $\varphi_n(A,x)$, instead of $\varphi_n(x)$. Similarly, we will set $E_n(A,x) := E_n(x)$ for all $n \in \mathbb{N}$. According to (5.34), $E_n(0,x) = 1$ for all $n \in \mathbb{N}$ and $x \in [0,n]$. Thus, (5.37) yields

$$\varphi_n(0,x) = \varphi_{n-1}(0,x) - 1 + x$$

for all $n \in \mathbb{N}$ and $x \in [0,n]$. Therefore, iterating $n-1$ times, it becomes apparent that

$$\varphi_n(0,x) = n(x-1) \quad \text{for all } \; n \in \mathbb{N}. \tag{5.50}$$

As the zeros of $\varphi_n(A,x)$ provide us with the nT-periodic positive solutions of (5.1), it follows from (5.50) that $x = 1$ is the unique nT-periodic solution, for all $n \in \mathbb{N}$, at the particular value of the parameter $A = 0$.

The next list collects the polynomials $p_n(A)$ for $1 \leq n \leq 13$.

$$p_1(A) = 1$$
$$p_2(A) = -A + 2$$
$$p_3(A) = -A^2 + 3$$
$$p_4(A) = A^3 - 2A^2 - 2A + 4$$
$$p_5(A) = A^4 - 5A^2 + 5$$
$$p_6(A) = -A^5 + 2A^4 + 4A^3 - 8A^2 - 3A + 6$$
$$p_7(A) = -A^6 + 7A^4 - 14A^2 + 7$$
$$p_8(A) = A^7 - 2A^6 - 6A^5 + 12A^4 + 10A^3 - 20A^2 - 4A + 8$$
$$p_9(A) = A^8 - 9A^6 + 27A^4 - 30A^2 + 9$$
$$p_{10}(A) = -A^9 + 2A^8 + 8A^7 - 16A^6 - 21A^5 + 42A^4 + 20A^3 - 40A^2 - 5A + 10$$
$$p_{11}(A) = -A^{10} + 11A^8 - 44A^6 + 77A^4 - 55A^2 + 11$$
$$p_{12}(A) = A^{11} - 2A^{10} - 10A^9 + 20A^8 + 36A^7 - 72A^6 - 56A^5 + 112A^4 + 35A^3 - 70A^2 - 6A + 12$$
$$p_{13}(A) = A^{12} - 13A^{10} + 65A^8 - 156A^6 + 182A^4 - 91A^2 + 13.$$

The next table collects the coefficients of all the polynomials listed above.

A^{12}	A^{11}	A^{10}	A^9	A^8	A^7	A^6	A^5	A^4	A^3	A^2	A^1	A^0
0	0	0	0	0	0	0	0	0	0	0	0	1
0	0	0	0	0	0	0	0	0	0	0	-1	2
0	0	0	0	0	0	0	0	0	0	-1	0	3
0	0	0	0	0	0	0	0	0	1	-2	-2	4
0	0	0	0	0	0	0	0	1	0	-5	0	5
0	0	0	0	0	0	0	-1	2	4	-8	-3	6
0	0	0	0	0	0	-1	0	7	0	-14	0	7
0	0	0	0	0	1	-2	-6	12	10	-20	-4	8
0	0	0	0	1	0	-9	0	27	0	-30	0	9
0	0	0	-1	2	8	-16	-21	42	20	-40	-5	10
0	0	-1	0	11	0	-44	0	77	0	-55	0	11
0	1	-2	-10	20	36	-72	-56	112	35	-70	-6	12
1	0	-13	0	65	0	-156	0	182	0	-91	0	13

Table 5.1: First thirteen polynomials coefficients.

By simply having a glance to these polynomials, it becomes apparent that the following properties hold:

(a) The constant terms of $p_n(A)$ equals n.

(b) The degree of $p_n(A)$ equals $n-1$.

(c) The leading coefficients of $p_{4n}(A)$ and $p_{4n+1}(A)$ equal 1, while the leading coefficients of $p_{4n+2}(A)$ and $p_{4n+3}(A)$ equal -1.

(d) $p_{2n}(2) = 0$ for all integer $n \geq 1$. Thus, $p_2 | p_{2n}$ for all $n \geq 1$.

(e) $p_{2n+1}(A)$ is an even function.

Besides these properties, it seems all the coefficients of $p_n(A)$, except the leading one, must be multiples of n if n is a prime integer, though this property will not be used in this chapter. The next result shows the property (a).

Lemma 5.3.4. *$p_n(0) = n$ for all $n \geq 1$.*

Proof. By (5.49), $\frac{dE_n(0,1)}{dx} = 0$. Hence, due to (5.48), $p_n(0) = n$ for all $n \geq 1$. □

The next result establishes the properties (b) and (c).

Lemma 5.3.5. *For every integer $n \geq 1$, $\deg(p_n) = n - 1$. Moreover, the leading coefficients of p_n equal 1 if $n \in 4\mathbb{N} \cup (4\mathbb{N}+1)$ and -1 if $n \in (4\mathbb{N}+2) \cup (4\mathbb{N}+3)$.*

Proof. By the proof of Lemma 5.3.1, we already know that

$$E_n'(A,1) := \frac{dE_n}{dx}(A,1)$$

is a polynomial in A for all integer $n \geq 1$. Next, we will show that it has degree n. To prove it, a complete induction argument will be used. According to (5.34), we already know that

$$\deg(E_0'(A,1)) = \deg(0) = 0 \quad \text{and} \quad \deg(E_1'(A,1)) = \deg(-A) = 1.$$

As the induction assumption, assume that

$$\deg(E_j'(A,1)) = j \quad \text{for all} \;\; j < n.$$

Then, owing to (5.49), it follows that

$$\deg(E_n'(A,1)) = n, \qquad n \geq 0. \tag{5.51}$$

Therefore, by (5.48),

$$\deg(p_n) = n - 1.$$

Subsequently, for any given polynomial, $q \in \mathbb{Z}[A]$, we will denote by $\ell(q)$ the leading coefficient of $q(A)$. According to Table 5.1, we already know that

$$\ell(p_5) = 1.$$

As an induction hypothesis, assume that

$$\ell(p_{4(n-1)+1}) = 1. \tag{5.52}$$

By (5.48), (5.49) and (5.51)

$$\begin{aligned}
\ell(p_{4n-2}) &= \ell(E_{4n-3}'(A,1)) = -\ell(E_{4(n-1)}'(A,1)) = -\ell(p_{4(n-1)+1}),\\
\ell(p_{4n-1}) &= \ell(E_{4n-2}'(A,1)) = \ell(E_{4n-3}'(A,1)) = -\ell(p_{4(n-1)+1}),\\
\ell(p_{4n}) &= \ell(E_{4n-1}'(A,1)) = -\ell(E_{4n-2}'(A,1)) = \ell(p_{4(n-1)+1}),\\
\ell(p_{4n+1}) &= \ell(E_{4n}'(A,1)) = \ell(E_{4n-1}'(A,1)) = \ell(p_{4(n-1)+1}).
\end{aligned}$$

By (5.52), the proof is complete. □

As a consequence of these lemmas, the next result holds.

Proposition 5.3.6. *Suppose* (5.29). *Then, the problem* (5.1) *possesses infinitely many subharmonics. In other words, there exists a sequence of integers* $\{n_m\}_{m\geq 1}$ *with*

$$\lim_{m\to+\infty} n_m = +\infty,$$

such that (5.1) *has at least a* $n_m T$*-periodic coexistence state for every* $m \geq 1$.

Proof. Since $p_n(0) = n$ for all $n \in \mathbb{N}$ and, thanks to Lemma 5.3.5, for every integer $n \geq 1$,

$$\ell(p_{4n+2}) = \ell(p_{4n+3}) = -1,$$

it becomes apparent that $p_{4n+2}(A)$ (resp. $p_{4n+3}(A)$) possesses a root, A_{4n+2} (resp. A_{4n+3}), where it changes of sign. Thus, for every integer $n \geq 1$, there exist two odd integers, $i_n, j_n \geq 1$, for which

$$\begin{aligned} p_{4n+2}^{k)}(A_{4n+2}) &= 0, \quad 0 \leq k \leq i_n - 1, \quad p_{4n+2}^{i_n)}(A_{4n+2}) \neq 0, \\ p_{4n+3}^{k)}(A_{4n+3}) &= 0, \quad 0 \leq k \leq j_n - 1, \quad p_{4n+3}^{j_n)}(A_{4n+3}) \neq 0. \end{aligned}$$

Thus, the algebraic multiplicity of [66] for these polynomials at those roots is given by

$$\chi[p_{4n+2}(A); A_{4n+2}] = i_n, \qquad \chi[p_{4n+3}(A); A_{4n+3}] = j_n.$$

As these integers are odd, by Theorem 5.6.2 of [124], the local topological indexes of $p_{4n+2}(A)$ and $p_{4n+3}(A)$ change as A crosses A_{4n+2} and A_{4n+3}, respectively. Therefore, by Theorem 6.2.1 of [124], there exist two components of $(4n+2)T$-periodic solutions and $(4n+3)T$-periodic solutions bifurcating from the trivial solution $(A, 1)$ at the roots A_{4n+2} and A_{4n+3}, respectively. This ends the proof. □

The next result establishes Property (d).

Lemma 5.3.7. $p_2 | p_{2n}$ *for all* $n \geq 1$. *Thus, since* $p_2(A) = -A + 2$, $r = 2$ *is a root of* $p_{2n}(A)$ *for all integer* $n \geq 1$.

Proof. By (5.43), any $2T$-periodic solution is a $2nT$-periodic solution for all $n \geq 1$. Thus, any bifurcation point from $(A, 1)$ to $2T$-periodic solutions must be a bifurcation point to $2nT$-periodic solutions. Since the unique bifurcation value to $2T$-periodic solutions is the root of $p_2(A) = -A + 2$, given by $r = 2$, it becomes apparent that $p_{2n}(2) = 0$ for all integer $n \geq 1$. Therefore, $p_2 | p_{2n}$ for all $n \geq 1$. This ends the proof. □

The next list of polynomials, collecting $p_{2n+1}(A)$ and $\frac{p_{2n}(A)}{2-A}$, for $1 \leq n \leq 6$, might be helpful to understand the (very sharp) identity established by the next result.

$$
\begin{aligned}
\frac{p_2(A)}{2-A} &= 1\\
p_3(A) &= -A^2+3\\
\frac{p_4(A)}{2-A} &= -A^2+2\\
p_5(A) &= A^4-5A^2+5\\
\frac{p_6(A)}{2-A} &= A^4-4A^2+3\\
p_7(A) &= -A^6+7A^4-14A^2+7\\
\frac{p_8(A)}{2-A} &= -A^6+6A^4-10A^2+4\\
p_9(A) &= A^8-9A^6+27A^4-30A^2+9\\
\frac{p_{10}(A)}{2-A} &= A^8-8A^6+21A^4-20A^2+5\\
p_{11}(A) &= -A^{10}+11A^8-44A^6+77A^4-55A^2+11\\
\frac{p_{12}(A)}{2-A} &= -A^{10}+10A^8-36A^6+56A^4-35A^2+6\\
p_{13}(A) &= A^{12}-13A^{10}+65A^8-156A^6+182A^4-91A^2+13.
\end{aligned}
$$

Theorem 5.3.8. *The following identity holds*

$$\frac{p_n(A)}{2-A} = p_{n-1}(A) - \frac{p_{n-2}(A)}{2-A}$$

for all $n \in 2\mathbb{N}$, whereas

$$\frac{p_n(A)}{2+A} = p_{n-1}(A) - \frac{p_{n-2}(A)}{2+A}$$

for all $n \in 2\mathbb{N}+1$.

Proof. First, we will prove the next relationships

$$\begin{cases} -\dfrac{n}{2} - 1 - \displaystyle\sum_{\substack{j=1\\ j\in 2\mathbb{N}}}^{n} E_j'(A,1) = 1 - A + \sum_{j=3}^{n+1}(-1)^j p_j, & n \in 2\mathbb{N}, \\ \left[\dfrac{n}{2}\right] + 1 + \displaystyle\sum_{\substack{j=1\\ j\in 2\mathbb{N}+1}}^{n} E_j'(A,1) = 1 - A + \sum_{j=3}^{n+1}(-1)^j p_j, & n \in 2\mathbb{N}+1. \end{cases} \tag{5.53}$$

Since $p_2(A) = 2 - A$, particularizing (5.47) at $n = 3$ yields

$$-2 - E_2'(A,1) = 1 - A - p_3(A),$$

which is (5.53) for $n = 2$. As the induction assumption, assume that (5.53) holds for some $n = 2m$ with $m \geq 1$, i.e.,

$$-m - 1 - \sum_{\substack{j=1\\ j\in 2\mathbb{N}}}^{2m} E_j'(A,1) = 1 - A + \sum_{j=3}^{2m+1} (-1)^j p_j(A). \tag{5.54}$$

According to (5.48),

$$\begin{aligned} 2m + 2 + E_1'(A,1) + E_2'(A,1) + \cdots \\ + E_{2m}'(A,1) + E_{2m+1}'(A,1) = p_{2m+2}(A). \end{aligned} \tag{5.55}$$

Thus, adding (5.54) and (5.55), we obtain that

$$m + 1 + \sum_{\substack{j=1\\ j\in 2\mathbb{N}+1}}^{2m+1} E_j'(A,1) = 1 - A + \sum_{j=3}^{2m+2} (-1)^j p_j(A). \tag{5.56}$$

Equivalently,

$$\left[\frac{2m+1}{2}\right] + 1 + \sum_{\substack{j=1\\ j\in 2\mathbb{N}+1}}^{2m+1} E_j'(A,1) = 1 - A + \sum_{j=3}^{2m+2} (-1)^j p_j(A),$$

which shows the validity of (5.53) for $n = 2m + 1$. To prove the validity of (5.53) for $n = 2(m+1) = 2m + 2$, we can argue similarly. Again by (5.48),

$$\begin{aligned} 2m + 3 + E_1'(A,1) + E_2'(A,1) + \cdots \\ + E_{2m+1}'(A,1) + E_{2m+2}'(A,1) = p_{2m+3}(A). \end{aligned} \tag{5.57}$$

Hence, subtracting (5.57) from (5.56) yields

$$-m - 2 - \sum_{\substack{j=1\\ j\in 2\mathbb{N}}}^{2m+2} E_j'(A,1) = 1 - A + \sum_{j=3}^{2m+3} (-1)^j p_j(A). \tag{5.58}$$

Since

$$-\frac{2m+2}{2}-1=-m-2,$$

(5.58) provides us with (5.53) for $n=2m+2$, which ends the proof of (5.53).

By (5.46), it follows from (5.47) and (5.49) that

$$p_n(A)=\begin{cases} p_{n-1}(A)+1+A\Big[-\dfrac{n}{2}-\displaystyle\sum_{\substack{j=1\\ j\in 2\mathbb{N}}}^{n-2}E_j'(A,1)\Big] & \text{if } n\in 2\mathbb{N},\\[2ex] p_{n-1}(A)+1+A\Big[\dfrac{n-1}{2}+\displaystyle\sum_{\substack{j=1\\ j\in 2\mathbb{N}+1}}^{n-2}E_j'(A,1)\Big] & \text{if } n\in 2\mathbb{N}+1.\end{cases} \tag{5.59}$$

On the other hand, when $n\in 2\mathbb{N}$, it follows from (5.53) and (5.59) that

$$\begin{aligned} p_n(A)-p_{n-1}(A) &= 1+A\Big[-\frac{n}{2}-\sum_{\substack{j=1\\ j\in 2\mathbb{N}}}^{n-2}E_j'(A,1)\Big]\\ &= 1+A\Big[-\frac{n-2}{2}-1-\sum_{\substack{j=1\\ j\in 2\mathbb{N}}}^{n-2}E_j'(A,1)\Big]\\ &= 1+A\Big[1-A+\sum_{j=3}^{n-1}(-1)^j p_j\Big]\\ &= 1-Ap_{n-1}(A)+A\Big[1-A+\sum_{j=3}^{n-2}(-1)^j p_j\Big]\\ &= -Ap_{n-1}(A)+1+A\Big[\frac{n-2}{2}+\sum_{\substack{j=1\\ j\in 2\mathbb{N}+1}}^{n-3}E_j'(A,1)\Big]\\ &= -Ap_{n-1}(A)+p_{n-1}(A)-p_{n-2}(A). \end{aligned}$$

Therefore, for every $n\in 2\mathbb{N}$,

$$p_n(A)=(2-A)p_{n-1}(A)-p_{n-2}(A).$$

The proof is complete for n even. Subsequently, we assume that n is odd. Arguing as in the previous case, from (5.59) and (5.53) the following chain of identities holds

$$\begin{aligned}
p_n(A) - p_{n-1}(A) &= 1 + A\Big[\frac{n-1}{2} + \sum_{\substack{j=1 \\ j\in 2\mathbb{N}+1}}^{n-2} E_j'(A)\Big] \\
&= 1 + A\Big[1 - A + \sum_{j=3}^{n-1}(-1)^j p_j\Big] \\
&= 1 + Ap_{n-1}(A) + A\Big[1 - A + \sum_{j=3}^{n-2}(-1)^j p_j\Big] \\
&= Ap_{n-1}(A) + 1 + A\Big[-\frac{n-1}{2} - \sum_{\substack{j=1 \\ j\in 2\mathbb{N}}}^{n-3} E_j'(1)\Big] \\
&= Ap_{n-1}(A) + p_{n-1}(A) - p_{n-2}(A).
\end{aligned}$$

Therefore, for every $n \in 2\mathbb{N}+1$,

$$p_n(A) = (2+A)p_{n-1}(A) - p_{n-2}(A).$$

This ends the proof. $\square$

Theorem 5.3.8 can be summarized into the next generalized identity

$$p_n(A) = [2 - (-1)^n A]p_{n-1}(A) - p_{n-2}(A), \qquad n \in \mathbb{N}. \tag{5.60}$$

As a by-product of these identities, the next result, establishing Property (e) at the beginning of the section, holds.

Corollary 5.3.9. *For every $n \geq 1$, the polynomials $\dfrac{p_{2n}(A)}{2-A}$ and $p_{2n+1}(A)$ are even.*

Proof. We already know that

$$\frac{p_2(A)}{2-A} = 1 \qquad \text{and} \qquad p_3(A) = -A^2 + 3.$$

Arguing by induction, assume that $\dfrac{p_{2m-2}(A)}{2-A}$ and $p_{2m-1}(A)$ are even polynomials for some $m \geq 1$. Then, by (5.60),

$$\frac{p_{2m}(A)}{2-A} = p_{2m-1}(A) - \frac{p_{2m-2}(A)}{2-A}$$

must be also even, because it is sum of two even functions. Similarly, since p_{2m+1} can be expressed in the form

$$p_{2m+1}(A) = (2+A)p_{2m}(A) - p_{2m-1}(A) = (4-A^2)\frac{p_{2m}(A)}{2-A} - p_{2m-1}(A),$$

it becomes apparent that $p_{2m+1}(A)$ is also an even polynomial. The proof is completed. $\square$

5.4 Characterizing the bifurcation points from $(A,1)$

The following definition will be used in the statement of the main theorem of this section.

Definition 5.4.1. *Given two arbitrary polynomials $q_1, q_2 \in \mathbb{Z}[A]$, it is said that the roots of q_1 are separated by the roots of q_2 if all the roots of q_2 lye in between the maximal and minimal roots of q_1 and any pair of consecutive roots of q_2 contains exactly one root of q_1.*

The main theorem of this section can be stated as follows. It counts the number of roots of each of the polynomials $p_n(A)$, $n \geq 1$, establishing that there are as many roots as indicated by the degree, that all of them are real and algebraically simple and that the positive roots of $p_{n+1}(A)$ are always separated by the positive roots (less than 2 if $n \in 2\mathbb{N}$) of $p_n(A)$. So, it counts all roots establishing their relative positions.

Theorem 5.4.2. *For every $n \geq 2$, the positive roots of $p_{2n}(A)$ are separated by the positive roots of $p_{2n-1}(A)$, and the positive roots of $p_{2n+1}(A)$ are separated by those of $p_{2n}(A)$ less than 2. Moreover, for every $n \geq 1$, the even polynomials $\frac{p_{2n}(A)}{2-A}$ and $p_{2n-1}(A)$ have (exactly) $n-1$ positive roots. Thus, since they are even with degree $2n-2$, they must have another $n-1$ negative roots and, therefore, all roots are real and simple.*

Proof. As we have already constructed the associated polynomials above, it is easily seen that all the thesis of Theorem 5.4.2 hold to be true for $2 \leq n \leq 6$. This task can be easily accomplished by simply looking at Figure 5.3, where we have plotted all the positive roots of $p_n(A)$ for $2 \leq n \leq 13$. These roots are located in the interval $(0,2]$ and have been represented in abscisas at different levels according to n. As inserting in the same interval $(0,2]$ all the zeros of the first 13 polynomials would not be of any real help for understanding their fine distribution, we have superimposed them at 13 different levels, each of them containing the positive roots of each of the polynomials p_n, $2 \leq n \leq 13$. In total we are representing 42 roots, though some of them are common roots of different polynomials as a result of the fact that any kT-periodic solution must be a nkT-periodic solution for all $n \geq 1$. These common roots have been represented in vertical dashed lines to emphasize that all roots on them share the same abscisa value. In such case, the ordinates provide us with the corresponding value of n. By simply having a glance at Figure 5.3, it is easily realized how the two roots of the polynomial p_4 are separated by the root of p_3, the 3 roots of p_6 are separated by the 2 roots of p_5, the 4 roots of p_8 are separated by the 3 of p_7, and so on... Similarly, the two roots of p_5 are separated by the unique root of p_4 different from 2, the 3 roots of p_7 are separated by the 2 roots of p_6 different from 2, and so on... The proof of the theorem will be delivered in two steps by induction in both cases. Since $\frac{p_2(A)}{2-A} = 1$ does not admit any root, this is a very special case that will not play any rol in these induction arguments.

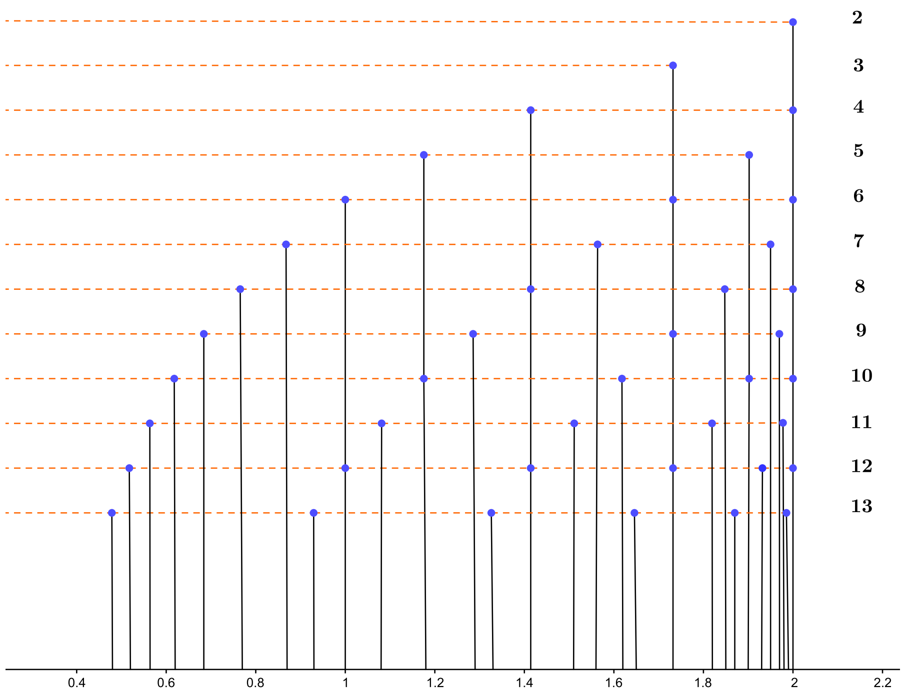

Figure 5.3: Positive roots of p_n, $2 \leq n \leq 13$.

Step 1: Passing from $p_{2n}(A)$ to $p_{2n+1}(A)$, $n \geq 2$. According to Figure

5.3, it becomes apparent that the two positive roots of $p_4(A)$ are separated by the unique root of $p_3(A)$. Moreover, all these zeros are real and simple and each of the polynomials

$$p_3(A) = -A^2 + 3, \qquad \frac{p_4(A)}{2-A} = -A^2 + 2,$$

has a unique positive root. Arguing by induction, assume that $p_{2n-1}(A)$ and $p_{2n}(A)$ satisfy all the assertions of the statement of the theorem for some $n \geq 2$. In other words, all the positive roots of these polynomials are real and algebraically simple, the positive roots of $p_{2n}(A)$ are separated by the positive roots of $p_{2n-1}(A)$, and the polynomials $\frac{p_{2n}(A)}{2-A}$ and $p_{2n-1}(A)$ have (exactly) $n-1$ positive roots. We claim that the positive roots of the polynomial $p_{2n+1}(A)$ are real and simple, that they are separated by the positive roots of $p_{2n}(A)$, except for 2, and that it has (exactly) n positive roots. Indeed, by Theorem 5.3.8 , we already know that

$$p_{2n+1}(A) = (2+A)p_{2n}(A) - p_{2n-1}(A). \tag{5.61}$$

First, we will show the previous claim in the case when $2n \in 4\mathbb{N} + 2$. So, suppose $2n \in 4\mathbb{N}+2$. Figure 5.4 shows the plots of the polynomials $p_{2n-1}(A)$ and $(2+A)p_{2n}(A)$ in one of such cases: $p_{2n-1}(A)$ has been plotted in brown

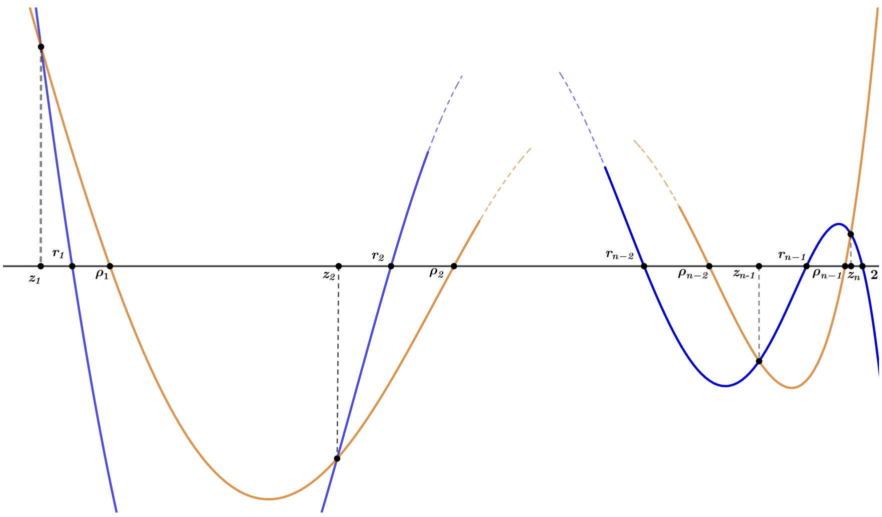

Figure 5.4: Sketch of the construction of $p_{2n+1}(A)$.

and $(2+A)p_{2n}(A)$ in blue. According to Lemmas 5.3.4 and 5.3.5, we already know that

$$\begin{aligned} 2n-1 = p_{2n-1}(0) < 4n = 2p_{2n}(0), \\ \deg(p_{2n-1}) = 2n-2, \\ \deg((2+A)p_{2n}) = 2n, \end{aligned} \tag{5.62}$$

and, since $2n \in 4\mathbb{N}+2$, the leading coefficient of $p_{2n-1}(A)$ equals 1, while the leading coefficient of $p_{2n}(A)$ equals -1. Thus, $p_{2n-1}(A) > 0$ and $(2+A)p_{2n}(A) < 0$ for $A > 2$. By the induction assumption, the polynomials $\frac{p_{2n}(A)}{2-A}$ and $p_{2n-1}(A)$ have (exactly) $n-1$ positive roots. Hence, each of the polynomials $p_{2n-1}(A)$ and $(2+A)p_{2n}(A)$ possesses (exactly) $n-1$ simple roots in the interval $(0,2)$ and, in addition, $p_{2n}(2) = 0$. In Figure 5.4, we have named by ρ_i, $1 \le i \le n-1$, the $n-1$ positive roots of $p_{2n-1}(A)$,

$$0 < \rho_1 < \rho_2 < \cdots < \rho_{n-2} < \rho_{n-1} < 2,$$

while those of $p_{2n}(A)$ less than 2 have been named by r_i, $1 \le i \le n-1$. So,

$$0 < r_1 < r_2 < \cdots < r_{n-1} < r_{n-1} < r_n := 2.$$

As, again by the induction hypothesis, the positive roots of $(2+A)p_{2n}(A)$ are separated by the positive roots of $p_{2n-1}(A)$, necessarily

$$0 < r_1 < \rho_1 < r_2 < \rho_2 < \cdots < r_{n-2} < \rho_{n-2} < r_{n-1} < \rho_{n-1} < r_n = 2. \tag{5.63}$$

Consequently, by (5.61), the polynomial $p_{2n+1}(A)$ must have, at least, n different roots in the interval $(0,2)$. These roots have been named by z_i, $1 \le i \le n$, in Figure 5.4 and they satisfy

$$0 < z_1 < r_1 < \rho_1 < z_2 < r_2 < \rho_2 < \cdots < z_{n-1} < r_{n-1} < \rho_{n-1} < z_n < 2. \tag{5.64}$$

On the other hand, by Corollary 5.3.9, $p_{2n+1}(A)$ is an even polynomial. Thus, since, due to Lemma 5.3.5, it has degree $2n$ and, by the previous construction, $\pm z_i$, $1 \le i \le n$, provides us with a set of $2n$ different roots of $p_{2n+1}(A)$, necessarily

$$p_{2n+1}(A) = -\prod_{j=1}^{n}(A^2 - z_j^2), \qquad A > 0.$$

Therefore, all the roots of $p_{2n+1}(A)$ are real and algebraically simple. As a direct consequence of (5.64) it is apparent that the positive roots of $p_{2n+1}(A)$ are separated by the positive roots of $p_{2n}(A)$, except for 2.

Subsequently, we should prove the result in the special case when $2n \in 4\mathbb{N}$. In this situation, owing to Lemmas 5.3.4 and 5.3.5, the plots of the polynomials $p_{2n-1}(A)$ and $(2+A)p_{2n}(A)$ look like illustrated by Figure 5.5. Apart from the fact that now $p_{2n-1}(A) > 0$ and $(2+A)p_{2n}(A) < 0$ for all $A > 2$, because the leading coefficients change sign, the previous analysis can be easily adapted to cover the present situation in order to infer that $p_{2n+1}(A)$ satisfies all the requirements also in this case. By repetitive the technical details of the proof are omitted here in.

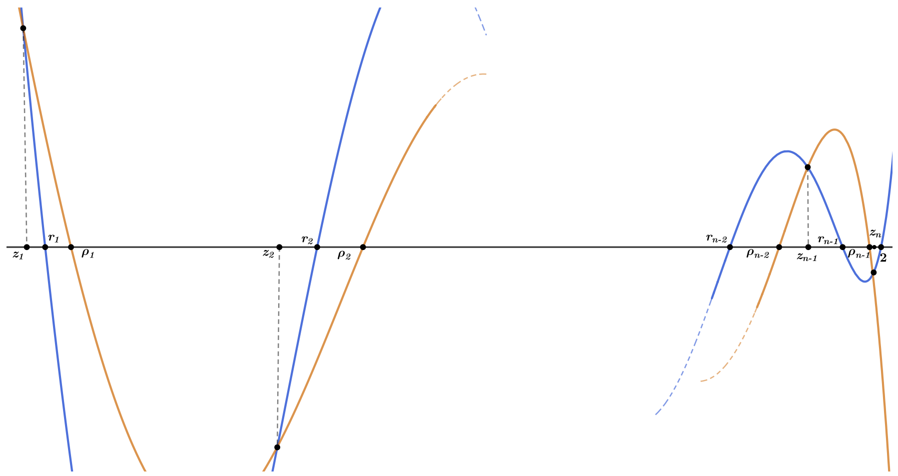

Figure 5.5: Sketch of the construction of $p_{2n+1}(A)$.

Step 2: Passing from $p_{2n+1}(A)$ to $p_{2n+2}(A)$, $n \geq 2$. According to Figure 5.3, it becomes apparent that the two positive roots of $p_5(A)$ are separated by the unique root of $p_4(A)$ less than 2. Moreover, all their roots are real and simple. Note that the polynomials

$$\frac{p_4(A)}{2-A} = -A^2 + 2, \qquad p_5(A) = A^4 - 5A^2 + 5,$$

have one and two positive roots respectively. Arguing by induction, assume that $p_{2n}(A)$ and $p_{2n+1}(A)$ satisfy all the requirements in the statement of the theorem for some $n \geq 2$, i.e., all the positive roots of these polynomials are real and algebraically simple, the positive roots of $p_{2n+1}(A)$ are separated by the positive roots less than 2 of $p_{2n}(A)$, and the polynomials $\frac{p_{2n}(A)}{2-A}$ and $p_{2n+1}(A)$ have, respectively, $n-1$ and n positive roots. We claim that the roots of the polynomial $p_{2n+2}(A)$ are real and simple, that they are separated by the roots of $p_{2n+1}(A)$, and that $p_{2n+2}(A)$ possesses $n+1$ positive roots.

Indeed, by Theorem 5.3.8 ,

$$p_{2n+2}(A) = (2-A)p_{2n+1}(A) - p_{2n}(A). \tag{5.65}$$

As in the previous step, we first deal with the case when $2n \in 4\mathbb{N}+2$. By Lemmas 5.3.4 and 5.3.5, we already know that

$$\begin{aligned} 2n = p_{2n}(0) < 4n+2 = 2p_{2n+1}(0), \\ \deg(p_{2n}) = 2n-1, \\ \deg((2-A)p_{2n+1}) = 2n+1, \end{aligned} \tag{5.66}$$

and, since $2n \in 4\mathbb{N}+2$, the leading coefficient of $p_{2n}(A)$ equals -1, and the leading coefficient of $p_{2n+1}(A)$ equals also -1. Thus,

$$p_{2n}(A) < 0, \qquad (2-A)p_{2n+1}(A) > 0 \qquad \text{for all } \; A > 2.$$

By the induction assumption, the polynomials $\frac{p_{2n}(A)}{2-A}$ and $p_{2n+1}(A)$ have (exactly) $n-1$ and n positive roots, respectively. Thus, each of the polynomials $p_{2n}(A)$ and $(2-A)p_{2n+1}(A)$ possesses (exactly) n simple roots in $(0,2)$ and, obviously, $(2-A)p_{2n+1}(A)$ also vanishes at $A=2$. Figure 5.6 shows the plots of $p_{2n}(A)$, in blue, and $(2-A)p_{2n+1}(A)$, in brown. In Figure 5.6, we have

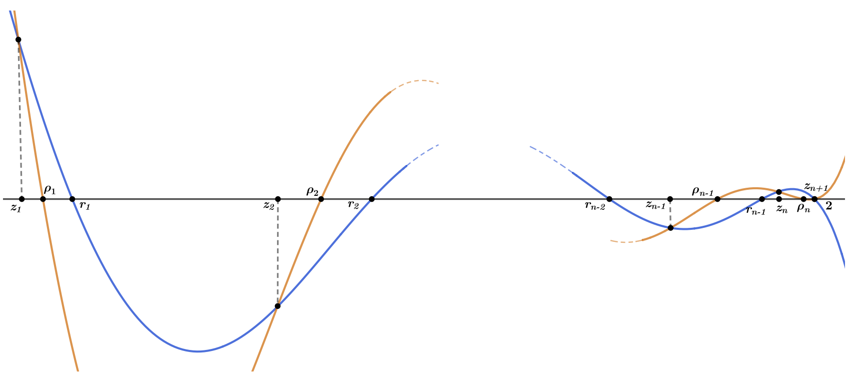

Figure 5.6: Sketch of the construction of $p_{2n+2}(A)$ in case $2n \in 4\mathbb{N}+2$.

named by ρ_i, $1 \le i \le n$, the n positive roots less than 2 of $(2-A)p_{2n+1}(A)$,

$$0 < \rho_1 < \rho_2 < \cdots < \rho_{n-1} < \rho_n < 2 := \rho_{n+1},$$

whereas r_i, $1 \le i \le n$, stand for the positive roots of $p_{2n}(A)$. Since $p_{2n}(2) = 0$, $r_n = 2$. Since the positive roots of $p_{2n+1}(A)$ are separated by the positive roots less than 2 of $p_{2n}(A)$, the following holds

$$0 < \rho_1 < r_1 < \rho_2 < r_2 < \cdots < \rho_{n-1} < r_{n-1} < \rho_n < 2 := \rho_{n+1} = r_n,$$

as illustrated by Figure 5.6. Thanks to (5.65), it becomes apparent that the polynomial $p_{2n+2}(A)$ admits, at least, an interior root in each of the intervals (ρ_i, ρ_{i+1}), $i = 0, ..., n$, denoted by z_i in Figure 5.6, plus $z_{n+1} = 2$. Here we are setting $\rho_0 := 0$. Consequently, $p_{2n+2}(A)$ has, at least, $n + 1$ positive roots.

On the other hand, thanks to Corollary 5.3.9, $\frac{p_{2n+2}(A)}{2-A}$ is an even function and hence, $p_{2n+2}(A)$ has, at least, $2n + 1$ different roots. Since, by Lemma 5.3.5,

$$\deg(p_{2n+2}) = 2n + 1,$$

all these roots are real and algebraically simple. By construction, it is apparent that the positive roots of $p_{2n+2}(A)$ are separated by the positive roots of $p_{2n+1}(A)$ (see Figure 5.6 if necessary).

If, instead of $2n \in 4\mathbb{N} + 2$, we impose $2n \in 4\mathbb{N}$, then the previous arguments can be easily adapted to complete the proof of the theorem from Figure 5.7, where the graphs of $(2 + A)p_{2n+1}(A)$ and $p_{2n}(A)$ have been superimposed in order to show their crossing points, which, owing to Theorem 5.3.8 , are the roots of $p_{2n+2}(A)$. By repetitive, the technical details of this case are not included here. $\square$

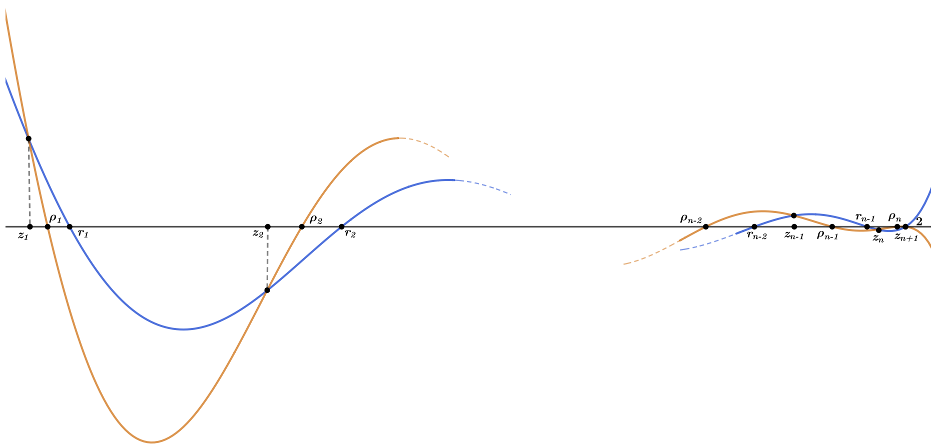

Figure 5.7: Sketch of the construction of $p_{2n+2}(A)$ in case $2n \in 4\mathbb{N}$.

A careful reading of the proof of Theorem 5.61 reveals that, actually, not only the roots of $p_n(A)$ are separated by those of $p_{n-1}(A)$, but that they are also separated by those of $p_{n-2}(A)$, taking always into account the exceptional role played by the root 2.

5.5 Global bifurcation diagram

This section analyzes the global structure of the set of zeros of the maps φ_n, $n \geq 1$, introduced in (5.32). These zeros are the positive fixed points of the Poincaré maps $\mathcal{P}_n$, $n \geq 1$, constructed in Section 3. They provide us with the nT-periodic coexistence states of (5.1) under the additional assumption (5.29). It should be remembered that, according to (5.44), for every integer $n \geq 1$

$$p_n(A) = \frac{d\varphi_n(A,1)}{dx} = \mathfrak{L}(n;A), \qquad A > 0, \tag{5.67}$$

provides us with the linearization at the *trivial curve*, $(A,1)$, of $\varphi_n(A,x)$. In our analysis, A is always regarded as a bifurcation parameter to nT-periodic coexistence states from the T-periodic ones (i.e., from $x = 1$). As a consequence of the simplicity of all the roots of $p_n(A)$, $n \geq 1$, guaranteed by Theorem 5.4.2, the following result holds.

Theorem 5.5.1. *For every $n \geq 1$ and $r \in p_n^{-1}(0)$ the following algebraic transversality condition holds*

$$\mathfrak{L}_1(N\left[\mathfrak{L}(n;r)\right]) \oplus R\left[\mathfrak{L}(n;r)\right] = \mathbb{R}, \tag{5.68}$$

where

$$\mathfrak{L}_1 := \frac{d\mathfrak{L}(n;r)}{dA}, \qquad n \geq 1, \;\; r \in p_n^{-1}(0).$$

Therefore, by Theorem 1.7 of M. G. Crandall and P. H. Rabinowitz [37], there exists an analytic curve of nT-periodic coexistence states of (5.1) bifurcating from $(A,1)$ at the root $A = r$. Actually, there exists $\varepsilon > 0$ and a real analytic map $A : (-\varepsilon,\varepsilon) \to \mathbb{R}$ such that $A(0) = r$ and

$$\varphi_n(A(s), 1+s) = 0 \quad \textit{for all} \;\; s \in (-\varepsilon,\varepsilon).$$

Moreover, any non-trivial zero of φ_n, (A,x) with $x \neq 1$, in a neighborhood of $(r,1)$ must be of the form $(A(s), 1+s)$ for some $s \in (-\varepsilon,\varepsilon)$. In other words, there exists $\varrho > 0$ such that

$$\left.\begin{array}{r} \varphi_n(A,x) = 0 \\ |A-r| + |x-1| < \varrho \\ x \neq 1 \end{array}\right\} \Longrightarrow (A,x) = (A(s), 1+s) \quad \textit{for some} \;\; s \in (-\varepsilon,\varepsilon).$$

Furthermore, setting

$$A(s) = r + A_1 s + A_2 s^2 + \mathcal{O}(s^3) \quad \textit{as} \;\; s \to 0, \tag{5.69}$$

one has that

(a) $A_1 = 0$ *and* $A_2 > 0$ *if* $n = 2$ *and* $r = 2$, *in complete agreement with Figure 7.1;*

(b) $A_1 < 0$ *if* $n = 3$ *and* $r = \sqrt{3}$*;*

(c) $A_1 = 0$ *and* $A_2 < 0$ *(resp.* $A_2 > 0$*) if* $n = 4$ *and* $r = r_{4,1} = \sqrt{2}$ *(resp.* $r = r_{4,2} = 2$*).*

Proof. According to (5.67), $\mathfrak{L}(n;r) = p_n(r) = 0$. Thus, $N[\mathfrak{L}(n;r)] = \mathbb{R}$ and (5.68) can be equivalently expressed as $\mathfrak{L}_1(\mathbb{R}) = \mathbb{R}$, which holds true because, thanks to Theorem 5.61, we already know that r is an algebraically simple root of $p_n(A)$, i.e.,

$$\mathfrak{L}_1 = p_n'(r) \neq 0.$$

So, (5.68) indeed holds and [37, Th. 1.7] applies to $\varphi_n(A,x) = 0$ at $(A,x) = (r,1)$. Since we can take $\psi = 1$ as a generator of $N[\mathfrak{L}(n;r)] = \mathbb{R}$ and $Y = [0]$ as a supplement of $N[\mathfrak{L}(n;r)] = \mathbb{R}$ in $\mathbb{R}$, owing to [37, Th. 1.7], there exist $\varepsilon > 0$ and a real analytic map

$$(A,y) : (-\varepsilon,\varepsilon) \to \mathbb{R} \times Y$$

such that $(A(0), y(0)) = (r, 0)$ and

$$\varphi_n(A(s), 1 + s(\psi + y(s))) = 0 \quad \text{for all} \;\; s \in (-\varepsilon,\varepsilon), \tag{5.70}$$

it becomes apparent, by construction, that

$$\varphi_n(A(s), 1+s) = 0 \quad \text{for all} \;\; s \in (-\varepsilon,\varepsilon),$$

because $y \equiv 0$ and $\psi = 1$. This ends the proof of the first two claims of the theorem: the existence of the analytic curve of nontrivial solutions and the uniqueness.

As far as concerns to the problem of ascertaining the nature of these *local bifurcations* at $(r,1)$, we can proceed as follows. In order to prove Part (a), note that, thanks to (5.70), setting $x(s) := 1 + s$ and expanding in Taylor series, we have that

$$0 = \varphi_2(A(s), x(s)) = \varphi_2(r,1) + \frac{d\varphi_2}{ds}(r,1)s + \frac{1}{2}\frac{d^2\varphi_2}{ds^2}(r,1)s^2 + \cdots$$

for all $s \in (-\varepsilon,\varepsilon)$, where $r = 2$. Moreover, by construction, we already know that

$$\varphi_2(r,1) = 0, \qquad \frac{\partial\varphi_2}{\partial x}(r,1) = p_2(r) = p_2(2) = 0$$

(see (5.67), if necessary). Thus, since by (5.37)

$$\varphi_2(A,x) = x\,(E_1(A,x)+1) - 2, \tag{5.71}$$

it follows from (5.69) and $\frac{\partial E_1}{\partial A}(r,1)=0$ that

$$\frac{d\varphi_2}{ds}(r,1) = \frac{\partial \varphi_2}{\partial A}(r,1)A'(0) = \frac{\partial E_1}{\partial A}(r,1)A_1 = 0,$$

where $' := \frac{d}{ds}$. Hence, these terms do not provide us with any neat information concerning A_1. So, we must consider higher order terms to find out A_1. As

$$\frac{\partial \varphi_2}{\partial A}(r,1) = 0 = \frac{\partial \varphi_2}{\partial x}(r,1),$$

applying the chain rule it readily follows that

$$0 = \frac{d^2\varphi_2}{ds^2}(r,1) = \frac{\partial^2 \varphi_2}{\partial x^2}(r,1) + 2\frac{\partial^2 \varphi_2}{\partial A \partial x}(r,1)A_1 + \frac{\partial^2 \varphi_2}{\partial A^2}(r,1)A_1^2. \tag{5.72}$$

On the other hand, differentiating with respect to x the identity (5.71) yields

$$\frac{\partial \varphi_2}{\partial x}(A,x) = E_1(A,x) + 1 + x\frac{\partial E_1}{\partial x}(A,x). \tag{5.73}$$

So,

$$\frac{\partial^2 \varphi_2}{\partial x^2}(A,x) = 2\frac{\partial E_1}{\partial x}(A,x) + x\frac{\partial^2 E_1}{\partial x^2}(A,x).$$

Consequently, particularizing at $(A,x)=(r,1)$, it follows from (5.34) that

$$\frac{\partial^2 \varphi_2}{\partial x^2}(r,1) = r^2 - 2r = 4 - 4 = 0. \tag{5.74}$$

Similarly, differentiating (5.73) with respect to A shows that

$$\frac{\partial^2 \varphi_2}{\partial x \partial A}(A,x) = \frac{\partial E_1}{\partial A}(A,x) + x\frac{\partial^2 E_1}{\partial x \partial A}(A,x)$$

and hence, owing to (5.34),

$$\frac{\partial^2 \varphi_2}{\partial x \partial A}(r,1) = \frac{\partial E_1}{\partial A}(r,1) + \frac{\partial^2 E_1}{\partial x \partial A}(r,1) = \frac{\partial^2 E_1}{\partial x \partial A}(r,1) = -1. \tag{5.75}$$

Lastly,

$$\frac{\partial^2 \varphi_2}{\partial A^2}(A,x) = x\frac{\partial^2 E_1}{\partial A^2}(A,x) = (1-x)^2 E_1(A,x)$$

and hence,

$$\frac{\partial^2 \varphi_2}{\partial A^2}(A,1) = 0. \tag{5.76}$$

Therefore, substituting (5.74), (5.75) and (5.76) into (5.72) it becomes apparent that $A_1 = 0$. Thanks to this fact, the third derivative admits the next (simple) expression:

$$0 = \frac{d^3\varphi_2}{ds^3}(r,1) = 6\frac{\partial^2\varphi_2}{\partial x \partial A}(r,1)A_2 + \frac{\partial^3\varphi_2}{\partial x^3}(r,1) = -6A_2 + 3r^2 - r^3,$$

which implies that

$$A_2 = \frac{4}{3} > 0$$

and ends the proof of Part (a).

To prove Part (b), note that, much like in Part (a), one has that

$$0 = \varphi_3(A(s), x(s)) = \varphi_3(r,1) + \frac{d\varphi_3}{ds}(r,1)s + \frac{1}{2}\frac{d^2\varphi_3}{ds^2}(r,1)s^2 + \cdots$$

for all $s \in (-\varepsilon, \varepsilon)$. Similarly,

$$\frac{\partial\varphi_3}{\partial A}(r,1) = 0 = \frac{\partial\varphi_3}{\partial x}(r,1).$$

So,

$$\frac{d\varphi_3}{ds}(r,1) = 0.$$

Moreover, differentiating twice with respect to s yields

$$\begin{aligned} 0 &= \frac{d^2\varphi_3}{ds^2}(r,1) \\ &= \frac{\partial^2\varphi_3}{\partial x^2}(r,1) + 2\frac{\partial^2\varphi_3}{\partial x\partial A}(r,1)A_1 + \frac{\partial^2\varphi_3}{\partial A^2}(r,1)A_1^2 \\ &= r^4 - r^3 - 2r^2 - 4rA_1. \end{aligned}$$

Consequently, since $r = \sqrt{3}$, it follows from this identity that

$$A_1 = \frac{\sqrt{3}-3}{4} < 0,$$

which ends the proof of Part (b).

Finally, much like before, we have that

$$0 = \varphi_4(A(s), x(s)) = \varphi_4(r,1) + \frac{d\varphi_4}{ds}(r,1)s + \frac{1}{2}\frac{d^2\varphi_4}{ds^2}(r,1)s^2 + \cdots$$

for all $s \in (-\varepsilon, \varepsilon)$, and, in addition,

$$\frac{\partial \varphi_4}{\partial A}(r,1) = 0 = \frac{\partial \varphi_4}{\partial x}(r,1).$$

Thus, $\frac{d\varphi_4}{ds}(r,1) = 0$. Moreover, differentiating twice yields

$$\begin{aligned} 0 &= \frac{d^2\varphi_4}{ds^2}(r,1) \\ &= \frac{\partial^2\varphi_4}{\partial x^2}(r,1) + 2\frac{\partial^2\varphi_4}{\partial x \partial A}(r,1)A_1 + \frac{\partial^2\varphi_4}{\partial A^2}(r,1)A_1^2 \\ &= r^6 - 3r^5 - r^4 + 8r^3 - 2r^2 - 4r + 2(r^3 - 2r^2 - 2r)A_1. \end{aligned}$$

Therefore, since $r = \sqrt{2}$ it follows from this identity that $A_1 = 0$. Furthermore,

$$\begin{aligned} 0 &= \frac{d^3\varphi_2}{ds^3}(r,1) \\ &= 6\frac{\partial^2\varphi_2}{\partial x \partial A}(r,1)A_2 + \frac{\partial^3\varphi_2}{\partial x^3}(r,1) \\ &= 6(3r^2 - 4r - 2)A_2 - r^8 + r^7 + 9r^6 - 11r^5 - 10r^4 + 20r^3 - 2r^2. \end{aligned}$$

Consequently, we find from $r = \sqrt{2}$ that

$$A_2 = -\frac{2(5+4\sqrt{2})}{3} < 0,$$

which ends the proof. □

Figure 5.8 shows the local bifurcation diagrams of the $2T$, $3T$ and $4T$-periodic coexistence states of (5.1) under condition (5.29). We are plotting x, in ordinates, versus A, in abscisas. By the analysis already done at the beginning of Section 2, and, in particular, by Theorem 5.1.1, which was sketched in Figure 5.2, we already know that, under condition (5.29), the problem (5.1) admits a $2T$-periodic coexistence state if, and only if, $A > 2$. Moreover, the local bifurcation of these solutions must be supercritical. Thus $A_2 \geq 0$. As a byproduct of Theorem 5.5.1, it turns out that $A_2 > 0$. So, it is a genuine supercritical pitchfork bifurcation of quadratic type. However, since $A_1 < 0$, the bifurcation to $3T$-periodic coexistence states from $(A, x) = (\sqrt{3}, 1)$ is transcritical, whereas the $4T$-periodic solutions emanate from $(A, x) = (\sqrt{2}, 1)$ through a subcritical quadratic pitchfork bifurcation, because $A_1 = 0$ and $A_2 < 0$ in this case.

The fact that the local nature of the first three bifurcation phenomena possess a completely different character shows that, in general, ascertaining the precise type of these local bifurcations for large n might not be possible, much like happened with the problem of determining the fine structure of the set of bifurcation points from the trivial solution $(A, 1)$. The higher is the order of the bifurcating subharmonics, measured by n, the higher is the complexity of the associated function φ_n and hence, the more involved is finding out the values of A_1 and A_2 in (5.69) by the intrinsic nature of the functions E_n defined in (5.34).

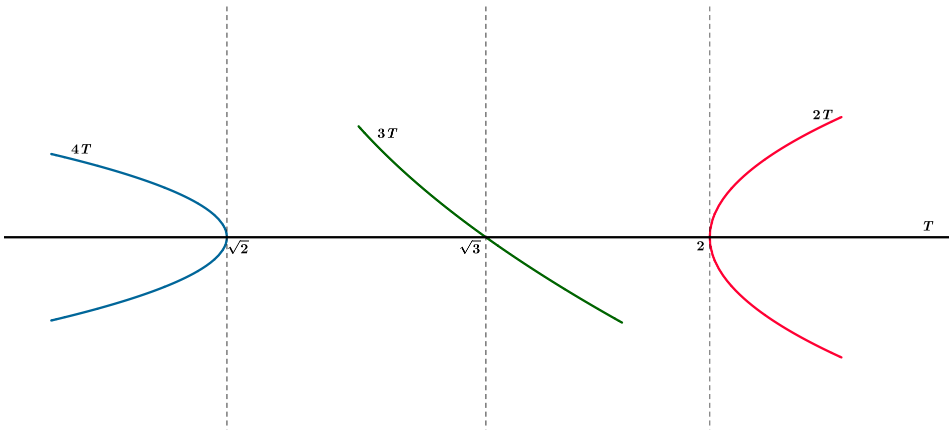

Figure 5.8: Local bifurcation diagrams from $(A, x) = (A, 1)$ of the nT-periodic coexistence states for $n \in \{2, 3, 4\}$.

Remark 5.5.2. Thanks to Theorem 5.5.1, it becomes apparent that the set of bifurcation points from $(A, 1)$ to nT-periodic coexistence states of (5.1) is the set of roots of $p_n(A)$. Since the number of roots of a polynomial is finite, the set of bifurcation points is numerable, as it is a numerable union of finite sets.

Since every nT-periodic coexistence state of (5.1) provides us with a knT-periodic coexistence state for all $k \geq 1$, owing Theorem 5.5.1, the roots of $p_n(A)$ must be roots of $p_{kn}(A)$ for all $n, k \geq 1$, i.e., $p_n | p_{kn}$ for all $n, k \geq 1$.

Remark 5.5.3. Thanks to Theorem 5.4.2 and Remark 5.5.2, the set of bifurcation points to a nT-periodic solution is a subset of the interval $(0, 2]$. Complementing [123, Th. 5.2], where the non-degeneration of the positive T-periodic coexistence states of (5.1) with respect to the T-periodic solutions was established, Theorem 5.5.1 shows that the T-periodic solutions are degenerated with respect to the nT-periodic solutions of (5.1) for all $n \geq 2$ at every positive root, r, of $p_n(A)$. Nevertheless, the T-periodic solutions are non-degenerated with respect to the nT-periodic solutions, $n \geq 2$, if $A > 2$, because in this range there is not any bifurcation point from $(A, 1)$.

Subsequently, we will discuss the global character of all the local bifurcations documented by Theorem 5.5.1 in the context of global bifurcation theory. In this discussion, by a (connected) component it is understood any closed and connected subset that is maximal for the inclusion. For any given integer $n \geq 1$, the set of non-trivial nT-periodic solutions of (5.1), $\mathcal{S}_n$, consists of all nT-periodic coexistence states different from $(A, 1)$ plus the set of points $(r, 1)$ with $p_n(r) = 0$. In other words, setting $\mathbb{R}_+ := (0, +\infty)$,

$$\mathcal{S}_n = \{(A, x) \in \mathbb{R}_+ \times (\mathbb{R}_+ \setminus \{1\}) \;:\; \varphi_n(A, x) = 0\} \cup \{(r, 1) \;:\; p_n(r) = 0\}.$$

Note that, owing to Theorem 5.5.1, $\{(r, 1) \;:\; p_n(r) = 0\}$ is the set of bifurcation points to nT-periodic solutions from the trivial curve $(A, 1)$. Thanks to (5.68), the algebraic multiplicity of J. Esquinas and J. López-Gómez [66] equals one,

$$\chi[\mathfrak{L}(n; A); r] = 1 \in 2\mathbb{N} + 1,$$

for all $r \in p_n^{-1}(0)$, $r > 0$. Thus, by [124, Th. 5.6.2], the local degree at $(A, 1)$ of the one-dimensional $\varphi_n(A, \cdot)$ changes as A crosses r (see also J. López-Gómez and C. Mora-Corral [133, Prop. 12.3.1] if necessary). Therefore, according to [124, Th. 6.2.1], for every integer $n \geq 2$ and each root $r > 0$ of $p_n(A)$, there is a component of $\mathcal{S}_n$, $\mathfrak{C}_{n,r}$, such that

$$(r, 1) \in \mathfrak{C}_{n,r} \subset \mathbb{R}_+ \times \mathbb{R}.$$

Moreover, by the local uniqueness about $(r, 1)$ guaranteed by Theorem 5.5.1, in a neighborhood of $(r, 1)$ the component $\mathfrak{C}_{n,r}$ consists of an analytic curve, $(A(s), 1 + s)$, $|s| < \varepsilon$. Note that any real continuous map must be compact. So, the Leray–Schauder degree (see, e.g., N. G. Lloyd [118], or [133, Ch. 12], if necessary) can be applied to get these global results. Alternatively, one might use the degree of P. Benevieri and M. Furi [12], as in Theorem 5.4 and Corollary 5.5 of [132] (see [128] for a recent survey on global bifurcation theory).

By Remark 5.2.4, for every $r \in p_n^{-1}(0) \cap \mathbb{R}_+$, the component $\mathfrak{C}_{n,r}$ must be separated away from $x = 0$ and hence, all their solutions must be positive, because $\varphi_n(0) = -n$. Thus, they indeed provide us with coexistence states of (5.1). Similarly, for every $n \geq 2$, since $\varphi_n(n) > 0$, $\mathfrak{C}_{n,r}$ is bounded above by n, in the sense that $x < n$ if $(A, x) \in \mathfrak{C}_{n,r}$ with $A > 0$. Therefore,

$$\mathcal{P}_x(\mathfrak{C}_{n,r}) \subset (0, n), \tag{5.77}$$

where $\mathcal{P}_x$ stands for the x-projection operator, $\mathcal{P}_x(A,x) := x$. Moreover, due to (5.50), $x=1$ is the unique zero of $\varphi_n(A,x)$ at $A=0$. Note that, due to Remark 5.5.2, $(A,1)=(0,1)\notin \mathfrak{C}_{n,r}$ because $p_n(0)=n>0$.

Throughout the rest of this section, we will also consider the (unilateral) subcomponents

$$\mathfrak{C}^+_{n,r} := \mathfrak{C}_{n,r}\cap [x>1], \qquad \mathfrak{C}^-_{n,r} := \mathfrak{C}_{n,r}\cap [x<1]. \tag{5.78}$$

Thanks to Theorem 5.5.1, these subcomponents are non-empty. Moreover, arguing as in [124, p. 182], it is easily seen that they equal the components $\mathfrak{C}^+$ and $\mathfrak{C}^-$ introduced on page [124, p. 187]. This feature heavily relies on the fact that x is a one-dimensional variable. Therefore, the unilateral theorem [124, Th. 6.4.3] can be applied to infer that each of the components $\mathfrak{C}^+_{n,r}$ and $\mathfrak{C}^-_{n,r}$ satisfies the *global alternative* of P. H. Rabinowitz [175], because the supplement of $N[\mathfrak{L}(n;r)]=\mathbb{R}$ in $\mathbb{R}$ is $Y=[0]$ and, due to (5.77), $\mathfrak{C}_{n,r}$ cannot admit an element, (A,x) with $x=0$. Therefore, $\mathfrak{C}^+_{n,r}$ (resp. $\mathfrak{C}^-_{n,r}$) satisfies some of the following two conditions, which are far from being excluding:

(a) There exists $s\in p_n^{-1}(0)\setminus\{r\}$ (resp. $t\in p_n^{-1}(0)\setminus\{r\}$) such that $(s,1)\in \mathfrak{C}^+_{n,r}$ (resp. $(t,1)\in\mathfrak{C}^-_{n,r}$).

(b) The component $\mathfrak{C}^+_{n,r}$ (resp. $\mathfrak{C}^-_{n,r}$) is unbounded in A, because of (5.77).

Note that the counterexample of E. N. Dancer [45] shows that Theorems 1.27 and 1.40 of P. H. Rabinowitz [175] are not true as originally stated. To show that the second option occurs in both cases we need the next result.

Lemma 5.5.4. *Each of the unilateral subcomponents satisfies*

$$\mathfrak{C}^\pm_{n,r}\cap\{(A,1)\ :\ A\geq 0\}=\{(r,1)\}. \tag{5.79}$$

Thus, also

$$\mathfrak{C}_{n,r}\cap\{(A,1)\ :\ A\geq 0\}=\{(r,1)\},$$

i.e., $(r,1)$ is the unique bifurcation point of $\mathfrak{C}_{n,r}$ from $(A,1)$.

Proof. Subsequently, we will denote by $\nu(n)$ the total number of positive roots of the polynomial $p_n(A)$. By Theorem 5.62, we already know that $\nu(n)=\frac{n}{2}$ if n is even and $\nu(n)=\frac{n-1}{2}$ if n is odd. We will prove the result only for $\mathfrak{C}^+_{n,r}$, as the same argument also works out to prove the corresponding assertion for the component $\mathfrak{C}^-_{n,r}$. The proof will proceed by contradiction. We already know that $\mathfrak{C}^+_{n,r}$ can only meet the trivial solution $(A,1)$ at the roots of $p_n(A)$. Suppose that $r=r_{n,i}$ for some $i\in\{1,...,\nu(n)\}$, and that there exists $j>i$, $j\in\{1,...,\nu(n)\}$, such that

$$\{(r_{n,i},1),(r_{n,j},1)\}\subset\mathfrak{C}^+_{n,r}\cap\{(A,1)\ :\ A\geq 0\}. \tag{5.80}$$

Then, by the definition of component, it becomes apparent that

$$\mathfrak{C}^+_{n,r_{n,i}} = \mathfrak{C}^+_{n,r_{n,j}} \tag{5.81}$$

as sketched by Figure 5.9. Thanks to Theorem 5.4.2, there exists

$$r_{n-1,k} \in (r_{n,i}, r_{n,j}) \cap p_{n-1}^{-1}(0).$$

By the incommensurability of nT with $(n-1)T$, $\mathfrak{C}^+_{n-1,r_{n-1,k}}$ cannot reach the component (5.81). Thus, must be bounded. Consequently, as $\mathfrak{C}^+_{n-1,r_{n-1,k}}$ also satisfies the global alternative of P. H. Rabinowitz, there exists $r_{n-1,\ell} \in p_{n-1}^{-1}(0)$, with $k \neq \ell$, such that

$$\{(r_{n-1,k}, 1), (r_{n-1,\ell}, 1)\} \subset \mathfrak{C}^+_{n-1,r_{n-1,k}} \cap \{(A,1) \;:\; A \geq 0\},$$

as sketched in Figure 5.9. Since the set of roots

$$\bigcup_{2 \leq \kappa \leq n} p_\kappa^{-1}(0)$$

is finite, it becomes apparent that, after finite many steps, there exists a component, $\mathfrak{C}^+_{n-h,r_{n-h,m}}$, for some $2 \leq h \leq n-3$ and $1 \leq m \leq \nu(n-h)$, that should meet the last component linking two different roots sketched in Figure 5.9,

$$\mathfrak{C}^+_{n-h+1,r_{n-h+1,v}} = \mathfrak{C}^+_{n-h+1,r_{n-h+1,w}},$$

because there is no any additional root of $p_{n-h}(A)$ in between $r_{n-h+1,v}$ and $r_{n-h+1,w}$. But this is impossible, by the incommensurability of $(n-h)T$ with $(n-h+1)T$. This contradiction ends the proof. $\square$

As an immediate consequence of the previous analysis, the next result holds. As for the x-projection operator, $\mathcal{P}_x$, we will denote by $\mathcal{P}_A$ the A-projection operator,

$$\mathcal{P}_A(A,x) := A.$$

Theorem 5.5.5. *For every integer $n \geq 2$ and each root $r > 0$ of $p_n(A)$, the component $\mathfrak{C}^+_{n,r}$ satisfies*

(a) $\mathcal{P}_x(\mathfrak{C}^+_{n,r}) \subset [1,n)$;

(b) $\mathcal{P}_A(\mathfrak{C}^+_{n,r}) = [A^+_{n,r}, +\infty)$ *for some* $A^+_{n,r} \in (0,r]$. *In particular,* $\mathfrak{C}^+_{n,r}$ *is unbounded.*

(c) $\mathfrak{C}^+_{n,r} \cap \{(A,1) \;:\; A \geq 0\} = \{(r,1)\}$;

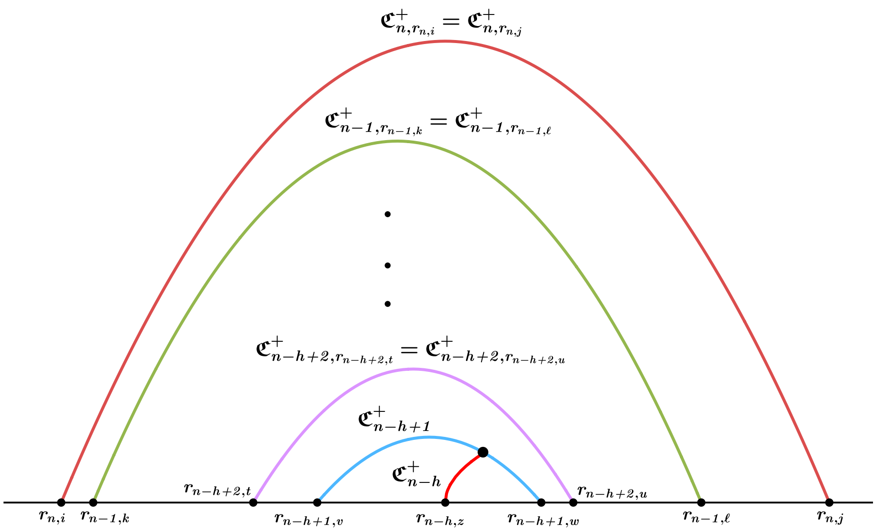

Figure 5.9: Sketch of the proof of Lemma 5.5.4.

(d) *For every* $n, m \geq 2$, $\mathfrak{C}^+_{n,r} \cap \mathfrak{C}^+_{m,s} = \emptyset$ *if* $r \neq s$.

Moreover, by Theorem 5.5.1, in a neighborhood of $(r, 1)$ *the component* $\mathfrak{C}^+_{n,r}$ *consists of an analytic curve,* $(A(s), 1 + s)$, $0 \leq s < \varepsilon$. *Similarly, the component* $\mathfrak{C}^-_{n,r}$ *satisfies* (c), (d) *and*

(A) $\mathcal{P}_x(\mathfrak{C}^-_{n,r}) \subset (0, 1]$*;*

(B) $\mathcal{P}_A(\mathfrak{C}^-_{n,r}) = [A^-_{n,r}, +\infty)$ *for some* $A^-_{n,r} \in (0, r]$. *In particular,* $\mathfrak{C}^-_{n,r}$ *is unbounded.*

Analogously, in a neighborhood of $(r, 1)$ *the component* $\mathfrak{C}^-_{n,r}$ *consists of an analytic curve,* $(A(s), 1 + s)$, $-\varepsilon < s \leq 0$.

Proof. At this stage, the only delicate point is Part (d). Suppose that $\mathfrak{C}^+_{n,r} \cap \mathfrak{C}^+_{m,s} \neq \emptyset$ for some $r \neq s$. Then, by the definition of component, necessarily

$$\mathfrak{C}^+_{n,r} = \mathfrak{C}^+_{m,s}.$$

Thus, $(r, 1), (s, 1) \in \mathfrak{C}^+_{n,r}$, which contradicts Lemma 5.5.4. The proof is complete. □

Except for the local bifurcations from the trivial line $(A,1)$, the global diagramas of the components $\mathfrak{C}^{\pm}_{n,r}$ plotted in Figure 5.1 respect the general properties established by Theorem 5.5.5. Although the components have been plotted with no secondary bifurcations along them, there are some numerical evidences that $\mathfrak{C}^{-}_{2,2}$ possesses a secondary bifurcation to $4T$-periodic solutions. Nevertheless, thanks to Theorem 5.5.5, even in the case that they might occur higher order bifurcations along these components, they must be disjoint.

According to Theorems 5.5.1 and 5.5.5, it becomes apparent that some $3T$ and $4T$-periodic solutions must be degenerated. Namely, those on the turning points of $\mathfrak{C}^{+}_{3,\sqrt{3}}$, $\mathfrak{C}^{+}_{4,\sqrt{2}}$ and $\mathfrak{C}^{-}_{4,\sqrt{2}}$ in Figure 5.8. Similarly, the bifurcation points accumulating from the left to $\sqrt{2}$ and $\sqrt{3}$ must provide us with additional degenerate solutions: those on the turning points of their corresponding components.

5.6 General cases

The main goal of this section is sharpening and generalizing as much as possible the main findings of the past subsections of this chapter for the same Volterra predator-prey model

$$\begin{cases} u' = \alpha(t)u(1-v) \\ v' = \beta(t)v(-1+u). \end{cases} \tag{5.82}$$

Precisely, as in Chapter 3, we analyze the existence of nT-periodic coexistence states of (5.82) for any integer $n \geq 1$ under the following structural constraints on the weight functions α and β. That is, for some integers $k, \ell \geq 1$, with $|k-\ell| \leq 1$, it is assumed the existence of $k+\ell$ continuous functions in the interval $[0,T]$, $\alpha_i \gneq 0$, $1 \leq i \leq k$, and $\beta_j \gneq 0$, $1 \leq j \leq \ell$, such that

$$\alpha = \alpha_1 + \alpha_2 + \cdots + \alpha_k, \quad \beta = \beta_1 + \beta_2 + \cdots + \beta_\ell,$$

with

$$\operatorname{supp} \alpha_i \subseteq [t_0^i, t_1^i] \;\text{ and }\; \operatorname{supp} \beta_j \subseteq [t_2^j, t_3^j], \tag{5.83}$$

for some partition of $[0,T]$

$$0 \leq t_0^1 < t_1^1 \leq t_2^1 < t_3^1 \leq t_0^2 < t_1^2 \leq t_2^2 < t_3^2 \leq \cdots \leq t_0^k < t_1^k \leq t_2^k < t_3^k \leq T$$

if $k = \ell$, or

$$0 \leq t_0^1 < t_1^1 \leq t_2^1 < t_3^1 \leq t_0^2 < t_1^2 \leq t_2^2 < t_3^2 \leq \cdots \leq t_0^k < t_1^k \leq T$$

if $k = \ell + 1$. Similarly, we also consider the case when, instead of (5.83),

$$\operatorname{supp} \beta_j \subseteq [t_0^j, t_1^j] \ \text{ and } \ \operatorname{supp} \alpha_i \subseteq [t_2^i, t_3^i], \tag{5.84}$$

for some partition of $[0, T]$

$$0 \le t_0^1 < t_1^1 \le t_2^1 < t_3^1 \le t_0^2 < t_1^2 \le t_2^2 < t_3^2 \le \cdots \le t_0^\ell < t_1^\ell \le t_2^\ell < t_3^\ell \le T$$

if $\ell = k$, or

$$0 \le t_0^1 < t_1^1 \le t_2^1 < t_3^1 \le t_0^2 < t_1^2 \le t_2^2 < t_3^2 \le \cdots \le t_0^\ell < t_1^\ell \le T$$

if $\ell = k + 1$. We refer again to an α-interval (resp. β-interval) as a maximal interval where $\beta \equiv 0$ (resp. $\alpha \equiv 0$) and we set

$$A_i := \int_0^T \alpha_i, \qquad B_j := \int_0^T \beta_j. \tag{5.85}$$

There are two fundamental aims in this section. The first one is to show that the complexity of the global bifurcation diagram of subharmonics of (5.82) when $k = \ell$ depends on the size of k, rather than on the particular structure of the α_i's and the β_j's on each of the intervals of the partition of $[0, T]$. In fact, all admissible global bifurcation diagrams when $k = \ell$ can be constructed systematically, through the algorithm already found in Sections 5.2-5.5, regardless the particular locations of each of the points of the partitions, t_r^s's. The second aim of this section is to determine a lower bound for the number of nT-periodic coexistence states of model (5.82).

5.6.1 The case when $k = \ell = 1$

Assume first that

$$\operatorname{supp} \alpha_1 \subseteq [t_0^1, t_1^1] \ \text{ and } \ \operatorname{supp} \beta_1 \subseteq [t_2^1, t_3^1], \tag{5.86}$$

where

$$0 \le t_0^1 < t_1^1 \le t_2^1 < t_3^1 \le T.$$

Figure 5.10 illustrates this case.

It is worth noting that all the results developed in Sections 5.1-5.5 are independent of the weights α and β location. Indeed, the construction of the Poincaré maps at time nT depends only on the integrals A and B. Hence, under condition (5.86), the next result holds.

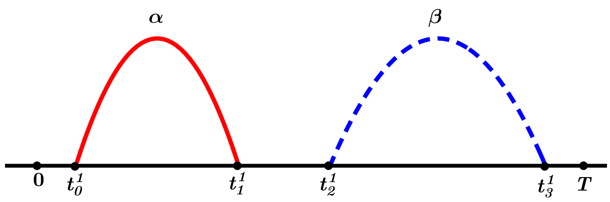

Figure 5.10: α and β satisfying (5.86)

Theorem 5.6.1. *Assume (5.86). Then, the equilibrium* $(1,1)$ *is the unique* T*-periodic coexistence state of (5.82). Thus, (5.82) cannot admit non-trivial* T*-periodic coexistence states. Moreover, (5.82) possesses exactly two non-trivial* $2T$*-periodic coexistence states for every*

$$\lambda > \frac{2}{\sqrt{A_1 B_1}},$$

where A_1 *and* B_1 *are those defined in (5.85). Furthermore, in the special case when* $A_1 = B_1$ *and* $u(0) = v(0)$*, for every* $\lambda > \frac{2}{A_1}$ *and* $n \geq 2$*, (5.82) has, at least,* n *non-trivial* nT*-periodic coexistence states if* n *is even, and* $n-1$ *if* n *is odd.*

Moreover, as the set of subharmonics obeys identical equations, it is apparent that also in this more general case the topological structure of the global bifurcation diagram of the positive subharmonics of (5.82) follows the general patterns sketched in Figure 5.1. Thus, the global bifurcation diagram of (5.82) remains invariant regardless the concrete values of t_0^1, t_1^1, t_2^1, t_3^1 and the number and distribution of the components of the supports of the weight functions $\alpha(t)$ and $\beta(t)$ on each of the intervals of the partition of $[0,T]$ induced by these values. Naturally, as in the discussion of Section 5.5, the local behavior of most of the bifurcations from $(1,1)$ is unknown, except for $n \in \{2,3,4\}$.

On the other hand, we can also assume that

$$\operatorname{supp}\beta_1 \subseteq [t_0^1, t_1^1] \quad \text{and} \quad \operatorname{supp}\alpha_1 \subseteq [t_2^1, t_3^1], \tag{5.87}$$

where

$$0 \leq t_0^1 < t_1^1 \leq t_2^1 < t_3^1 \leq T.$$

Figure 5.11 shows a simple example within this case. The next result focuses attention into the case when condition (5.87) holds.

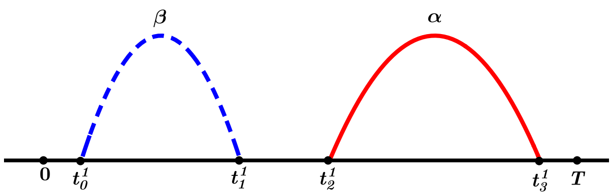

Figure 5.11: α and β satisfying (5.87).

Theorem 5.6.2. *Under condition (5.87), the equilibrium* $(1,1)$ *is the unique* T*-periodic coexistence state of (5.82). Moreover, (5.82) possesses exactly two non-trivial* $2T$*-periodic coexistence states for every*

$$\lambda > \frac{2}{\sqrt{A_1 B_1}}. \tag{5.88}$$

If, in addition, $A_1 = B_1$*, then the problem (5.82) has, for every* $\lambda > \frac{2}{A_1}$ *and* $n \geq 3$*, at least* $n-1$ *non-trivial* nT*-periodic coexistence states with* $u_0 = v_0$ *if* n *is odd, whereas if* n *is even, then (5.82) possesses, at least,* $n-2$ *non-trivial* nT*-periodic coexistence states with* $u_0 = v_0$*, and exactly two with* $u_0 + v_0 = 2$*.*

Notice that, based on Theorem 5.6.1, one can get, very easily, solutions of (5.82) satisfying (5.87) in the interval $[0, T]$. Indeed, if (u_0, v_0) is the initial value to an nT-periodic solution of (5.82) for the weight distribution (5.86), then, a solution with initial values $(u_0 e^{(1-v_0)A_1}, v_0)$ provides us with an nT-periodic solution of (5.82) for the configuration (5.87). Next section goes further by establishing that, for the distribution (5.87), there are periodic solutions of (5.86) with initial data on the line $u = v$ by means of similar symmetry reductions and techniques as in the proof of Theorem 5.6.1. Equivalently, fixing a time $\tau_0 \in (t_1^1, t_2^1)$, and setting

$$\tilde{\alpha}(t) := \alpha(t + \tau_0), \qquad \tilde{\beta}(t) := \beta(t + \tau_0),$$

the pair $(\tilde{\alpha}, \tilde{\beta})$ lies within the configuration of Figure 5.10. Thus, Theorem 5.6.1 applies. Note that this is equivalent to consider the Poincaré map with τ_0 as initial time. Hence, the importance of Theorem 5.6.2 relies in the fact that the multiplicity result is preserved when $u_0 = v_0$ and condition (5.87) holds.

The main difference in the result between Theorems 5.6.1 and 5.6.2 is that all the solutions of (5.82) when $A_1 = B_1$ and n is even have been constructed to satisfy $u_0 = v_0$ under condition (5.86), while (5.82) only admits $n-2$ solutions with $u_0 = v_0$ and 2 solutions with $u_0 + v_0 = 2$ when (5.87) holds.

Proof. Since, for every $(u_0, v_0) \in \mathbb{R}^2$, the unique solution of (5.82) with $(u(0), v(0)) = (u_0, v_0)$ is given through

$$u(t) = u_0 e^{(1-v(T))\lambda \int_0^t \alpha(s)ds}, \qquad v(t) = v_0 e^{(-1+u_0)\lambda \int_0^t \beta(s)ds}, \quad t \in [0, T],$$

the T-time and $2T$-time Poincaré maps of (5.82) are given by

$$(u_1, v_1) := \mathcal{P}_1(u_0, v_0) := (u(T), v(T)) = (u_0 e^{(1-v_1)\lambda A_1}, v_0 e^{(-1+u_0)\lambda B_1})$$

and

$$\begin{aligned}(u_2, v_2) := \mathcal{P}_2(u_0, v_0) = \mathcal{P}_1(u_1, v_1) &= (u_1 e^{(1-v_2)\lambda A_1}, v_1 e^{(-1+u_1)\lambda B_1}) \\ &= (u_0 e^{(2-v_1-v_2)\lambda A_1}, v_0 e^{(-2+u_0+u_1)\lambda B_1}).\end{aligned}$$

It is easily seen that $(u_0, v_0) = (1, 1)$ is the unique fixed point of $\mathcal{P}_1$. Moreover, a solution of (5.82), $(u(t), v(t))$, is a $2T$-periodic coexistence state if, and only if, $u_0 > 0$, $v_0 > 0$ and

$$(u_2, v_2) = \mathcal{P}_2(u_0, v_0) = (u_0, v_0).$$

In other words,

$$u_0, \;\; v_0 > 0, \qquad 2 - u_0 = u_1 = u_0 e^{(v_0-1)\lambda A_1}, \qquad 2 - v_0 = v_1 = v_0 e^{(u_0-1)\lambda B_1}. \tag{5.89}$$

Setting $(A, B) \equiv (A_1, B_1)$ and arguing as in the proof of Theorem 5.1.1, it becomes apparent that the non-trivial $2T$-periodic coexistence states of (5.82) are given by the zeroes of the map

$$\psi(x) := x \left(e^{\frac{1-e^{(x-1)\lambda A}}{1+e^{(x-1)\lambda A}}\lambda B} + 1 \right) - 2 \tag{5.90}$$

with $x = v_0 \neq 1$. By definition, it is obvious that

$$\psi(x) < 0 \;\text{ for all } x \leq 0, \;\; \psi(1) = 0, \;\; \psi(x) > 0 \;\text{ for all } x \geq 2.$$

Moreover, by differentiating with respect to x, after rearranging terms, yields

$$\psi'(x) = e^{\frac{1-e^{(x-1)\lambda A}}{1+e^{(x-1)\lambda A}}\lambda B} \left[1 - 2\lambda^2 ABx \frac{e^{(x-1)\lambda A}}{(1+e^{(x-1)\lambda A})^2} \right] + 1,$$

$$\psi''(x) = e^{\frac{1-e^{(x-1)\lambda A}}{1+e^{(x-1)\lambda A}}\lambda B} \left[x \left(\frac{2\lambda^2 ABe^{(x-1)\lambda A}}{(1+e^{(x-1)\lambda A})^2} \right)^2 - \frac{4\lambda^2 ABe^{(x-1)\lambda A}}{(1+e^{(x-1)\lambda A})^2} + \frac{2\lambda^3 A^2 Bxe^{(x-1)\lambda A}(e^{(x-1)2\lambda A}-1)}{(1+e^{(x-1)\lambda A})^4} \right],$$

for all $x \geq 0$. In particular,

$$\psi'(1) = 2 - \lambda^2 \frac{AB}{2}.$$

Thus, owing to (5.88), $\psi'(1) < 0$. Summarizing, (5.88) implies that

$$\psi(0) = -2 < 0, \quad \psi(1) = 0, \quad \psi'(1) < 0, \quad \psi(2) > 0.$$

Hence, the function ψ possesses, at least, one zeroes in each of the intervals $(0, 1)$ and $(1, 2)$. Therefore, (5.82) has, at least, two $2T$-periodic coexistence states. Moreover, adapting the analysis carried out in the proof of Theorem 5.1.1, from the previous value of $\psi''(x)$, it is easily seen that any critical point, x_c, of ψ satisfies $\psi''(x_c) < 0$ if $x_c \in (0, 1)$ and $\psi''(x_c) > 0$ if $x_c \in (1, 2)$. Consequently, (5.82) possesses exactly two $2T$-periodic coexistence states under condition (5.88). This ends the proof of the first assertion.

Subsequently, we assume that

$$A = B, \qquad u_0 = v_0 = x. \tag{5.91}$$

In this case the nT-time map is defined as follows

$$\begin{aligned}(u_n, v_n) &:= \mathcal{P}_n(u_0, v_0) = \mathcal{P}_1^n(u_0, v_0) \\ &= (u_0 e^{(n - v_1 - v_2 - \cdots - v_n)\lambda A}, v_0 e^{(u_0 + u_2 + \cdots + u_{n-1} - n)\lambda A}).\end{aligned}$$

Thus, $(u_n, v_n) = (u_0, v_0)$, i.e., (u_0, v_0) provides us with a subharmonic of order $n \geq 1$ of (5.82), if and only if

$$\begin{cases} n &= v_0 + v_1 + \cdots + v_{n-1}, \\ n &= u_0 + u_1 + \cdots + u_{n-1}. \end{cases} \tag{5.92}$$

Adapting the argument of the proof of Lemma 5.2.1, it is easily seen that the two equations of (5.92) coincide under condition (5.91). Thus, the solutions of the system (5.92) are the zeroes of the function

$$\psi_n(x) := x + u_1(x) + \ldots + u_{n-1}(x) - n, \qquad x > 0.$$

Consequently, the nT-periodic coexistence states of (5.82) are given through $\psi^{-1}(0)$.

Arguing as in the proof of Proposition 5.2.2, it becomes apparent that

$$(u_n, v_n) := \mathcal{P}_n(x, x) = (xE_{2n}(-\lambda, x), xE_{2n-1}(-\lambda, x))$$

for all $n \geq 1$. Hence,

$$(1, 1) = \mathcal{P}_n(1, 1) = (E_{2n}(-\lambda, 1), E_{2n-1}(-\lambda, 1)) \tag{5.93}$$

for all $n \geq 1$. Further, by the proof of Theorem 5.2.3, we find that

$$\psi_n(\lambda, x) = x \sum_{j=0}^{n-1} E_j(-\lambda, x) - n = \psi_{n-1}(x) - 1 + xE_{n-1}(-\lambda, x)$$

for all $x > 0$. Note that ψ_n also depends on the parameter $\lambda > 0$. To make explicit this dependence, we will subsequently write $\psi_n(\lambda, x)$, instead of $\psi_n(x)$, for all $n \geq 1$.

By (5.93), differentiating with respect to x and particularizing at $x = 1$ yields

$$q_n(\lambda) := \frac{\partial \psi_n}{\partial x}(\lambda, 1) = n + \sum_{j=1}^{n-1} E_j'(-\lambda, 1). \tag{5.94}$$

Adapting the induction argument of the proof of Lemma 5.3.1, it follows from the definition of the E_j's that the function $q_n(\lambda)$ is a polynomial for all $n \geq 1$.

The next result relates the sequence $\{q_n\}_{n\geq 1}$ with the corresponding sequence $\{p_n\}_{n\geq 1}$ constructed in Section 5.3 under condition (5.86).

Proposition 5.6.3. *For every $n \geq 1$,*

$$q_{2n-1}(\lambda) = p_{2n-1}(\lambda), \qquad \frac{q_{2n}(\lambda)}{2 + A\lambda} = \frac{p_{2n}(\lambda)}{2 - A\lambda}, \tag{5.95}$$

and

$$q_n(\lambda) = [2 + (-1)^n A\lambda] q_{n-1}(\lambda) - q_{n-2}(\lambda). \tag{5.96}$$

Proof. According to 5.48, p_n is defined as

$$p_n(\lambda) := \frac{\partial \varphi_n}{\partial x}(\lambda, 1) = n + \sum_{j=1}^{n-1} E_j'(\lambda, 1).$$

Thus, by (5.94), $q_n(\lambda) = p_n(-\lambda)$. By Corollary 5.3.9, $p_{2n-1}(\lambda)$ and $\frac{p_{2n}(\lambda)}{2-A\lambda}$ are even functions in λ. Hence,

$$q_{2n-1}(\lambda) = p_{2n-1}(\lambda)$$

and

$$q_{2n}(\lambda) = p_{2n}(-\lambda) = \frac{p_{2n}(-\lambda)}{2 - A(-\lambda)}(2 + A\lambda) = \frac{p_{2n}(\lambda)}{2 - A\lambda}(2 + A\lambda).$$

This concludes the proof of (5.95).

On the other hand, by Theorem 5.3.8, we already know that

$$p_{2n-1}(\lambda) = (2 + A\lambda) p_{2n-2}(\lambda) - p_{2n-3}(\lambda) \tag{5.97}$$

and

$$\frac{p_{2n}(\lambda)}{2 - A\lambda} = p_{2n-1}(\lambda) - \frac{p_{2n-2}(\lambda)}{2 - A\lambda}. \tag{5.98}$$

Therefore, owing to (5.95), (5.97) and (5.98), we find that, for every $n \geq 1$,

$$\frac{q_{2n-1}(\lambda)}{2-A\lambda} = \frac{p_{2n-1}(\lambda)}{2-A\lambda} = (2+A\lambda)\frac{p_{2n-2}(\lambda)}{2-A\lambda} - \frac{p_{2n-3}(\lambda)}{2-A\lambda} = q_{2n-2}(\lambda) - \frac{q_{2n-3}(\lambda)}{2-A\lambda}$$

and

$$\frac{q_{2n}(\lambda)}{2+A\lambda} = \frac{p_{2n}(\lambda)}{2-A\lambda} = p_{2n-1}(\lambda) - \frac{p_{2n-2}(\lambda)}{2-A\lambda} = q_{2n-1}(\lambda) - \frac{q_{2n-2}(\lambda)}{2+A\lambda}.$$

So, (5.96) holds, and the proof is complete. □

As a direct consequence of (5.95), the corresponding sets of bifurcation points from the curve $(\lambda, x) = (\lambda, 1)$ coincide under conditions (5.86) and (5.87) as soon as $u_0 = v_0 (= x)$ and $A = B$, except for the bifurcation point $(\lambda, x) = (2/A, 1)$, because

$$2/A \in p_{2n}^{-1}(0) \setminus q_{2n}^{-1}(0) \quad \text{for all} \;\; n \geq 1.$$

Moreover, also by (5.95), the mathematical analysis carried out in Sections 5.4 and 5.5 applies *mutatis mutandis* to cover the case when (5.87) holds, instead of (5.86). As a byproduct, also in the case when (5.87) holds, all the zeroes of the polynomials $q_n(\lambda)$ are simple. Thus, the Crandall–Rabinowitz theorem [37] provides us with a local analytic curve of nT-periodic solutions. Moreover, since the generalized algebraic multiplicity of Esquinas and López-Gómez [66] equals one, according to [124, Th. 6.2.1] and the unilateral theorem [124, Th. 6.4.3], these local curves of subharmonics can be extended to maximal connected components of the set of nT-subharmonics of (5.82). This proves the theorem when $u_0 = v_0 = x$ and $A = B$, regardless the oddity of $n \geq 1$.

Finally, assume that $2 = u_0 + v_0$ and $A = B$. As we already know that a solution $(u(t), v(t))$ is $2T$-periodic if, and only if,

$$2 = u_0 + v_0 \qquad 2 = v_0 + v_1 = v_0 + v_0 e^{(u_0-1)\lambda A},$$

it becomes apparent that the non-trivial $2T$-periodic coexistence states of (5.82) are the zeroes of the function

$$\varphi_2(x) = x[e^{(1-x)\lambda A} + 1] - 2, \qquad x \in (0,2) \setminus \{1\}.$$

As, according to the proof of Theorem 5.6.1, φ_2 possesses exactly two zeroes, the proof of Theorem 5.6.2 is completed. □

Since, according to (5.95), we already know that

$$\{r \in q_n^{-1}(0) \ : \ r > 0, \ n \geq 1\} = \{r \in p_n^{-1}(0) \ : \ r > 0, \ n \geq 1\} \setminus \{2\},$$

the global bifurcation diagram of subharmonics of (5.82) when (5.87), instead of (5.86), holds true, can be obtained from the global bifurcation diagram plotted in Figure 5.1 by removing the component of subharmonics of order two. However, even the local behavior of the corresponding components of subharmonics of order n in each of the cases (5.86) and (5.87) might be different, because, in general, $\varphi_n \neq \psi_n$ for all $n \geq 2$ and, hence, the identity $\varphi_n^{-1}(0) = \psi_n^{-1}(0)$ cannot be guaranteed.

By (5.17), $0 < v_0 < 1$ if $0 < u_0 < 1$. Similarly, $1 < v_0 < 2$ if $1 < u_0 < 2$. Thus, the $2T$-periodic coexistence states of (5.82) under condition (5.86) are localized in the shadowed region of the left plot in Figure 5.12. Moreover, by (5.89), $1 < v_0 < 2$ if $0 < u_0 < 1$, and $0 < v_0 < 1$ if $1 < u_0 < 2$. Thus, under condition (5.87), the $2T$-periodic coexistence states of (5.82) lye in the shadowed area of the right plot of Figure 5.12. This explains why (5.82) cannot admit a subharmonic of order two if $u_0 = v_0$.

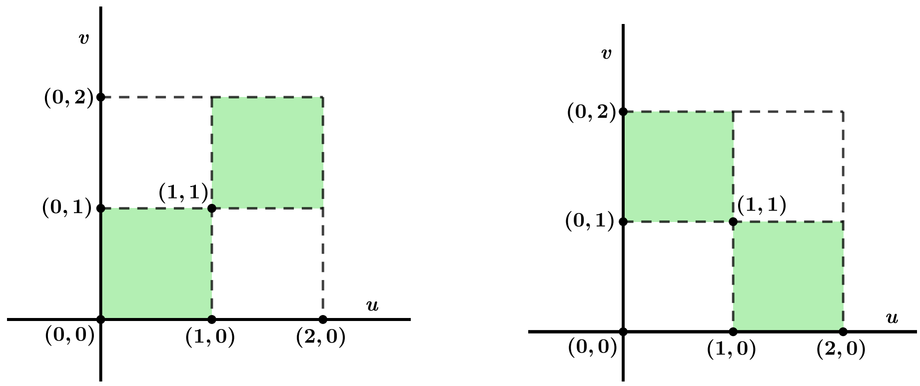

Figure 5.12: The shadow regions on each of these figures represent the quadrants of the phase-plane containing the initial data to $2T$-periodic coexistence states of (5.82) under the conditions (5.86) (left) and (5.87) (right).

5.6.2 The case when $k = \ell \geq 2$

Then, either

$$\operatorname{supp} \alpha_j \subseteq [t_0^j, t_1^j] \ \text{ and } \ \operatorname{supp} \beta_j \subseteq [t_2^j, t_3^j] \text{ for every } j \in \{1, 2, \ldots, k\}, \qquad (5.99)$$

or

$$\operatorname{supp}\beta_j \subseteq [t_0^j, t_1^j] \text{ and } \operatorname{supp}\alpha_j \subseteq [t_2^j, t_3^j] \text{ for every } j \in \{1,2,\dots,k\}, \quad (5.100)$$

for some

$$0 \le t_0^1 < t_1^1 \le t_2^1 < t_3^1 \le \cdots \le t_0^k < t_1^k \le t_2^k < t_3^k \le T.$$

As in Theorems 5.6.1 and 5.6.2, to analyze the higher order subharmonics of (5.82) we need to impose the constraints

$$A_1 := \int_0^T \alpha_1 = \cdots = \int_0^T \alpha_k = \int_0^T \beta_1 = \cdots = \int_0^T \beta_k, \;\; u_0 = v_0 > 0. \quad (5.101)$$

Even in the simplest case when $k = \ell = 1$ it is far from evident that the analysis of Sections 5.1-5.5 will be possible to refine as to sharpen Theorems 5.6.1 and 5.6.2 to cover the general case when

$$\int_0^T \alpha \neq \int_0^T \beta.$$

Essentially, (5.101) reduces the problem of finding out the subharmonics of (5.82) to the problem of getting the zeroes of a sequence of real functions, instead of vectorial ones, much like in the simplest case when $k = \ell = 1$ already covered by Section 5.6.1. The next lemma is pivotal in the proof of the main theorem of this section. We observe that it holds independently of (5.101).

Lemma 5.6.4. *Assume*

$$A_1 := \int_0^T \alpha_1 = \cdots = \int_0^T \alpha_k \quad \text{and} \quad B_1 := \int_0^T \beta_1 = \cdots = \int_0^T \beta_k.$$

Then, under condition (5.99) (resp. (5.100)), for any integers $n, m, q, r \ge 1$ such that

$$nm = qr,$$

the Poincaré map of (5.82) at time nT for $k = \ell = m$, denoted by $\mathcal{P}_n^{m,\alpha,\beta}$ (resp. $\mathcal{P}_n^{m,\beta,\alpha}$), equals the Poincaré map of (5.82) at time qT for $k = \ell = r$; denoted, naturally, by $\mathcal{P}_q^{r,\alpha,\beta}$ (resp. $\mathcal{P}_q^{r,\beta,\alpha}$).

Proof. Assume (5.99) and $k = \ell = m$. Then, integrating in $[0, t_0^2]$ yields

$$u(t) = u_0 e^{(1-v(t_0^1))\lambda \int_0^t \alpha_1(s)ds}, \qquad v(t) = v_0 e^{(u(t_0^2)-1)\lambda \int_0^t \beta_1(s)ds},$$

for all $t \in [0, t_0^2]$, because $v(t_0^1) = v_0$ and $u(t_0^2) = u(t_2^1)$. Arguing by induction, assume that

$$u(t) = u_0 e^{\sum_{j=1}^{m-1}(1-v(t_0^j))\lambda \int_0^t \alpha_j(s)ds}, \qquad v(t) = v_0 e^{\sum_{j=2}^{m}(u(t_0^j)-1)\lambda \int_0^t \beta_{j-1}(s)ds},$$

for all $t \in [0, t_0^m]$. Then, integrating in $[t_0^m, T]$, it becomes apparent that

$$\begin{aligned} u(t) &= u_0 e^{\sum_{j=1}^{m}(1-v(t_0^j))\lambda \int_0^t \alpha_j(s)ds}, \\ v(t) &= v_0 e^{\sum_{j=2}^{m}(u(t_0^j)-1)\lambda \int_0^t \beta_{j-1}(s)ds + (u(t_0^1+T)-1)\int_0^t \beta_m(s)ds} \end{aligned}$$

for all $t \in [0, T]$. Thus, iterating n times, we find that, for every $t \in [0, nT]$,

$$\begin{cases} u(t) = u_0 e^{\sum_{i=0}^{n-1}\sum_{j=1}^{m}(1-v(t_0^j+iT))\lambda \int_0^t \alpha_j(s)ds} \\ v(t) = v_0 e^{\sum_{i=0}^{n-1}[\sum_{j=2}^{m}(u(t_0^j+iT)-1)\lambda \int_0^t \beta_{j-1}(s)ds + (u(t_0^1+(i+1)T)-1)\int_0^t \beta_m(s)ds]} \end{cases} \tag{5.102}$$

for all $t \in [0, nT]$. Moreover, the interval $[0, nT]$ can be viewed as an interval consisting of nm pairs of α and β intervals, instead of made of n copies of $[0, T]$. Thus, setting for every $1 \leq j \leq m$ and $0 \leq i \leq n-1$,

$$t_0^j + iT \equiv j + mi, \qquad (u(t_0^j + iT), v(t_0^j + iT)) \equiv (u_{j+mi}, v_{j+mi}),$$

and

$$\alpha_j(t) = \alpha_j(t + iT) \equiv \alpha_{j+mi}(t), \qquad \beta_j(t) = \beta_j(t + iT) \equiv \beta_{j+mi}(t),$$

(5.102) can be equivalently expressed as

$$u(t) = u_0 e^{\sum_{h=1}^{nm}(1-v_h)\lambda \int_0^t \alpha_h(s)ds}, \qquad v(t) = v_0 e^{\sum_{h=2}^{nm+1}(u_h-1)\lambda \int_0^t \beta_{h-1}(s)ds},$$

for all $t \in [0, nT]$. Thus, it becomes apparent that

$$\begin{aligned} \mathcal{P}_n^{m,\alpha,\beta}(u_0, v_0) &:= (u(nT), v(nT)) \\ &= \left(u_0 e^{(nm - \sum_{h=1}^{nm} v_h)\lambda A_1}, v_0 e^{(\sum_{h=2}^{nm+1} u_h - nm)\lambda B_1}\right). \end{aligned} \tag{5.103}$$

As in (5.103) n and m are arbitrary integer numbers, it is apparent that

$$\mathcal{P}_q^{r,\alpha,\beta} = \mathcal{P}_n^{m,\alpha,\beta}$$

for all integers $q, r \geq 1$ such that $nm = qr$, Lastly, assume (5.100) and $k=\ell=m$. Then, arguing as above yields

$$\begin{aligned}\mathcal{P}_n^{m,\beta,\alpha}(u_0,v_0) &:= (u(nT),v(nT))\\ &= \left(u_0 e^{(\sum_{h=2}^{nm+1} v_h - nm)\lambda A_1}, v_0 e^{(nm-\sum_{h=1}^{nm} u_h)\lambda B_1}\right)\end{aligned}$$

and, therefore, taking integers $q,r\geq 1$ such that $nm=qr$, we find that

$$\mathcal{P}_q^{r,\beta,\alpha} = \mathcal{P}_n^{m,\beta,\alpha}.$$

The proof is complete. □

Since $\mathcal{P}_q^{r,\alpha,\beta} = \mathcal{P}_n^{m,\alpha,\beta}$, their fixed points are the same. Thus, if $nm=qr$, then, the set of positive fixed points of the Poincaré map of (5.82) at time nT for $k=\ell=m$ equals the set of positive fixed points of the Poincaré map of (5.82) at time qT for $k=\ell=r$. The main result of this section invokes this feature to estimate the number of subharmonics of arbitrary order of (5.82) in any of the cases (5.99) and (5.100).

Theorem 5.6.5. *Suppose (5.101), $u_0=v_0>0$, and $k=\ell=m\geq 2$, and set*

$$\nu(z) := \begin{cases} z & \text{if } z\in 2\mathbb{N}, \\ z-1 & \text{if } z\in 2\mathbb{N}+1, \end{cases} \qquad \mu(z) := \begin{cases} z-2 & \text{if } z\in 2\mathbb{N}, \\ z-1 & \text{if } z\in 2\mathbb{N}+1. \end{cases} \tag{5.104}$$

Then, for every integer $n\geq 1$ and $\lambda>2/A_1$, (5.82) has $\nu(nm)$ (resp. $\mu(nm)$) nT-periodic coexistence states under condition (5.99) (resp. (5.100)).

Proof. Assume (5.99). By the semigroup property of the flow, Lemma 5.99 implies that

$$(\mathcal{P}_n^{1,\alpha,\beta})^m := \mathcal{P}_{nm}^{1,\alpha,\beta} = \mathcal{P}_n^{m,\alpha,\beta}.$$

Thus, the set of positive fixed points of $\mathcal{P}_{nm}^{1,\alpha,\beta}$, already described by Theorem 5.6.1, equals the set of positive fixed points of $\mathcal{P}_n^{m,\alpha,\beta}$. As, due to Theorem 5.6.1, the map $\mathcal{P}_{nm}^{1,\alpha,\beta}$ has, at least, $\nu(nm)$ positive fixed points, the map $\mathcal{P}_n^{m,\alpha,\beta}$ also admits, at least, $\nu(nm)$ positive fixed points for all $\lambda>2/A_1$. When, instead of (5.99), the condition (5.100) holds, then one should invoke to Theorem 5.6.2, instead of Theorem 5.6.1. As the proof follows the same patterns, we will omit any further technical detail. □

Crucially, since $\mathcal{P}_n^{m,\alpha,\beta} = \mathcal{P}_q^{r,\alpha,\beta}$, the global bifurcation diagram of the nT-periodic coexistence states for $k=\ell=m$ coincides with the global bifurcation diagram of the qT-periodic coexistence states for $k=\ell=r$ if $nm=qr$. For instance, if $m=2$, then the set of components of nT-periodic coexistence states provides us with the set of components of $2nT$-periodic coexistence states for $m=1$. Thus, for $m=2$ the global bifurcation diagram of subharmonics can be obtained by removing from Figure 5.1 the set of components filled in by odd order subharmonics. Therefore, the global bifurcation diagram sketched in Figure 5.1 provides us with all the global bifurcation diagrams for every $k = \ell = m \geq 2$ by choosing the appropriate subharmonic components in that diagram.

Finally, the next result ascertains the number of coexistence states with minimal period nT among those given by Theorem 5.6.5. By minimal period nT it is meant that the coexistence states are nT-periodic but not mT-periodic if $m < n$. To state that result, we first need to deliver two well-known facts on number theory. For every integer $n \geq 1$, the Euler *totient function* is defined as

$$\Phi(n) := \operatorname{card}(\{1 \leq m \leq n \mid \gcd(n, m) = 1\}).$$

According to Gauss [83, p. 21], the Euler totient function satisfies the next identity

$$n = \sum_{d|n} \Phi(d). \tag{5.105}$$

The next result relates, through (5.105), the Euler totient function with a very special class of univariate polynomials.

Proposition 5.6.6. *Let $\mathbb{K}[X]$ be the univariate polynomials ring over a zero characteristic field, $\mathbb{K}$. Then, for every sequence $\{h_n\}_{n\geq 2} \subset \mathbb{K}[X]$ satisfying:*

1. $\deg(h_n) = n - 1$,
2. $\operatorname{card}\{r \in \mathbb{R} \,:\, h_n(r) = 0\} = n - 1$, *and*
3. $h_{n_1} | h_{n_2}$ *if, and only if,* $n_1 | n_2$,

the following identity holds

$$\Phi(n) = \operatorname{card}\left\{r \in \mathbb{R} \,:\, h_n(r) = 0 \textit{ and } h_d(r) \neq 0 \textit{ if } d|n\right\}.$$

Proof. Setting

$$\begin{aligned} \mathcal{C}_h(n) &:= \operatorname{card}\{r \in \mathbb{R} \,:\, h_n(r) = 0\}, \\ \mathcal{C}_h^{\min}(n) &:= \operatorname{card}\{r \in \mathbb{R} \,:\, h_n(r) = 0 \text{ and } h_d(r) \neq 0 \text{ if } d|n\}, \end{aligned}$$

it is apparent that

$$\mathcal{C}_h^{\min}(n) = \mathcal{C}_h(n) - \sum_{\substack{d|n \\ d\neq 1,n}} \mathcal{C}_h^{\min}(d).$$

By definition, $\mathcal{C}_h^{\min}(p) = \Phi(p)$ for every prime integer $p \geq 2$, because $\mathcal{C}_h^{\min}(p) = \mathcal{C}_h(p) = p - 1$. Moreover, for any given prime integers $p_1, p_2 \geq 2$,

$$\begin{cases} \mathcal{C}_h^{\min}(p_1 p_2) & = \mathcal{C}_h(p_1 p_2) - \mathcal{C}_h^{\min}(p_1) - \mathcal{C}_h^{\min}(p_2) \\ & = p_1 p_2 - 1 - \Phi(p_1) - \Phi(p_2) \qquad\qquad \text{if } p_1 \neq p_2, \\ \mathcal{C}_h^{\min}(p_1 p_2) & = \mathcal{C}_h(p_1 p_2) - \mathcal{C}_h^{\min}(p_1) = p_1 p_2 - 1 - \Phi(p_1) \quad \text{if } p_1 = p_2. \end{cases}$$

Thus, by (5.105), $\mathcal{C}_h^{\min}(p_1 p_2) = \Phi(p_1 p_2)$. Now, given $i \geq 2$, assume as a complete induction hypothesis, that, for every $j \in \{1, 2, \ldots, i\}$,

$$\mathcal{C}_h^{\min}(p_1 p_2 \ldots p_j) = \Phi(p_1 p_2 \ldots p_j). \tag{5.106}$$

Then, denoting $\gamma := p_1 p_2 \ldots p_{j+1}$, it follows from (5.106) that

$$\mathcal{C}_h^{\min}(\gamma) = \mathcal{C}_h(\gamma) - \sum_{\substack{d|\gamma \\ d \neq 1, \gamma}} \mathcal{C}_h^{\min}(d) = \gamma - 1 - \sum_{\substack{d|\gamma \\ d \neq 1, \gamma}} \Phi(d) = \gamma - \sum_{\substack{d|\gamma \\ d \neq \gamma}} \Phi(d).$$

Therefore, by (5.105), $\mathcal{C}_h^{\min}(\gamma) = \Phi(\gamma)$, which concludes the induction. As any integer, n, can be factorized as a (unique) finite product of prime integers, it becomes apparent that $\mathcal{C}_h^{\min}(n) = \Phi(n)$. This ends the proof. $\square$

Next theorem is a direct consequence of Proposition 5.6.6.

Theorem 5.6.7. *Assume (5.101), $k = \ell = m \geq 1$, and either (5.99), or (5.100). Then, (5.82) possesses, at least, $\Phi(nm)$ coexistence states with minimal period nT for all $nm > 2$.*

Proof. First, assume that (5.99). Then, by Lemma 5.3.1 4.3 and Theorem 5.4.2, the sequence of polynomials p_{nm} whose positive roots are the bifurcation points to the nT-periodic coexistence states, satisfies the hypothesis of Proposition 5.6.6. Thus,

$$\mathcal{C}_p^{\min}(nm) = \Phi(nm).$$

Subsequently, we denote by

$$\mathcal{C}_{p,+}^{\min}(nm) := \operatorname{card}\{r \in \mathbb{R},\, r > 0 \,:\, p_{nm}(r) = 0 \text{ and } p_d(r) \neq 0 \text{ if } d|nm\}$$

the cardinality of the set of bifurcations points of (5.82) to minimal nT-periodic coexistence states. As, thanks to Corollary 5.3.9, we already know that $\frac{p_{2nm}(\lambda)}{2 - A\lambda}$ and $p_{2nm+1}(\lambda)$ are even polynomials, it is apparent that

$$\mathcal{C}_{p,+}^{\min}(nm) = \frac{\Phi(nm)}{2}.$$

Thus, as they emerge at least two solutions from each positive root, there are, at least, $\Phi(nm)$ coexistence states with minimal period nT for $nm > 2$.

Finally, assume (5.100). Then, owing to (5.95),

$$\mathcal{C}_{q,+}^{\min}(nm) = \mathcal{C}_{p,+}^{\min}(nm) = \frac{\Phi(nm)}{2}.$$

Therefore, the same conclusion holds. This ends the proof. $\square$

Now we will ascertain, under the assumptions of Theorem 5.6.7, the classes of periodicity of the subharmonics of (5.82). Recall that, thanks to Lemma 5.6.4, $\mathcal{P}_n^m = \mathcal{P}_{nm}^1$. Thus, for $k = \ell = m$, the nT-periodic coexistence states of (5.82) are the same as the nmT-periodic coexistence states for $k = \ell = 1$. Remember that, in case $k = \ell = 1$, we already know from Lemma 5.2.1 that

$$u_h = v_{nm-h} \qquad \text{for all } \; h \in \{1, 2, \dots, nm-1\}. \tag{5.107}$$

Proposition 5.6.8. *Assume (5.101), $k = \ell = 1$, and either (5.99), or (5.100), and let (u, v) be a minimal nmT-periodic coexistence state of (5.82) with $nm > 2$. Then,*

$$u_h = v_h \;\; \textit{if and only if} \;\; nm \in 2\mathbb{N} \;\; \textit{and} \;\; h = \tfrac{nm}{2}. \tag{5.108}$$

Therefore:

1. *The $\Phi(nm)$ subharmonics of order nm of (5.82) given by Theorem 5.6.7 lie in different periodicity classes if $nm \in 2\mathbb{N} + 1$, $nm \geq 3$, and*

2. *At least $\Phi(nm)/2$ of these subharmonics lie in different periodicity classes if $nm \in 2\mathbb{N}$, $nm \geq 2$.*

Proof. The proof of (5.108) proceeds by contradiction. Assume that $u_h = v_h$ for some $h \neq nm/2$. Then, by (5.107),

$$v_{nm-h} = u_h = v_h = u_{nm-h} \qquad \text{for all } \; h \in \{1, 2, \dots, nm-1\},$$

which, in particular, implies that

$$z_h := (u_h, v_h) = (u_{nm-h}, v_{nm-h}) =: z_{nm-h}. \tag{5.109}$$

Note that, by the structure of (5.82),

$$z_h \neq z_{h+1} \quad \text{for all } \; h \in \{1, 2, \dots, nm-2\}. \tag{5.110}$$

Subsequently, we set

$$\omega_{\min} := \min\{h, nm-h\}, \quad \omega_{\max} := \max\{h, nm-h\}, \quad \omega^* := \omega_{\max} - \omega_{\min}.$$

Thanks to (5.109), by the T-periodicity of (5.82), we find that, for every $k \in \mathbb{N}$,

$$z_{\omega_{\max}} = z_{\omega_{\min}+k\omega^* \,(\mathrm{mod}\, nm)}.$$

Suppose $\gcd(\omega^*, nm) = 1$. Then, by the Bézout's Identity, there exists an integer $k_0 \geq 1$ such that $(k_0+1)\omega^* = \omega^* + 1\,(\mathrm{mod}\, nm)$, which contradicts (5.110). Thus, $\gcd(\omega^*, nm) > 1$ and, hence, there exists $k < nm$ such that $k\omega^* = 0\,(\mathrm{mod}\, nm)$. Therefore,

$$\omega_{\min} + k\omega^* = \omega_{\min}\,(\mathrm{mod}\, nm)$$

which implies that the solution is kT-periodic with $k < nm$. This contradicts the minimality of the period and ends the proof. □

In [159] (see also [21, Sec.4.1.2]), where the Poincaré–Birkhoff theorem was improved from several perspectives, another lower bound, also related to $\Phi(n)$, was given for the number of subharmonics of order n of (5.82).

5.6.3 The case when $k \neq \ell$

Necessarily, either $k = \ell+1$, or $\ell = k+1$. Moreover, setting $m := \min\{k, \ell\}$, there exist

$$0 \leq t_0^1 < t_1^1 \leq t_2^1 < t_3^1 \leq \cdots \leq t_0^m < t_1^m \leq t_2^m < t_3^m \leq t_1^{m+1} < t_2^{m+1} \leq T,$$

such that

$$\operatorname{supp}\alpha_i \subseteq [t_0^i, t_1^i] \quad \text{and} \quad \operatorname{supp}\beta_j \subseteq [t_2^j, t_3^j] \tag{5.111}$$

if $k = \ell+1$, whereas

$$\operatorname{supp}\beta_j \subseteq [t_0^j, t_1^j] \quad \text{and} \quad \operatorname{supp}\alpha_i \subseteq [t_2^i, t_3^i] \tag{5.112}$$

if $\ell = k+1$.

The next result shows that also in this case (5.82) has as many subharmonics as in the context of Theorem 5.6.5 with $k = \ell$.

Theorem 5.6.9. *Assume*

$$A_1 := \int_0^T (\alpha_1 + \alpha_{m+1}) = \int_0^T \alpha_2 = \cdots = \int_0^T \alpha_m = \int_0^T \beta_1 = \int_0^T \beta_2 = \cdots = \int_0^T \beta_m \tag{5.113}$$

if (5.111) *holds, and*

$$B_1 := \int_0^T (\beta_1 + \beta_{m+1}) = \int_0^T \beta_2 = \cdots = \int_0^T \beta_m = \int_0^T \alpha_1 = \int_0^T \alpha_2 = \cdots = \int_0^T \alpha_m \tag{5.114}$$

under condition (5.112). *Then, much like in Theorem* 5.6.5*, for every integer* $n \geq 1$ *and* $\lambda > 2/A_1$, (5.82) *has* $\nu(nm)$ *(resp.* $\mu(nm)$*)* nT*-periodic coexistence states under condition* (5.111) *(resp.* (5.112)*).*

Proof. Assume (5.111) and (5.113), and let denote the Poincaré map in the time interval $[s_1, s_2]$ by $\mathcal{P}^{k=\ell}_{[s_1,s_2]}$ if $k = \ell$, and by $\mathcal{P}^{k=\ell+1}_{[s_1,s_2]}$ if $k = \ell + 1$. Then, the value $\int_0^T \alpha_1$ in case $k = \ell$ equals $\int_0^T (\alpha_1 + \alpha_{m+1})$ in case $k = \ell + 1$.

Let (u_0, v_0) be a fixed point of $\mathcal{P}^{k=\ell}_{[0,nT]} = \mathcal{P}^{k=\ell}_{[0,t_3^{nm}]}$. Then, it is clear that the point $(u_0 e^{(1-v_0)\int_0^T \alpha_{m+1}}, v_0)$ is a fixed point of $\mathcal{P}^{k=\ell+1}_{[0,nT]} = \mathcal{P}^{k=\ell+1}_{[0,t_1^{nm+1}]}$. Indeed, by the structure of (5.82),

$$\begin{aligned}
\mathcal{P}^{k=\ell+1}_{[0,t_1^1]}(u_0 e^{(1-v_0)\int_0^T \alpha_{m+1}}, v_0) &= (u_0 e^{(1-v_0)\int_0^T (\alpha_{m+1}+\alpha_1)}, v_0) \\
&= (u_0 e^{(1-v_0)A_1}, v_0) = \mathcal{P}^{k=\ell}_{[0,t_1^1]}(u_0, v_0).
\end{aligned}$$

Moreover, thanks to (5.113), we also have that $\mathcal{P}^{k=\ell+1}_{[t_1^1,t_3^{nm}]} = \mathcal{P}^{k=\ell}_{[t_1^1,t_3^{nm}]}$. Thus, since (u_0, v_0) is a fixed point of $\mathcal{P}^{k=\ell}_{[0,t_3^{nm}]}$, it becomes apparent that

$$\mathcal{P}^{k=\ell+1}_{[0,t_3^{nm}]}(u_0 e^{(1-v_0)\int_0^T \alpha_{m+1}}, v_0) = (u_0, v_0).$$

Therefore,

$$\mathcal{P}^{k=\ell+1}_{[0,t_1^{nm+1}]}(u_0 e^{(1-v_0)\int_0^T \alpha_{m+1}}, v_0) = (u_0 e^{(1-v_0)\int_0^T \alpha_{m+1}}, v_0),$$

i.e., $(u_0 e^{(1-v_0)\int_0^T \alpha_{m+1}}, v_0)$ is an nT-periodic coexistence state. This establishes a bijection between the nT-coexistence states of (5.82) in cases $\ell = k$ and $k = \ell + 1$, and shows that (5.82) has $\nu(nm)$ nT-periodic coexistence states under condition (5.111).

As the proof when $\ell = k + 1$ can be accomplished similarly, we will omit its technical details here. □

Our next result gives some sufficient conditions for non-existence.

Lemma 5.6.10. *The following non-existence results hold:*

(i) (5.82) *cannot admit any non-trivial* nT*-periodic coexistence state,* $n \in \mathbb{N}$*, if* $k + \ell = 1$*.*

(ii) (5.82) *cannot admit any non-trivial T-periodic coexistence state if $k+\ell=3$.*

Proof. If $k+\ell=1$, then either $k=1$ and $\ell=0$, or $\ell=1$ and $k=0$. Thus, either u, or v, are constant for all $t\in[0,T]$, which ends the proof.

Now, suppose that $k+\ell=3$. Then, there exist

$$0\leq t_0^1<t_1^1\leq t_2^1<t_3^1\leq t_0^2<t_1^2\leq T,$$

such that either

$$\operatorname{supp}\alpha_1\subseteq[t_0^1,t_1^1],\quad \operatorname{supp}\beta_1\subseteq[t_2^2,t_3^1],\qquad \operatorname{supp}\alpha_2\subseteq[t_0^2,t_1^2],$$

or

$$\operatorname{supp}\beta_1\subseteq[t_0^1,t_1^1],\quad \operatorname{supp}\alpha_1\subseteq[t_2^2,t_3^1],\quad \operatorname{supp}\beta_2\subseteq[t_0^2,t_1^2],$$

as illustrated in Figure 5.13.

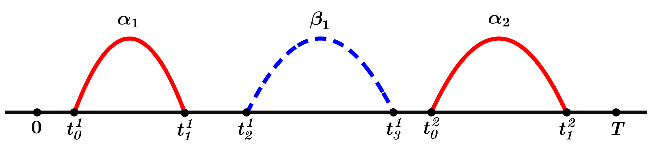

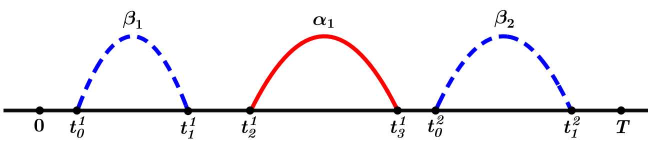

Figure 5.13: Two admissible examples with $k=2$, $\ell=1$, and $k=1$, $\ell=2$.

By the special structure of (5.82), where $\alpha\beta=0$, the orbit of any solution in the interval $[0,T]$ consists of three lines, two of them parallel in the phase-plane to one of the axis, while the third one is parallel to the other axis. So, these orbits cannot be closed. Therefore, (5.82) cannot admit any T-periodic solution. □

The next theorem summarizes the results found in the previous four sections. It characterizes the existence of T-periodic coexistence states, and subharmonics of all orders of (5.82), in terms of the number of α-intervals and β-intervals in $[0,T]$.

Theorem 5.6.11. *The system (5.82) admits, for sufficiently large λ, some T-periodic coexistence state if, and only if, $k+\ell \geq 4$. Moreover, for every $\lambda > 2/A_1$, under the appropriate symmetry properties, (5.82) has subharmonics of all orders, $n \geq 2$, if, and only if, $k+\ell \geq 2$.*

5.6.4 The limiting T-periodic case $k = \ell = 2$

According to Theorem 5.6.11, the condition $k + \ell \geq 4$ is necessary and sufficient so that (5.82) can admit a T-periodic coexistence state. In this section, we deal with the limiting case when $k = \ell = 2$ and ascertain the bifurcation directions to T-periodic coexistence states. Note that when $k = \ell \geq 2$, then there exist

$$0 \leq t_0^1 < t_1^1 \leq t_2^1 < t_3^1 \leq t_0^2 < t_1^2 \leq t_2^2 < t_3^2 \leq T.$$

such that either

$$\operatorname{supp} \alpha_1 \subseteq [t_0^1, t_1^1], \quad \operatorname{supp} \beta_1 \subseteq [t_2^1, t_3^1], \quad \operatorname{supp} \alpha_2 \subseteq [t_0^2, t_1^2], \quad \operatorname{supp} \beta_2 \subseteq [t_2^2, t_3^2], \tag{5.115}$$

or

$$\operatorname{supp} \beta_1 \subseteq [t_0^1, t_1^1], \quad \operatorname{supp} \alpha_1 \subseteq [t_2^1, t_3^1], \quad \operatorname{supp} \beta_2 \subseteq [t_0^2, t_1^2], \quad \operatorname{supp} \alpha_2 \subseteq [t_2^2, t_3^2]. \tag{5.116}$$

Figure 5.14 shows two admissible configurations.

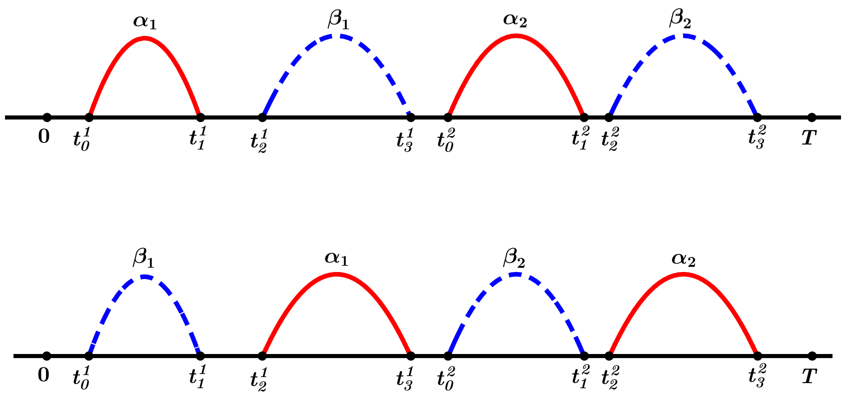

Figure 5.14: Two examples, with $k = \ell = 2$, satisfying (5.115) (above) and (5.116) (below).

Theorem 5.6.12. *Under the assumption (5.115), or (5.116), (5.82) has, at least, two T-periodic coexistence states for every $\lambda > \lambda_0$, where for $i = 1, 2$,*

$$\lambda_0 := \sqrt{\frac{(A_1+A_2)(B_1+B_2)}{A_1A_2B_1B_2}}, \qquad A_i := \int_0^T \alpha_i,\ B_i := \int_0^T \beta_i. \tag{5.117}$$

In general, although $\lambda > \lambda_0$ is a sufficient condition, it is far from necessary. Actually, regarding λ as the main bifurcation parameter, λ_0 provides with a bifurcation value to T-periodic coexistence states of (5.82) from the line $(\lambda, u, v) = (\lambda, 1, 1)$, and there are some ranges of values of the parameters, A_j, B_j, $j \in \{1, 2\}$, for which this bifurcation is transcritical.

Proof. Assume (5.115). Then, integrating (5.82) yields

$$\begin{aligned} u(T) &= u_0 e^{(1-v_0)\lambda A_1 + (1-v(t_0^2))\lambda A_2}, \\ v(T) &= v_0 e^{(-1+u(t_0^2))\lambda B_1 + (-1+u(T))\lambda B_2}. \end{aligned} \tag{5.118}$$

Thus, a solution $(u(t), v(t))$ of (5.82) with initial data (u_0, v_0) is a T-periodic coexistence state if, and only, if $u_0, v_0 > 0$ and $\mathcal{P}_1(u_0, v_0) = (u_0, v_0)$, i.e, by (5.118), if, and only, if $u_0, v_0 > 0$ and

$$(1-v_0)A_1 = (v(t_0^2) - 1)A_2, \qquad (1-u_0)B_2 = (u(t_0^2) - 1)B_1,$$

which, again integrating (5.82), is equivalent to

$$\begin{cases} (1-v_0)A_1 = (v_0 e^{(-1+u_0 e^{(1-v_0)\lambda A_1})\lambda B_1} - 1)A_2, \\ (1-u_0)B_2 = (u_0 e^{(1-v_0)\lambda A_1} - 1)B_1. \end{cases} \tag{5.119}$$

Hence, eliminating u_0 from the second equation of (5.119),

$$u_0 = \frac{B_1 + B_2}{B_2 + B_1 e^{(1-v_0)\lambda A_1}}. \tag{5.120}$$

So, substituting (5.120) into the first equation of (5.119), it follows that

$$(1-v_0)A_1 = (v_0 e^{(-1 + \frac{B_1+B_2}{B_2 + B_1 e^{(1-v_0)\lambda A_1}} e^{(1-v_0)\lambda A_1})\lambda B_1} - 1)A_2.$$

Consequently, naming $x \equiv v_0$ and setting

$$\Phi(x) := x(A_2 e^{\frac{B_2(e^{(1-x)\lambda A_1} - 1)}{B_1 e^{(1-x)\lambda A_1} + B_2}\lambda B_1} + A_1) - (A_1 + A_2), \tag{5.121}$$

it is apparent that $\Phi^{-1}(0)$ provides us with the set of T-periodic coexistence states of (5.82). As $\Phi(x) < 0$ for all $x \le 0$, its zeroes are always positive. Since

$$\Phi(0) = -(A_1 + A_2) < 0, \qquad \Phi(1) = 0,$$

$$\Phi(x) > 0 \quad \text{if} \quad x \geq M := 1 + A_2/A_1,$$

and

$$\Phi'(1) = A_1 + A_2 - \lambda^2 \frac{A_1 A_2 B_1 B_2}{B_1 + B_2},$$

we find that $\Phi'(1) < 0$ if and only if, $\lambda > \lambda_0$ (see (5.117)). Therefore, (5.82) possesses two T-periodic solutions, $(\lambda, x_\pm)$, with $0 < x_- < 1$ and $1 < x_+ < M$. This ends the proof when (5.115) holds. Note that $x_\pm \in (0, M)$.

Assume (5.116). Then, repeating the previous argument it is apparent that the T-periodic coexistence states of (5.82) are the zeroes of the map

$$\Psi(x) := x(B_2 e^{\frac{A_2(1-e^{(x-1)\lambda B_1})}{A_1 e^{(x-1)\lambda B_1} + A_2}\lambda A_1} + B_1) - (B_1 + B_2). \tag{5.122}$$

As above, since $\Psi(x) < 0$ for all $x \leq 0$, its zeroes are always positive. Thus, as $\Psi(x)$ satisfies

$$\Psi(0) = -(B_1 + B_2) < 0, \qquad \Psi(1) = 0,$$

$$\Psi(x) > 0 \quad \text{if} \quad x \geq N := 1 + B_2/B_1,$$

and

$$\Psi'(1) = B_1 + B_2 - \lambda^2 \frac{A_1 A_2 B_1 B_2}{A_1 + A_2},$$

it is apparent that $\Psi'(1) < 0$ if $\lambda > \lambda_0$. Therefore, in this case, (5.82) admits, at least, two T-periodic coexistence states, $(\lambda, x^\pm)$, with $0 < x^+ < 1$ and $1 < x^- < N$. Note that $x^\pm \in (0, N)$. This concludes the proof that $\lambda > \lambda_0$ is sufficient for the existence of, at least, two T-periodic coexistence states.

It remains to determine the bifurcation directions from $(\lambda, x) = (\lambda_0, 1)$ in both cases. Now, it is appropriate to made explicit the dependence of the functions Φ and Ψ not only on x but also on λ, for as λ will be though as a bifurcation parameter.

Assume (5.115) and let $\Phi(\lambda, x)$ denote the function defined by (5.121). Then, the linearization of this function at $(\lambda, 1)$ is given by

$$\mathfrak{L}(\lambda) := \frac{\partial \Phi}{\partial x}(\lambda, 1) = A_1 + A_2 - \lambda^2 \frac{A_1 A_2 B_1 B_2}{B_1 + B_2}. \tag{5.123}$$

Thus, using the notations of [124], we find that, by the definition of λ_0,

$$\mathfrak{L}_0 := \mathfrak{L}(\lambda_0) = \frac{\partial \Phi}{\partial x}(\lambda_0, 1) = 0, \qquad \mathfrak{L}_1 := \frac{d\mathfrak{L}}{d\lambda}(\lambda_0).$$

We claim that the next algebraic transversality condition holds

$$\mathfrak{L}_1(N[\mathfrak{L}_0]) \oplus R[\mathfrak{L}_0] = \mathbb{R}. \tag{5.124}$$

Indeed, since $\mathfrak{L}_0 = 0$, it is apparent that $R[\mathfrak{L}_0] = [0]$ and hence, $N[\mathfrak{L}_0] = \mathbb{R} = \mathrm{span}[1]$. Moreover, differentiating with respect to λ (5.123) yields

$$\mathfrak{L}_1 = -\frac{2\lambda_0 A_1 A_2 B_1 B_2}{B_1 + B_2} \neq 0.$$

Therefore, $\mathfrak{L}_1 1 \notin R[\mathfrak{L}_0]$ and (5.124) holds. Consequently, by Theorem 7.1 of Crandall and Rabinowitz [37], there exist $\varepsilon > 0$ and two analytic functions $\lambda, x : (-\varepsilon, \varepsilon) \to \mathbb{R}$ such that, for some $\lambda_1 \in \mathbb{R}$ to be determined,

$$\lambda(s) = \lambda_0 + \lambda_1 s + \mathcal{O}(s^2), \qquad x(s) = 1 + s + \mathcal{O}(s^2), \qquad \text{as } \; s \to 0,$$

and $\Phi(\lambda(s), x(s)) = 0$ for all $s \in (-\varepsilon, \varepsilon)$. Moreover, besides $(\lambda, 1)$, these are the unique solutions of (5.82) in a neighborhood of $(\lambda_0, 1)$.

Setting

$$\varphi(s) := \Phi(\lambda(s), x(s)), \qquad |s| < \varepsilon,$$

it is apparent that

$$0 = \varphi(s) = \varphi(0) + \varphi'(0)s + \frac{1}{2}\varphi''(0)s^2 + \mathcal{O}(s^3) \qquad |s| < \varepsilon,$$

where $'$ stands for differentiation with respect to s. So,

$$\varphi(0) = \varphi'(0) = \varphi''(0) = 0.$$

By construction,

$$0 = \varphi(0) = \Phi(\lambda_0, 1) = 0, \qquad \frac{\partial \Phi}{\partial x}(\lambda_0, 1).$$

Moreover, differentiating (5.121) with respect to λ, it becomes apparent that

$$\frac{\partial \Phi}{\partial \lambda}(\lambda_0, 1) = 0.$$

Thus, since $\lambda'(0) = \lambda_1$,

$$\varphi'(0) = \frac{\partial \Phi}{\partial \lambda}(\lambda_0, 1)\lambda_1 + \frac{\partial \Phi}{\partial x}(\lambda_0, 1) = 0$$

does not provide any information on the sign of λ_1. So, we must analyze the second order terms of $\Phi(\lambda, x)$ at $(\lambda_0, 1)$. By differentiating Φ, after some straightforward, but tedious, manipulations, we find that

$$\frac{\partial^2\Phi}{\partial x^2}(\lambda_0,1) = \lambda_0^2 \frac{A_1A_2B_1B_2}{(B_1+B_2)^2}\left[(B_1+B_2)(\lambda_0 A_1 - 2) + \lambda_0 A_1 B_1(\lambda_0 B_2 - 2)\right],$$

$$\frac{\partial^2\Phi}{\partial x\partial\lambda}(\lambda_0,1) = -2\lambda_0\frac{A_1A_2B_1B_2}{B_1+B_2}, \qquad \frac{\partial^2\Phi}{\partial\lambda^2}(\lambda_0,1) = 0.$$

Consequently, differentiating and substituting the previous values of the second derivatives, it is apparent that

$$\begin{aligned} 0 = \varphi''(0) &= 2\lambda_1\frac{\partial^2\Phi}{\partial x\partial\lambda}(\lambda_0,1) + \frac{\partial^2\Phi}{\partial x^2}(\lambda_0,1) + \frac{\partial^2\Phi}{\partial\lambda^2}(\lambda_0,1) \\ &= \lambda_1\left(-4\lambda_0\frac{A_1A_2B_1B_2}{B_1+B_2}\right) \\ &+ \lambda_0^2\frac{A_1A_2B_1B_2}{(B_1+B_2)^2}\left[(B_1+B_2)(\lambda_0A_1-2)+\lambda_0A_1B_1(\lambda_0B_2-2)\right] \end{aligned}$$

and therefore,

$$\lambda_1 = \frac{\lambda_0}{4(B_1+B_2)}\left[(B_1+B_2)(\lambda_0A_1-2)+\lambda_0A_1B_1(\lambda_0B_2-2)\right]. \qquad (5.125)$$

It is clear that (5.125) can reach both positive and negative values depending on the values of the several parameters A_1, A_2, B_1 and B_2. For instance, if

$$2A_1 < A_2, \quad 2B_2 < B_1, \quad \frac{2}{3} < \frac{B_2}{A_1} < \frac{3}{2}, \qquad (5.126)$$

then,

$$\lambda_0^2A_1^2 = \frac{(A_1+A_2)(B_1+B_2)}{A_2B_1B_2}A_1 = \left(\frac{A_1}{A_2}+1\right)\left(1+\frac{B_2}{B_1}\right)\frac{A_1}{B_2} < \left(\frac{3}{2}\right)^3 < 4.$$

Similarly,

$$\lambda_0^2B_2^2 = \frac{(A_1+A_2)(B_1+B_2)}{A_1A_2B_1}B_2 = \left(\frac{A_1}{A_2}+1\right)\left(1+\frac{B_2}{B_1}\right)\frac{B_2}{A_1} < \left(\frac{3}{2}\right)^3 < 4.$$

Since the estimates (5.126) are satisfied, for example, if $B_2 = A_1$, $B_1 = A_2$ and $2B_2 < B_1$, it becomes apparent that (5.126) holds for wide open ranges of values of the several parameters involved in the setting of (5.82).

Now, assume (5.116), instead of (5.115). Then, the T-periodic coexistence states are given by the zeros of the map $\Psi(\lambda, x)$ defined in (5.122). In this case, the linearization of $\Psi(\lambda, x)$ at $(\lambda, 1)$ is given by

$$\mathfrak{M}(\lambda) := \frac{\partial \Psi}{\partial x}(\lambda, 1) = B_1 + B_2 - \lambda^2 \frac{A_1 A_2 B_1 B_2}{A_1 + A_2}.$$

Thus, setting

$$\mathfrak{M}_0 := \mathfrak{M}(\lambda_0) = 0, \qquad \mathfrak{M}_1 := \frac{d\mathfrak{M}}{d\lambda}(\lambda_0),$$

and adapting the argument given above, it is apparent that the transversality condition

$$\mathfrak{M}_1(N[\mathfrak{M}_0]) \oplus R[\mathfrak{M}_0] = \mathbb{R}$$

holds true. Moreover, also

$$\frac{\partial \Psi}{\partial x}(\lambda_0, 1) = 0 = \frac{\partial \Psi}{\partial \lambda}(\lambda_0, 1).$$

Hence, to find out the bifurcation direction, we must proceed as in the previous case. A rather straightforward, but tedious, calculation shows that

$$\frac{\partial^2 \Psi}{\partial x^2}(\lambda_0, 1) = \lambda_0^2 \frac{A_1 A_2 B_1 B_2}{(A_1 + A_2)^2} \left[(A_1 + A_2)(-\lambda_0 B_1 - 2) + \lambda_0 A_1 B_1 (\lambda_0 A_2 - 2) \right],$$

$$\frac{\partial^2 \Psi}{\partial x \partial \lambda}(\lambda_0, 1) = -2\lambda_0 \frac{A_1 A_2 B_1 B_2}{A_1 + A_2}, \qquad \frac{\partial^2 \Psi}{\partial \lambda^2}(\lambda_0, 1) = 0.$$

Therefore,

$$\lambda_1 = \frac{\lambda_0}{4(A_1 + A_2)} \left[-(B_1 + B_2)(\lambda_0 A_1 + 2) + \lambda_0 A_1 B_1 (\lambda_0 B_2 - 2) \right],$$

which can reach negative values also in this case. Indeed, if

$$B_2 < A_1 < B_1, \quad A_1 < A_2,$$

then

$$\lambda_0^2 B_2^2 = \frac{(A_1 + A_2)(B_1 + B_2)}{A_1 A_2 B_1} B_2 < 4$$

and consequently $\lambda_1 < 0$. This concludes the proof. $\square$

Note that Theorem 5.6.12 generalizes Theorems 5.6.1 and 5.6.2. Indeed, if $A_1 = A_2$ and $B_1 = B_2$, then $\varphi(x) = \Phi(x)$ and $\psi(x) = \Psi(x)$. Thus,

$$\lambda_0 = \frac{2}{\sqrt{A_1 B_1}},$$

which provides us with Theorems 5.6.1 and 5.6.2. Moreover, by Lemma 5.6.10, Theorem 5.6.12 holds also for the cases

$$\operatorname{supp}\alpha_i \subseteq [t_0^i, t_1^i] \quad \text{and} \quad \operatorname{supp}\beta_j \subseteq [t_2^j, t_3^j], \tag{5.127}$$

and

$$\operatorname{supp}\beta_i \subseteq [t_0^i, t_1^i] \quad \text{and} \quad \operatorname{supp}\alpha_j \subseteq [t_2^j, t_3^j], \tag{5.128}$$

with $i \in \{1,2,3\}$, $j \in \{1,2\}$ and for some

$$0 \le t_0^1 < t_1^1 \le t_2^1 < t_3^1 \le t_0^2 < t_1^2 \le t_2^2 < t_3^2 \le t_0^3 < t_1^3 \le T.$$

If (5.127) holds, then

$$\lambda_0 = \sqrt{\frac{(B_1+B_2+B_3)(A_1+A_2)}{B_2(B_1+B_3)A_1A_2}},$$

while

$$\lambda_0 = \sqrt{\frac{(A_1+A_2+A_3)(B_1+B_2)}{A_2(A_1+A_3)B_1B_2}}$$

if (5.128) holds.

Part II

Parabolic predator-prey models

Chapter 6

An heterogeneous predator-prey model

This chapter analyzes the existence and the uniqueness of coexistence states for the generalized spatially heterogeneous predator-prey model

$$\begin{cases} \mathfrak{L}_1 u = \lambda u - a(x)u^2 - \tilde{b}(x)\dfrac{uv}{\tilde{\gamma}(x)+\tilde{m}(x)u} & \text{in } \Omega, \\ \mathfrak{L}_2 v = \mu v + \tilde{c}(x)\dfrac{uv}{\tilde{\gamma}(x)+\tilde{m}(x)u} - d(x)v^2 & \text{in } \Omega, \\ \mathfrak{B}_1 u = \mathfrak{B}_2 v = 0 & \text{on } \partial\Omega, \end{cases} \tag{6.1}$$

where Ω is a bounded domain of $\mathbb{R}^N$ whose boundary, $\partial\Omega$, is a $N-1$ dimensional manifold of class C^2, and $\mathfrak{L}_1$ and $\mathfrak{L}_2$ are second order uniformly elliptic operators of the form

$$\mathfrak{L}_k := -\mathrm{div}\,(A^k(x)\nabla) + \sum_{j=1}^{N} b_j^k(x)\partial_j + c^k(x), \qquad k=1,2, \tag{6.2}$$

where, for every $k=1,2$, $A^k(x) := \left(a_{ij}^k(x)\right)_{1\le i,j\le N}$ is a symmetric matrix of order N such that

$$a_{ij}^k = a_{ji}^k \in W^{1,\infty}(\Omega) \quad \text{and} \quad b_j^k, c^k \in L^\infty(\Omega) \quad \text{for all} \quad 1\le i,j\le N.$$

In this model, $\mathfrak{B}_1$ and $\mathfrak{B}_2$ are general boundary operators of mixed type such that, for every $k=1,2$ and $w\in\mathcal{C}(\bar{\Omega})\cap\mathcal{C}^1(\Omega\cup\Gamma_1^k)$,

$$\mathfrak{B}_k w := \begin{cases} w & \text{on } \Gamma_0^k, \\ \partial_{\nu_k} w + \beta_k(x) w & \text{on } \Gamma_1^k, \end{cases} \tag{6.3}$$

where Γ_0^k and Γ_1^k are two closed and open disjoint subsets of $\partial\Omega$ such that

$$\Gamma_0^k \cup \Gamma_1^k = \partial\Omega.$$

In (6.3), $\beta_k \in \mathcal{C}(\Gamma_1^k;\mathbb{R})$ and $\nu_k \in \mathcal{C}^1(\Gamma_1^k;\mathbb{R}^N)$ is an outward pointing nowhere tangent vector field. Moreover, the functions coefficients $a(x)$, $\tilde{b}(x)$, $\tilde{c}(x)$, $d(x)$, $\tilde{\gamma}(x)$ and $\tilde{m}(x)$ are continuous in $\bar{\Omega}$ and satisfy $\tilde{b} \gneq 0$, $\tilde{c} \gneq 0$, $\tilde{m} \geq 0$ and

$$a(x) > 0, \quad d(x) > 0, \quad \tilde{\gamma}(x) > 0 \quad \text{for all} \quad x \in \bar{\Omega}. \tag{6.4}$$

Since $\tilde{\gamma}(x) > 0$ for all $x \in \bar{\Omega}$, the interaction coefficients between u and v in the setting of (6.1) can be equivalently expressed as

$$\tilde{b}(x)\frac{uv}{\tilde{\gamma}(x)+\tilde{m}(x)u} = \frac{\tilde{b}(x)}{\tilde{\gamma}(x)}\frac{uv}{1+\frac{\tilde{m}(x)}{\tilde{\gamma}(x)}u}, \quad \tilde{c}(x)\frac{uv}{\tilde{\gamma}(x)+\tilde{m}(x)u} = \frac{\tilde{c}(x)}{\tilde{\gamma}(x)}\frac{uv}{1+\frac{\tilde{m}(x)}{\tilde{\gamma}(x)}u}.$$

Thus, renaming

$$b(x) := \frac{\tilde{b}(x)}{\tilde{\gamma}(x)}, \qquad c(x) := \frac{\tilde{c}(x)}{\tilde{\gamma}(x)}, \qquad m(x) := \frac{\tilde{m}(x)}{\tilde{\gamma}(x)},$$

(6.1) can be finally written down as

$$\begin{cases} \mathfrak{L}_1 u = \lambda u - a(x)u^2 - b(x)\dfrac{uv}{1+m(x)u} & \text{in } \ \Omega, \\ \mathfrak{L}_2 v = \mu v + c(x)\dfrac{uv}{1+m(x)u} - d(x)v^2 & \text{in } \ \Omega, \\ \mathfrak{B}_1 u = \mathfrak{B}_2 v = 0 & \text{on } \ \partial\Omega. \end{cases} \tag{6.5}$$

In this model, $a(x)$ and $d(x)$ satisfy (6.4) and

$$b \gneq 0, \quad c \gneq 0, \quad m \geq 0. \tag{6.6}$$

From an ecological point of view, (6.5) models the interaction between a prey with density u and a predator with density v in the inhabiting territory Ω, where both species are assumed to have a logistic growth, or decay, in the absence of each other. In the special case when $m = 0$, (6.5) provides us with a rather generalized diffusive counterpart of the classical Lotka–Volterra predator-prey model, while if $m(x)$ is a positive constant, it is a generalized heterogeneous counterpart of the diffusive Holling–Tanner model studied by A. Casal et al. [34]. Such kinetics take into account the saturation effects of the predator in the presence of a high population of preys; the constant $m > 0$ measuring the predator saturation level (see, e.g., H. Freedman [81] and R. May [150]). In a non-spatial context, these predator-prey interactions had been already analyzed in the late seventies by S. B. Hsu [95], where a rather pioneering criterium for the global stability of the coexistence state was given (see also S. B. Hsu and T. W. Huang [96]).

In (6.5), $m(x)$ measures the level of saturation of the predator at any particular location $x \in \Omega$ where $m(x) > 0$, while saturation effects do not play any role if $m(x) = 0$. Thus, (6.5) combines, within the same territory, the classical interactions of Lotka–Volterra type in the region $m^{-1}(0)$ with the Holling-Tanner functional responses in $\{x \in \Omega : m(x) > 0\}$. So, integrating at a single prototype model the classical Lotka–Volterra and Holling–Tanner kinetics. Throughout this chapter, $\lambda > 0$ and $\mu \in \mathbb{R}$ are regarded as bifurcation parameters. In applications, $\lambda - c^1(x)$ and $\mu - c^2(x)$ are the growth rates of the prey and the predator in the absence of each other.

Although there is a huge amount of literature on this type of models, beginning with A. Casal et al. [34], in most of the available literature

$$\mathfrak{L}_1 = \mathfrak{L}_2 = -\Delta = -\sum_{j=1}^{N} \frac{\partial^2}{\partial x_j^2}$$

is the Laplace operator in $\mathbb{R}^N$, and either $\Gamma_1^1 = \Gamma_1^2 = \emptyset$, i.e., $\mathfrak{B}_1$ and $\mathfrak{B}_2$ equal the Dirichlet operator on $\partial\Omega$, or $\Gamma_0^1 = \Gamma_0^2 = \emptyset$, $\beta_1 = \beta_2 = 0$ and $\nu_1 = \nu_2$ is the exterior normal vector field; so, $\mathfrak{B}_1$ and $\mathfrak{B}_2$ equal the Neumann boundary operator. Among the contributions within the first category count those of R. Peng, M. X. Wang and W. Y. Chen [170], M. X. Wang and Q. Wu [207], H. Nie and J. Wu [161], G. Guo and J. Wu [86], [87], J. Zhou and C. Mu [216], J. Zhou and J. P. Shi [218], H. Jiang and L. Wang [100], H. Yuan, J. Wu, Y. Jia and H. Nie [212], S. Li, J. Wu and Y. Dong [114], and X. Feng, Y. Song and X. An [68]. Among those in the second category count P. Y. H. Pang and M. Wang [163], [164], Y. Du and S. B. Hsu [59], W. Ko and K. Ryu [103], [105], Y. Du and J. P. Shi [64], J. Zhou and C. Mu [217], Y. Jia, J. Wu and H. K. Xu [99], S. Li, J. Wu and Y. Dong [113], and X. Zeng, W. Zeng and L. Liu [213]. Another fraction of available literature, like K. Ryu and I. Ahn [183] and W. Ko and K. Ryu [104] dealt with Robin boundary conditions. The paper of Y. Du and J. P. Shi [63] dealt with a model of a slightly different nature.

According to its greatest generality, the prototype (6.5) integrates almost all available models in the literature, except for the fact that we are not considering in this chapter any kind of degeneracies for the function coefficients $a(x)$ and $d(x)$, which might provoke metasolutions, as discussed in J. López-Gómez [127] and the references there in. The first general Reaction-Diffusion systems incorporating spatial heterogeneities seem to be those introduced by

J. López-Gómez in [121], later revisited in [124, Ch. 7]. Actually, as it will be shown later, most of the available results on the existence of coexistence states can be derived as a rather direct consequence of Theorem 7.2.2 of [124].

The main goal of this chapter is characterizing the existence of coexistence states of (6.5) and analyzing their uniqueness in terms of the level of the saturation effects, measured by $m(x)$. As a result of our analysis we have found the next intriguing feature of the model (6.5). When $m(x) > 0$ for all $x \in \bar{\Omega}$, like in most of the existing papers, (6.5) cannot admit a coexistence state for

$$\mu \leq \sigma_0 \left[\mathfrak{L}_2 - \tfrac{c(x)}{m(x)}, \mathfrak{B}_2, \Omega \right],$$

where $\sigma_0[\mathfrak{L}_2 - c/m, \mathfrak{B}_2, \Omega]$ stands for the principal eigenvalue of the problem $(\mathfrak{L}_2 - c/m, \mathfrak{B}_2, \Omega)$, whereas if

$$\Omega_0 \equiv \operatorname{Int} m^{-1}(0) \neq \emptyset, \tag{6.7}$$

regardless the size and the internal structure of Ω_0, (6.5) admits coexistence states for all $\mu < 0$.

As far as concerns the uniqueness, we have adopted the methodology of J. López-Gómez and R. M. Pardo [143], [144], to establish that the one-dimensional counterpart of (6.5) has a unique coexistence state if $m(x)$ is sufficiently small for all $x \in \Omega$, which enables us to recover the uniqueness theorems of [143] and [144]. Astonishingly, no real serious advance has been done on this particular issue in the last three decades, except for the multiplicity results of J. López-Gómez [123] and [134] (see also Chapter 5) in the context of the periodic Lotka–Volterra predator model.

Although the techniques used in this chapter are already classical, it should be emphasized that the construction of supersolutions and, hence, of a priori bounds, in the general case when $\beta_1(x)$ and $\beta_2(x)$ change of sign is far from straightforward and it uses a recent technical device introduced by D. Aleja et al. [5] based on Lemma 2.1 of the monograph [126]. Similarly, by the lack of singular perturbation results for logistic equations under general non-classical mixed boundary conditions, we must invoke the (very recent) Theorem 1.2 of S. Fernández-Rincón and J. López-Gómez [69]. Besides our extensions of the existing results here are far from straightforward, some of them are fraught with a number of technical difficulties whose resolution might contribute to facilite our understanding of the effects of the spatial heterogeneities on the dynamics of Reaction Diffusion systems, much like Theorem 7.10 of [126] enhanced the mathematical analysis of the effects of the spatial heterogeneities in the context of degenerate problems.

This chapter is organized as follows. Section 2 collects some preliminaries that are going to be used throughout this chapter. Among them, the characterization of the strong maximum principle, [126, Th. 7.10], and the singular perturbation result established by [69, Th. 1.2]. Section 3 characterizes the linearized stability of the trivial and semitrivial positive solutions of (6.5). Section 4 derives some necessary conditions for the existence of a coexistence state of (6.5). Section 5 establishes that (6.5) possesses a coexistence state provided that any of the semitrivial positive solutions is linearly unstable. The analysis of A. Casal et al. [34] already established that this is far from characterizing the existence of a coexistence state when m is a positive constant, while, thanks to Theorem 3.1 of J. López-Gómez and R. M. Pardo [142], the instability of the semitrivial positive solutions characterizes the existence of a coexistence state in the classical diffusive Lotka–Volterra system under Dirichlet boundary conditions. Section 6 ascertains the nature of the local bifurcations to coexistence states from the semitrivial positive solutions. Finally, Section 7 delivers our main uniqueness result of coexistence states, establishing that, regardless the nodal structure of $m(x)$, in one spatial dimension, the problem (6.5) admits a unique coexistence state provided $\|m\|_{\mathcal{C}(\bar{\Omega})}$ is sufficiently small.

6.1 Preliminaries

This section collects some well known results that are going to be used throughout this chapter and in the following chapter. As a direct consequence of the elliptic L^p-theory (see, e.g., Chapter 5 of [126]), it is apparent that any non-negative weak solution of (6.5), (u, v), satisfies

$$u \in U_1 := \bigcap_{p=N}^{\infty} W^{2,p}_{\mathfrak{B}_1}(\Omega), \qquad v \in U_2 := \bigcap_{p=N}^{\infty} W^{2,p}_{\mathfrak{B}_2}(\Omega),$$

where, for every $k = 1, 2$ and $p > N$, $W^{2,p}_{\mathfrak{B}_k}(\Omega)$ stands for the Sobolev space of the functions $w \in W^{2,p}(\Omega)$ such that $\mathfrak{B}_k w = 0$ on $\partial\Omega$. By the Sobolev embeddings and the Rellich–Kondrashov theorem, it is easily seen that

$$U_k \hookrightarrow \mathcal{C}^1_{\mathfrak{B}_k}(\bar{\Omega}) \qquad k = 1, 2,$$

with compact embeddings, where $\mathcal{C}^1_{\mathfrak{B}_k}(\bar{\Omega})$ stands for the set of functions $z \in \mathcal{C}^1(\bar{\Omega})$ such that $\mathfrak{B}_k z = 0$ on $\partial\Omega$ (see [126, Ch. 4] if necessary). Hence, there is enough regularity along the boundary as to consider $\mathfrak{B}_k w$ in the classical sense. Actually, according to [126, Th. 5.11], (u, v) must be a strong solution of (6.5). In particular, u and v are twice classically differentiable almost everywhere in Ω and they are classical solutions in the sense of [126, Def. 4.1].

Throughout this chapter, for any given $V \in L^\infty(\Omega)$ and $k = 1, 2$, we denote by

$$\sigma_0[\mathfrak{L}_k + V, \mathfrak{B}_k, \Omega]$$

the principal eigenvalue of the linear eigenvalue problem

$$\begin{cases} (\mathfrak{L}_k + V)\varphi = \tau\varphi & \text{in } \Omega, \\ \mathfrak{B}_k\varphi = 0 & \text{on } \partial\Omega, \end{cases} \tag{6.8}$$

whose existence and uniqueness in our general setting was established in [126, Ch. 7]. It is folklore that the principal eigenvalue is the lowest real eigenvalue of the problem, as well as strictly dominant and algebraically simple. The associated principal eigenfunction, unique up to a multiplicative positive constant, can be taken strongly positive in Ω, $\varphi \gg_k 0$, in the sense that

$$\varphi(x) > 0 \text{ for all } x \in \Omega \cup \Gamma_1^k \text{ and } \frac{\partial\varphi}{\partial n}(x) < 0 \text{ for all } x \in \Gamma_0^k,$$

where n stands for the outward unit vector field to Ω. Throughout this chapter we will use two important properties of the principal eigenvalue: its monotonicity with respect to the potential and the theorem of characterization of the strong maximum principle. They have been collected into the next two results. With the greatest generality in this chapter, the next result goes back to S. Cano-Casanova and J. López-Gómez [28].

Theorem 6.1.1. *Let $V_1, V_2 \in L^\infty(\Omega)$ be such that $V_1 < V_2$. Then, for every $k = 1, 2$,*

$$\sigma_0\left[\mathfrak{L}_k + V_1, \mathfrak{B}_k, \Omega\right] < \sigma_0\left[\mathfrak{L}_k + V_2, \mathfrak{B}_k, \Omega\right].$$

Thus, the map $V \mapsto \sigma_0\left[\mathfrak{L}_k + V, \mathfrak{B}_k, \Omega\right]$ is continuous and increasing.

The next characterization goes back to J. López-Gómez and M. Molina-Meyer [129] for cooperative systems under Dirichlet boundary conditions, and to H. Amann and J. López-Gómez [7] and J. López-Gómez [125] for general boundary conditions of mixed type. It is [126, Th. 7.10], where the interested reader is sent for further details.

Incidentally, simultaneously to [129], the equivalence between (a) and (c) was also established for the single equation under Dirichlet boundary conditions by H. Berestycki, L. Nirenberg and S. R. S. Varadhan [14] (see the Preface of [126] for any further details and a complete discussion). However, (b) is the most useful condition from the point of the applications.

Theorem 6.1.2. *For every $V \in L^\infty(\Omega)$ and $k = 1, 2$, the next conditions are equivalent:*

(a) $\sigma_0 [\mathfrak{L}_k + V, \mathfrak{B}_k, \Omega] > 0$.

(b) *The tern* $(\mathfrak{L}_k + V, \mathfrak{B}_k, \Omega)$ *admits a positive strict supersolution,* $h \in U_k$, *i.e., for some* $h \in U_k$ *such that* $h \gneq 0$, *the next estimates hold*

$$\begin{cases} (\mathfrak{L}_k + V)h \geq 0 & \text{in } \Omega, \\ \mathfrak{B}_k h \geq 0 & \text{on } \partial\Omega, \end{cases}$$

with some of these inequalities strict.

(c) *The tern* $(\mathfrak{L}_k + V, \mathfrak{B}_k, \Omega)$ *satisfies the strong maximum principle, i.e.,* $w \gg_k 0$ *for every function* $w \in U_k$ *such that*

$$\begin{cases} (\mathfrak{L}_k + V)w \geq 0 & \text{in } \Omega, \\ \mathfrak{B}_k w \geq 0 & \text{on } \partial\Omega, \end{cases}$$

with some of these inequalities strict. By $w \gg_k 0$, *it is meant that*

$$w(x) > 0 \text{ for all } x \in \Omega \cup \Gamma_1^k \text{ and } \frac{\partial w}{\partial n}(x) < 0 \text{ for all } x \in w^{-1}(0) \cap \Gamma_0^k.$$

Similarly, through this chapter, we will often invoke the next result. In the special case when $\beta_k \geq 0$, it goes back to J. M. Fraile et al. [79, Th. 3.5]. In the general case when β_k changes of sign one can use the change of variable of S. Fernández-Rincón and J. López-Gómez [69, Sect. 3] to reduce the problem to the setting of [79], or one might derive it directly from Theorem 1.1 of D. Daners and J. López-Gómez [50].

Theorem 6.1.3. *Suppose* $\rho \in \mathbb{R}$ *and* $\xi \in C(\bar{\Omega}; (0, \infty))$. *Then, for every* $k = 1, 2$ *and* $V \in L^\infty(\Omega)$, *the semilinear boundary value problem*

$$\begin{cases} (\mathfrak{L}_k + V)w = \rho w - \xi(x) w^2 & \text{in } \Omega, \\ \mathfrak{B}_k w = 0 & \text{on } \partial\Omega, \end{cases} \tag{6.9}$$

admits a positive solution if, and only if,

$$\rho > \sigma_0 [\mathfrak{L}_k + V, \mathfrak{B}_k, \Omega].$$

Moreover, it is unique if it exists, and if we denote it by

$$w_{\rho,k} \equiv \theta_{[\mathfrak{L}_k + V, \rho, \xi]} \in U_k,$$

then $w_{\rho,k} \gg_k 0$ *and the map* $\rho \to w_{\rho,k}$ *is point-wise increasing if*

$$\rho > \sigma_0 [\mathfrak{L}_k + V, \mathfrak{B}_k, \Omega].$$

Furthermore,

$$\lim_{\rho \downarrow \sigma_0[\mathfrak{L}_k + V, \mathfrak{B}_k, \Omega]} w_{\rho,k} = 0.$$

In other words, $w_{\rho,k}$ *bifurcates from* $w = 0$ *at* $\rho = \sigma_0 [\mathfrak{L}_k + V, \mathfrak{B}_k, \Omega]$.

More precisely, through this chapter we denote by $\theta_{[\mathfrak{L}_k+V,\rho,\xi]}$ the maximal non-negative solution of (6.9). Thus,

$$\theta_{[\mathfrak{L}_k+V,\rho,\xi]} := 0 \quad \text{if} \;\; \rho \leq \sigma_0\left[\mathfrak{L}_k+V,\mathfrak{B}_k,\Omega\right],$$

whereas

$$\theta_{[\mathfrak{L}_k+V,\rho,\xi]} \gg_k 0 \quad \text{if} \;\; \rho > \sigma_0\left[\mathfrak{L}_k+V,\mathfrak{B}_k,\Omega\right].$$

J. M. Fraile et al. [79] also gave a version of Theorem 6.1.3 for the special case when $\rho \geq 0$ and ξ vanishes on some nice subdomain of Ω. Theorem 1.1 of D. Daners and J. López-Gómez [50] characterized the range of ρ's for which (6.9) admits a positive solution under no additional restrictions on the nature of $\xi^{-1}(0)$. The next result, of technical nature, will be often invoked in this chapter.

Lemma 6.1.4. *Under the assumptions of Theorem 6.1.3, $w_{\rho_2,k} \gg_k w_{\rho_1,k}$ if*

$$\rho_2 > \rho_1 > \sigma_0\left[\mathfrak{L}_k+V,\mathfrak{B}_k,\Omega\right],$$

in the sense that $w_{\rho_2,k} - w_{\rho_1,k} \gg_k 0$. More generally, if $\bar{u}$ is a positive strict supersolution of (6.9), then $\bar{u} \gg_k w_{\rho,k}$. Similarly, if $\underline{u}$ is a positive strict subsolution of (6.9), then $\underline{u} \ll_k w_{\rho,k}$.

Proof. First we show that any positive strict supersolution of (6.9), $\bar{u}$, satisfies $\bar{u} \gg_k w_{\rho,k}$. Indeed,

$$\begin{aligned}(\mathfrak{L}_k+V)(\bar{u}-w_{\rho,k}) &\geq \rho\bar{u} - \xi(x)\bar{u}^2 - \rho w_{\rho,k} + \xi(x)w_{\rho,k}^2 \\ &= \rho(\bar{u}-w_{\rho,k}) - \xi(x)(\bar{u}+w_{\rho,k})(\bar{u}-w_{\rho,k})\end{aligned}$$

and hence,

$$\begin{cases} \left[\mathfrak{L}_k+V+\xi(x)(\bar{u}+w_{\rho,k})-\rho\right](\bar{u}-w_{\rho,k}) \geq 0 & \text{in } \;\Omega, \\ \mathfrak{B}_k(\bar{u}-w_{\rho,k}) \geq 0 & \text{on } \;\partial\Omega, \end{cases} \tag{6.10}$$

with some of these inequalities strict, for as $\bar{u}$ is a strict supersolution of (6.9). On the other hand, by Theorem 6.1.1,

$$\sigma_0\left[\mathfrak{L}_k+V+\xi(x)(\bar{u}+w_{\rho,k})-\rho,\mathfrak{B}_k,\Omega\right] > \sigma_0\left[\mathfrak{L}_k+V+\xi(x)w_{\rho,k}-\rho,\mathfrak{B}_k,\Omega\right] = 0,$$

because $\bar{u} \gneq 0$ and $\xi(x) > 0$ for all $x \in \Omega$. The last identity follows, by the Krein–Rutman theorem, from the fact that $w_{\rho,k}$ is a positive solution of (6.9). Therefore, according to Theorem 6.1.2, it follows from (6.10) that

$$\bar{u} - w_{\rho,k} \gg_k 0.$$

Now, suppose that $\underline{u}$ is a positive strict subsolution of (6.9). Then,

$$\begin{aligned}(\mathfrak{L}_k + V)(w_{\rho,k} - \underline{u}) &\geq \rho w_{\rho,k} - \xi(x) w_{\rho,k}^2 - \rho \underline{u} + \xi(x)\underline{u}^2 \\ &= \rho(w_{\rho,k} - \underline{u}) - \xi(x)(w_{\rho,k} + \underline{u})(w_{\rho,k} - \underline{u})\end{aligned}$$

and hence,

$$\begin{cases} \left[\mathfrak{L}_k + V + \xi(x)(w_{\rho,k} + \underline{u}) - \rho\right](w_{\rho,k} - \underline{u}) \geq 0 & \text{in } \Omega, \\ \mathfrak{B}_k(w_{\rho,k} - \underline{u}) \geq 0 & \text{on } \partial\Omega, \end{cases}$$

with some of these inequalities strict. Therefore, arguing as above yields

$$\underline{u} \ll_k w_{\rho,k}.$$

This ends the proof. □

As a byproduct of Theorem 6.1.3, the next result holds

Corollary 6.1.5. *According to Theorem 6.1.3, (6.5) has a semitrivial positive solution of the form $(u, 0)$ if, and only if,*

$$\lambda > \sigma_{0,1} \equiv \sigma_0[\mathfrak{L}_1, \mathfrak{B}_1, \Omega]$$

and, in such case, $(u, 0) = \left(\theta_{[\mathfrak{L}_1,\lambda,a(x)]}, 0\right)$. Similarly, (6.5) has a semitrivial positive solution of the form $(0, v)$ if, and only if,

$$\mu > \sigma_{0,2} \equiv \sigma_0[\mathfrak{L}_2, \mathfrak{B}_2, \Omega]$$

and, in such case, $(0, v) = \left(0, \theta_{[\mathfrak{L}_2,\mu,d(x)]}\right)$.

By making the change of variable

$$\theta_{[\mathfrak{L}_k+V,\rho,\xi]} = \rho\, \psi_{[\mathfrak{L}_k+V,\rho,\xi]} \tag{6.11}$$

in the problem (6.9) and dividing the resulting differential equation by ρ^2 yields

$$\begin{cases} \frac{1}{\rho}(\mathfrak{L}_k + V)\psi_{[\mathfrak{L}_k+V,\rho,\xi]} = \psi_{[\mathfrak{L}_k+V,\rho,\xi]} - \xi(x)\psi^2_{[\mathfrak{L}_k+V,\rho,\xi]} & \text{in } \Omega, \\ \mathfrak{B}_k \psi_{[\mathfrak{L}_k+V,\rho,\xi]} = 0 & \text{on } \partial\Omega. \end{cases}$$

Thus, thanks to Theorem 1.2 of S. Fernández-Rincón and J. López-Gómez [69], the next result holds.

Theorem 6.1.6. *Suppose $\rho > 0$ and $\xi \in C(\bar{\Omega}; (0, \infty))$. Then, for every compact subset, $K \subset \Omega \cup \Gamma_k^1$,*

$$\lim_{\rho \uparrow +\infty} \psi_{[\mathfrak{L}_k+V,\rho,\xi]} = \xi^{-1} \quad \textit{uniformly in } K.$$

In other words,

$$\lim_{\rho \uparrow +\infty} \frac{\theta_{[\mathfrak{L}_k+V,\rho,\xi]}}{\rho} = \xi^{-1} \quad \textit{uniformly in } K.$$

6.2 Linearized stability of the semitrivial positive solutions

This section analyzes the linearized stability of the semitrivial positive solutions of (6.5), which are given by $(\theta_{[\mathfrak{L}_1,\lambda,a]},0)$ if $\lambda>\sigma_{0,1}$, and $(0,\theta_{[\mathfrak{L}_2,\mu,d]})$ if $\mu>\sigma_{0,2}$. Their linearized stabilities provide us with their local attractive, or repulsive, characters as positive steady-state solutions of the associated parabolic model

$$\begin{cases} \partial_t u+\mathfrak{L}_1 u=\lambda u-a(x)u^2-b(x)\dfrac{uv}{1+m(x)u} & x\in\Omega,\quad t>0,\\ \partial_t v+\mathfrak{L}_2 v=\mu v+c(x)\dfrac{uv}{1+m(x)u}-d(x)v^2 & x\in\Omega,\quad t>0,\\ \mathfrak{B}_1 u=\mathfrak{B}_2 v=0 & x\in\partial\Omega,\quad t>0,\\ u(\cdot,0)=u_0\geq 0,\quad v(\cdot,0)=v_0\geq 0, \end{cases} \tag{6.12}$$

where u_0 and v_0 are the initial distributions in the inhabiting area Ω of the species u and v. The next result provides us with the linearized stability of $(\theta_{[\mathfrak{L}_1,\lambda,a]},0)$.

Theorem 6.2.1. *Suppose $\lambda>\sigma_{0,1}$. Then, the semitrivial positive solution $(\theta_{[\mathfrak{L}_1,\lambda,a]},0)$ is linearly unstable (l.u.) if, and only if,*

$$\mu>\sigma_0\Big[\mathfrak{L}_2-c\frac{\theta_{[\mathfrak{L}_1,\lambda,a]}}{1+m\theta_{[\mathfrak{L}_1,\lambda,a]}},\mathfrak{B}_2,\Omega\Big], \tag{6.13}$$

while it is linearly stable (l.s.) if, and only if,

$$\mu<\sigma_0\Big[\mathfrak{L}_2-c\frac{\theta_{[\mathfrak{L}_1,\lambda,a]}}{1+m\theta_{[\mathfrak{L}_1,\lambda,a]}},\mathfrak{B}_2,\Omega\Big]. \tag{6.14}$$

Therefore, the curve

$$\mu=\Psi(\lambda)\equiv\sigma_0\Big[\mathfrak{L}_2-c\frac{\theta_{[\mathfrak{L}_1,\lambda,a]}}{1+m\theta_{[\mathfrak{L}_1,\lambda,a]}},\mathfrak{B}_2,\Omega\Big],\qquad \lambda>\sigma_{0,1}, \tag{6.15}$$

provides us with the curve of change of stability of $(\theta_{[\mathfrak{L}_1,\lambda,a]},0)$, i.e., it is the curve of neutral stability of $(\theta_{[\mathfrak{L}_1,\lambda,a]},0)$.

Proof. The linearized stability of $(\theta_{[\mathfrak{L}_1,\lambda,a]},0)$ is determined by the signs of the eigenvalues of the linearization of (6.5) at $(\theta_{[\mathfrak{L}_1,\lambda,a]},0)$, i.e., by the signs of the τ's for which the eigenvalue problem

$$\begin{cases} \mathfrak{L}_1 u=\lambda u-2a\theta_{[\mathfrak{L}_1,\lambda,a]}u-b\frac{\theta_{[\mathfrak{L}_1,\lambda,a]}}{1+m\theta_{[\mathfrak{L}_1,\lambda,a]}}v+\tau u & \text{in }\ \Omega,\\ \mathfrak{L}_2 v=\mu v+c\frac{\theta_{[\mathfrak{L}_1,\lambda,a]}}{1+m\theta_{[\mathfrak{L}_1,\lambda,a]}}v+\tau v & \text{in }\ \Omega,\\ \mathfrak{B}_1 u=\mathfrak{B}_2 v=0 & \text{on }\ \partial\Omega. \end{cases} \tag{6.16}$$

admits a nontrivial eigenfunction, (u,v). First, we will look for eigenvalues with $v=0$. Those are given by the values of τ for which the eigenvalue problem

$$\begin{cases} \mathfrak{L}_1 u = \lambda u - 2a\theta_{[\mathfrak{L}_1,\lambda,a]}u + \tau u & \text{in } \Omega, \\ \mathfrak{B}_1 u = 0 & \text{on } \partial\Omega, \end{cases} \tag{6.17}$$

admits a solution $u \neq 0$. Since, by definition,

$$\begin{cases} \mathfrak{L}_1 \theta_{[\mathfrak{L}_1,\lambda,a]} = \lambda\theta_{[\mathfrak{L}_1,\lambda,a]} - a\theta^2_{[\mathfrak{L}_1,\lambda,a]} & \text{in } \Omega, \\ \mathfrak{B}_1 \theta_{[\mathfrak{L}_1,\lambda,a]} = 0 & \text{on } \partial\Omega, \end{cases}$$

it becomes apparent that

$$\left(\mathfrak{L}_1 + a\theta_{[\mathfrak{L}_1,\lambda,a]}\right)\theta_{[\mathfrak{L}_1,\lambda,a]} = \lambda\theta_{[\mathfrak{L}_1,\lambda,a]}$$

and hence, by the uniqueness of the principal eigenvalue (see, e.g., [124, Ch. 7]),

$$\lambda = \sigma_0[\mathfrak{L}_1 + a\theta_{[\mathfrak{L}_1,\lambda,a]}, \mathfrak{B}_1, \Omega].$$

Thus, by Theorem 6.1.1,

$$\sigma_0[\mathfrak{L}_1 + 2a\theta_{[\mathfrak{L}_1,\lambda,a]} - \lambda, \mathfrak{B}_1, \Omega] > \sigma_0[\mathfrak{L}_1 + a\theta_{[\mathfrak{L}_1,\lambda,a]} - \lambda, \mathfrak{B}_1, \Omega] = 0. \tag{6.18}$$

Consequently, since the principal eigenvalue is dominant, it becomes apparent that all the eigenvalues, τ, of (6.17) have a positive real part. So, they provide us with eigenfunctions on the stable manifold of the steady state solution $(\theta_{[\mathfrak{L}_1,\lambda,a]}, 0)$. Next, we will look for eigenfunctions of (6.16), (u,v), with $v \neq 0$. Since $v \neq 0$ satisfies

$$\begin{cases} \mathfrak{L}_2 v = \mu v + c\frac{\theta_{[\mathfrak{L}_1,\lambda,a]}}{1+m\theta_{[\mathfrak{L}_1,\lambda,a]}}v + \tau v & \text{in } \Omega, \\ \mathfrak{B}_2 v = 0 & \text{on } \partial\Omega, \end{cases} \tag{6.19}$$

τ must be an eigenvalue of the differential operator

$$\mathfrak{L}_2 - c\frac{\theta_{[\mathfrak{L}_1,\lambda,a]}}{1+m\theta_{[\mathfrak{L}_1,\lambda,a]}} - \mu$$

in Ω subject to the boundary operator $\mathfrak{B}_2$ on $\partial\Omega$. By the dominance of the principal eigenvalue, all these eigenvalues are positive if (6.14) holds. Thus, $(\theta_{[\mathfrak{L}_1,\lambda,a]}, 0)$ is linearly stable under condition (6.14).

Now, suppose (6.13). Then,

$$\tau := \sigma_0\left[\mathfrak{L}_2 - c\frac{\theta_{[\mathfrak{L}_1,\lambda,a]}}{1+m\theta_{[\mathfrak{L}_1,\lambda,a]}} - \mu, \mathfrak{B}_2, \Omega\right] < 0$$

provides us with a negative eigenvalue of (6.19) and, for this choice, the first equation of (6.16) can be equivalently expressed as

$$\begin{cases} \left(\mathfrak{L}_1 + 2a\theta_{[\mathfrak{L}_1,\lambda,a]} - \lambda - \tau\right) u = -b\frac{\theta_{[\mathfrak{L}_1,\lambda,a]}}{1+m\theta_{[\mathfrak{L}_1,\lambda,a]}} v & \text{in } \Omega, \\ \mathfrak{B}_1 u = 0 & \text{on } \partial\Omega. \end{cases} \tag{6.20}$$

As $\tau < 0$, it follows from (6.18) that also

$$\sigma_0 \left[\mathfrak{L}_1 + 2a\theta_{[\mathfrak{L}_1,\lambda,a]} - \lambda - \tau, \mathfrak{B}_1, \Omega\right] > 0.$$

Thus, it follows from (6.20) that

$$u = -\left(\mathfrak{L}_1 + 2a\theta_{[\mathfrak{L}_1,\lambda,a]} - \lambda - \tau\right)^{-1} \left(b\frac{\theta_{[\mathfrak{L}_1,\lambda,a]}}{1 + m\theta_{[\mathfrak{L}_1,\lambda,a]}} v\right).$$

Therefore, (6.16) possesses a negative eigenvalue under (6.13). Hence, the semitrivial solution $(\theta_{[\mathfrak{L}_1,\lambda,a]}, 0)$ is linearly unstable, as claimed in the statement.

Lastly, thanks to the previous analysis, it becomes apparent that the curve (6.15) provides us with the set of values of the parameters λ and μ for which $(\theta_{[\mathfrak{L}_1,\lambda,a]}, 0)$ is linearly neutrally stable, i.e., is the curve of change of stability of this semitrivial solution. This ends the proof. □

Similarly, the next result holds.

Theorem 6.2.2. *Suppose $\mu > \sigma_{0,2}$. Then, the semitrivial solution $(0, \theta_{[\mathfrak{L}_2,\mu,d]})$ is linearly unstable (l.u.) if, and only if,*

$$\lambda > \sigma_0 \left[\mathfrak{L}_1 + b\theta_{[\mathfrak{L}_2,\mu,d]}, \mathfrak{B}_1, \Omega\right], \tag{6.21}$$

while it is linearly stable (l.s.) if, and only if,

$$\lambda < \sigma_0 \left[\mathfrak{L}_1 + b\theta_{[\mathfrak{L}_2,\mu,d]}, \mathfrak{B}_1, \Omega\right]. \tag{6.22}$$

Therefore, the curve

$$\lambda = \Phi(\mu) \equiv \sigma_0 \left[\mathfrak{L}_1 + b\theta_{[\mathfrak{L}_2,\mu,d]}, \mathfrak{B}_1, \Omega\right], \quad \mu > \sigma_{0,2}, \tag{6.23}$$

provides us with the curve of change of stability of $(0, \theta_{[\mathfrak{L}_2,\mu,d]})$.

Proof. The linearized stability of $(0, \theta_{[\mathfrak{L}_2,\mu,d]})$ is determined by the signs of the τ's for which the eigenvalue problem

$$\begin{cases} \mathfrak{L}_1 u = \lambda u - b\theta_{[\mathfrak{L}_2,\mu,d]} u + \tau u & \text{in } \Omega, \\ \mathfrak{L}_2 v = \mu v - 2d\theta_{[\mathfrak{L}_2,\mu,d]} v + c\theta_{[\mathfrak{L}_2,\mu,d]} u + \tau v & \text{in } \Omega, \\ \mathfrak{B}_1 u = \mathfrak{B}_2 v = 0 & \text{on } \partial\Omega. \end{cases}$$

which can be equivalently written as

$$\begin{cases} \left(\mathfrak{L}_1 + b\theta_{[\mathfrak{L}_2,\mu,d]} - \lambda\right) u = \tau u & \text{in } \Omega, \\ \left(\mathfrak{L}_2 + 2d\theta_{[\mathfrak{L}_2,\mu,d]} - \mu\right) v = c\theta_{[\mathfrak{L}_2,\mu,d]} u + \tau v & \text{in } \Omega, \\ \mathfrak{B}_1 u = \mathfrak{B}_2 v = 0 & \text{on } \partial\Omega. \end{cases} \tag{6.24}$$

As in the proof of Theorem 6.2.1, we first search for eigenvalues with $u = 0$. Those are given by the values of τ for which the eigenvalue problem

$$\begin{cases} \left(\mathfrak{L}_2 + 2d\theta_{[\mathfrak{L}_2,\mu,d]} - \mu\right) v = \tau v & \text{in } \Omega, \\ \mathfrak{B}_2 v = 0 & \text{on } \partial\Omega, \end{cases} \tag{6.25}$$

admits a solution $v \neq 0$. Arguing as in the proof of Theorem 6.2.1, it becomes apparent that

$$\sigma_0[\mathfrak{L}_2 + 2d\theta_{[\mathfrak{L}_2,\mu,d]} - \mu, \mathfrak{B}_2, \Omega] > \sigma_0[\mathfrak{L}_2 + d\theta_{[\mathfrak{L}_2,\mu,d]} - \mu, \mathfrak{B}_2, \Omega] = 0.$$

Thus, since the principal eigenvalue is dominant, all eigenvalues of (6.25) have positive real part. So, these eigenvalues cannot destabilize $(0, \theta_{[\mathfrak{L}_2,\mu,d]})$. Now, we will focus attention on the eigenvalues τ with $u \neq 0$. Those are given by the eigenvalues of the problem

$$\begin{cases} \left(\mathfrak{L}_1 + b\theta_{[\mathfrak{L}_2,\mu,d]} - \lambda\right) u = \tau u & \text{in } \Omega, \\ \mathfrak{B}_1 u = 0 & \text{on } \partial\Omega. \end{cases} \tag{6.26}$$

Suppose (6.22) holds. Then,

$$\sigma_0\left[\mathfrak{L}_1 + b\theta_{[\mathfrak{L}_2,\mu,d]} - \lambda, \mathfrak{B}_1, \Omega\right] > 0$$

and hence, since the principal eigenvalue is dominant, any other eigenvalue of (6.26), τ, has a positive real part. Thus, $(0, \theta_{[\mathfrak{L}_2,\mu,d]})$ is linearly stable.

Now, suppose (6.21). Then,

$$\tau := \sigma_0\left[\mathfrak{L}_1 + b\theta_{[\mathfrak{L}_2,\mu,d]} - \lambda, \mathfrak{B}_1, \Omega\right] < 0$$

provides us with a negative eigenvalue of (6.26) and the second equation of (6.24) can be equivalently expressed as

$$\left(\mathfrak{L}_2 + 2d\theta_{[\mathfrak{L}_2,\mu,d]} - \mu - \tau\right) v = c\theta_{[\mathfrak{L}_2,\mu,d]} u.$$

Thus, since

$$\sigma_0[\mathfrak{L}_2 + 2d\theta_{[\mathfrak{L}_2,\mu,d]} - \mu - \tau, \mathfrak{B}_2, \Omega] > \sigma_0[\mathfrak{L}_2 + d\theta_{[\mathfrak{L}_2,\mu,d]} - \mu, \mathfrak{B}_2, \Omega] = 0,$$

we find that

$$v = \left(\mathfrak{L}_2 + 2d\theta_{[\mathfrak{L}_2,\mu,d]} - \mu - \tau\right)^{-1} \left(c\theta_{[\mathfrak{L}_2,\mu,d]}u\right)$$

and therefore, (6.24) possesses a negative eigenvalue. Consequently, $(0, \theta_{[\mathfrak{L}_2,\mu,d]})$ is linearly unstable. This ends the proof. □

Subsequently, we will consider the curves of change of stability of the semitrivial solutions, $\lambda = \Phi(\mu)$ and $\mu = \Psi(\lambda)$, introduced in (6.23) and (6.15). As, according to Lemma 6.1.4, the map $\mu \mapsto \theta_{[\mathfrak{L}_2,\mu,d]}$ is increasing, it follows from Theorem 6.1.1 that $\Phi(\mu)$ is strictly increasing with respect to μ. Moreover, thanks to Theorem 6.1.6, it is easily seen that

$$\lim_{\mu\uparrow\infty} \Phi(\mu) = \lim_{\mu\uparrow\infty} \sigma_0 \left[\mathfrak{L}_1 + \mu b \frac{\theta_{[\mathfrak{L}_2,\mu,d]}}{\mu}, \mathfrak{B}_1, \Omega\right] = \infty,$$

because $\frac{b(x)}{d(x)} > 0$ for all $x \in \bar{\Omega}$. Moreover, owing to Theorems 6.1.3 and 6.1.1,

$$\lim_{\mu\downarrow\sigma_{0,2}} \Phi(\mu) = \sigma_{0,1}.$$

Therefore, the curve of change of stability of $(0, \theta_{[\mathfrak{L}_2,\mu,d]})$, $\lambda = \Phi(\mu)$, passes through the point $(\sigma_{0,1}, \sigma_{0,2})$, it is increasing with respect to μ and

$$\lim_{\mu\uparrow\infty} \Phi(\mu) = \infty.$$

In particular, for every $\lambda > \sigma_{0,1}$ there exists a unique $\mu > \sigma_{0,2}$ such that $\lambda = \Phi(\mu)$. Similarly,

$$\lim_{\lambda\downarrow\sigma_{0,1}} \Psi(\lambda) = \sigma_{0,2}$$

and hence, the curve $\mu = \Psi(\lambda)$ also passes through $(\sigma_{0,1}, \sigma_{0,2})$. Moreover, since the mappings $\lambda \mapsto \theta_{[\mathfrak{L}_1,\lambda,a]}$ and $\zeta \mapsto \frac{\zeta}{1+m\zeta}$ are increasing, Theorem 6.1.1 reveals that $\Psi(\lambda)$ is strictly decreasing with respect to λ. Furthermore,

$$\Psi(\lambda) < \sigma_{0,2} \quad \text{for all} \quad \lambda > \sigma_{0,1}.$$

As far as concerns the behavior of $\Psi(\lambda)$ for $\lambda \uparrow \infty$, we will differentiate two rather different situations.

Case 1. Suppose that

$$\operatorname{Int} m^{-1}(0) \neq \emptyset.$$

Then, there exist $x_0 \in \Omega$ and $R > 0$ such that $\bar{B}_R(x_0) \subset \Omega$ and $m \equiv 0$ in $B_R(x_0)$. Thus, by Proposition 3.2 of S. Cano-Casanova and J. López-Gómez [28],

$$\Psi(\lambda) = \sigma_0\left[\mathfrak{L}_2 - c\frac{\theta_{[\mathfrak{L}_1,\lambda,a]}}{1+m\theta_{[\mathfrak{L}_1,\lambda,a]}}, \mathfrak{B}_2, \Omega\right] < \sigma_0\left[\mathfrak{L}_2 - c\frac{\theta_{[\mathfrak{L}_1,\lambda,a]}}{1+m\theta_{[\mathfrak{L}_1,\lambda,a]}}, \mathfrak{D}, B_R(x_0)\right].$$

Hence, since $m = 0$ on $B_R(x_0)$,

$$\Psi(\lambda) < \sigma_0\Big[\mathfrak{L}_2 - c\theta_{[\mathfrak{L}_1,\lambda,a]}, \mathfrak{D}, B_R(x_0)\Big] \quad \text{for all} \quad \lambda > \sigma_{0,1}.$$

On the other hand, thanks to Theorem 6.1.6,

$$\lim_{\lambda\uparrow\infty} \frac{\theta_{[\mathfrak{L}_1,\lambda,a]}}{\lambda} = a^{-1} \quad \text{uniformly in} \quad \bar{B}_R(x_0).$$

Therefore, much like in the classical Lotka–Volterra model ($m \equiv 0$),

$$\lim_{\lambda\uparrow\infty} \Psi(\lambda) = -\infty.$$

Case 2. Suppose that $m(x) > 0$ for all $x \in \bar{\Omega}$. Then, much like in the classical Holling–Tanner models with $m > 0$ constant, we may infer from Theorem 6.1.6 that

$$\begin{aligned}\lim_{\lambda\uparrow\infty} \Psi(\lambda) &= \lim_{\lambda\uparrow\infty} \sigma_0\Big[\mathfrak{L}_2 - c\frac{\theta_{[\mathfrak{L}_1,\lambda,a]}}{1 + m\theta_{[\mathfrak{L}_1,\lambda,a]}}, \mathfrak{B}_2, \Omega\Big] \\ &= \lim_{\lambda\uparrow\infty} \sigma_0\Big[\mathfrak{L}_2 - c\frac{\frac{\theta_{[\mathfrak{L}_1,\lambda,a]}}{\lambda}}{\frac{1}{\lambda} + m\frac{\theta_{[\mathfrak{L}_1,\lambda,a]}}{\lambda}}, \mathfrak{B}_2, \Omega\Big] = \sigma_0\Big[\mathfrak{L}_2 - \frac{c}{m}, \mathfrak{B}_2, \Omega\Big],\end{aligned}$$

in strong contrast with the previous case.

Figure 6.1 represents the curves $\mu = \Psi(\lambda)$ and $\lambda = \Phi(\mu)$ in Case 1. The curve $\mu = \Psi(\lambda)$ divides the half-plane $\lambda > \sigma_{0,1}$ into two regions. The solution $(\theta_{[\mathfrak{L}_1,\lambda,a]}, 0)$ is linearly asymptotically stable if $\mu < \Psi(\lambda)$, whereas it is linearly unstable if $\mu > \Psi(\lambda)$. Similarly, the curve $\lambda = \Phi(\mu)$ divides the half-plane $\mu > \sigma_{0,2}$ into two regions. The solution $(0, \theta_{[\mathfrak{L}_2,\mu,d]})$ is linearly stable if $\lambda < \Phi(\mu)$, while it is linearly unstable if $\lambda > \Phi(\mu)$. In particular, the region enclosed by these curves,

$$\mu > \Psi(\lambda), \qquad \lambda > \Phi(\mu), \tag{6.27}$$

which is the shadowed green region in Figure 6.1, is the region where any of the semitrivial positive solutions of (6.5) is linearly unstable. By the Lyapunov theorems, the semitrivial positive solutions are unstable in this region.

Figure 6.2 shows the stability of the trivial solution, $(0, 0)$ according to the each of the quadrants of the (λ, μ) plane centered at the point $(\sigma_{0,1}, \sigma_{0,2})$. At the light of the proofs of Theorems 6.2.1 and 6.2.2, checking these properties is straightforward. So, the technical details are omitted here.

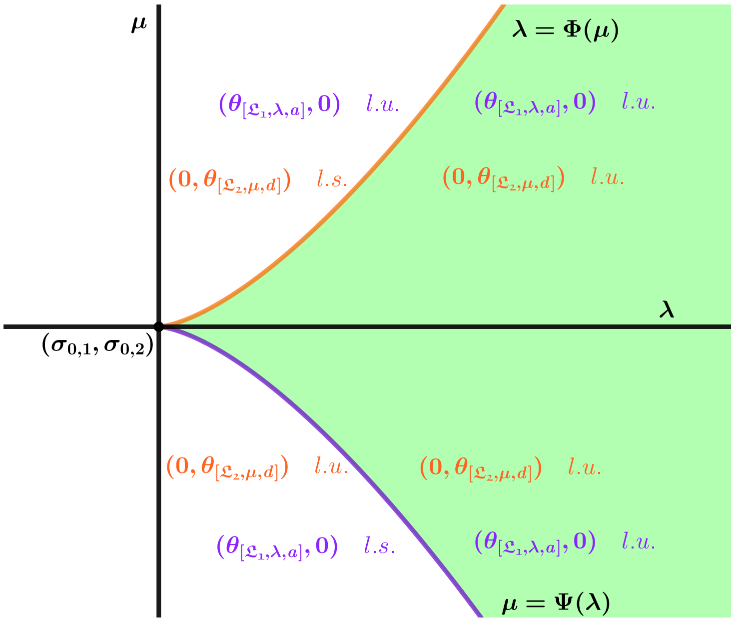

Figure 6.1: Stability of the semitrivial solutions

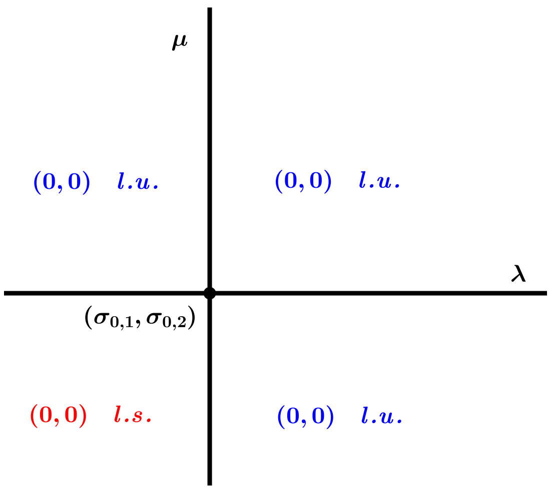

Figure 6.2: Stability of $(0, 0)$

6.3 Necessary conditions for the existence of coexistence states

The main result of this section establishes some necessary conditions for the existence of a coexistence state for (6.5). A coexistence state is a solution (u, v) with $u \gneq 0$ and $v \gneq 0$. These conditions are optimal in a sense to be precised later.

Theorem 6.3.1. *Suppose that* (6.5) *has a coexistence state,* (u, v)*. Then,* $u \gg_1 0$*,* $v \gg_2 0$*, and*

$$\lambda = \sigma_0 \left[\mathfrak{L}_1 + au + b\tfrac{v}{1+mu}, \mathfrak{B}_1, \Omega \right], \tag{6.28}$$

$$\mu = \sigma_0 \left[\mathfrak{L}_2 + dv - c\tfrac{u}{1+mu}, \mathfrak{B}_2, \Omega \right]. \tag{6.29}$$

Thus,

$$\lambda > \sigma_0 \left[\mathfrak{L}_1 + b\tfrac{\theta_{[\mathfrak{L}_2,\mu,d]}}{1+m\theta_{[\mathfrak{L}_1,\lambda,a]}}, \mathfrak{B}_1, \Omega \right], \ \mu > \sigma_0 \left[\mathfrak{L}_2 - c\tfrac{\theta_{[\mathfrak{L}_1,\lambda,a]}}{1+m\theta_{[\mathfrak{L}_1,\lambda,a]}}, \mathfrak{B}_2, \Omega \right]. \tag{6.30}$$

Proof. Let (u, v) be a coexistence state of (6.5). Then,

$$\begin{cases} \left(\mathfrak{L}_1 + au + b\dfrac{v}{1+mu} \right) u = \lambda u & \text{in } \Omega, \\ \left(\mathfrak{L}_2 + dv - c\dfrac{u}{1+mu} \right) v = \mu v & \text{in } \Omega, \\ \mathfrak{B}_1 u = \mathfrak{B}_2 v = 0 & \text{on } \partial\Omega. \end{cases}$$

Thus, thanks to the uniqueness of the principal eigenvalue, (6.28) and (6.29) hold. Moreover, since u and v are principal eigenfunctions associated to each of these principal eigenvalues, it follows from [126, Ch. 7] that $u \gg_1 0$ and $v \gg_2 0$. Hence, by the first equation of (6.5),

$$\mathfrak{L}_1 u = \lambda u - au^2 - b\frac{uv}{1+mu} \lneq \lambda u - au^2.$$

So, u is a positive strict subsolution of the problem

$$\begin{cases} \mathfrak{L}_1 w = \lambda w - a(x)w^2 & \text{in } \Omega, \\ \mathfrak{B}_1 w = 0 & \text{on } \partial\Omega. \end{cases} \tag{6.31}$$

To show the existence of large supersolutions of (6.31) we will use a technical device borrowed from D. Aleja et al. [5]. Since Ω is of class $\mathcal{C}^2$, by [126, Lem. 2.1], there exist $\psi \in \mathcal{C}^2(\bar{\Omega})$ and $\gamma > 0$ such that

$$\frac{\partial \psi}{\partial \nu}(x) \geq \gamma > 0 \ \text{ for all } \ x \in \Gamma_1. \tag{6.32}$$

We claim that, for sufficiently large $C > 0$ and $M > 0$, the function

$$\bar{u}(x) := Ce^{M\psi(x)}, \qquad x \in \bar{\Omega},$$

is a supersolution of (6.31). Indeed, for every $M > 0$ and $C > 0$, $\bar{u} > 0$ on Γ_0. Moreover, for every $x \in \Gamma_1$,

$$\frac{\partial \bar{u}}{\partial \nu_1}(x) = CM\frac{\partial \psi}{\partial \nu_1}(x)e^{M\psi(x)} + C\beta_1(x)e^{M\psi(x)} = Ce^{M\psi(x)}\left(M\frac{\partial \psi}{\partial \nu_1}(x) + \beta_1(x)\right).$$

So, thanks to (6.32),

$$\frac{\partial \bar{u}}{\partial \nu_1}(x) \geq Ce^{M\psi(x)}\left(M\gamma + \beta_1(x)\right) > 0$$

for sufficiently large $M > 0$. Therefore,

$$\mathfrak{B}_1\bar{u} \gneq 0 \qquad \text{on } \partial\Omega$$

for every $C > 0$ and sufficiently large $M > 0$. On the other hand, once fixed one of these M's, it is easily seen that

$$\mathfrak{L}_1\bar{u} = C\mathfrak{L}_1 e^{M\psi} \geq \lambda Ce^{M\psi} - a(x)C^2e^{2M\psi}$$

if, and only if,

$$e^{-M\psi}\mathfrak{L}_1 e^{M\psi} \geq \lambda - a(x)Ce^{M\psi}$$

which holds true for sufficiently large $C > 0$, because $a(x) > 0$ and $e^{M\psi(x)} > 0$ for all $x \in \bar{\Omega}$. Consequently, $\bar{u}$ provides us with a positive strict supersolution of (6.31) for sufficiently large $C > 0$ and $M > 0$.

Enlarging C, if necessary, we also can get the estimate $u \leq \bar{u}$. Thus, (6.31) admits a positive solution, w_λ, such that

$$u \leq w_\lambda \leq \bar{u}.$$

By Theorem 6.1.3, $w_\lambda = \theta_{[\mathfrak{L}_1,\lambda,a]} \gg_1 0$ and $\lambda > \sigma_{0,1}$. So, due to Lemma 6.1.4,

$$u \ll_1 \theta_{[\mathfrak{L}_1,\lambda,a]} \ll_1 \bar{u} \tag{6.33}$$

as soon as $\bar{u}$ is a strict supersolution of (6.31).

Going back to the second equation of (6.5), we also have that

$$\mathfrak{L}_2 v = \mu v - dv^2 + c\frac{uv}{1+mu} \gneq \mu v - dv^2$$

and hence, v is a positive strict supersolution of

$$\begin{cases} \mathfrak{L}_2 w = \mu w - d(x)w^2 & \text{in } \Omega, \\ \mathfrak{B}_2 w = 0 & \text{on } \partial\Omega. \end{cases} \tag{6.34}$$

Suppose $\mu \leq \sigma_{0,2}$. Then, $\theta_{[\mathfrak{L}_2,\mu,d]} = 0$ and hence the next estimate holds

$$v \gg_1 \theta_{[\mathfrak{L}_2,\mu,d]}. \tag{6.35}$$

Now, suppose that $\mu > \sigma_{0,2}$. Then, $\theta_{[\mathfrak{L}_2,\mu,d]} \gg_2 0$ is the unique positive solution of (6.34) and (6.35) holds from Lemma 6.1.4. Thus, going back to the first equation of (6.5) and using (6.33) and (6.35), it becomes apparent that

$$\mathfrak{L}_1 u = \lambda u - au^2 - b\frac{uv}{1+mu} \lneq \lambda u - au^2 - b\frac{\theta_{[\mathfrak{L}_2,\mu,d]}}{1+m\theta_{[\mathfrak{L}_1,\lambda,a]}}u.$$

Thus, u is a positive strict subsolution of the problem

$$\begin{cases} \left(\mathfrak{L}_1 + b\frac{\theta_{[\mathfrak{L}_2,\mu,d]}}{1+m\theta_{[\mathfrak{L}_1,\lambda,a]}}\right) w = \lambda w - aw^2 & \text{in } \Omega, \\ \mathfrak{B}_1 w = 0 & \text{on } \partial\Omega. \end{cases} \tag{6.36}$$

Arguing as above, it is easily seen that $\bar{u} := Ce^{M\psi}$ also provides us with a supersolution of (6.36) for sufficiently large $M > 0$ and $C > 0$. Therefore, the problem (6.36) admits a positive solution in the interval $[u, \bar{u}]$. Consequently, by Theorem 6.1.3,

$$\lambda > \sigma_0\left[\mathfrak{L}_1 + b\frac{\theta_{[\mathfrak{L}_2,\mu,d]}}{1+m\theta_{[\mathfrak{L}_1,\lambda,a]}}, \mathfrak{B}_1, \Omega\right],$$

which provides us with the first estimate of (6.30). Moreover, by Lemma 6.1.4,

$$0 \ll_1 u \ll_1 \theta_{\left[\mathfrak{L}_1 + b\frac{\theta_{[\mathfrak{L}_2,\mu,d]}}{1+m\theta_{[\mathfrak{L}_1,\lambda,a]}},\lambda,a\right]} \ll_1 Ce^{M\psi}. \tag{6.37}$$

Finally, since the mapping $u \mapsto \frac{u}{1+mu}$ is increasing, we can infer from (6.33) that

$$\mathfrak{L}_2 v = \mu v - dv^2 + c\frac{uv}{1+mu} < \mu v - dv^2 + c\frac{\theta_{[\mathfrak{L}_1,\lambda,a]}}{1+m\theta_{[\mathfrak{L}_1,\lambda,a]}}v.$$

Thus, v provides us with a positive strict subsolution of

$$\begin{cases} \left(\mathfrak{L}_2 - c\frac{\theta_{[\mathfrak{L}_1,\lambda,a]}}{1+m\theta_{[\mathfrak{L}_1,\lambda,a]}}\right) w = \mu w - dw^2 & \text{in } \Omega, \\ \mathfrak{B}_2 w = 0 & \text{on } \partial\Omega. \end{cases} \tag{6.38}$$

Since (6.38) admits strict supersolutions of the form $Ce^{M\psi}$ for sufficiently large $M>0$ and $C>0$, it becomes apparent that

$$\mu > \sigma_0\Big[\mathfrak{L}_2 - c\frac{\theta_{[\mathfrak{L}_1,\lambda,a]}}{1+m\theta_{[\mathfrak{L}_1,\lambda,a]}}, \mathfrak{B}_2, \Omega\Big].$$

Moreover, according to Lemma 6.1.4,

$$v \ll_2 \theta_{\Big[\mathfrak{L}_2 - c\frac{\theta_{[\mathfrak{L}_1,\lambda,a]}}{1+m\theta_{[\mathfrak{L}_1,\lambda,a]}},\mu,d\Big]}. \tag{6.39}$$

This ends the proof. □

6.4 Sufficient conditions for the existence of coexistence states

Our main existence theorem can be stated as follows.

Theorem 6.4.1. *Suppose (6.27) holds, i.e.,*

$$\begin{aligned} &\lambda > \Phi(\mu) \equiv \sigma_0[\mathfrak{L}_1 + b\theta_{[\mathfrak{L}_2,\mu,d]}, \mathfrak{B}_1, \Omega], \\ &\mu > \Psi(\lambda) \equiv \sigma_0\Big[\mathfrak{L}_2 - c\frac{\theta_{[\mathfrak{L}_1,\lambda,a]}}{1+m\theta_{[\mathfrak{L}_1,\lambda,a]}}, \mathfrak{B}_2, \Omega\Big]. \end{aligned} \tag{6.40}$$

Then, (6.5) has, at least, one coexistence state. Moreover, when $\mu \le \sigma_{0,2}$, by definition, $\theta_{[\mathfrak{L}_2,\mu,d]} = 0$ and hence, (6.40) becomes

$$\lambda > \sigma_{0,1}, \qquad \mu > \sigma_0\Big[\mathfrak{L}_2 - c\frac{\theta_{[\mathfrak{L}_1,\lambda,a]}}{1+m\theta_{[\mathfrak{L}_1,\lambda,a]}}, \mathfrak{B}_2, \Omega\Big]. \tag{6.41}$$

In such case, (6.41) is not only sufficient but also necessary for the existence of a coexistence state.

In other words, according to Theorems 6.2.1 and 6.2.2, (6.5) admits a coexistence state if any of the existing semitrivial positive solutions is linearly unstable.

Proof. By fixing $\lambda > 0$ and regarding μ as the main bifurcation parameter the proof is a direct application of [124, Th. 7.2.2]. Indeed, since $(\theta_{[\mathfrak{L}_1,\lambda,a]}, 0)$ is a nondegenerate solution of

$$\begin{cases} \mathfrak{L}_1 u = \lambda u - a(x)u^2 & \text{in } \Omega, \\ \mathfrak{B}_1 u = 0 & \text{on } \partial\Omega, \end{cases} \tag{6.42}$$

by [124, Th. 7.2.2] there exists a continuum of coexistence states, $\mathfrak{C}$, in $\mathbb{R} \times U_1 \times U_2$ emanating from

$$(\mu, u, v) = (\Phi(\lambda), \theta_{[\mathfrak{L}_1,\lambda,a]}, 0)$$

such that either

(i) $\mathfrak{C}$ is unbounded in $\mathbb{R} \times \mathcal{C}(\bar{\Omega}) \times \mathcal{C}(\bar{\Omega})$; or

(ii) there exists a positive solution, $(\mu^*, \theta_{[\mathfrak{L}_2,\mu^*,d]})$ of

$$\begin{cases} \mathfrak{L}_2 v = \mu v - d(x)v^2 & \text{in } \Omega, \\ \mathfrak{B}_2 v = 0 & \text{on } \partial\Omega, \end{cases} \tag{6.43}$$

such that $(\mu^*, 0, \theta_{[\mathfrak{L}_2,\mu^*,d]}) \in \bar{\mathfrak{C}}$.

Obviously, since (6.42) admits at most a unique positive solution, Alternative 3 of [124, Th. 7.2.2] cannot happen. Similarly, as we are assuming that $\lambda > \sigma_{0,1}$, Alternative 4 of [124, Th. 7.2.2] cannot occur neither. Subsequently, $\mathcal{P}_\mu$ stands for the μ-projection operator, $\mathcal{P}_\mu(\mu, u, v) = \mu$. Thanks to the estimates (6.37) and (6.39), it becomes apparent that $\mathcal{P}_\mu(\mathfrak{C})$ should be unbounded if Alternative (i) holds. On the other hand, by Theorem 6.3.1, (6.30) holds if (6.5) admits a coexistence state. Thus, $\mathcal{P}_\mu(\mathfrak{C})$ is bounded. Therefore, Alternative (ii) holds. To make sure that indeed $\mathcal{P}_\mu(\mathfrak{C})$ is bounded we can argue as follows. The second estimate of (6.30) shows that μ must be bounded below. The first one provides us with an upper bound for μ, because

$$\lim_{\mu\uparrow\infty} \sigma_0[\mathfrak{L}_1 + b\frac{\theta_{[\mathfrak{L}_2,\mu,d]}}{1 + m\theta_{[\mathfrak{L}_1,\lambda,a]}}, \mathfrak{B}_1, \Omega] = \infty. \tag{6.44}$$

Note that (6.44) relies on the fact that, thanks to Theorem 6.1.6,

$$\lim_{\mu\uparrow\infty} \theta_{[\mathfrak{L}_2,\mu,d,\Omega]} = \infty \tag{6.45}$$

uniformly on compact subsets of Ω.

The fact that $(\mu^*, 0, \theta_{[\mathfrak{L}_2,\mu^*,d]}) \in \bar{\mathfrak{C}}$ entails

$$\lambda = \sigma_0[\mathfrak{L}_1 + b\theta_{[\mathfrak{L}_2,\mu^*,d]}, \mathfrak{B}_1, \Omega].$$

Therefore, the continuum of coexistence states $\mathfrak{C}$ bifurcates from $(\theta_{[\mathfrak{L}_1,\lambda,a]}, 0)$ at

$$\mu = \Phi(\lambda) \equiv \sigma_0\left[\mathfrak{L}_2 - c\frac{\theta_{[\mathfrak{L}_1,\lambda,a]}}{1 + m\theta_{[\mathfrak{L}_1,\lambda,a]}}, \mathfrak{B}_2, \Omega\right] < \sigma_{0,2}$$

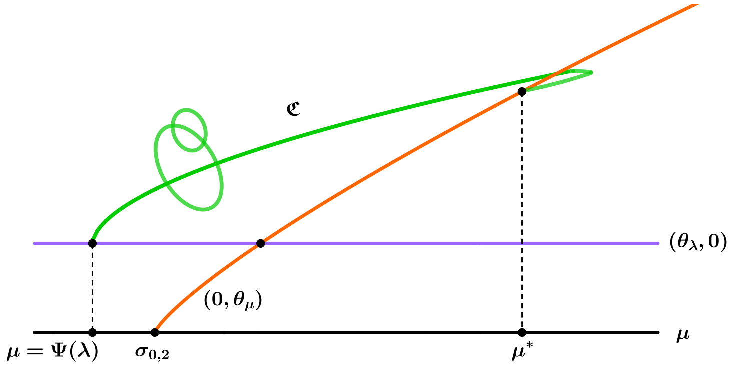

Figure 6.3: An admissible component $\mathfrak{C}$

and from $(0, \theta_{[\mathfrak{L}_2,\mu,d]})$ at $\mu^* > \sigma_{0,2}$. Figure 6.3 represents an admissible $\mathfrak{C}$.

Although we have not ascertained the bifurcation directions from the semitrivial states yet, it is apparent that (6.5) possesses a coexistence state for every $\mu \in (\Phi(\lambda), \mu^*)$, because, since $\mathcal{P}_\mu$ is continuous and $\mathfrak{C}$ is connected, the projection $\mathcal{P}_\mu(\mathfrak{C})$ is also connected. from this fact, it is easily inferred that (6.5) has a coexistence state under condition (6.40).

When $\mu \le \sigma_{0,2}$, by definition, $\theta_{[\mathfrak{L}_2,\mu,d]} = 0$. Thus, (6.40) reduces to (6.41). Combining Theorems 6.3.1 and 6.4.1 it is easily seen that (6.41) is not only sufficient but also necessary for the existence of a coexistence state. This ends the proof. □

In the example of Figure 6.3 there exists $\varepsilon > 0$ such that (6.5) admits a coexistence state for all $\mu \in [\mu^*, \mu^* + \varepsilon]$, in complete agreement with Theorem 6.3.1.

In Figure 6.4 we have represented the curve of change of stability of the semitrivial positive solutions $(0, \theta_{[\mathfrak{L}_2,\mu,d]})$, $\lambda = \Phi(\mu)$, together with the curve

$$\begin{aligned}\lambda = \varphi(\mu) &\equiv \sigma_0 \left[\mathfrak{L}_1 + b\frac{\theta_{[\mathfrak{L}_2,\mu,d]}}{1 + m\theta_{[\mathfrak{L}_1,\lambda,a]}}, \mathfrak{B}_1, \Omega\right] \\ &< \sigma_0 \left[\mathfrak{L}_1 + b\theta_{[\mathfrak{L}_2,\mu,d]}, \mathfrak{B}_1, \Omega\right] \equiv \Phi(\mu),\end{aligned}$$

and the curve of change of stability of $(\theta_{[\mathfrak{L}_1,\lambda,a]}, 0)$, $\mu = \Psi(\lambda)$, in the special case when $m(x) > 0$ for all $x \in \bar{\Omega}$. In such case, we already know that

$$\lim_{\lambda \uparrow \infty} \Psi(\lambda) = \sigma_0 \left[\mathfrak{L}_2 - \frac{c}{m}, \mathfrak{B}_2, \Omega\right].$$

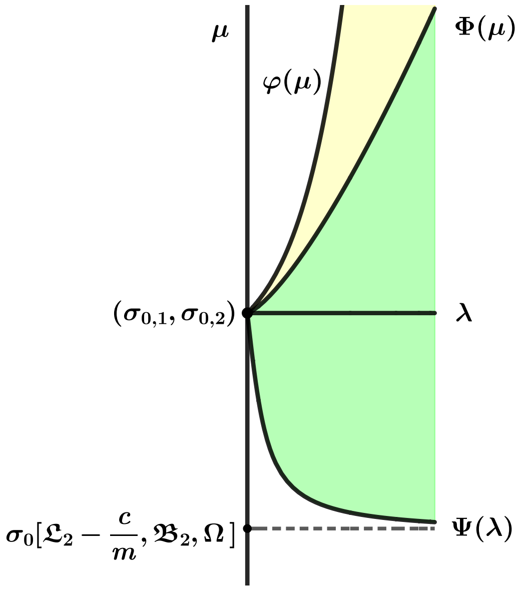

Figure 6.4: By Theorem 6.4.1, (6.5) admits a coexistence state for each (λ, μ) in the green region, while it cannot admit a coexistence state in the white one. Within the yellow region, (6.5) might admit, or not, a coexistence state as it will become apparent later.

Figure 6.5 represents the same curves in the most general case when $\operatorname{Int} m^{-1}(0) \neq \emptyset$, which should be more realistic from a biological point of view. Note that, for every $\mu \in \mathbb{R}$, there exists $\lambda > \sigma_{0,1}$ such that (6.5) possesses a coexistence region, while in the case described in Figure 6.4, the problem (6.5) cannot admit a coexistence state if

$$\mu \leq \sigma_0 \left[\mathfrak{L}_2 - \frac{c}{m}, \mathfrak{B}_2, \Omega \right].$$

6.5 Bifurcation to coexistence states from the semitrivial solutions

Throughout this section the solutions of (6.5) are viewed as zeroes of the operator

$$\mathfrak{F} : (\sigma_{0,1}, \infty) \times \mathbb{R} \times \mathcal{C}(\bar{\Omega}) \times \mathcal{C}(\bar{\Omega}) \to U_1 \times U_2,$$

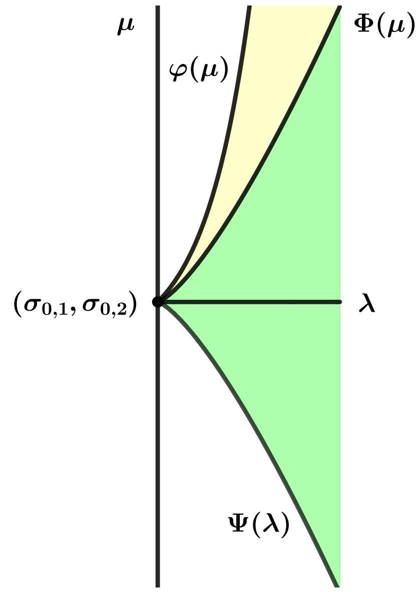

Figure 6.5: The coexistence wedges of Figure 6.4 when $\operatorname{Int} m^{-1}(0) \neq \emptyset$.

defined by

$$\mathfrak{F}(\lambda,\mu,u,v) := \begin{pmatrix} u - (\mathfrak{L}_1+\omega)^{-1}\left[(\lambda+\omega)u - au^2 - b\frac{uv}{1+mu}\right] \\ v - (\mathfrak{L}_2+\omega)^{-1}\left[(\mu+\omega)v - dv^2 + c\frac{uv}{1+mu}\right] \end{pmatrix} \tag{6.46}$$

where ω is any real number satisfying

$$\omega > \max\{-\sigma_{0,1}, -\sigma_{0,2}\},$$

and, for every $k=1,2$, $(\mathfrak{L}_k+\omega)^{-1}$ stands for the resolvent operator of $(\mathfrak{L}_k+\omega, \mathfrak{B}_k, \Omega)$. The operator $\mathfrak{F}$ is a compact perturbation of the identity map and hence it is Fredholm of index zero. Moreover, it is real analytic in an open region containing the positive cone $u \geq 0$, $v \geq 0$.

Our first result establishes the structure of the set of coexistence states in a neighborhood of the bifurcation point

$$(\mu,u,v) = \left(\Psi(\lambda), \theta_{[\mathfrak{L}_1,\lambda,a]}, 0\right)$$

for every $\lambda > \sigma_{0,1}$. As, due to Theorem 6.3.1, (6.5) cannot admit a coexistence state if $\mu < \Psi(\lambda)$, it is apparent that the bifurcation to coexistence states must be supercritical.

Theorem 6.5.1. *For every $\lambda > \sigma_{0,1}$, there exist $\varepsilon > 0$, and an analytic map*

$$(\mu, u, v) : (-\varepsilon, \varepsilon) \to \mathbb{R} \times U_1 \times U_2$$

such that

(a) $(\mu(0), u(0), v(0)) = \big(\Psi(\lambda), \theta_{[\mathfrak{L}_1,\lambda,a]}, 0\big)$.

(b) $\mathfrak{F}(\lambda, \mu(s), u(s), v(s)) = 0$ *for all* $s \in (-\varepsilon, \varepsilon)$.

(c) $u(s) > 0$ *for all* $s \in (-\varepsilon, \varepsilon)$*,* $v(s) > 0$ *for all* $s \in (0, \varepsilon)$ *and* $v(s) < 0$ *for all* $s \in (-\varepsilon, 0)$*. Thus, for every* $s \in (0, \varepsilon)$*,* $(u(s), v(s))$ *is a coexistence state of* (7.5) *for* $(\lambda, \mu) = (\lambda, \mu(s))$.

(d) *The set of solutions of* (6.5) *in a neighborhood of* $\big(\Psi(\lambda), \theta_{[\mathfrak{L}_1,\lambda,a]}, 0\big)$ *consists of the curves* $\big(\lambda, \mu, \theta_{[\mathfrak{L}_1,\lambda,a]}, 0\big)$*,* $\mu \sim \Psi(\lambda)$*, and* $(\lambda, \mu(s), u(s), v(s))$*,* $s \in (-\varepsilon, \varepsilon)$.

Moreover, $\mu'(0) > 0$*. Therefore, the bifurcation to coexistence states from* $(\theta_{[\mathfrak{L}_1,\lambda,a]},$
$0)$ *at* $\mu = \Psi(\lambda)$ *is supercritical, in complete agreement with Theorem 6.3.1.*

Proof. It is a direct consequence of the Theorem of M. G. Crandall and P. H. Rabinowitz [37] applied to the function $\mathfrak{F}$ at the semitrivial branch $\big(\mu, \theta_{[\mathfrak{L}_1,\lambda,a]}, 0\big)$. Indeed, by definition,

$$\mathfrak{F}(\lambda, \mu, \theta_{[\mathfrak{L}_1,\lambda,a]}, 0) = 0 \quad \text{for all} \quad \mu \in \mathbb{R}.$$

Moreover, the Fréchèt differential

$$\mathfrak{L}(\mu) := D_{(u,v)}\mathfrak{F}(\lambda, \mu, \theta_{[\mathfrak{L}_1,\lambda,a]}, 0)$$

is the integral operator defined by

$$\mathfrak{L}(\mu)(u, v) = \begin{pmatrix} u - (\mathfrak{L}_1 + \omega)^{-1} \left[(\lambda + \omega)u - 2a\theta_{[\mathfrak{L}_1,\lambda,a]}u - b\frac{\theta_{[\mathfrak{L}_1,\lambda,a]}}{1+m\theta_{[\mathfrak{L}_1,\lambda,a]}}v\right] \\ v - (\mathfrak{L}_2 + \omega)^{-1} \left[(\mu + \omega)v + c\frac{\theta_{[\mathfrak{L}_1,\lambda,a]}}{1+m\theta_{[\mathfrak{L}_1,\lambda,a]}}v\right] \end{pmatrix}.$$

Thus,

$$N[\mathfrak{L}(\Psi(\lambda))] = \text{span}[\varphi_0], \qquad \varphi_0 = \begin{pmatrix} u_1 \\ v_1 \end{pmatrix},$$

where

$$\begin{cases} (\mathfrak{L}_1 + 2a\theta_{[\mathfrak{L}_1,\lambda,a]} - \lambda)u_1 = -b\frac{\theta_{[\mathfrak{L}_1,\lambda,a]}}{1+m\theta_{[\mathfrak{L}_1,\lambda,a]}}v_1, \\ \left(\mathfrak{L}_2 - c\dfrac{\theta_{[\mathfrak{L}_1,\lambda,a]}}{1 + m\theta_{[\mathfrak{L}_1,\lambda,a]}}\right) v_1 = \Psi(\lambda)v_1. \end{cases} \tag{6.47}$$

Hence, $v_1 \gg_2 0$ can be chosen as the principal eigenfunction associated to $\Psi(\lambda)$ normalized so that

$$\int_\Omega v_1^2(x)\, dx = 1.$$

On the other hand, by Theorem 6.1.1,

$$\sigma_0 \left[\mathfrak{L}_1 + 2a\theta_{[\mathfrak{L}_1,\lambda,a]} - \lambda, \mathfrak{B}_1, \Omega\right] > \sigma_0 \left[\mathfrak{L}_1 + a\theta_{[\mathfrak{L}_1,\lambda,a]}, \mathfrak{B}_1, \Omega\right] - \lambda = 0.$$

Thus, thanks to Theorem 6.1.2, the first equation of (6.47) yields

$$u_1 = -(\mathfrak{L}_1 + 2a\theta_{[\mathfrak{L}_1,\lambda,a]} - \lambda)^{-1} \left(d\frac{\theta_{[\mathfrak{L}_1,\lambda,a]}}{1 + m\theta_{[\mathfrak{L}_1,\lambda,a]}}\varphi_0 \right) \ll_1 0. \tag{6.48}$$

In order to apply the main theorem of [37] one should make sure that the next transversality condition holds

$$\mathfrak{L}'(\Psi(\lambda))\varphi_0 \notin R[\mathfrak{L}(\Psi(\lambda))], \tag{6.49}$$

where $\mathfrak{L}'(\mu)$ stands for the derivative of $\mathfrak{L}(\mu)$ with respect to μ. Since

$$\mathfrak{L}'(\Psi(\lambda))(u,v) = \begin{pmatrix} 0 \\ -(\mathfrak{L}_2 + \omega)^{-1} v \end{pmatrix},$$

(6.49) can be expressed as

$$\begin{pmatrix} 0 \\ -(\mathfrak{L}_2 + \omega)^{-1} v_1 \end{pmatrix} \notin R[\mathfrak{L}(\Psi(\lambda))].$$

On the contrary, assume that

$$\mathfrak{L}(\Psi(\lambda))(u,v) = \begin{pmatrix} 0 \\ -(\mathfrak{L}_2 + \omega)^{-1} v_1 \end{pmatrix}$$

for some (u, v). Then,

$$v - (\mathfrak{L}_2 + \omega)^{-1} \left[(\Psi(\lambda) + \omega)v + c\frac{\theta_{[\mathfrak{L}_1,\lambda,a]}}{1 + m\theta_{[\mathfrak{L}_1,\lambda,a]}} v \right] = -(\mathfrak{L}_2 + \omega)^{-1} v_1$$

and hence, $v \in U_2$ satisfies

$$\left[\mathfrak{L}_2 - c\frac{\theta_{[\mathfrak{L}_1,\lambda,a]}}{1 + m\theta_{[\mathfrak{L}_1,\lambda,a]}} - \Psi(\lambda) \right] v = -v_1,$$

which is impossible, because $-v_1 \ll_2 0$ cannot be orthogonal in $L^2(\Omega)$ to the principal eigenfunction, $v_1^* \gg_2 0$, of the differential operator

$$\mathfrak{L}_2^* - c\frac{\theta_{[\mathfrak{L}_1,\lambda,a]}}{1+m\theta_{[\mathfrak{L}_1,\lambda,a]}} - \Psi(\lambda),$$

where $\mathfrak{L}_2^*$ stands for the adjoint operator of $(\mathfrak{L}_2, \mathfrak{B}_2, \Omega)$. Therefore, the main theorem of [37] can be applied to get the first assertions of the theorem. It remains to prove that $\mu'(0) > 0$. Setting

$$(\mu(s), u(s), v(s)) = \left(\Psi(\lambda) + \sum_{j=1}^{\infty} s^j \mu_j, \theta_{[\mathfrak{L}_1,\lambda,a]} + \sum_{j=1}^{\infty} s^j u_j, \sum_{j=1}^{\infty} s^j v_j\right), \quad s \sim 0,$$

substituting in (6.5) and taking into account the definitions of $\Psi(\lambda)$, u_1 and v_1, it becomes apparent that

$$\left(\mathfrak{L}_2 - c\frac{\theta_{[\mathfrak{L}_1,\lambda,a]}}{1+m\theta_{[\mathfrak{L}_1,\lambda,a]}} - \Psi(\lambda)\right)v_2 = \left(\mu_1 + \frac{cu_1}{(1+m\theta_{[\mathfrak{L}_1,\lambda,a]})^2} - dv_1\right)v_1. \quad (6.50)$$

Therefore, the Fredholm's alternative yields

$$\mu_1 = \int_\Omega dv_1^2 v_1^* - \int_\Omega \frac{cu_1}{(1+m\theta_{[\mathfrak{L}_1,\lambda,a]})^2} v_1 v_1^*, \quad (6.51)$$

provided that v_1^* is normalized so that

$$\int_\Omega v_1(x) v_1^*(x)\, dx = 1.$$

By (6.48), $u_1 \ll_1 0$ in Ω. Thus, by (6.51), $\mu_1 > 0$ for all $\lambda > \sigma_{0,1}$. This ends the proof. □

The next result provides us with the local structure of the set of coexistence states bifurcating from

$$(\lambda, u, v) = \left(\Phi(\mu), 0, \theta_{[\mathfrak{L}_2,\mu,d]}\right)$$

for every $\mu > \sigma_{0,2}$.

Theorem 6.5.2. *For every $\mu > \sigma_{0,2}$, there exist $\varepsilon > 0$, and an analytic map*

$$(\lambda, u, v) : (-\varepsilon, \varepsilon) \to \mathbb{R} \times U_1 \times U_2$$

such that

(a) $(\lambda(0), u(0), v(0)) = \left(\Phi(\mu), 0, \theta_{[\mathfrak{L}_2,\mu,d]}\right)$.

(b) $\mathfrak{F}(\lambda(s), \mu, u(s), v(s)) = 0$ *for all* $s \in (-\varepsilon, \varepsilon)$.

(c) $v(s) > 0$ *for all* $s \in (-\varepsilon, \varepsilon)$, $u(s) > 0$ *for all* $s \in (0, \varepsilon)$ *and* $u(s) < 0$ *for all* $s \in (-\varepsilon, 0)$. *Thus, for every* $s \in (0, \varepsilon)$, $(u(s), v(s))$ *is a coexistence state of* (6.5) *for* $(\lambda, \mu) = (\lambda(s), \mu)$.

(d) *The set of solutions of* (6.5) *in a neighborhood of* $\left(\lambda, \Phi(\mu), 0, \theta_{[\mathfrak{L}_2,\mu,d]}\right)$ *consists of the curves* $\left(\lambda, \mu, 0, \theta_{[\mathfrak{L}_2,\mu,d]}\right)$, $\lambda \sim \Phi(\mu)$, *and* $(\lambda(s), \mu, u(s), v(s))$, $s \in (-\varepsilon, \varepsilon)$.

Moreover,

$$\begin{aligned}\lambda'(0) = &\int_\Omega \left(a - bm\theta_{[\mathfrak{L}_2,\mu,d]}\right) u_1^2 u_1^* \\ &+ \int_\Omega b\left(\mathfrak{L}_2 + 2d\theta_{[\mathfrak{L}_2,\mu,d]} - \mu\right)^{-1}\left(c\theta_{[\mathfrak{L}_2,\mu,d]} u_1\right) u_1 u_1^*,\end{aligned} \tag{6.52}$$

where $u_1 \gg_1 0$ *is the principal eigenfunction of* $\Phi(\mu)$, *normalized so that* $\int_\Omega u_1^2 = 1$, *and* $u_1^* \gg_1 0$ *stands for the principal eigenfunction associated to* $\mathfrak{L}_1^* + b\theta_{[\mathfrak{L}_2,\mu,d]} - \Phi(\mu)$, *normalized so that* $\int_\Omega u_1 u_1^* = 1$.

Proof. As the previous theorem, this result also is a direct consequence of the main theorem of [37] applied to the function $\mathfrak{F}$ at the semitrivial branch $\left(\lambda, 0, \theta_{[\mathfrak{L}_2,\mu,d]}\right)$. Indeed, by definition,

$$\mathfrak{F}(\lambda, \mu, 0, \theta_{[\mathfrak{L}_2,\mu,d]}) = 0 \quad \text{for all} \quad \mu \in \mathbb{R}.$$

Moreover, the Fréchèt differential

$$\mathfrak{M}(\lambda) := D_{(u,v)}\mathfrak{F}(\lambda, \mu, 0, \theta_{[\mathfrak{L}_2,\mu,d]})$$

is given by

$$\mathfrak{M}(\lambda)(u, v) = \begin{pmatrix} u - (\mathfrak{L}_1 + \omega)^{-1}\left[(\lambda + \omega)u - b\theta_{[\mathfrak{L}_2,\mu,d]}u\right] \\ v - (\mathfrak{L}_2 + \omega)^{-1}\left[(\mu + \omega)v - 2d\theta_{[\mathfrak{L}_2,\mu,d]}v + c\theta_{[\mathfrak{L}_2,\mu,d]}u\right] \end{pmatrix}.$$

Thus,

$$N[\mathfrak{M}(\Phi(\mu))] = \operatorname{span}[\varphi_0], \qquad \varphi_0 = \begin{pmatrix} u_1 \\ v_1 \end{pmatrix},$$

where

$$\begin{cases} \left(\mathfrak{L}_1 + b\theta_{[\mathfrak{L}_2,\mu,d]}\right) u_1 = \Phi(\mu) u_1, \\ \left(\mathfrak{L}_2 + 2d\theta_{[\mathfrak{L}_2,\mu,d]} - \mu\right) v_1 = c\theta_{[\mathfrak{L}_2,\mu,d]} u_1. \end{cases} \tag{6.53}$$

Hence, $u_1 \gg_1 0$ can be chosen as the principal eigenfunction associated to $\Phi(\mu)$ normalized so that

$$\int_\Omega u_1^2(x)\,dx = 1.$$

By Theorem 6.1.1,

$$\sigma_0\left[\mathfrak{L}_2 + 2d\theta_{[\mathfrak{L}_2,\mu,d]} - \mu, \mathfrak{B}_2, \Omega\right] > \sigma_0\left[\mathfrak{L}_2 + d\theta_{[\mathfrak{L}_2,\mu,d]}, \mathfrak{B}_2, \Omega\right] - \mu = 0.$$

So, due to Theorem 6.1.2, we find from the second equation of (6.53) that

$$v_1 = \left(\mathfrak{L}_2 + 2d\theta_{[\mathfrak{L}_2,\mu,d]} - \mu\right)^{-1}\left(c\theta_{[\mathfrak{L}_2,\mu,d]} u_1\right) \gg_2 0. \tag{6.54}$$

To apply the main theorem of [37] one should make sure that the next condition holds

$$\mathfrak{M}'(\Phi(\mu))\varphi_0 \notin R[\mathfrak{M}(\Phi(\mu))], \tag{6.55}$$

where $\mathfrak{M}'(\lambda)$ stands for the derivative of $\mathfrak{M}(\lambda)$ with respect to λ. Since

$$\mathfrak{M}'(\Phi(\mu))(u,v) = \begin{pmatrix} -(\mathfrak{L}_1 + \omega)^{-1} u \\ 0 \end{pmatrix},$$

(6.55) can be written as

$$\begin{pmatrix} -(\mathfrak{L}_1 + \omega)^{-1} u_1 \\ 0 \end{pmatrix} \notin R[\mathfrak{M}(\Phi(\mu))].$$

On the contrary, assume that there exists (u,v) such that

$$\mathfrak{M}(\Phi(\mu))(u,v) = \begin{pmatrix} -(\mathfrak{L}_1 + \omega)^{-1} u_1 \\ 0 \end{pmatrix}.$$

Then,

$$u - (\mathfrak{L}_1 + \omega)^{-1}\left[(\Phi(\mu) + \omega)u - b\theta_{[\mathfrak{L}_2,\mu,d]} u\right] = -(\mathfrak{L}_1 + \omega)^{-1} u_1$$

and hence, $u \in U_1$ satisfies

$$\left[\mathfrak{L}_1 + b\theta_{[\mathfrak{L}_2,\mu,d]} - \Phi(\mu)\right] u = -u_1,$$

which is impossible, because $-u_1 \ll_1 0$ cannot be orthogonal in $L^2(\Omega)$ to the principal eigenfunction, $u_1^* \gg_1 0$, of the differential operator

$$\mathfrak{L}_1^* + b\theta_{[\mathfrak{L}_2,\mu,d]} - \Phi(\mu),$$

where $\mathfrak{L}_1^*$ stands for the adjoint operator of $(\mathfrak{L}_1, \mathfrak{B}_1, \Omega)$. Therefore, thanks to the main theorem of [37], the first assertions of the theorem follow readily. It remains to find out $\lambda'(0)$. Setting

$$(\lambda(s), u(s), v(s)) = \left(\Phi(\mu) + \sum_{j=1}^{\infty} s^j \lambda_j, \sum_{j=1}^{\infty} s^j u_j, \theta_{[\mathfrak{L}_2,\mu,d]} + \sum_{j=1}^{\infty} s^j v_j\right), \quad s \sim 0,$$

substituting in (6.5) and taking into account the definitions of $\Phi(\mu)$, u_1 and v_1, it is easily seen that

$$\left(\mathfrak{L}_1 + b\theta_{[\mathfrak{L}_2,\mu,d]} - \Phi(\mu)\right) v_2 = \left(\lambda_1 + bm\theta_{[\mathfrak{L}_2,\mu,d]} u_1 - au_1 - bv_1\right) u_1.$$

Consequently, choosing u_1^* such that $\int_\Omega u_1 u_1^* = 1$, combining the Fredholm's alternative with (6.54), the identity (6.52) holds. This ends the proof. $\square$

As a byproduct of (6.52), the next result holds.

Theorem 6.5.3. *Let $\mathfrak{m} \in \mathcal{C}(\bar{\Omega})$ be such that $\mathfrak{m} \gneq 0$ and consider $m = M\mathfrak{m}$, where $M > 0$ is a positive constant. Then, for every $\mu > \sigma_{0,2}$, there exist $M_1, M_2 > 0$ such that $M_1 < M_2$ and*

(a) $\lambda'(0) > 0$ *if* $M < M_1$.

(b) $\lambda'(0) < 0$ *if* $M > M_2$.

Moreover, when $\lambda'(0) < 0$, there exists $\varepsilon > 0$ such that, for every $\lambda \in (\Phi(\mu) - \varepsilon, \Phi(\mu))$, the problem (6.5) possesses, at least, two coexistence states.

Proof. The first assertion of the theorem is a direct consequence of (6.52), for as there exist $x_0 \in \Omega$ and $\eta > 0$ such that $x \in \Omega$ and $\mathfrak{m}(x) > 0$ if $|x - x_0| \leq \eta$.

The second assertion of the theorem can be inferred with the next argument. Suppose $\lambda'(0) < 0$. Then, the bifurcation to coexistence states from the curve $(\lambda, u, v) = \left(\lambda, 0, \theta_{[\mathfrak{L}_2,\mu,d]}\right)$ at $\lambda = \Phi(\mu)$ is subritical. Moreover, by Theorem 6.2.2, $(0, \theta_{[\mathfrak{L}_2,\mu,d]})$ is linearly unstable if $\lambda < \Phi(\mu)$. Thus, thanks to the exchange stability principle of M. G. Crandall and P. H. Rabinowitz [38], the coexistence state $(\lambda(s), \mu, u(s), v(s))$ must be linearly unstable with one-dimensional unstable manifold for sufficiently small $s > 0$. Thus, its fixed point index, as discussed in [120], equals -1. Therefore, adapting the technical devices of [120] it readily follows the existence of a further coexistence state for sufficiently close $\lambda < \Phi(\mu)$, because the total index of the underlying fixed point operator equals 1, and, whenever $\lambda < \Phi(\mu)$, the local fixed point indices of $(0,0)$ and $(\theta_{[\mathfrak{L}_1,\lambda,a]},0)$ equal 0, while the local index of $(0,\theta_{[\mathfrak{L}_2,\mu,d]})$ equals 1. The technical details of these calculations are omitted here. □

As suggested by the numerical experiments of A. Casal et al. [34] (see Figure 3 and the subsequent discussion of [34]), even in the simplest prototypes of model (6.5), the fact that $\lambda'(0) > 0$ in Theorem 6.5.2 does not necessarily guarantee the uniqueness of the coexistence state.

6.6 Uniqueness of the coexistence state in the 1-d model

The main result of this section is a substantial improvement of the classical uniqueness 1-d theorem of J. López-Gómez and R. M. Pardo [143], later sharpened by A. Casal et al. [34], E. N. Dancer et al. [46], and J. López-Gómez and R. M. Pardo [144], and revisited in [123] in a rather different context. It can be stated as follows.

Theorem 6.6.1. *Suppose that $\Omega = (p,q)$ for some real numbers $p < q$, that $\lambda > \sigma_{0,1}$, $\lambda > \Phi(\mu)$, $\mu > \Psi(\lambda)$, and that (7.39) admits a positive supersolution, $\bar{v}$, such that*

$$\bar{v} \le \frac{a}{bm}. \tag{6.56}$$

Then, (7.5) possesses a unique coexistence state.

Proof. The existence of a coexistence state is guaranteed by Theorem 7.3.1. Let (u,v), $(\tilde{u},\tilde{v})$ be two arbitrary coexistence states of (7.5). Then,

$$\begin{cases} [\mathfrak{L}_1 - \lambda + a(u+\tilde{u})](u-\tilde{u}) + b\left(\dfrac{uv}{1+mu} - \dfrac{\tilde{u}\tilde{v}}{1+m\tilde{u}}\right) = 0, \\ [\mathfrak{L}_2 - \mu + d(v+\tilde{v})](v-\tilde{v}) - c\left(\dfrac{uv}{1+mu} - \dfrac{\tilde{u}\tilde{v}}{1+m\tilde{u}}\right) = 0. \end{cases} \tag{6.57}$$

Moreover,

$$\begin{aligned} \frac{uv}{1+mu} - \frac{\tilde{u}\tilde{v}}{1+m\tilde{u}} &= \frac{\tilde{v}}{(1+mu)(1+m\tilde{u})}(u-\tilde{u}) + \frac{u(1+m\tilde{u})}{(1+mu)(1+m\tilde{u})}(v-\tilde{v}) \\ &= \frac{\tilde{v}}{(1+mu)(1+m\tilde{u})}(u-\tilde{u}) + \frac{u}{1+mu}(v-\tilde{v}). \end{aligned}$$

Thus, setting

$$\tilde{\mathfrak{L}}_1 := \mathfrak{L}_1 - \lambda + a(u+\tilde{u}) + b\frac{\tilde{v}}{(1+mu)(1+m\tilde{u})},$$
$$\tilde{\mathfrak{L}}_2 := \mathfrak{L}_2 - \mu + d(v+\tilde{v}) - c\frac{u}{1+mu},$$

and

$$\varphi_1 := u - \tilde{u}, \qquad \varphi_2 := v - \tilde{v},$$

it is apparent that (6.57) can be expressed as

$$\begin{cases} \tilde{\mathfrak{L}}_1\varphi_1 = -b\dfrac{u}{1+mu}\varphi_2 & \text{in } (p,q), \\ \tilde{\mathfrak{L}}_2\varphi_2 = c\dfrac{\tilde{v}}{(1+mu)(1+m\tilde{u})}\varphi_1 & \text{in } (p,q), \\ \mathfrak{B}_1 u = \mathfrak{B}_2 v = 0 & \text{on } \{p,q\}. \end{cases} \tag{6.58}$$

On the other hand, according to the proof of Theorem 7.2.3, we already know that $\tilde{v} \gg_2 0$ is a positive strict subsolution of

$$\begin{cases} \left(\mathfrak{L}_2 - c\frac{\theta_{[\mathfrak{L}_1,\lambda,a]}}{1+m\theta_{[\mathfrak{L}_1,\lambda,a]}}\right) w = \mu w - dw^2 & \text{in } \Omega, \\ \mathfrak{B}_2 w = 0 & \text{on } \partial\Omega. \end{cases} \tag{6.59}$$

Moreover, we are assuming that (6.59) admits a positive strict supersolution, $\bar{v}$, satisfying (6.56). Consequently, by Lemma 6.1.4, it becomes apparent that

$$\tilde{v} \lneq w \lneq \bar{v} \leq \frac{a}{bm},$$

where w stands for the unique positive solution of (6.59), which exists because $\mu > \Psi(\lambda)$. As this estimate implies

$$a \gneq bm\tilde{v} \geq \frac{bm\tilde{v}}{(1+mu)(1+m\tilde{u})} = \frac{1}{u}\frac{b\tilde{v}(1+mu) - b\tilde{v}}{(1+mu)(1+m\tilde{u})}$$

one has that

$$au + \frac{b\tilde{v} - b\tilde{v}(1+mu)}{(1+mu)(1+m\tilde{u})} \gneq 0$$

or, equivalently,

$$au + \frac{b\tilde{v}}{(1+mu)(1+m\tilde{u})} \gneq \frac{b\tilde{v}}{1+m\tilde{u}},$$

which implies

$$\sigma_0[\tilde{\mathfrak{L}}_1, \mathfrak{B}_1, (p,q)] > \sigma_0\Big[\mathfrak{L}_1 - \lambda + a\tilde{u} + b\frac{\tilde{v}}{1+m\tilde{u}}, \mathfrak{B}_1, (p,q)\Big] = 0.$$

Similarly, by Theorem 6.1.1,

$$\sigma_0[\tilde{\mathfrak{L}}_2, \mathfrak{B}_2, (p,q)] > \sigma_0\Big[\mathfrak{L}_2 - \mu + dv - c\frac{u}{1+mu}, \mathfrak{B}_2, (p,q)\Big] = 0.$$

Thus, owing to the next lemma, we can infer that $(\varphi_1, \varphi_2) = (0,0)$ is the unique solution of (6.58). Therefore, $(u,v) = (\tilde{u}, \tilde{v})$. The proof is complete. □

Lemma 6.6.2. *Suppose that $\Omega = (p,q)$ for some real numbers $p < q$ and that $\alpha, \beta \in \mathcal{C}(\bar{\Omega})$ satisfy $\alpha(x) > 0$ and $\beta(x) > 0$ for all $x \in (p,q)$. Then, $(u,v) = (0,0)$ is the unique solution of*

$$\begin{cases} \tilde{\mathfrak{L}}_1 u = -\alpha v & \textit{in } (p,q), \\ \tilde{\mathfrak{L}}_2 v = \beta u & \textit{in } (p,q), \\ \mathfrak{B}_1 u = \mathfrak{B}_2 v = 0 & \textit{on } \{p,q\}. \end{cases} \tag{6.60}$$

Proof of Lemma 6.6.2. Let (u,v) be a solution of (6.60). To show that $(u,v) = (0,0)$ we will argue by contradiction assuming that $(u,v) \neq (0,0)$. Suppose $u \neq 0$. Then, it follows from the v-equation of (6.60) that $v \neq 0$. Similarly, if $v \neq 0$, the u-equation implies that $u \neq 0$. Thus, $u \neq 0$ and $v \neq 0$. Suppose $u \gneq 0$. Then, since $\tilde{\mathfrak{L}}_2^{-1}$ is strongly positive, we can infer from the v-equation of (6.60) that $v \gg_2 0$. But, in such case, the right hand side of the u-equation of (6.60) becomes negative and hence, since $\tilde{\mathfrak{L}}_1^{-1}$ is strongly positive, we can infer that also $u \ll_1 0$, which is impossible. Therefore, u changes of sign in (p,q). This argument can be easily adapted to show that v must change of sign too. Adapting the proof of [46], it is easily seen that the zeros of u and v are isolated, i.e., they cannot accumulate in (p,q). Thus, there is a partition of $[p,q]$,

$$Q := \{p = x_0 < x_1 < x_2 < ... < x_{m-1} < x_m = q\}, \quad m \geq 2,$$

such that

$$\begin{aligned} u(x) > 0 \ \text{ for all } \ x \in (x_{2j}, x_{2j+1}), \quad j \geq 0, \quad 2j+1 \leq m, \\ u(x) < 0 \ \text{ for all } \ x \in (x_{2j-1}, x_{2j}), \quad j \geq 1, \quad 2j \leq m, \\ u(x_j) = 0 \ \text{ for all } \ j \in \{1, ..., m-1\} \ \text{ and } \ \mathfrak{B}_1 u(p) = \mathfrak{B}_1 u(q) = 0. \end{aligned} \tag{6.61}$$

We claim that

$$v(x_{2j}) > 0, \quad v(x_{2j+1}) < 0, \quad x_{2j}, x_{2j+1} \in Q \setminus \{p, q\}.$$

Indeed, by (6.61), we have that $u(x) > 0$ for all $x \in (x_0, x_1)$, $\mathfrak{B}_1 u(x_0) = 0$ and $u(x_1) = 0$. Thus, owing to (6.60), we find that

$$\tilde{\mathfrak{L}}_2 v = \beta u > 0 \quad \text{in} \quad (x_0, x_1).$$

Moreover, $\mathfrak{B}_2 v(x_0) = 0$. Suppose that $v(x_1) \geq 0$. As, according to [28, Pr. 3.2], the operator $\tilde{\mathfrak{L}}_2$ subject to the boundary conditions

$$\mathfrak{B}_2 v(x_0) = 0, \qquad v(x_1) = 0,$$

in the interval (x_0, x_1) has a positive principal eigenvalue, from Theorem 6.1.2 it becomes apparent that $v(x) > 0$ for all $x \in (x_0, x_1)$. Thus, going back to (6.60) yields

$$\tilde{\mathfrak{L}}_1 u = -\alpha v < 0 \quad \text{in} \quad (x_0, x_1).$$

As due to [28, Pr. 3.2], the operator $\tilde{\mathfrak{L}}_1$ subject to the boundary conditions

$$\mathfrak{B}_1 u(x_0) = 0, \qquad u(x_1) = 0,$$

in the interval (x_0, x_1) has a positive principal eigenvalue, Theorem 6.1.2 also implies that $u(x) < 0$ for all $x \in (x_0, x_1)$, which is a contradiction. Therefore, $v(x_1) < 0$. The previous argument can be easily adapted to show that $v(x_2) > 0$, $v(x_3) < 0$, ... and so on and so forth.

If m is odd, one has that

$$u(x) > 0 \ \text{ for all } \ x \in (x_m, q) \ \text{ and } \ v(x_m) > 0, \tag{6.62}$$

while, if m is even,

$$u(x) < 0 \ \text{ for all } \ x \in (x_{2k+1}, q) \ \text{ and } \ v(x_{2k+1}) < 0.$$

Suppose that m is odd. Then, (6.62) holds and hence, by (6.60),

$$\tilde{\mathfrak{L}}_2 v = \beta u > 0 \quad \text{in} \ (x_{2k}, q).$$

Since $v(x_{2k}) > 0$ and $\mathfrak{B}_2 v(q) = 0$, arguing as above, it follows from [28, Pr. 3.2] and Theorem 6.1.2 that $v(x) > 0$ for all $x \in (x_{m-1}, q)$. Thus,

$$\tilde{\mathfrak{L}}_1 u = -\alpha v < 0 \quad \text{in} \quad (x_{m-1}, q)$$

and therefore, since $u(x_{m-1}) = 0$ and $\mathfrak{B}_u(q) = 0$, it becomes apparent that $u(x) < 0$ for all $x \in (x_{m-1}, q)$, which contradicts (6.62). A similar contradiction can be reached when, instead, m is even. These contradictions end the proof. $\square$

Since

$$\frac{\theta_{[\mathfrak{L}_1,\lambda,a]}}{1+m\theta_{[\mathfrak{L}_1,\lambda,a]}} \leq \theta_{[\mathfrak{L}_1,\lambda,a]},$$

we have that

$$-c\frac{\theta_{[\mathfrak{L}_1,\lambda,a]}}{1+m\theta_{[\mathfrak{L}_1,\lambda,a]}} \geq -c\theta_{[\mathfrak{L}_1,\lambda,a]},$$

and hence, any positive strict supersolution, $\bar{v}$ of

$$\begin{cases} \left(\mathfrak{L}_2 - c\theta_{[\mathfrak{L}_1,\lambda,a]}\right) w = \mu w - dw^2 & \text{in } \Omega, \\ \mathfrak{B}_2 w = 0 & \text{on } \partial\Omega, \end{cases} \tag{6.63}$$

provides us with a positive strict supersolution of (6.59). On the other hand, arguing as in the proof of Theorem 7.2.3 it becomes apparent that (6.63) admits a positive strict supersolution of the form

$$\bar{v} = Ce^{M\psi}$$

for sufficiently large constants $C > 0$ and $M > 0$, independent of $m(x)$. Therefore, the assumption (6.56) of Theorem 6.6.1 holds true as soon as

$$Ce^{M\psi} \leq \frac{a}{bm}. \tag{6.64}$$

Consequently, the uniqueness of a coexistence state occurs for sufficiently small $m(x)$, in complete agreement with the available results in the literature.

Chapter 7

A robust multiplicity result

This chapter studies the existence and multiplicity of coexistence states for the generalized spatially heterogeneous predator-prey model

$$\begin{cases} \mathfrak{L}_1 u = \lambda u - a(x)u^2 - b(x)\dfrac{uv}{1+\gamma m(x)u} & \text{in } \Omega, \\ \mathfrak{L}_2 v = \mu v - d(x)v^2 + c(x)\dfrac{uv}{1+\gamma m(x)u} & \text{in } \Omega, \\ \mathfrak{B}_1 u = \mathfrak{B}_2 v = 0 & \text{on } \partial\Omega, \end{cases} \tag{7.1}$$

where Ω is a bounded domain of $\mathbb{R}^N$ with boundary, $\partial\Omega$, of class $\mathcal{C}^2$, and $\mathfrak{L}_k$, $k = 1, 2$, are second order uniformly elliptic operators in Ω of the form

$$\mathfrak{L}_k := -\mathrm{div}\,(A_k \nabla) + \langle b_k, \nabla \rangle + c_k, \qquad k = 1, 2, \tag{7.2}$$

where, for every $k = 1, 2$, $A_k = \left(a_{ij}^k\right)_{1 \le i,j \le N} \in \mathscr{M}_N^{\mathrm{sym}}(W^{1,\infty}(\Omega))$,

$$b_k = (b_1^k, ..., b_N^k) \in (L^\infty(\Omega))^N, \quad c_k \in L^\infty(\Omega).$$

For a given Banach space X, we are denoting by $\mathscr{M}_N^{\mathrm{sym}}(X)$ the space of the symmetric square matrices of order N with entries in X, and $W^{1,\infty}(\Omega)$ stands for the Sobolev space of all bounded and measurable functions in Ω with weak derivatives in $L^\infty(\Omega)$. In (7.1), for every $k = 1, 2$, $\mathfrak{B}_k$ is a general boundary operator of mixed type such that, for every $\psi \in \mathcal{C}(\bar{\Omega}) \cap \mathcal{C}^1(\Omega \cup \Gamma_1^k)$,

$$\mathfrak{B}_k \psi = \begin{cases} \psi & \text{on } \Gamma_0^k, \\ \partial_{\nu_k}\psi + \beta_k(x)\psi & \text{on } \Gamma_1^k, \end{cases} \tag{7.3}$$

where Γ_0^k and Γ_1^k are two closed and open disjoint subsets of $\partial\Omega$ such that $\Gamma_0^k \cup \Gamma_1^k = \partial\Omega$, and $\nu_k = A_k n$ is the co-normal vector field, i.e., n is the outward unit normal vector field of Ω. In (7.3), $\beta_k \in \mathcal{C}(\Gamma_1^k)$ is not required to have any special sign. As for the coefficient functions $a(x)$, $b(x)$, $c(x)$, $d(x)$ and $m(x)$ in the setting of (7.1), we assume that they are functions in $\mathcal{C}(\bar{\Omega};\mathbb{R})$ such that $b \neq 0$, $c \neq 0$, and

$$a(x) > 0, \quad d(x) > 0, \quad b(x) \geq 0, \quad c(x) \geq 0, \quad m(x) \geq 0 \quad \text{for all } x \in \bar{\Omega}. \tag{7.4}$$

In other words, $a \gg 0$, $d \gg 0$, $b \gneq 0$, $c \gneq 0$ and $m \geq 0$. Finally, in (7.1), λ, μ and $\gamma > 0$ are regarded as real parameters.

Except for the incorporation of the new parameter $\gamma > 0$, this model, in its greatest generality, Has been introduced in Chapter 6 (see [135]) to establish an homotopy between the classical diffusive Lotka–Volterra predator-prey system, when $m = 0$, and the diffusive Holling–Tanner model introduced by Casal, Eilbeck and López-Gómez [34], where m is a positive constant. The case when m is constant has been also analyzed by Du and Lou in [60], [61] and [62], under Dirichlet or Neumann boundary conditions, and Du and Shi [63] assuming the existence of a protection zone for the prey. Some pioneering non-spatial models of this type were studied by Freedman [81], May [151] and Hsu [95], among others.

In Population Dynamics, (7.1) represents the interaction in a common habitat, Ω, between a prey, with population density u, and a predator, with population density v. According to (7.1), in the absence of the other, each species has a logistic growth determined by the relative sizes of λ and μ with respect to the thresholds $\sigma_0[\mathfrak{L}_1 - c_1, \mathfrak{B}_1, \Omega]$ and $\sigma_0[\mathfrak{L}_2 - c_2, \mathfrak{B}_2, \Omega]$, respectively. Throughout this chapter, for any given second order elliptic operator $\mathfrak{L}$ in Ω and any boundary operator $\mathfrak{B}$ on $\partial\Omega$, we denote by $\sigma_0[\mathfrak{L}, \mathfrak{B}, \Omega]$ the principal eigenvalue of $(\mathfrak{L}, \mathfrak{B}, \Omega)$ as discussed in [124]. In (7.1), the term $\gamma m(x)$ measures the saturation effects in Ω of the predator in the presence of a high population of preys. More precisely, for every $x \in \Omega$, $\gamma m(x)$ measures the predator saturation level at the location $x \in \Omega$ if $m(x) > 0$, while the saturation effects at x do not play any role if $m(x) = 0$. By normalizing $m(x)$ so that $\max_{x\in\bar{\Omega}} m(x) = 1$, γ becomes the maximal intensity of the saturations effects. So, throughout this chapter we will assume that

$$\|m\|_\infty \equiv \max_{x\in\bar{\Omega}} m(x) = 1. \tag{7.5}$$

Furthermore, we assume that $\Omega_0 := \operatorname{int} m^{-1}(0)$ is a nice open subset of class $\mathcal{C}^2$ of Ω with finitely many connected components and $\bar{\Omega}_0 = m^{-1}(0) \subset \Omega$. Thus, (7.1) combines in the same habitat, Ω, functional responses of Lotka–Volterra type in the components of $m^{-1}(0)$ together with Holling–Tanner responses in $m^{-1}(\mathbb{R}_+)$, where $\mathbb{R}_+ := (0, +\infty)$. As noticed in Sections 6.3 and

6.5, the existence of both functional responses can lead to global effects in the dynamics of the species, regardless the sizes of the patches where $m = 0$ or $m > 0$. Moreover, the size of the regions where $m(x)$ or $b(x)$ degenerate can also affect the global dynamics. Indeed, as shown in Section 7.2, the greater is the support of $m(x)$, or $b^{-1}(0)$, the smaller can be λ so that (7.1) can still admit a coexistence state.

Essentially, this chapter (see also [136]) is a continuation of Chapter 6 (see also [135]), where the existence and the uniqueness of coexistence states was established for the generalized problem (7.1), by fixing $\mu \in \mathbb{R}$ and regarding $\lambda \in \mathbb{R}$ as a bifurcation parameter. According to Theorem 7.1 of [135], we already know that the one-dimensional counterpart of (7.1) has a unique coexistence state for sufficiently small $\gamma > 0$. The main goal of this chapter is to study the dynamics of (7.1) as $\gamma \uparrow +\infty$. Thus, it is rather natural to perform the change of variables

$$w := \gamma\, u, \qquad \varepsilon = \frac{1}{\gamma}. \tag{7.6}$$

In these variables, (7.1) can be expressed, equivalently, as

$$\begin{cases} \mathfrak{L}_1 w = \lambda w - \varepsilon a(x) w^2 - b(x)\dfrac{wv}{1+m(x)w} & \text{in } \ \Omega, \\ \mathfrak{L}_2 v = \mu v - d(x) v^2 + \varepsilon c(x)\dfrac{wv}{1+m(x)w} & \text{in } \ \Omega, \\ \mathfrak{B}_1 w = \mathfrak{B}_2 v = 0 & \text{on } \ \partial\Omega. \end{cases} \tag{7.7}$$

According to (7.6), analyzing the dynamics of (7.1) for sufficiently large γ is equivalent to analyze (7.7) for sufficiently small $\varepsilon > 0$. Thus, it is rather natural to focus attention into (7.7) as a system perturbing from

$$\begin{cases} \mathfrak{L}_1 w = \lambda w - b(x)\dfrac{wv}{1+m(x)w} & \text{in } \ \Omega, \\ \mathfrak{L}_2 v = \mu v - d(x) v^2 & \text{in } \ \Omega, \\ \mathfrak{B}_1 w = \mathfrak{B}_2 v = 0 & \text{on } \ \partial\Omega. \end{cases} \tag{7.8}$$

This problem has the tremendous advantage that it is uncoupled.

Our main results establish, for every $\varepsilon \geq 0$, the existence of a component $\mathscr{C}_\varepsilon^+$ of the set of coexistence states of (7.7), or (7.8), and ascertain their global structures according to weather $\varepsilon > 0$, or $\varepsilon = 0$. Precisely, when $\varepsilon = 0$, Theorems 7.2.3 and 7.2.4 show that $\mathscr{C}_0^+$ behaves much like sketched in Figure 7.3, where the constants $\Phi(\mu)$ and $\varphi_0(\mu)$ are defined in (7.24) and (7.27), respectively. Later, Theorem 7.3.1 shows that, as $\varepsilon > 0$ perturbs from

$\varepsilon = 0$, the component $\mathscr{C}_0^+$ perturbs into $\mathscr{C}_\varepsilon^+$ and that, since the coexistence states of (7.7) have uniform a priori bounds on compact subintervals of the parameter λ, for any given $\eta > 0$, there exists $\varepsilon_0 = \varepsilon_0(\eta) > 0$ such that $\mathscr{C}_\varepsilon^+$ has, at least, two coexistence states for every $\lambda \in [\varphi_0(\mu) - \eta, \Phi(\mu) - \eta]$ if $\varepsilon \in (0, \varepsilon_0]$, as illustrated by Figure 7.4. This multiplicity result is new even for the simplest prototype model introduced by Casal et al. [34].

Although in the classical setting of Casal et al. [34], Du and Lou [61] proved the existence of the S-shaped diagrams computed in [34] for sufficiently large $\gamma > 0$ and $c > 0$, with $\mu > \sigma_{0,2} \equiv \sigma_0[\mathfrak{L}_2, \mathfrak{B}_2, \Omega]$ sufficiently close to $\sigma_{0,2}$, the reader should be aware that, in this chapter, $c(x)$ can degenerate and take arbitrary values, and that $\mu > \sigma_{0,2}$ is arbitrary. Actually, the multiplicity result of this chapter has a different nature than the inherent to the S-shaped diagrams discovered in [34]. In S-shaped bifurcation diagrams, the problem has, at least, two coexistence states if $\lambda \in [\Phi(\mu) - \eta, \Phi(\mu)]$, while it has, at least, three, if $\lambda \in (\Phi(\mu), \Phi(\mu) + \eta]$, for sufficiently small $\eta > 0$, as illustrated in the second picture of Figure 7.8. In strong contrast, the main result of this chapter establishes that, for sufficiently large $\gamma > 0$, (7.1) has, at least, two coexistence states in any compact subinterval of $(\varphi_0(\mu), \Phi(\mu))$, regardless the size and shape of the function coefficient $c(x)$ and how large is μ. Rather surprisingly, this occurs regardless the size of the support of the saturation term, measured by $m(x)$, which might be arbitrarily small, as is an atom in a Galaxy. A similar phenomenon, though in a very different problem, was observed by López-Gómez and Rabinowitz [145].

We end this chapter by analyzing a simple prototype model with constant coefficients and non-flux boundary conditions, where the constant steady-states are given by a simple algebraic system. Among other things, we will establish the existence of S-shaped curves of coexistence states when $bc > ad$ and ε is sufficiently large. This example shows that our multiplicity theorem, for sufficiently small $\varepsilon > 0$, has nothing to do with the formation of S-shaped components of coexistence states.

The notations and abstract results that are used throughout the chapter are the ones presented in Section 6.2. The plan of this chapter is the following. Section 7.1 studies the stability of the semitrivial curve $(0, \theta_{[\mathfrak{L}_2, \mathfrak{B}_2, \Omega]})$, where $\theta_{[\mathfrak{L}_2, \mathfrak{B}_2, \Omega]}$ stands for the unique positive solution of

$$\begin{cases} \mathfrak{L}_2 = \mu v - dv^2 & \text{in } \Omega, \\ \mathfrak{B}_2 v = 0 & \text{on } \partial\Omega, \end{cases}$$

which exists if, and only if, $\mu > \sigma_{0,2}$, and analyzes the local bifurcation to coexistence states of (7.7) from it, with special emphasis on the uniform dependence of these local bifurcations on the parameter $\varepsilon \geq 0$, which is a subtle issue. Section 7.2 studies the uncoupled system (7.8), establishing the global structure of the component $\mathscr{C}_0^+$ near $\varphi_0(\mu)$, its bifurcation point from infinity, and $\Phi(\mu)$, its bifurcation point from the semitrivial positive solution $(0, \theta_{[\mathfrak{L}_2,\mathfrak{B}_2,\Omega]})$. Then, the analysis carried out in Sections 7.1 and 7.2 combined with some sophisticated topological and global continuation arguments, will drive us to the proof of Theorem 7.3.1 of Section 7.3, which is our main multiplicity result. Finally, in Section 7.4 we analyze a very simple example with S-shaped components of coexistence states. A previous analysis of this example is imperative for tackling the problem of the global existence of S-shaped bifurcation diagrams in its greatest generality, which will be pursued in a forthcoming investigation.

7.1 Bifurcation of coexistence states from $(0, \theta_{[\mathfrak{L}_2,\mu,d]})$

In this section we analyze the bifurcation of coexistence states from the semitrivial curve $(0, \theta_{[\mathfrak{L}_2,\mu,d]})$ in the problem (7.7). We are particularly interested in ascertaining the nature of the local bifurcation according to the value of the parameter $\varepsilon > 0$. The linearized stability of $(0, \theta_{[\mathfrak{L}_2,\mu,d]})$ is determined by the signs of the real parts of the eigenvalues of the problem

$$\begin{cases} \begin{pmatrix} \mathfrak{L}_1 + b\theta_{[\mathfrak{L}_2,\mu,d]} - \lambda & 0 \\ -\varepsilon c\theta_{[\mathfrak{L}_2,\mu,d]} & \mathfrak{L}_2 + 2d\theta_{[\mathfrak{L}_2,\mu,d]} - \mu \end{pmatrix} \begin{pmatrix} w \\ v \end{pmatrix} = \tau \begin{pmatrix} w \\ v \end{pmatrix} & \text{in } \Omega, \\ \mathfrak{B}_1 w = \mathfrak{B}_2 v = 0 & \text{on } \partial\Omega. \end{cases} \tag{7.9}$$

The next result holds.

Theorem 7.1.1. *Setting* $\Phi(\mu) \equiv \sigma_0\left[\mathfrak{L}_1 + b\theta_{[\mathfrak{L}_2,\mu,d]}, \mathfrak{B}_1, \Omega\right]$ *for every* $\mu > \sigma_0[\mathfrak{L}_2, \mathfrak{B}_2, \Omega]$, *the semitrivial solution* $(0, \theta_{[\mathfrak{L}_2,\mu,d]})$ *is linearly unstable if, and only if,* $\lambda > \Phi(\mu)$, *whereas it is linearly stable if, and only if,* $\lambda < \Phi(\mu)$. *Thus,* $\lambda = \Phi(\mu)$ *is the curve of change of stability of* $(0, \theta_{[\mathfrak{L}_2,\mu,d]})$.

Proof. We first determine the eigenvalues with associated eigenvectors (w, v) such that $w = 0$ and $v \neq 0$. By (7.9), these eigenvalues satisfy

$$\begin{cases} (\mathfrak{L}_2 + 2d\theta_{[\mathfrak{L}_2,\mu,d]} - \mu)v = \tau v & \text{in } \Omega, \\ \mathfrak{B}_2 v = 0 & \text{on } \partial\Omega. \end{cases} \tag{7.10}$$

By Theorem 6.1.1, the definition of $\theta_{[\mathfrak{L}_2,\mu,d]}$, and the uniqueness of the principal eigenvalue,

$$\sigma_0\left[\mathfrak{L}_2 + 2d\theta_{[\mathfrak{L}_2,\mu,d]} - \mu, \mathfrak{B}_2, \Omega\right] > \sigma_0\left[\mathfrak{L}_2 + d\theta_{[\mathfrak{L}_2,\mu,d]} - \mu, \mathfrak{B}_2, \Omega\right] = 0. \tag{7.11}$$

Thus, by the dominance of the principal eigenvalue (see [126, Th. 7.8]),

$$\operatorname{Re}\tau \geq \sigma_0\left[\mathfrak{L}_2 + 2d\theta_{[\mathfrak{L}_2,\mu,d]} - \mu, \mathfrak{B}_2, \Omega\right] > 0$$

for any eigenvalue, τ, of (7.10).

Now, we will ascertain the real parts of the eigenvalues of (7.9) with associated eigenfunctions, (w, v), such that $w \neq 0$. By (7.9), they should satisfy

$$\begin{cases} (\mathfrak{L}_1 + b\theta_{[\mathfrak{L}_2,\mu,d]} - \lambda)w = \tau w & \text{in } \Omega, \\ \mathfrak{B}_1 w = 0 & \text{on } \partial\Omega. \end{cases} \tag{7.12}$$

These eigenvalues consist of the sequence

$$\tau_j := \sigma_j\left[\mathfrak{L}_1 + b\theta_{[\mathfrak{L}_2,\mu,d]}, \mathfrak{B}_1, \Omega\right] - \lambda \qquad \text{for } j \geq 0, \tag{7.13}$$

where $\left\{\sigma_j\left[\mathfrak{L}_1 + b\theta_{[\mathfrak{L}_2,\mu,d]}, \mathfrak{B}_1, \Omega\right]\right\}_{j\geq 0}$ is the sequence of eigenvalues of (6.8) with $k = 1$ and $V = b\theta_{[\mathfrak{L}_2,\mu,d]}$. As the principal eigenvalue is dominant, it is apparent that

$$\operatorname{Re}\tau_j \geq \tau_0 = \Phi(\mu) - \lambda \quad \text{for all } \ j \geq 0.$$

Assume $\lambda < \Phi(\mu)$. Then, $\operatorname{Re}\tau_j > 0$ for all $j \geq 0$. Thus, any eigenvalue of (7.9) has a positive real part, i.e., $(0, \theta_{[\mathfrak{L}_2,\mu,d]})$ is linearly stable.

Assume now $\lambda > \Phi(\mu)$. Then, $\tau_0 < 0$. Let $w \neq 0$ be a principal eigenfunction associated to τ_0. Then, the second equation of (7.9) becomes

$$\begin{cases} (\mathfrak{L}_2 + 2d\theta_{[\mathfrak{L}_2,\mu,d]} - \mu - \tau_0)v = \varepsilon c\theta_{[\mathfrak{L}_2,\mu,d]}w, & \text{in } \ \Omega, \\ \mathfrak{B}_2 v = 0 & \text{in } \ \partial\Omega. \end{cases} \tag{7.14}$$

Since $-\tau_0 > 0$, it follows from Theorem 6.1.1 and (7.11) that

$$\sigma_0[\mathfrak{L}_2 + 2d\theta_{[\mathfrak{L}_2,\mu,d]} - \mu - \tau_0, \mathfrak{B}_2, \Omega] > \sigma_0[\mathfrak{L}_2 + 2d\theta_{[\mathfrak{L}_2,\mu,d]} - \mu, \mathfrak{B}_2, \Omega] > 0.$$

Thus, thanks to Theorem 6.1.2,

$$v = \left(\mathfrak{L}_2 + 2d\theta_{[\mathfrak{L}_2,\mu,d]} - \mu - \tau_0\right)^{-1}(\varepsilon c\theta_{[\mathfrak{L}_2,\mu,d]}w)$$

provides us with the unique solution of (7.14). Therefore, (w, v) is an eigenfunction of (7.9) associated to $\tau_0 < 0$ and hence, $(0, \theta_{[\mathfrak{L}_2,\mu,d]})$ is linearly unstable. □

Remark 7.1.2. According to the theorems of Lyapunov on linearized stability, it becomes apparent that $(0, \theta_{[\mathfrak{L}_2,\mu,d]})$ is exponentially asymptotically stable if $\lambda < \Phi(\mu)$, while it is unstable if $\lambda > \Phi(\mu)$ (see, e.g., Henry [91, Sec. 5.1]).

Subsequently, we set

$$\sigma_{0,k} \equiv \sigma_0[\mathfrak{L}_k, \mathfrak{B}_k, \Omega], \qquad k = 1, 2, \tag{7.15}$$

and pick any real number, e, such that $e > \max\{-\sigma_{0,1}, -\sigma_{0,2}\}$. Then, for every $k = 1, 2$,

$$\sigma_0[\mathfrak{L}_k + e, \mathfrak{B}_k, \Omega] = \sigma_{0,k} + e > 0$$

and hence, by Theorem 6.1.2, $(\mathfrak{L}_k + e, \mathfrak{B}_k, \Omega)$ is an invertible operator with strongly positive inverse. Obviously, the solutions of the problem (7.7) are given by the zeroes of the operator

$$\mathfrak{F} : \mathbb{R} \times \mathbb{R} \times \mathbb{R} \times \mathcal{C}^1_{\mathfrak{B}_1}(\bar{\Omega}) \times \mathcal{C}^1_{\mathfrak{B}_2}(\bar{\Omega}) \to U_1 \times U_2,$$

defined, for every $\lambda, \mu, \varepsilon \in \mathbb{R}$, $w \in \mathcal{C}^1_{\mathfrak{B}_1}(\bar{\Omega})$ and $v \in \mathcal{C}^1_{\mathfrak{B}_2}(\bar{\Omega})$, by

$$\mathfrak{F}(\lambda, \mu, \varepsilon, w, v) := \begin{pmatrix} w - (\mathfrak{L}_1 + e)^{-1}\left[(\lambda + e)w - \varepsilon a w^2 - b\frac{wv}{1+mw}\right] \\ v - (\mathfrak{L}_2 + e)^{-1}\left[(\mu + e)v - dv^2 + \varepsilon c\frac{wv}{1+mw}\right] \end{pmatrix}. \tag{7.16}$$

The operator $\mathfrak{F}$ is a compact perturbation of the identity map in $\mathcal{C}^1_{\mathfrak{B}_1}(\bar{\Omega}) \times \mathcal{C}^1_{\mathfrak{B}_2}(\bar{\Omega})$. Moreover, it is Fréchèt differentiable and, since $D_{(w,v)}\mathfrak{F}$ is a linear compact perturbation of the identity map, $D_{(w,v)}\mathfrak{F}$ is a Fredholm operator of index zero. Actually, $\mathfrak{F}$ is real analytic in an open region containing the first quadrant $w \geq 0$, $v \geq 0$.

The next result shows that the coexistence states bifurcate from the semitrivial positive solution $(0, \theta_{[\mathfrak{L}_2,\mu,d]})$ along the curve $\lambda = \Phi(\mu)$. It is a direct consequence of the theorem of bifurcation from simple eigenvalues of Crandall and Rabinowitz [37]. It provides us with the local structure of the set of bifurcating coexistence states.

Theorem 7.1.3. *For every $\mu > \sigma_{0,2}$ and $\varepsilon \in \mathbb{R}$, there exist $\delta = \delta(\mu, \varepsilon) > 0$ and an analytic map $(\lambda, w, v) : (-\delta, \delta) \to \mathbb{R} \times U_1 \times U_2$ such that:*

(i) $(\lambda(0), w(0), v(0)) = \left(\Phi(\mu), 0, \theta_{[\mathfrak{L}_2,\mu,d]}\right)$.

(ii) $\mathfrak{F}(\lambda(s), \mu, \varepsilon, w(s), v(s)) = 0$ *for all* $s \in (-\delta, \delta)$.

(iii) $v(s) \gg_2 0$ *if* $s \in (-\delta, \delta)$, $w(s) \gg_1 0$ *if* $s \in (0, \delta)$, *and* $w(s) \ll_1 0$ *if* $s \in (-\delta, 0)$.

(iv) *The set of solutions of* (7.7) *in a neighborhood of the point* $(\lambda, w, v) = \left(\Phi(\mu), 0, \theta_{[\mathfrak{L}_2,\mu,d]}\right)$ *consists of the curves* $\left(\lambda, 0, \theta_{[\mathfrak{L}_2,\mu,d]}\right)$, $\lambda \sim \Phi(\mu)$, *and* $(\lambda(s), w(s), v(s))$, $s \in (-\delta, \delta)$.

Moreover, there are two functions $w_1, w_1^* \gg_1 0$ *such that*

$$\lambda'(\varepsilon) \equiv \frac{\partial \lambda}{\partial s}(0,\varepsilon) = \int_\Omega \left(\varepsilon a - b\theta_{[\mathfrak{L}_2,\mu,d]}\right) w_1^2 w_1^* \\ + \int_\Omega b \left(\mathfrak{L}_2 + 2d\theta_{[\mathfrak{L}_2,\mu,d]} - \mu\right)^{-1} \left(\varepsilon c \theta_{[\mathfrak{L}_2,\mu,d]} w_1\right) w_1 w_1^*. \tag{7.17}$$

Proof. By definition, $\mathfrak{F}(\lambda,\mu,\varepsilon,0,\theta_{[\mathfrak{L}_2,\mu,d]}) = 0$. Moreover, the Fréchèt differential

$$\mathscr{L}(\lambda,\varepsilon) := D_{(w,v)}\mathfrak{F}(\lambda,\mu,\varepsilon,0,\theta_{[\mathfrak{L}_2,\mu,d]})$$

is the operator defined by

$$\mathscr{L}(\lambda,\varepsilon)(w,v) = \begin{pmatrix} w - (\mathfrak{L}_1 + e)^{-1}\left[(\lambda + e)w - b\theta_{[\mathfrak{L}_2,\mu,d]} w\right] \\ v - (\mathfrak{L}_2 + e)^{-1}\left[(\mu + e)v - 2d\theta_{[\mathfrak{L}_2,\mu,d]} v + \varepsilon c \theta_{[\mathfrak{L}_2,\mu,d]} w\right] \end{pmatrix}.$$

Thus, at $\lambda = \Phi(\mu)$ we have that $(w_1, v_1) \in N[\mathscr{L}(\Phi(\mu),\varepsilon)]$ if, and only if,

$$\begin{cases} \left(\mathfrak{L}_1 + b\theta_{[\mathfrak{L}_2,\mu,d]}\right) w_1 = \Phi(\mu) w_1, \\ \left(\mathfrak{L}_2 + 2d\theta_{[\mathfrak{L}_2,\mu,d]} - \mu\right) v_1 = \varepsilon c \theta_{[\mathfrak{L}_2,\mu,d]} w_1, \end{cases} \tag{7.18}$$

in Ω and $\mathfrak{B}_1 w_1 = \mathfrak{B}_2 v_1 = 0$ in $\partial\Omega$. Since $\Phi(\mu) \equiv \sigma_0\left[\mathfrak{L}_1 + b\theta_{[\mathfrak{L}_2,\mu,d]}, \mathfrak{B}_1, \Omega\right]$, by the simplicity of $\Phi(\mu)$, w_1 is unique, up to multiplicative constants. Actually, it can be chosen to satisfy $w_1 \gg_1 0$. Moreover, by (7.11) and Theorem 6.1.2, the second equation of (7.18) implies that

$$v_1 = \left(\mathfrak{L}_2 + 2d\theta_{[\mathfrak{L}_2,\mu,d]} - \mu\right)^{-1} \left(\varepsilon c \theta_{[\mathfrak{L}_2,\mu,d]} w_1\right). \tag{7.19}$$

Note that $\operatorname{sign} v_1 = \operatorname{sign} \varepsilon$, by Theorem 6.1.2. Therefore,

$$N[\mathscr{L}(\Phi(\mu),\varepsilon)] = \operatorname{span}[\varphi_0], \qquad \varphi_0 \equiv (w_1, v_1), \quad w_1 \gg_1 0.$$

Subsequently, we normalize $w_1 \gg_1 0$ so that $\int_\Omega w_1^2(x)\,dx = 1$, and denote by $D_\lambda \mathscr{L}(\lambda,\varepsilon)$ the derivative of $\mathscr{L}(\lambda,\varepsilon)$ with respect to λ. Then,

$$D_\lambda \mathscr{L}(\Phi(\mu),\varepsilon)\varphi_0 = \begin{pmatrix} -(\mathfrak{L}_1 + e)^{-1} w_1 \\ 0 \end{pmatrix} \notin R[\mathscr{L}(\Phi(\mu),\varepsilon)], \tag{7.20}$$

i.e., the transversality condition of Crandall and Rabinowitz [37] holds. Indeed, arguing by contradiction, assume that there exists (w,v) such that

$$\mathscr{L}(\Phi(\mu),\varepsilon)(w,v) = \begin{pmatrix} -(\mathfrak{L}_1 + e)^{-1} w_1 \\ 0 \end{pmatrix}.$$

Then, we find from the first equation of this system that

$$\begin{cases} \left[\mathfrak{L}_1 + b\theta_{[\mathfrak{L}_2,\mu,d]} - \Phi(\mu)\right] w = -w_1 & \text{in } \Omega, \\ \mathfrak{B}_1 w = 0 & \text{on } \partial\Omega. \end{cases}$$

By Corollary 7.1(f) of [126] this is impossible. This contradiction shows (7.20). Consequently, the first four assertions of the theorem follow from the main theorem of [37]. To complete the proof it remains to show (7.17). Setting

$$(\lambda(s), w(s), v(s)) = \left(\Phi(\mu) + \sum_{j=1}^{\infty} s^j \lambda_j, \sum_{j=1}^{\infty} s^j w_j, \theta_{[\mathfrak{L}_2,\mu,d]} + \sum_{j=1}^{\infty} s^j v_j\right), \quad s \sim 0,$$

and substituting into (7.7), it becomes apparent that

$$\begin{cases} \left(\mathfrak{L}_1 + b\theta_{[\mathfrak{L}_2,\mu,d]} - \Phi(\mu)\right) w_2 = \left(\lambda_1 + b\theta_{[\mathfrak{L}_2,\mu,d]} w_1 - \varepsilon a w_1 - b v_1\right) w_1 & \text{in } \Omega, \\ \mathfrak{B}_1 w_2 = 0 & \text{on } \partial\Omega. \end{cases} \tag{7.21}$$

Thanks to Corollary 7.1(e) of [126], it is easily seen that the $L^2(\Omega)$-orthogonal to the kernel of the adjoint problem of $\left(\mathfrak{L}_1 + b\theta_{[\mathfrak{L}_2,\mu,d]} - \Phi(\mu), \mathfrak{B}_1, \Omega\right)$ is generated by some $w_1^* \gg_1 0$. Therefore, multiplying by w_1^* the problem (7.21) and integrating in Ω, it follows from (7.19) that (7.17) holds. This ends the proof. $\square$

Remark 7.1.4. As the dependence of $\mathfrak{F}$ on $\varepsilon \in \mathbb{R}$ is also analytic, by the implicit function theorem used in the proof of the theorem of Crandall and Rabinowitz [37], it becomes apparent that the bifurcated curve

$$(\lambda(s), w(s), v(s)) \equiv (\lambda(s,\varepsilon), w(s,\varepsilon), v(s,\varepsilon))$$

also is analytic with respect to the parameter ε, though in Theorem 7.1.3 we have refrained to emphasize this dependence on the parameter ε to simplify the notations as much as possible.

As a further application of the exchange stability principle of Crandall and Rabinowitz [38, Th. 1.16], the next result holds.

Theorem 7.1.5. *The curve of coexistence states of (7.7) emanating from $\left(\Phi(\mu), 0, \theta_{[\mathfrak{L}_2,\mu,d]}\right)$, denoted in Theorem 7.1.3 by $(\lambda(s), \mu, w(s), v(s))$ for sufficiently small $s > 0$, is unstable, with one-dimensional unstable manifold, if $\lambda'(0) < 0$, and exponentially stable if $\lambda'(0) > 0$.*

Proof. According to (7.13), it is apparent that

$$\begin{cases} \tau_0 > 0 \;\text{ and }\; \tau_j > 0 \;\text{ for all } j \geq 1 \;\text{ if }\; \lambda < \Phi(\mu), \\ \tau_0 = 0 \;\text{ and }\; \tau_j > 0 \;\text{ for all } j \geq 1 \;\text{ if }\; \lambda = \Phi(\mu), \\ \tau_0 < 0 \;\text{ and }\; \tau_j > 0 \;\text{ for all } j \geq 1 \;\text{ if }\; \lambda \gtrsim \Phi(\mu). \end{cases} \tag{7.22}$$

Thus, by the exchange stability principle, [38, Th. 1.16], $(\lambda(s),\mu,w(s),v(s))$ is linearly unstable (resp. stable) for sufficiently small $s>0$ if $\lambda'(0)<0$ (resp. $\lambda'(0)>0$). Moreover, maintaining the notations of the proof of Theorem 7.1.3, it follows from [124, Sec. 2.4] that, for sufficiently small $s>0$,

$$\mathfrak{m}\left[D_{(w,v)}\mathfrak{F}(\lambda(s),\mu,\varepsilon,w(s),v(s))\right] = \begin{cases} \mathfrak{m}\left[\mathscr{L}(\Phi(\mu),\varepsilon)\right]+1 & \text{if } \lambda'(0)<0, \\ \mathfrak{m}\left[\mathscr{L}(\Phi(\mu),\varepsilon)\right] & \text{if } \lambda'(0)>0, \end{cases}$$

where $\mathfrak{m}(L)$ stands for the sum of the algebraic multiplicities of the real negative eigenvalues of L. By (7.22), $\mathfrak{m}\left[\mathscr{L}(\Phi(\mu),\varepsilon)\right]=0$. Therefore,

$$\mathfrak{m}\left[D_{(w,v)}\mathfrak{F}(\lambda(s),\mu,\varepsilon,w(s),v(s))\right] = \begin{cases} 1 & \text{if } \lambda'(0)<0, \\ 0 & \text{if } \lambda'(0)>0. \end{cases}$$

The principle of linearized stability of Lyapunov ends the proof. □

Figure 7.1 sketches the corresponding local bifurcation diagrams in the transcritical case when $\lambda'(0)\neq 0$, according to the sign of $\lambda'(0)$. The arcs of analytic curve filled in by exponentially asymptotically stable solutions have been plotted using continuous lines, whereas unstable solutions with one-dimensional unstable manifold are plotted using dashed lines. The λ-axis stands for the constant λ-curve $(\lambda,\mu,0,\theta_{[\mathfrak{L}_2,\mu,d]})$. Thanks to Theorem 7.1.1, this solution is linearly unstable if $\lambda>\Phi(\mu)$ and linearly stable if $\lambda<\Phi(\mu)$.

We end this section applying Theorems 6.3.1 and 6.4.1 to (7.7), with $\varepsilon>0$. As a direct consequence, the next result holds.

Theorem 7.1.6. *Suppose (7.7), with $\varepsilon>0$, has a coexistence state, (w,v). Then,*

$$\begin{aligned} \lambda > \varphi_\varepsilon(\mu) &\equiv \sigma_0\Big[\mathfrak{L}_1 + b\tfrac{\theta_{[\mathfrak{L}_2,\mu,d]}}{1+m\theta_{[\mathfrak{L}_1,\lambda,\varepsilon a]}},\mathfrak{B}_1,\Omega\Big], \\ \mu > \Psi_\varepsilon(\lambda) &\equiv \sigma_0\Big[\mathfrak{L}_2 - \varepsilon c\tfrac{\theta_{[\mathfrak{L}_1,\lambda,\varepsilon a]}}{1+m\theta_{[\mathfrak{L}_1,\lambda,\varepsilon a]}},\mathfrak{B}_2,\Omega\Big]. \end{aligned} \tag{7.23}$$

Conversely, under the following condition

$$\lambda > \Phi(\mu) \equiv \sigma_0\left[\mathfrak{L}_1 + b\theta_{[\mathfrak{L}_2,\mu,d]},\mathfrak{B}_1,\Omega\right] \quad \text{and} \quad \mu > \Psi_\varepsilon(\lambda), \tag{7.24}$$

the problem (7.7) has, at least, a coexistence state.

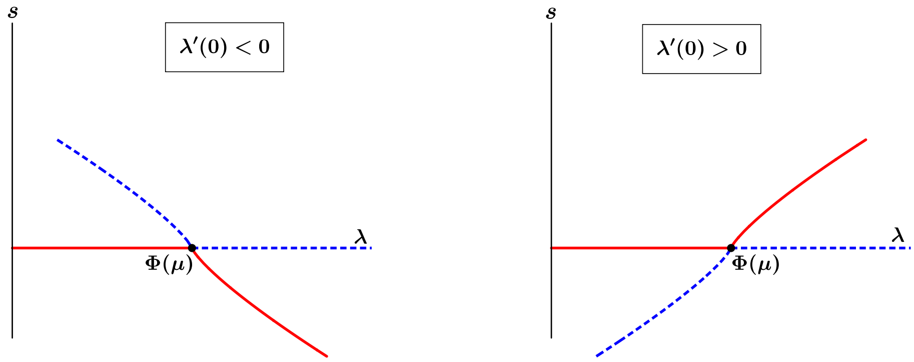

Figure 7.1: Stability of the solutions filling in the bifurcating branches

Since $\theta_{[\mathfrak{L}_2,\mu,d]}=0$ if $\mu\leq\sigma_{0,2}$, under this condition, both (7.23) and (7.24) become into

$$\lambda>\sigma_{0,1} \quad \text{and} \quad \mu>\Psi_\varepsilon(\lambda). \tag{7.25}$$

Therefore, (7.25) is not only necessary but also sufficient for the existence of a coexistence state if $\mu\leq\sigma_{0,2}$. Figure 7.2 sketches the construction of the wedges (7.23) and (7.24) given by Theorem 7.1.6. Note that, according to Theorem 6.1.1,

$$\varphi_\varepsilon(\mu)\equiv\sigma_0\left[\mathfrak{L}_1+b\tfrac{\theta_{[\mathfrak{L}_2,\mu,d]}}{1+m\theta_{[\mathfrak{L}_1,\lambda,\varepsilon a]}},\mathfrak{B}_1,\Omega\right]<\sigma_0[\mathfrak{L}_1+b\theta_{[\mathfrak{L}_2,\mu,d]},\mathfrak{B}_1,\Omega\Big]\equiv\Phi(\mu)$$

for all $\mu>\sigma_{0,2}$. More precisely, by Theorem 7.1.6, (7.7) has a coexistence state in the solid (dark) area of Figure 7.2, whereas outside the union of the solid and dashed patches of Figure 7.2, it cannot admit any coexistence state.

As already discussed by the authors in Section 6.3, the first picture of Figure 7.2 sketches the behavior of the curve $\mu=\Psi_\varepsilon(\lambda)$, $\lambda>\sigma_{0,1}$, when $m(x)>0$ for all $x\in\bar{\Omega}$, whereas the second picture shows it when $\Omega_0:=\operatorname{int}m^{-1}(0)$ is non-empty, which is the general case dealt with in this chapter. In the classical Holling–Tanner case when $m(x)>0$ for all $x\in\bar{\Omega}$, thanks to Theorem 6.1.2, it becomes apparent that for all $\lambda>\sigma_{0,1}$

$$\Psi_\varepsilon(\lambda)\equiv\sigma_0\left[\mathfrak{L}_2-\varepsilon c\tfrac{m\theta_{[\mathfrak{L}_1,\lambda,\varepsilon a]}}{m(1+m\theta_{[\mathfrak{L}_1,\lambda,\varepsilon a]})},\mathfrak{B}_2,\Omega\right]>\sigma_0\left[\mathfrak{L}_2-\frac{\varepsilon c}{m},\mathfrak{B}_2,\Omega\right],$$

as illustrated in the first picture of Figure 7.2. However, when the set $\Omega_0:=\operatorname{int}m^{-1}(0)$ is a nice (non-empty) open subset with $\bar{\Omega}_0\subset\Omega$, by [28, Pr. 3.2],

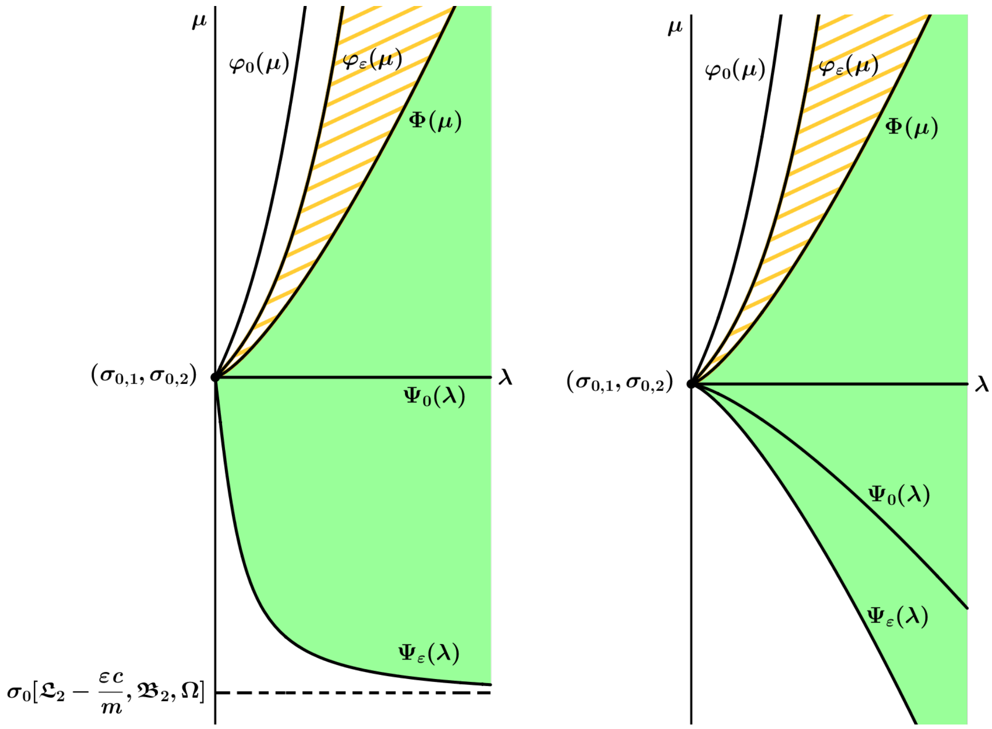

Figure 7.2: The coexistence regions of (7.7) according to Theorem 7.1.6

we have that

$$\Psi_\varepsilon(\lambda) \equiv \sigma_0\left[\mathfrak{L}_2 - \varepsilon c \tfrac{\theta_{[\mathfrak{L}_1,\lambda,\varepsilon a]}}{1+m\theta_{[\mathfrak{L}_1,\lambda,\varepsilon a]}}, \mathfrak{B}_2, \Omega\right] < \sigma_0\left[\mathfrak{L}_2 - \varepsilon c \theta_{[\mathfrak{L}_1,\lambda,\varepsilon a]}, \mathfrak{D}, \Omega_0\right],$$

where $\mathfrak{D}$ stands for the Dirichlet boundary operator on $\partial\Omega_0$. Thus,

$$\lim_{\lambda\uparrow\infty} \Psi_\varepsilon(\lambda) = -\infty \quad \text{for all } \ \varepsilon > 0,$$

as illustrated in the second picture of Figure 7.2, which is a behavior reminiscent of the one exhibited by the classical Lotka–Volterra model.

Since

$$\theta_{[\mathfrak{L}_1,\lambda,\varepsilon a]} = \varepsilon^{-1}\theta_{[\mathfrak{L}_1,\lambda,a]}, \tag{7.26}$$

it is apparent that

$$\begin{aligned}\lim_{\varepsilon\downarrow 0} \varphi_\varepsilon(\mu) &= \lim_{\varepsilon\downarrow 0} \sigma_0\left[\mathfrak{L}_1 + b\tfrac{\theta_{[\mathfrak{L}_2,\mu,d]}}{1+\frac{m}{\varepsilon}\theta_{[\mathfrak{L}_1,\lambda,a]}}, \mathfrak{B}_1, \Omega\right] \\ &= \sigma_0\left[\mathfrak{L}_1 + \left(1 - \chi_{\operatorname{int\,supp} m}\right) b(x)\theta_{[\mathfrak{L}_2,\mu,d]}, \mathfrak{B}_1, \Omega\right],\end{aligned}$$

where, for any subset $A \subset \mathbb{R}^N$, χ_A stands for the characteristic function of the set A, i.e., $\chi_A(x) = 1$ if $x \in A$, and $\chi_A(x) = 0$ if $x \in \mathbb{R}^N \setminus A$. In the next section, it will become apparent that the function

$$\varphi_0(\mu) := \sigma_0 \left[\mathfrak{L}_1 + \left(1 - \chi_{\mathrm{int\,supp}\, m}\right) b(x)\theta_{[\mathfrak{L}_2,\mu,d]}, \mathfrak{B}_1, \Omega\right], \qquad \mu > \sigma_{0,2}, \quad (7.27)$$

provides us with the left limiting curve to the region where the uncoupled model (7.8) possesses a coexistence state; recall that (7.8) is (7.7) with $\varepsilon = 0$. The curve $\lambda = \varphi_0(\mu)$ has been also plotted in Figure 7.2. According to Theorem 6.1.1, since

$$1 - \chi_{\mathrm{int\,supp}\, m} \lneq \tfrac{1}{1+m\theta_{[\mathfrak{L}_1,\lambda,\varepsilon a]}} \quad \text{in } \Omega,$$

it follows that, for every $\mu > \sigma_{0,2}$ and $\varepsilon > 0$,

$$\varphi_0(\mu) < \varphi_\varepsilon(\mu), \tag{7.28}$$

provided $bm \gneq 0$, as illustrated in Figure 7.2. Finally, note that, for every $\lambda > \sigma_{0,1}$,

$$\begin{aligned}\lim_{\varepsilon\downarrow 0} \Psi_\varepsilon(\lambda) &= \lim_{\varepsilon\downarrow 0} \sigma_0 \left[\mathfrak{L}_2 - c\tfrac{\theta_{[\mathfrak{L}_1,\lambda,a]}}{1+\frac{m}{\varepsilon}\theta_{[\mathfrak{L}_1,\lambda,a]}}, \mathfrak{B}_2, \Omega\right] \\ &= \sigma_0 \left[\mathfrak{L}_2 - \left(1 - \chi_{\mathrm{int\,supp}\, m}\right) c(x)\theta_{[\mathfrak{L}_1,\lambda,a]}, \mathfrak{B}_2, \Omega\right] \equiv \Psi_0(\lambda) \leq \sigma_{0,2}.\end{aligned}$$

Although $\Psi_0(\mu)$ can take different values depending on the distribution of the patches where $m(x)$ and $c(x)$ vanish, this does not affect the analysis of (7.8), for as the condition $\mu > \sigma_{0,2}$ is necessary for the existence of coexistence states.

7.2 The coexistence states of the limiting system (7.8)

This section determines the set of coexistence states of the limiting shadow problem (7.8). Since the component v satisfies

$$\begin{cases} \mathfrak{L}_2 v = \mu v - d(x)v^2 & \text{in } \Omega, \\ \mathfrak{B}_2 v = 0 & \text{on } \partial\Omega, \end{cases}$$

the condition $\mu > \sigma_{0,2} \equiv \sigma_0[\mathfrak{L}_2, \mathfrak{B}_2, \Omega]$ is imperative so that (7.8) can admit a coexistence state. Otherwise, $v = 0$ for any component-wise nonnegative solution, (w, v), of (7.8). Thus, throughout this section, we assume that $\mu > \sigma_{0,2}$. In such case, by Theorem 6.1.3, for every coexistence state (w, v)

of (7.8), necessarily $v=\theta_{[\mathfrak{L}_2,\mu,d]}\gg_2 0$, and $w\gg_1 0$ is a positive solution of the associated problem

$$\begin{cases} \mathfrak{L}_1 w = \lambda w - b(x)\theta_{[\mathfrak{L}_2,\mu,d]}\dfrac{w}{1+m(x)w} & \text{in } \Omega, \\ \mathfrak{B}_1 w = 0 & \text{on } \partial\Omega. \end{cases} \tag{7.29}$$

Note that, as soon as $b(x)$ and $m(x)$ have disjoint supports, i.e., $bm=0$, one has that

$$\left(1-\chi_{\mathrm{int\,supp}\,m}\right)b = \frac{b}{1+mw}$$

and, hence, (7.29) becomes into the linear problem

$$\begin{cases} \left[\mathfrak{L}_1 + \left(1-\chi_{\mathrm{int\,supp}\,m}\right)b\theta_{[\mathfrak{L}_2,\mu,d]}\right]w = \lambda w & \text{in } \Omega, \\ \mathfrak{B}_1 w = 0 & \text{on } \partial\Omega. \end{cases}$$

Therefore, when $bm=0$, (7.29) has a positive solution if, and only of, $\lambda = \varphi_0(\mu)$ (see (7.27)) and, in such case, w is a positive solution if, and only if, $w = sw_0$ for some $s>0$, where $w_0\gg_1 0$ stands for any principal eigenfunction associated to $\lambda=\varphi_0(\mu)$. The next result collects some useful properties of (7.29)

Lemma 7.2.1. *Suppose $w\neq 0$ is a positive solution of (7.29). Then, $w\gg_1 0$ and*

$$\lambda = \sigma_0\left[\mathfrak{L}_1 + \tfrac{b(x)\theta_{[\mathfrak{L}_2,\mu,d]}}{1+m(x)w}, \mathfrak{B}_1, \Omega\right]. \tag{7.30}$$

Thus,

$$\sigma_{0,1}\le \varphi_0(\mu)\le\lambda<\Phi(\mu), \tag{7.31}$$

where $\varphi_0(\mu)$ and $\Phi(\mu)$ are the functions defined in (7.27) and (7.24), respectively. More precisely,

$$\begin{cases} \sigma_{0,1}\le\varphi_0(\mu)<\lambda<\Phi(\mu) & \text{if } bm \gneq 0, \\ \sigma_{0,1}<\varphi_0(\mu)=\lambda<\Phi(\mu) & \text{if } bm=0. \end{cases}$$

In other words, either (λ,μ) lies in the wedges region between the curves $\varphi_0(\mu)$ and $\Phi(\mu)$ in Figure 7.2 if $bm\gneq 0$, or $\lambda=\varphi_0(\mu)$ if $bm=0$.

Proof. Since

$$\left(\mathfrak{L}_1 + \tfrac{b(x)\theta_{[\mathfrak{L}_2,\mu,d]}}{1+m(x)w}\right)w = \lambda w \quad \text{in } \Omega,$$

and $\mathfrak{B}_1 w = 0$, with $w\gneq 0$, the identity (7.30) is a direct consequence of the uniqueness of σ_0, and $w\gg_1 0$, by the properties of the positive principal eigenfunctions.

On the other hand, by our assumptions on $m(x)$,

$$1-\chi_{\mathrm{int\,supp}\,m} \lneq \frac{1}{1+mw} \quad \text{in } \ \Omega.$$

Thus, since $b\theta_{[\mathfrak{L}_2,\mu,d]} \gneq 0$, it is apparent that

$$0 \leq \left(1-\chi_{\mathrm{int\,supp}\,m}\right) b\theta_{[\mathfrak{L}_2,\mu,d]} \leq \frac{b\theta_{[\mathfrak{L}_2,\mu,d]}}{1+mw} \lneq b\theta_{[\mathfrak{L}_2,\mu,d]} \quad \text{in } \ \Omega. \tag{7.32}$$

Therefore, by (7.32) and Theorem 6.1.1, (7.31) holds.

Now, note that $\varphi_0(\mu)=\lambda$ unless $b(x)>0$ for some $x\in \mathrm{supp}\,m$. Thus, $\varphi_0(\mu)<\lambda$ if $bm \gneq 0$, and $\varphi_0(\mu)=\lambda>\sigma_{0,1}$ if $bm=0$. Moreover, in case $bm\gneq 0$, we have that, for every $\mu>\sigma_{0,2}$,

$$\varphi_0(\mu)=\sigma_0\left[\mathfrak{L}_1+\left(1-\chi_{\mathrm{int\,supp}\,m}\right)b\theta_{[\mathfrak{L}_2,\mu,d]},\mathfrak{B}_1,\Omega\right]=\sigma_{0,1}$$

if, and only if,

$$\left(1-\chi_{\mathrm{int\,supp}\,m}\right) b=0,$$

and this occurs provided $m(x)>0$ for all $x\in\Omega$, like in the Holling–Tanner model, or $m^{-1}(0)\subset b^{-1}(0)\neq\emptyset$, i.e., $\mathrm{supp}\ b\subset \mathrm{supp}\ m\neq\emptyset$. This ends the proof. □

It should not be forgotten that throughout this chapter we are assuming that $m=0$ in $\bar\Omega_0$ but $m\gneq 0$. Therefore, we are in a rather hybrid (different) situation between the Lotka–Volterra and the Holling–Tanner models.

Throughout the rest of this chapter, we will assume that $bm\gneq 0$, even if not expressed within text. This entails that $\varphi_0(\mu)<\lambda<\Phi(\mu)$ if (7.29) has some positive solution. The next results collects two important qualitative properties of the positive solutions of (7.29).

Lemma 7.2.2. *Let $\{(\lambda_n,w_n)\}_{n\geq 1}$ be a sequence of positive solutions of (7.29) such that*

$$\lim_{n\to+\infty}\lambda_n=\lambda_*.$$

Then $\lambda^*\in[\varphi_0(\mu),\Phi(\mu)]$. Moreover:

(a) $\lim_{n\to\infty}\|w_n\|_\infty=+\infty$ *if, and only if,* $\lambda_*=\varphi_0(\mu)$;

(b) $\lim_{n\to\infty}\|w_n\|_\infty=0$ *if, and only if,* $\lambda_*=\Phi(\mu)$.

Proof. By (7.31), necessarily,

$$\varphi_0(\mu)<\lambda_n<\Phi(\mu)\quad \text{for all } \ n\geq 1. \tag{7.33}$$

Thus, letting $n \to \infty$, yields to $\lambda^* \in [\varphi_0(\mu), \Phi(\mu)]$. Now, in order to prove the necessity of Part (a), suppose that

$$\lim_{n\to+\infty} \|w_n\|_\infty = +\infty. \tag{7.34}$$

Then, by expressing (7.29) as a fixed point equation and dividing by $\|w_n\|_\infty$, it becomes apparent that, for every $e > \sigma_{0,1}$ and $n \geq 1$,

$$\frac{w_n}{\|w_n\|_\infty} = (\mathfrak{L}_1 + e)^{-1}\Big[(\lambda_n + e)\frac{w_n}{\|w_n\|_\infty} - b\theta_{[\mathfrak{L}_2,\mu,d]}\frac{w_n}{\|w_n\|_\infty(1+m\frac{w_n}{\|w_n\|_\infty}\|w_n\|_\infty)}\Big]. \tag{7.35}$$

Since the sequence of continuous functions

$$(\lambda_n + e)\frac{w_n}{\|w_n\|_\infty} - b\theta_{[\mathfrak{L}_2,\mu,d]}\frac{w_n}{\|w_n\|_\infty(1+m\frac{w_n}{\|w_n\|_\infty}\|w_n\|_\infty)}, \qquad n \geq 1,$$

is bounded in $\mathcal{C}(\bar\Omega)$ and $(\mathfrak{L}_1+e)^{-1}$ is a compact operator, it follows from (7.35) that there exists $\psi \in \mathcal{C}^1_{\mathfrak{B}_1}(\bar\Omega)$ such that, along some subsequence, labeled by n_ℓ,

$$\lim_{\ell\to+\infty} \frac{w_{n_\ell}}{\|w_{n_\ell}\|_\infty} = \psi \quad \text{in } \mathcal{C}^1_{\mathfrak{B}_1}(\bar\Omega). \tag{7.36}$$

By (7.36), $\psi \gneq 0$ and $\|\psi\|_\infty = 1$. Moreover, by elliptic regularity, particularizing (7.35) at $n = n_\ell$ and letting $\ell \to +\infty$ in the resulting identity, shows that $\psi \in U_1$ and that it solves the problem

$$\begin{cases} \Big[\mathfrak{L}_1 + (1-\chi_{\operatorname{int}\operatorname{supp} m})b\theta_{[\mathfrak{L}_2,\mu,d]}\Big]\psi = \lambda_*\psi & \text{in } \Omega, \\ \mathfrak{B}_1\psi = 0 & \text{on } \partial\Omega. \end{cases} \tag{7.37}$$

From (7.37) it is apparent that $\psi \gg_1 0$ and that

$$\lambda_* = \sigma_0\Big[\mathfrak{L}_1 + (1-\chi_{\operatorname{int}\operatorname{supp} m})b\theta_{[\mathfrak{L}_2,\mu,d]}, \mathfrak{B}_1, \Omega\Big] \equiv \varphi_0(\mu).$$

This shows that, indeed, $\lambda_* = \varphi_0(\mu)$ if (7.34) holds.

Adapting the previous argument, it is easily seen that

$$\lim_{n\to+\infty} \|w_n\|_\infty = 0 \tag{7.38}$$

guarantees the existence of some $\psi \in U_1$, with $\|\psi\|_\infty = 1$, such that

$$\begin{cases} \Big(\mathfrak{L}_1 + b\theta_{[\mathfrak{L}_2,\mu,d]}\Big)\psi = \lambda_*\psi & \text{in } \Omega, \\ \mathfrak{B}_1\psi = 0 & \text{on } \partial\Omega. \end{cases}$$

Therefore, (7.38) implies that

$$\lambda_* = \sigma_0[\mathfrak{L}_1 + b\theta_{[\mathfrak{L}_2,\mu,d]}, \mathfrak{B}_1, \Omega] \equiv \Phi(\mu),$$

which ends the proof of the necessity in Part (b).

To prove the sufficiency in Part (a), assume that $\lambda_* = \varphi_0(\mu)$ and that (7.34) fails. Then, there exists a constant, $C > 0$, such that, along some subsequence of $\{w_n\}_{n\geq 1}$,

$$\|w_{n_\ell}\|_\infty \leq C \quad \text{for all } \ \ell \geq 1. \tag{7.39}$$

By the necessity of Part (b), $\{w_{n_\ell}\}_{n\geq 1}$ cannot admit any subsequence converging to zero in $\mathcal{C}(\bar{\Omega})$, because, in such case, $\varphi_0(\mu) = \lambda_* = \Phi(\mu)$, which contradicts $\varphi_0(\mu) < \Phi(\mu)$ (see (7.33)). On the other hand, since

$$w_{n_\ell} = (\mathfrak{L}_1 + e)^{-1}\left[(\lambda_{n_\ell} + e)w_{n_\ell} - b\theta_{[\mathfrak{L}_2,\mu,d]}\frac{w_{n_\ell}}{1+mw_{n_\ell}}\right] \quad \text{for all } \ \ell \geq 1 \tag{7.40}$$

and, due to (7.39), the sequence

$$(\lambda_{n_\ell} + e)w_{n_\ell} - b\theta_{[\mathfrak{L}_2,\mu,d]}\frac{w_{n_\ell}}{1+mw_{n_\ell}}, \qquad \ell \geq 1,$$

is bounded, by the compactness of $(\mathfrak{L}_1 + e)^{-1}$, we can extract a subsequence of $\{w_{n_\ell}\}_{n\geq 1}$, relabeled by n_ℓ, such that, for some $\Psi \in \mathcal{C}^1_{\mathfrak{B}_1}(\bar{\Omega})$,

$$\lim_{\ell\to\infty} w_{n_\ell} = \Psi \quad \text{in } \ \mathcal{C}^1_{\mathfrak{B}_1}(\bar{\Omega}). \tag{7.41}$$

As we already know that $\{w_{n_\ell}\}_{n\geq 1}$ cannot converge to zero in $\mathcal{C}(\bar{\Omega})$, it becomes apparent that $\Psi \gneq 0$. Moreover, letting $\ell \to \infty$ in (7.40) shows that

$$\Psi = (\mathfrak{L}_1 + e)^{-1}\left[(\varphi_0(\mu) + e)\Psi - b\theta_{[\mathfrak{L}_2,\mu,d]}\frac{\Psi}{1+m\Psi}\right] \quad \text{for all } \ \ell \geq 1. \tag{7.42}$$

By elliptic regularity, it follows from (7.42) that $\Psi \in U_1$ and that it provides us with a positive solution of

$$\begin{cases} \left(\mathfrak{L}_1 + \frac{b\theta_{[\mathfrak{L}_2,\mu,d]}}{1+m\Psi}\right)\Psi = \varphi_0(\mu)\Psi & \text{in } \ \Omega, \\ \mathfrak{B}_1\Psi = 0 & \text{on } \ \partial\Omega. \end{cases}$$

Therefore, $\Psi \gg_1 0$ and, by the uniqueness of σ_0, it becomes apparent that

$$\varphi_0(\mu) = \sigma_0\left[\mathfrak{L}_1 + \tfrac{b\theta_{[\mathfrak{L}_2,\mu,d]}}{1+m\Psi}, \mathfrak{B}_1, \Omega\right]. \tag{7.43}$$

On the other hand, since $bm \gneq 0$,

$$\left(1-\chi_{\text{int supp } m}\right) b \lneq \tfrac{b}{1+m\Psi} \quad \text{in } \; \Omega,$$

it follows from Theorem 6.1.1 and the definition of $\varphi_0(\mu)$ that, for every $\mu > \sigma_{0,2}$,

$$\varphi_0(\mu) := \sigma_0\left[\mathfrak{L}_1 + \left(1-\chi_{\text{int supp } m}\right) b\theta_{[\mathfrak{L}_2,\mu,d]}, \mathfrak{B}_1, \Omega\right] < \sigma_0\left[\mathfrak{L}_1 + \tfrac{b\theta_{[\mathfrak{L}_2,\mu,d]}}{1+m\Psi}, \mathfrak{B}_1, \Omega\right].$$

As this estimate contradicts (7.43), (7.39) fails. Therefore, (7.34) holds. This ends the proof of Part (a).

To complete the proof of Part (b), suppose that $\lambda_* = \Phi(\mu)$. Then, since $\varphi_0(\mu) < \Phi(\mu)$ for all $\mu > \sigma_{0,2}$, it follows from Part (a) that there exists a constant $C > 0$ such that

$$\|w_n\|_\infty \leq C \quad \text{for all } \; n \geq 1. \tag{7.44}$$

In such case, adapting the previous compactness arguments, it becomes apparent that there exist $\Psi \in U_1$, with $\Psi \geq 0$, and a subsequence of $\{w_n\}_{n\geq 1}$, relabeled by n_ℓ, $\ell \geq 1$, such that (7.41) holds. Thus, since $\lambda_* = \Phi(\mu)$, necessarily

$$\begin{cases} \left(\mathfrak{L}_1 + \frac{b\theta_{[\mathfrak{L}_1,\mu,d]}}{1+m\Psi}\right)\Psi = \Phi(\mu)\Psi & \text{in } \; \Omega, \\ \mathfrak{B}_1\Psi = 0 & \text{on } \; \partial\Omega. \end{cases} \tag{7.45}$$

Suppose that $\Psi \gneq 0$. Then, $\Psi \gg_1 0$ and (7.45) implies that

$$\Phi(\mu) = \sigma_0\left[\mathfrak{L}_1 + \tfrac{b\theta_{[\mathfrak{L}_1,\mu,d]}}{1+m\Psi}, \mathfrak{B}_1, \Omega\right]. \tag{7.46}$$

On the other hand, by Theorem 6.1.2 and the definition of $\Phi(\mu)$, we have that

$$\Phi(\mu) \equiv \sigma_0[\mathfrak{L}_1 + b\theta_{[\mathfrak{L}_2,\mu,d]}, \mathfrak{B}_1, \Omega\Big] > \sigma_0\left[\mathfrak{L}_1 + \tfrac{b\theta_{[\mathfrak{L}_1,\mu,d]}}{1+m\Psi}, \mathfrak{B}_1, \Omega\right],$$

which contradicts (7.46). Thus, $\Psi = 0$ and hence,

$$\lim_{\ell\to\infty} w_{n_\ell} = 0 \quad \text{in } \; \mathcal{C}^1_{\mathfrak{B}_1}(\bar{\Omega}). \tag{7.47}$$

As this argument can be repeated along any subsequence of $\{w_n\}_{n\geq 1}$, Part (b) holds. This ends the proof of the lemma. □

Particularizing (7.16) at $\varepsilon = 0$ yields to

$$\mathfrak{F}_0(\lambda,\mu,w,v) \equiv \mathfrak{F}(\lambda,\mu,0,w,v) := \begin{pmatrix} w - (\mathfrak{L}_1+e)^{-1}\left[(\lambda+e)w - b\frac{wv}{1+mw}\right] \\ v - (\mathfrak{L}_2+e)^{-1}\left[(\mu+e)v - dv^2\right] \end{pmatrix}.$$

As the v-component component of $\mathfrak{F}_0(\lambda,\mu,w,v)$ vanishes at $v=\theta_{[\mathfrak{L}_2,\mu,d]}$, it becomes apparent that w is a positive solution of (7.29) if, and only if, the w-component of

$$\mathfrak{F}_0(\lambda,\mu,w,\theta_{[\mathfrak{L}_2,\mu,d]}) := \begin{pmatrix} w-(\mathfrak{L}_1+e)^{-1}\left[(\lambda+e)w-b\theta_{[\mathfrak{L}_2,\mu,d]}\frac{w}{1+mw}\right] \\ 0 \end{pmatrix},$$

vanishes. Naturally, this is also a rather direct consequence of (7.29). Therefore, when applying Theorem 7.1.3 to (7.8) at $\varepsilon=0$ it becomes apparent that $v(s)=\theta_{[\mathfrak{L}_2,\mu,d]}$ and that $\mathfrak{F}_0(\lambda(s),\mu,w(s),\theta_{[\mathfrak{L}_2,\mu,d]})=0$ for all $s\in(-\delta,\delta)$. Moreover, particularizing (7.17) at $\varepsilon=0$ provides us with

$$\lambda'(0)=-\int_\Omega b\theta_{[\mathfrak{L}_2,\mu,d]}w_1^2w_1^*<0. \tag{7.48}$$

Therefore, there is a bifurcation to positive solutions of (7.29) from $(w,v)=(0,\theta_{[\mathfrak{L}_2,\mu,d]})$ at $\lambda=\Phi(\mu)$ and the bifurcation is subcritical, because of (7.48), or (7.31). Naturally, this entails the existence of an $\varepsilon_0>0$ such that $\lambda'(0)<0$ in (7.7) if $|\varepsilon|<\varepsilon_0$.

Subsequently, we denote by $\mathscr{S}_0$ the set of nontrivial solutions of (7.29) defined by

$$\begin{aligned}\mathscr{S}_0 :=&\{(\lambda,\mu,w,\theta_{[\mathfrak{L}_2,\mu,d]})\in\mathfrak{F}_0^{-1}(0)\;:\;w\neq 0\}\\ &\cup\{(\lambda,\mu,0,\theta_{[\mathfrak{L}_2,\mu,d]})\;:\;\lambda\in\Sigma(\mathscr{L}(\lambda,0))\},\end{aligned}$$

where $\Sigma(\mathscr{L}(\lambda,0))$ stands for the generalized spectrum of the Fredholm curve $\mathscr{L}(\lambda,0)$ introduced in the proof of Theorem 7.1.3. And $\mathscr{C}_0^+$ stands for the subcomponent of positive solutions of $\mathscr{S}_0$ such that $(\Phi(\mu),\mu,0,\theta_{[\mathfrak{L}_2,\mu,d]})\in\bar{\mathscr{C}}_0^+$. The next result provides us with some useful properties of $\mathscr{C}_0^+$. We are denoting by $\mathcal{P}_\lambda$ the λ-projection operator,

$$\mathcal{P}_\lambda(\lambda,\mu,w,\theta_{[\mathfrak{L}_2,\mu,d]})=\lambda.$$

Theorem 7.2.3. *The component $\mathscr{C}_0^+$ satisfies*

$$\mathcal{P}_\lambda(\mathscr{C}_0^+)=(\varphi_0(\mu),\Phi(\mu)). \tag{7.49}$$

Moreover, for every sequence of positive solutions in the component $\mathscr{C}_0^+$, $\{(\lambda_n,\mu,w_n,\theta_{[\mathfrak{L}_2,\mu,d]})\}_{n\geq1}$, such that $\lim_{n\to\infty}\lambda_n=\varphi_0(\mu)$, necessarily

$$\lim_{n\to\infty}\|w_n\|_\infty=+\infty. \tag{7.50}$$

In other words, $\mathscr{C}_0^+$ is unbounded at $\lambda=\varphi_0(\mu)$.

Proof. Owing to Lemma 7.2.2(b), $(\Phi(\mu), \mu, 0, \theta_{[\mathfrak{L}_2,\mu,d]})$ is the unique bifurcation point to positive solutions from $(\lambda, \mu, 0, \theta_{[\mathfrak{L}_2,\mu,d]})$. The existence of $\mathscr{C}_0^+$ follows from Theorem 7.1.3 and the Zorn–Kuratowski lemma. By [124, Th.7.1.3], $\mathscr{C}_0^+$ is unbounded in $\mathbb{R}^2 \times \mathcal{C}(\bar{\Omega})$. Since $\mu > \sigma_{0,2}$ is fixed and, due to Lemma 7.2.1, $\lambda \in (\varphi_0(\lambda), \Phi(\mu))$ if $bm \gneq 0$, $\mathscr{C}_0^+$ must be unbounded in w. Thus, thanks to Lemma 7.2.2(a), (7.49) and (7.50) hold. □

The next result provides us with the fine structure of the component $\mathscr{C}_0^+$ near $\lambda = \Phi(\mu)$ and $\lambda = \varphi_0(\mu)$. It is a pivotal result in getting the main multiplicity result of this chapter for (7.8) with sufficiently small $\varepsilon > 0$.

Theorem 7.2.4. *In a neighborhood of* $(\lambda, \mu, w, \theta_{[\mathfrak{L}_2,\mu,d]}) = (\Phi(\mu), \mu, 0, \theta_{[\mathfrak{L}_2,\mu,d]})$ *in* $\mathbb{R} \times \mathbb{R} \times U_1 \times \{\theta_{[\mathfrak{L}_2,\mu,d]}\}$, *the component* $\mathscr{C}_0^+$ *consists of the analytic curve* $(\lambda(s), \mu, w(s), \theta_{[\mathfrak{L}_2,\mu,d]})$ *given by Theorem 7.1.3. Moreover, the following properties are satisfied:*

(a) *For sufficiently small* $r > 0$ *and every* $\lambda \in [\Phi(\mu) - r, \Phi(\mu))$, (7.29) *has a unique positive solution, which is linearly unstable with one-dimensional unstable manifold.*

(b) *There exists* $r > 0$ *such that, for every* $\lambda \in (\varphi_0(\mu), \varphi_0(\mu)+r]$, (7.29) *has a unique positive solution,* $(\lambda, \mu, w_\lambda, \theta_{[\mathfrak{L}_2,\mu,d]})$, *which is non-degenerate. Thus, for these values of* λ, $\mathscr{C}_0^+$ *consists of an analytic curve of positive solutions bifurcating from* $+\infty$ *at* $\lambda = \varphi_0(\mu)$, *in the sense that*

$$\lim_{\lambda \downarrow \varphi_0(\mu)} w_\lambda(x) = +\infty \quad \text{for all } x \in \Omega. \tag{7.51}$$

Furthermore, these solutions have local Poincaré index -1, *calculated through the Leray–Schauder degree.*

Proof. According to (7.48), $\mathscr{C}_0^+$ bifurcates subcritically from $w = 0$ at $\lambda = \Phi(\mu)$. Combining this feature together with the uniqueness of the bifurcated curve in Theorem 7.1.3 and Lemma 7.2.2 (b), it becomes apparent the existence of a $r > 0$ such that (7.29) has a unique solution for each $\lambda \in [\Phi(\mu) - r, \Phi(\mu))$. The fact that $\mathscr{C}_0^+$ is analytic for λ sufficiently close to $\Phi(\mu)$ is a byproduct of Theorem 7.1.3, since $\mathscr{C}_0^+$ can be parameterized by λ, and $\mathfrak{F}$, or $\mathfrak{F}_0$, is an analytic function of λ. Furthermore, since $\lambda'(0) < 0$, it follows from Theorem 7.1.5 that, for sufficiently small $r > 0$ and every $\lambda \in [\Phi(\mu) - r, \Phi(\mu))$, the positive solution $(\lambda, \mu, w(\lambda))$ is linearly unstable with one-dimensional unstable manifold. In particular, by the Schauder formula, its local index as a fixed point of the compact operator $I - \mathfrak{F}_0$ equals -1.

On the other hand, by Lemma 7.2.2 (a), for every $\lambda \in (\varphi_0(\mu), \Phi(\mu))$, there exists $M_\lambda > 0$ such that any positive solution, $(\tilde{\lambda}, \tilde{w})$, of (7.29) with $\tilde{\lambda} \in [\lambda, \Phi(\mu))$ satisfies

$$\tilde{w} \in W_\lambda := \{w \in U_1 \, : \, 0 < \|w\|_\infty < M_\lambda\}\,.$$

Thus, combining the homotopy invariance with the excision property of the Leray–Schauder degree, it becomes apparent that

$$\mathrm{Deg}\,(\mathfrak{F}_0(\tilde{\lambda}, \mu, \cdot), W_\lambda) = \mathrm{Deg}\,(\mathfrak{F}_0(\Phi(\mu) - \tfrac{r}{2}, \mu, \cdot), W_\lambda) = -1$$

for all $\tilde{\lambda} \in [\lambda, \Phi(\mu))$. In particular,

$$\mathrm{Deg}\ (\mathfrak{F}_0(\lambda, \mu, \cdot,), W_\lambda) = -1 \quad \text{for all } \ \lambda \in (\varphi_0(\mu), \Phi(\mu)). \tag{7.52}$$

Therefore, for every $\lambda \in (\varphi_0(\mu), \Phi(\mu))$, the total sum of the local Poincaré indices of the (7.29) positive solutions, calculated through the Leray–Schauder degree, equals -1.

Subsequently, we will carry out the (sharp) analysis of $\mathscr{C}_0^+$ in a neighborhood of $\lambda = \varphi_0(\mu)$. Let $\{(\lambda_n, w_n)\}_{n\geq 1}$ be a sequence of positive solutions of $\mathscr{C}_0^+$ such that

$$\lim_{n\to+\infty} \lambda_n = \varphi_0(\mu). \tag{7.53}$$

Then, by Lemma (7.2.2) (a), we already know that

$$\lim_{n\to\infty} \|w_n\|_\infty = +\infty.$$

Note that, in particular, this implies that $\lim_{n\to\infty} M_{\lambda_n} = +\infty$. Moreover, according to the proof of Lemma (7.2.2) (a), there exists a subsequence, labeled again by n, such that

$$\lim_{n\to+\infty} \frac{w_n}{||w_n||_\infty} = \psi$$

for some $\psi \in U_1$ solving (7.37). Since $\psi \gg_1 0$ is a principal eigenfunction associated with $\varphi_0(\mu)$, it becomes apparent that

$$\lim_{n\to+\infty} w_n(x) = +\infty \quad \text{for all } \ x \in \Omega. \tag{7.54}$$

As this holds for every sequence of positive solutions, once established the uniqueness of w_λ, (7.51) holds. In order to prove the uniqueness of the positive solution for λ in a right-neighborhood of $\varphi_0(\mu)$, we will show that, for sufficiently large n, (λ_n, w_n) must be non-degenerate with a one-dimensional unstable manifold. Thanks again to the Schauder formula, this entails that the local index of these positive solutions equals -1 and therefore, combining (7.52) with the additivity property of the Leray–Schauder degree, (7.29) has a unique positive solution for λ sufficiently close to $\varphi_0(\lambda)$, denoted by $(\lambda,\mu,w_\lambda,\theta_{[\mathfrak{L}_2,\mu,d]})$ in the statement of the theorem. According to (7.49), necessarily $(\lambda,\mu,w_\lambda,\theta_{[\mathfrak{L}_2,\mu,d]})\in\mathscr{C}_0^+$ for $\lambda\sim\varphi_0(\mu)$.

The spectrum of the linearization of $\mathfrak{F}_0$ at $(\lambda_n,\mu,w_n,\theta_{[\mathfrak{L}_2,\mu,d]})$ is given by the eigenvalues of the boundary value problem

$$\begin{cases} \left(\mathfrak{L}_1+b\dfrac{\theta_{[\mathfrak{L}_2,\mu,d]}}{(1+mw_n)^2}-\lambda_n\right)w=\tau w & \text{in } \Omega,\\ \mathfrak{B}_1 w=0 & \text{on } \partial\Omega.\end{cases}$$

Since $1+mw_n\gneq 1$ for all $n\geq 1$, it follows from Theorem 6.1.1 and the identity (7.30) applied to $(\lambda,w)=(\lambda_n,w_n)$ that, for every $n\geq 1$,

$$\begin{aligned}\tau_0(n)&\equiv\sigma_0\left[\mathfrak{L}_1+b\tfrac{\theta_{[\mathfrak{L}_2,\mu,d]}}{(1+mw_n)^2}-\lambda_n,\mathfrak{B}_1,\Omega\right]\\ &<\sigma_0\left[\mathfrak{L}_1+b\tfrac{\theta_{[\mathfrak{L}_2,\mu,d]}}{1+mw_n},\mathfrak{B}_1,\Omega\right]-\lambda_n=0.\end{aligned}\tag{7.55}$$

On the other hand, it follows from (7.54) that

$$\lim_{n\to+\infty}\frac{b\theta_{[\mathfrak{L}_2,\mu,d]}}{(1+mw_n)^2}=\left(1-\chi_{\operatorname{int}\operatorname{supp} m}\right)b\theta_{[\mathfrak{L}_2,\mu,d]}.$$

Thus, thanks to (7.27) and (7.53), by letting $n\to\infty$ in (7.55), we find that

$$\lim_{n\to+\infty}\tau_0(n)=\varphi_0(\mu)-\varphi_0(\mu)=0,\tag{7.56}$$

though, due to (7.55), $\tau_0(n)<0$ for all $n\geq 1$. Similarly, by the strict dominance of the principal eigenvalues, any other eigenvalue, say $\tau_j(n)$, $j\geq 1$, satisfies

$$\lim_{n\to\infty}\operatorname{Re}\tau_j(n)=\operatorname{Re}\sigma_j\left[\mathfrak{L}_1+\left(1-\chi_{\operatorname{int}\operatorname{supp} m}\right)b\theta_{[\mathfrak{L}_2,\mu,d]},\mathfrak{B}_1,\Omega\right]-\varphi_0(\mu)>0.$$

Therefore, there exists $r>0$ such that any positive solution, (λ,w), of (7.29) with $\lambda\in(\varphi_0(\mu),\varphi_0(\mu)+r]$ is non-degenerate with one-dimensional unstable manifold. This ends the proof. □

Figure 7.3 shows an admissible component $\mathscr{C}_0^+$ of positive solutions of (7.29) respecting Theorems 7.2.3 and 7.2.4. Although (7.29) has a unique positive solution for λ sufficiently close to either $\Phi(\mu)$, or $\varphi_0(\mu)$, the problem might possess an arbitrarily large number of positive solutions for some intermediate range of values of the parameter λ, as illustrated in Figure 7.3.

Actually, besides $\mathscr{C}_0^+$, (7.29) might have some additional component of positive solutions not plotted in the figure. In spite of all these circumstances, thanks to Theorems 7.2.3 and 7.2.4, near the ends of the existence interval, $(\varphi_0(\mu), \Phi(\mu))$, the unique positive solution of (7.29) must be unstable with one-dimensional unstable manifold. It remains an open problem in this chapter to analyze the fine structure of the global bifurcation diagram.

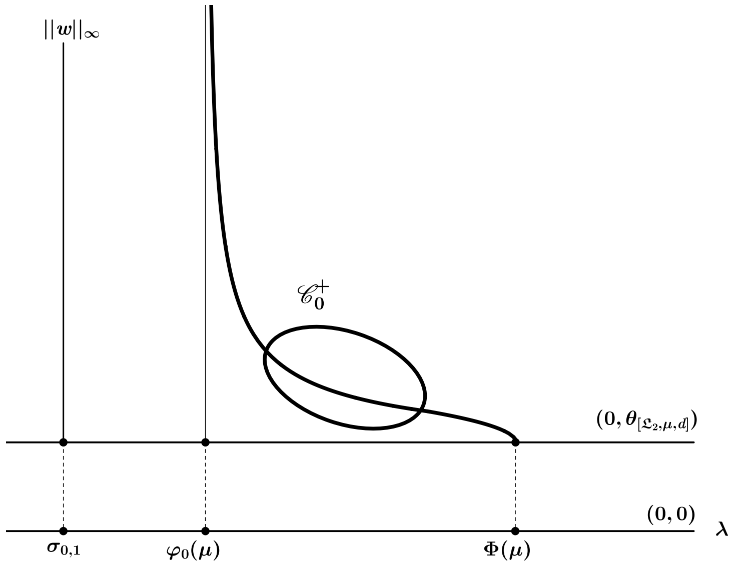

Figure 7.3: An admissible component $\mathscr{C}_0^+$ in case $bm \gneq 0$

7.3 An optimal multiplicity result for the original model

The next multiplicity result is the main theorem of this section. Remember that, owing to Theorem 7.1.6, for every $\mu > \sigma_{0,2}$, (7.7) has a coexistence state if $\lambda > \Phi(\mu)$. Moreover, in such case, $\lambda > \varphi_\varepsilon(\mu)$, because $\Phi(\mu) > \varphi_\varepsilon(\mu)$.

Theorem 7.3.1. *Fix $\lambda^* \in (\varphi_0(\mu), \Phi(\mu))$. Then, there exists $\varepsilon_0 \equiv \varepsilon_0(\lambda^*) > 0$ such that, for every $\varepsilon \in (0, \varepsilon_0)$, (7.7) possesses a component $\mathscr{C}_\varepsilon^+$ of coexistence states satisfying the following properties:*

(a) *$\mathcal{P}_\lambda(\mathscr{C}_\varepsilon^+) = [\lambda_T, +\infty)$ for some $\lambda_T \equiv \lambda_T(\varepsilon) \in (\varphi_\varepsilon(\mu), \lambda^*)$.*

(b) *For every $\lambda \in [\lambda^*, \Phi(\mu))$, (7.7) has, at least, two (different) coexistence states.*

(c) *$\mathscr{C}_\varepsilon^+$ is an analytic λ-curve in a neighborhood of the point* $(\lambda,\mu,w,v) = (\Phi(\mu),\mu,0,\theta_{[\mathfrak{L}_2,\mu,d]})$.

Naturally, $\mathscr{C}_\varepsilon^+$ is the perturbation of the component $\mathscr{C}_0^+$ constructed in Section 4 as $\varepsilon > 0$ leaves $\varepsilon = 0$. It turns out that, as ε perturbs from zero, the component $\mathscr{C}_0^+$ bends backwards towards the right providing us with a perturbed component like the one sketched in Figure 7.4.

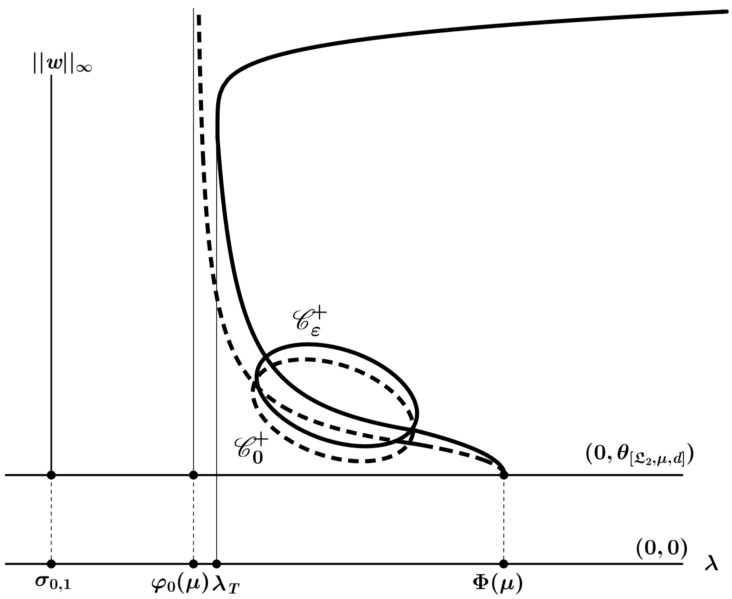

Figure 7.4: The components $\mathscr{C}_0^+$ (dashed line) and $\mathscr{C}_\varepsilon^+$ (solid line) for small $\varepsilon > 0$

The proof of Theorem 7.3.1 is based on Theorem 7.2.4, Theorem 7.2.2 of [124], and on the existence of a priori bounds for the coexistence states of (7.7) established by the following lemma.

Lemma 7.3.2. *Suppose $\varepsilon > 0$ and let (w,v) be a coexistence state of (7.7). Then,*

$$0 \ll_1 w \ll_1 \theta_{[\mathfrak{L}_1,\lambda,\varepsilon a]}, \qquad \theta_{[\mathfrak{L}_2,\mu,d]} \ll_2 v \ll_2 \theta_{\left[\mathfrak{L}_2,\mu+\varepsilon c\frac{\theta_{[\mathfrak{L}_1,\lambda,\varepsilon a]}}{1+m\theta_{[\mathfrak{L}_1,\lambda,\varepsilon a]}},d\right]}. \tag{7.57}$$

Proof. Since $w \gneq 0$, by the uniqueness of the principal eigenvalue, it follows from the w-equation of (7.7) that $w \gg_1 0$ and that

$$\lambda = \sigma_0\left[\mathfrak{L}_1 + \varepsilon a w + b\frac{v}{1+mw}, \mathfrak{B}_1, \Omega\right].$$

Moreover, it follows from $w \gg_1 0$ that

$$\mathfrak{L}_1 w = \lambda w - \varepsilon a w^2 - b\frac{wv}{1+mw} \lneq \lambda w - \varepsilon a w^2.$$

Thus, w is a positive strict subsolution of the problem

$$\begin{cases} \mathfrak{L}_1 w = \lambda w - \varepsilon a(x) w^2 & \text{in } \ \Omega, \\ \mathfrak{B}_1 w = 0 & \text{on } \ \partial\Omega. \end{cases}$$

Hence, since $\lambda > \sigma_{0,1}$, it follows from Theorem 6.1.4 that

$$w \ll_1 \theta_{[\mathfrak{L}_1,\lambda,\varepsilon a]}. \tag{7.58}$$

This completes the proof of the first two estimates of (7.57). Similarly, by (7.58),

$$\begin{aligned} \mu v - d v^2 \lneq \mathfrak{L}_2 v &= \mu v - d v^2 + \varepsilon c \frac{wv}{1+mw} \\ &\lneq \left(\mu + \varepsilon c \frac{\theta_{[\mathfrak{L}_1,\lambda,\varepsilon a]}}{1+m\theta_{[\mathfrak{L}_1,\lambda,\varepsilon a]}}\right) v - d v^2, \end{aligned}$$

which implies that v is a positive strict supersolution of

$$\begin{cases} \mathfrak{L}_2 v = \mu v - d v^2 & \text{in } \ \Omega, \\ \mathfrak{B}_2 v = 0 & \text{on } \ \partial\Omega, \end{cases}$$

as well as a positive strict subsolution of

$$\begin{cases} \mathfrak{L}_2 v = \mu v - d v^2 + \varepsilon c \dfrac{\theta_{[\mathfrak{L}_1,\lambda,\varepsilon a]} v}{1+m\theta_{[\mathfrak{L}_1,\lambda,\varepsilon a]}} & \text{in } \ \Omega, \\ \mathfrak{B}_2 v = 0 & \text{on } \ \partial\Omega. \end{cases}$$

Therefore, the last two estimates of (7.57) also follow analogously from Theorem 6.1.4. □

The rest of this section is devoted to the proof of Theorem 7.3.1. Throughout it, we fix $\mu > \sigma_{0,2}$ and $\lambda^* \in (\varphi_0(\mu), \Phi(\mu))$, consider a sufficiently small $r > 0$ satisfying the conclusions of Theorem 7.2.4, and pick $\lambda_0, \lambda_1 \in (\varphi_0(\mu), \Phi(\mu))$ such that

$$\lambda_0 < \varphi_0(\mu) + r < \lambda^* < \Phi(\mu) - r < \lambda_1 < \Phi(\mu).$$

Naturally, $r > 0$ can be shortened as much as necessary. Moreover, for every $t, s \in (\varphi_0(\mu), \Phi(\mu))$ with $t < s$, we denote by $\mathscr{C}^+_{0,[t,s]}$ the restriction of the component $\mathscr{C}^+_0$ to the interval $[t,s]$, i.e.,

$$\mathscr{C}^+_{0,[t,s]} \equiv \left\{(\lambda, \mu, w, \theta_{[\mathfrak{L}_2,\mu,d]}) \in \mathscr{C}^+_0 \ : \ \lambda \in [t,s]\right\}.$$

By the choice of λ_0 and λ_1, Theorem 7.2.4 guarantees that $\mathscr{C}^+_{0,[\lambda_0,\lambda_1]}$ has a unique non-degenerate positive solution for every

$$\lambda \in [\lambda_0, \varphi_0(\mu)+r] \cup [\Phi(\mu)-r, \lambda_1]. \tag{7.59}$$

Actually, by the application of the implicit function theorem, each of the components $\mathscr{C}^+_{0,[\lambda_0,\varphi_0(\mu)+r]}$ and $\mathscr{C}^+_{0,[\Phi(\mu)-r,\lambda_1]}$ consists of an analytic arc of λ-curve. This is a pivotal feature in the proof given here. As these solutions are non-degenerate, once again by the implicit function theorem, these two arcs perturb into two λ-arcs of non-degenerate solutions of (7.7) for sufficiently small $\varepsilon > 0$.

Now, we consider the bounded set

$$\mathcal{C}_\eta := \mathscr{C}^+_{0,[\lambda_0,\lambda_1]} + B_\eta,$$

where B_η stands for the open ball of radius η centered at $(\mu, w, v) = (\mu, 0, 0)$ in the product space

$$\mathscr{X} \equiv \mathbb{R} \times \mathcal{C}^1_{\mathfrak{B}_1}(\bar{\Omega}) \times \mathcal{C}^1_{\mathfrak{B}_2}(\bar{\Omega}).$$

Then, $\mathcal{C}_\eta$ is a η-neighborhood of $\mathscr{C}^+_{0,[\lambda_0,\lambda_1]}$ with side covers

$$\{\lambda_0\} \times [(\mu, w_{\lambda_0}, \theta_{[\mathfrak{L}_2,\mu,d]}) + B_\eta], \qquad \{\lambda_1\} \times [(\mu, w_{\lambda_1}, \theta_{[\mathfrak{L}_2,\mu,d]}) + B_\eta],$$

where w_λ denotes the unique positive solution of (7.29) for every λ satisfying (7.59). By construction, $\mathscr{C}^+_{0,[\lambda_0,\lambda_1]} \subset \mathcal{C}_\eta$. Moreover, for sufficiently small $\eta > 0$,

$$(\lambda, \mu, w, v) = (\lambda, \mu, w_\lambda, \theta_{[\mathfrak{L}_2,\mu,d]})$$

is the unique solution of (7.8) in $\mathcal{C}_\eta$ for each λ satisfying (7.59). Furthermore, since the w-components of the elements of $\mathscr{C}^+_{0,[\lambda_0,\lambda_1]}$ are separated away from zero, because $\lambda = \Phi(\mu)$ is the unique bifurcation value to coexistence states from $w = 0$, $\bar{\mathcal{C}}_\eta$ cannot admit any solution of the form $(\lambda, \mu, 0, v)$ with $v = 0$ or $v = \theta_{[\mathfrak{L}_2,\mu,d]}$ for sufficiently small $\eta > 0$.

Next, we will adapt the proof of [124, Th. 6.3.1], through a well known lemma of Whyburn [209, Ch. 1] on compact continua, to show that, if necessary, $\mathcal{C}_\eta$ can be shortened in the interval $[\varphi_0(\mu)+r, \Phi(\mu)-r]$ up to obtain an *isolating neighborhood* of $\mathscr{C}^+_0$, denoted by $\mathcal{O}$, in the sense that, besides the previous properties of $\mathcal{C}_\eta$, $\partial_L\mathcal{O} \cap \mathscr{S}_0$ cannot admit any positive solution of (7.8), $(\lambda, \mu, w, \theta_{[\mathfrak{L}_2,\mu,d]})$, with $\lambda \in [\varphi_0(\mu)+r, \Phi(\mu)-r]$. We are denoting by $\partial_L\mathcal{O}$ the set $\partial\mathcal{O}$, except for the two lateral side covers at $\lambda = \lambda_0$ and $\lambda = \lambda_1$, where $\mathscr{S}_0$ has exactly two non-degenerate coexistence states.

Indeed, should $\mathcal{C}_\eta$ satisfy this property we can take $\mathcal{O} = \mathcal{C}_\eta$. Otherwise, we consider the non-empty compact sets

$$\begin{aligned} M &:= \left\{(\lambda,\mu,w,\theta_{[\mathfrak{L}_2,\mu,d]}) \in \bar{\mathcal{C}}_\eta \cap \mathscr{S}_0 \;:\; \lambda \in [\varphi_0(\mu)+r, \Phi(\mu)-r]\right\}, \\ A &:= \left\{(\lambda,\mu,w,\theta_{[\mathfrak{L}_2,\mu,d]}) \in \partial\mathcal{C}_\eta \cap \mathscr{S}_0 \;:\; \lambda \in [\varphi_0(\mu)+r, \Phi(\mu)-r]\right\}, \\ B &:= \mathscr{C}^+_{0,[\varphi_0(\mu)+r,\Phi(\mu)-r]}. \end{aligned}$$

These sets are compact because they are closed and bounded sets consisting of fixed points of a compact operator. Moreover, A and B are disjoint. Thus, according to Whyburn [209, Ch.1], since B is a connected component, there are two disjoint compact subsets of M, M_A and M_B, such that $A \subset M_A$, $B \subset M_B$ and $M = M_A \cup M_B$. Thus, setting $\delta := \mathrm{dist}(M_A, M_B) > 0$, it is easily seen that

$$\mathcal{O} := \mathcal{C}_\eta \setminus \overline{M_A + B_{\frac{\delta}{2}}}$$

satisfies similar properties as $\mathcal{C}_\eta$ and, in addition, by construction,

$$\partial_L \mathcal{O} \cap \mathscr{S}_0 = \emptyset, \tag{7.60}$$

This construction has been sketched in Figure 7.5, where an admissible $\mathcal{O}$ has been plotted when $\mathcal{O} = \mathcal{C}_\eta$.

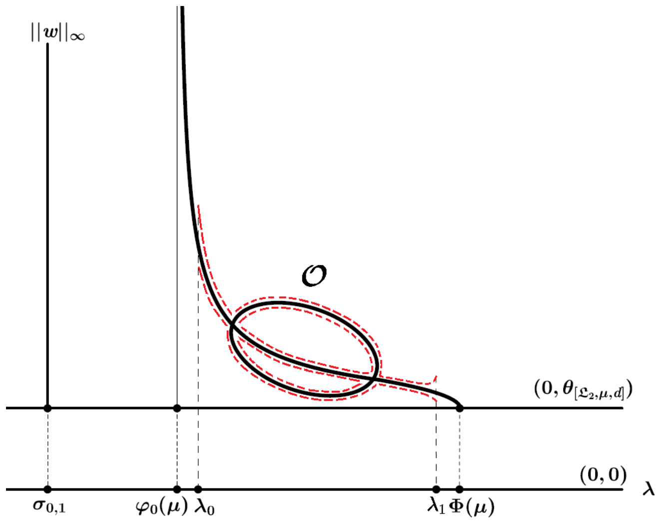

Figure 7.5: The isolating neighborhood $\mathcal{O}$ of $\mathscr{C}^+_{0,[\lambda_0,\lambda_1]}$

Subsequently, for sufficiently small $\varepsilon > 0$, we denote by $\mathscr{S}_\varepsilon$ the set of nontrivial solutions of (7.7),

$$\begin{aligned} \mathscr{S}_\varepsilon := &\{(\lambda,\mu,w,v) \in \mathfrak{F}^{-1}(0) \;:\; (w,v) \neq (0,\theta_{[\mathfrak{L}_2,\mu,d]})\} \\ &\cup \{(\lambda,\mu,0,\theta_{[\mathfrak{L}_2,\mu,d]}) \;:\; \lambda \in \Sigma(\mathscr{L}(\lambda,\varepsilon))\}, \end{aligned}$$

where $\Sigma(\mathscr{L}(\lambda,\varepsilon))$ is the generalized spectrum of $\mathscr{L}(\lambda,\varepsilon)$, as discussed in [124]. By [124, Th. 7.2.2], there exists a component of $\mathscr{S}_\varepsilon$, denoted by $\mathscr{C}_\varepsilon^+$, consisting of coexistence states of (7.7) such that

$$(\Phi(\mu),\mu,0,\theta_{[\mathfrak{L}_2,\mu,d]})\in\bar{\mathscr{C}}_\varepsilon^+.$$

However, contrarily to what happens with $\mathscr{C}_0^+$, Lemma 7.3.2 entails that, for every $\varepsilon>0$ and $\hat{\lambda}>\Phi(\mu)$, the set of coexistence states

$$\left\{(\lambda,\mu,w,v)\in\mathscr{C}_\varepsilon^+\;:\;\lambda\in(\varphi_\varepsilon(\mu),\hat{\lambda}]\right\}$$

is bounded, whereas, thanks to [124, Th. 7.2.2], $\mathscr{C}_\varepsilon^+$ is unbounded. Consequently, as soon as $\lambda'(0)<0$, which holds true for sufficiently small $\varepsilon>0$, there exists $\lambda_T\equiv\lambda_T(\varepsilon)\in(\varphi_\varepsilon(\mu),\Phi(\mu))$ such that

$$\mathcal{P}_\lambda\left(\mathscr{C}_\varepsilon^+\right)=[\lambda_T(\varepsilon),+\infty).$$

We claim that $\lambda_T(\varepsilon)<\lambda_0$ for sufficiently small $\varepsilon>0$. Since $\lambda_0<\lambda^*$, this ends the proof of Part (a). Note that $\lambda_T>\varphi_\varepsilon(\mu)$ by Theorem 7.1.6. To prove $\lambda_T(\varepsilon)<\lambda_0$, we first show that

$$[\lambda_0,\Phi(\mu))\subset\mathcal{P}_\lambda\left(\mathscr{C}_\varepsilon^+\right)\quad\text{for sufficiently small }\;\varepsilon>0. \tag{7.61}$$

This holds true thanks to the crucial feature that the isolating neighborhood of $\mathscr{C}_0^+$ in $[\lambda_0,\lambda_1]$, $\mathcal{O}$, also provides us with an isolating neighborhood of $\mathscr{C}_\varepsilon^+$ in $[\lambda_0,\lambda_1]$ for sufficiently small $\varepsilon>0$ if λ_1 is sufficiently close to $\Phi(\mu)$. Indeed, thanks to Theorem 7.1.3, one can choose λ_1 to be sufficiently close to $\Phi(\mu)$ so that, for sufficiently small $\varepsilon>0$, $\mathscr{C}_\varepsilon^+$ has a unique non-degenerate coexistence state close to $(w,v)=(0,\theta_{[\mathfrak{L}_2,\mu,d]})$ for all $\lambda\in[\lambda_1,\Phi(\mu))$, say

$$(\lambda,\mu,w,v)=(\lambda,\mu,w_{\lambda,\varepsilon},v_{\lambda,\varepsilon}),\qquad\lambda\in[\lambda_1,\Phi(\mu)),\;\;\varepsilon\in[0,\varepsilon_0).$$

Naturally, as Theorem 7.1.3 shows that $\mathscr{C}_\varepsilon^+$ is a regular perturbation of $\mathscr{C}_0^+$ through the implicit function theorem in a neighborhood of the bifurcation point, there exists $\varepsilon_0>0$ such that, for every $\varepsilon\in[0,\varepsilon_0)$, the coexistence state $(\lambda_1,\mu,w_{\lambda_1,\varepsilon},v_{\lambda_1,\varepsilon})$ lies in the interior of the right side cover of $\mathcal{O}$; actually, it is the unique coexistence state of (7.7) on $\partial\mathcal{O}$ for $\lambda=\lambda_1$. This argument combined with the local uniqueness of Theorem 7.1.3 shows Part (c). Figure 7.6 sketches this behavior. As in the remaining bifurcation diagramas plotted in this section, the dashed curve represents $\mathscr{C}_0^+$, while the continuous curve shows $\mathscr{C}_\varepsilon^+$ for sufficiently small $\varepsilon>0$. According to Theorem 7.1.3, these are the unique solutions of the model in a neighborhood of the bifurcation point for sufficiently small $\varepsilon\geq 0$. All are non-degenerate; actually, linearly

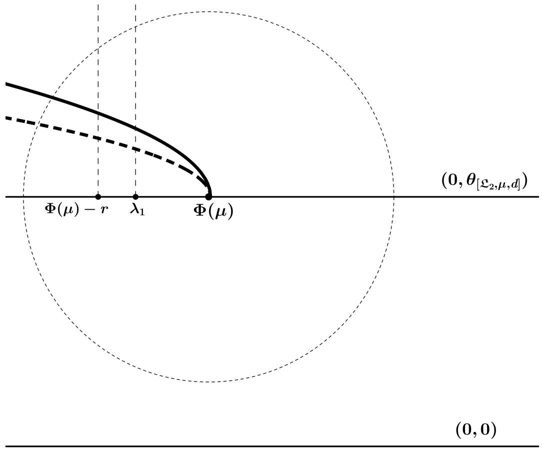

Figure 7.6: The ball where the solutions of (7.7) are analytic λ-curves

unstable with one-dimensional unstable manifold by the exchange stability principle.

Once shown that $\mathscr{C}_\varepsilon^+$ reaches $\mathcal{O}$ at $\lambda = \lambda_1$, and so enters into $\mathcal{O}$, we claim that these components must abandone $\mathcal{O}$ passing through some point with $\lambda = \lambda_0$, as illustrated by the left picture of Figure 7.7, so concluding the proof of (7.61). Since they must abandone $\mathcal{O}$ because they are unbounded, in order to prove our claim, it suffices to make sure that $\mathscr{C}_\varepsilon^+$ cannot leave $\mathcal{O}$ through $\partial_L \mathcal{O}$ for sufficiently small $\varepsilon > 0$, as illustrated by the right picture of Figure 7.7. Our proof of this fact proceeds by contradiction. Assume that there is a sequence ε_n, $n \geq 2$, such that $\lim_{n\uparrow\infty} \varepsilon_n = 0$, and, for every $n \geq 2$, $\lambda'(\varepsilon_n) < 0$ and the problem (7.7) has some coexistence state, $(\lambda_n, \mu, w_n, v_n) \in \partial_L \mathcal{O}$, for $\varepsilon = \varepsilon_n$ and some $\lambda_n \in [\varphi_0(\mu) + r, \Phi(\mu) - r]$, as sketched on the right picture of Figure 7.7.

Then, since $\{(\lambda_n, \mu, w_n, v_n)\}_{n\geq 2}$ is bounded in $[\lambda_0, \lambda_1] \times \{\mu\} \times \mathcal{C}^1_{\mathfrak{B}_1}(\bar\Omega) \times \mathcal{C}^1_{\mathfrak{B}_2}(\bar\Omega)$ and it consists of fixed points of a sequence of associated compact operators depending continuously on ε, $\varepsilon \sim 0$, by a rather standard compactness argument, we can extract a subsequence, relabeled by $n \geq 2$, such that

$$\lim_{n\to\infty} (\lambda_n, \mu, w_n, v_n) = (\lambda_\omega, \mu, w_\omega, v_\omega) \in \partial_L \mathcal{O}$$

for some $w_\omega \geq 0$, $v_\omega \geq 0$ and $\lambda_\omega \in [\lambda_0, \lambda_1]$ such that $(\lambda_\omega, \mu, w_\omega, v_\omega)$ solves (7.8). Since $\mathcal{O}$ is an isolating neighborhood of $\mathscr{C}_0^+$, it becomes apparent that $w_\omega \gg_1 0$ and $v_\omega \gg_2 0$. But this contradicts (7.60). Therefore, (7.61) holds true. Consequently, for every $\varepsilon \in [0, \varepsilon_0)$, we have that $\lambda_T(\varepsilon) \leq \lambda_0 < \lambda^*$, which ends the proof of Part (a).

Note that, as $\varepsilon > 0$ perturbs from zero, a further application of the

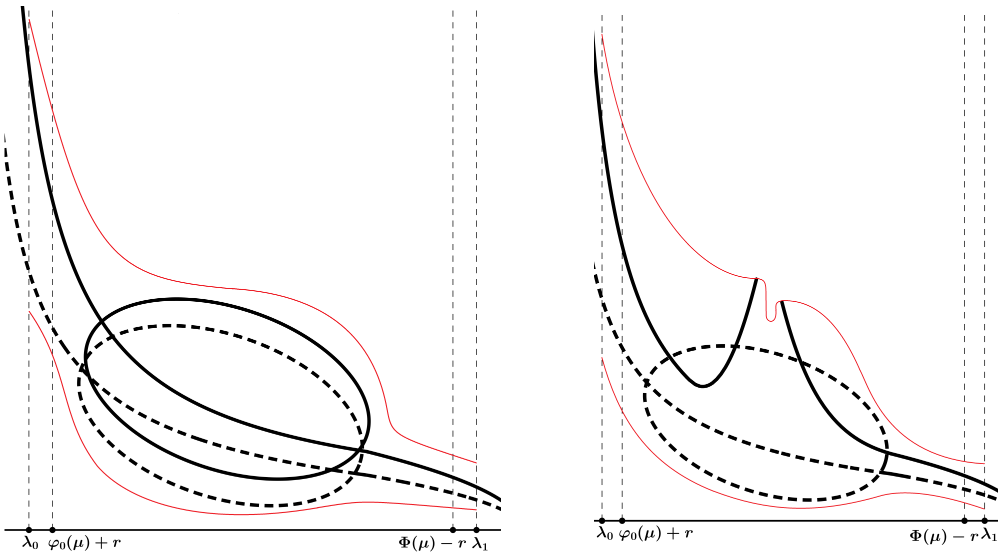

Figure 7.7: The isolating neighborhood $\mathcal{O}$ of $\mathscr{C}^+_{0,[\lambda_0,\lambda_1]}$

implicit function theorem shows that the analytic arcs of λ-curve $\mathscr{C}^+_{0,[\lambda_0,\varphi_0(\mu)+r]}$ and $\mathscr{C}^+_{0,[\Phi(\mu)-r,\lambda_1]}$ perturb into two λ-arcs of $\mathscr{C}^+_\varepsilon$ within $\mathcal{O}$, that we denote by $\mathscr{C}^+_{\varepsilon,[\lambda_0,\varphi_0(\mu)+r]}$ and $\mathscr{C}^+_{\varepsilon,[\Phi(\mu)-r,\lambda_1]}$, and that these arcs consist of non-degenerate solutions of (7.7) for sufficiently small $\varepsilon \geq 0$. By a further application of the implicit function theorem at the unique solution of $\mathscr{C}^+_\varepsilon$ on $\partial\mathcal{O}$ at λ_0, say $(\lambda_0, \mu, w_{\lambda_0,\varepsilon}, v_{\lambda_0,\varepsilon})$, this entails that actually for sufficiently small $\varepsilon > 0$ there exists $\delta(\varepsilon) > 0$ such that

$$[\lambda_0 - \delta(\varepsilon), \Phi(\mu)) \subset \mathcal{P}_\lambda\left(\mathscr{C}^+_\varepsilon\right).$$

Moreover,

$$\lim_{\varepsilon\downarrow 0}(w_{\lambda_0,\varepsilon}, v_{\lambda_0,\varepsilon}) = (w_{\lambda_0}, \theta_{[\mathfrak{L}_2,\mu,d]}).$$

Therefore, since

$$\mathscr{C}^+_\varepsilon \setminus \mathscr{C}^+_{\varepsilon,[\lambda_0,\varphi_0(\mu)+r]}$$

is unbounded, it follows from Lemma 7.3.2 that, for every $\lambda \in [\lambda_0, \Phi(\mu))$, (7.7) has, at least, two coexistence states for sufficiently small $\varepsilon > 0$. This proves Part (b) and concludes the proof of Theorem 7.3.1.

Another proof of the multiplicity result of Part (b) can be given by using the topological degree. Although this proof does not allow to show that each of the components $\mathscr{C}^+_\varepsilon$ bend backwards at some supercritical turning point for sufficiently small $\varepsilon > 0$, it provides with the local index of the additional solutions, which is imperative to ascertain their local stability character. The alternative proof proceeds as follows. Thanks to Theorem 7.2.4, it follows from the invariance by homotopy of the Leray–Schauder degree, that, for every $\varepsilon \in [0, \varepsilon_0)$ and $\lambda \in [\lambda_0, \lambda_1]$,

$$\mathrm{Deg}\,(\mathfrak{F}(\lambda, \mu, \varepsilon, \cdot, \cdot), \mathcal{O}_\lambda) = -1, \tag{7.62}$$

where $\mathfrak{F}$ is the operator defined in (7.16) and, for every $\lambda \in [\lambda_0, \lambda_1]$, we are denoting

$$\mathcal{O}_\lambda := \{(\mu, w, v) \in \mathscr{X} \;:\; (\lambda, \mu, w, v) \in \mathcal{O}\}.$$

Subsequently we will use the fixed point index in cones, as axiomatized by Amann [6] and Dancer [42], which was applied by the first time to the classical diffusive Lotka–Volterra models by López-Gómez and Pardo [142], López-Gómez [120] and, more recently, by Fernández-Rincón and López-Gómez [70], among many others. First, we consider, for every $i = 1, 2$, the positive cone of U_i,

$$\mathscr{P}_{U_i} := \{u \in U_i \;:\; u \geq 0 \;\text{ in } \Omega\}$$

and the associated system to (7.7)

$$\begin{cases} \mathfrak{L}_1 w = \lambda w - \varepsilon a(x) w^2 - \alpha b(x) \dfrac{wv}{1 + m(x) w} & \text{in } \Omega, \\ \mathfrak{L}_2 v = \mu v - d(x) v^2 + \alpha \varepsilon c(x) \dfrac{wv}{1 + m(x) w} & \text{in } \Omega, \\ \mathfrak{B}_1 w = \mathfrak{B}_2 v = 0 & \text{on } \partial\Omega, \end{cases} \tag{7.63}$$

where $\alpha \in [0, 1]$ is an homotopy parameter to uncouple (7.7) into two semilinear boundary value problems. By applying Lemma 7.3.2 uniformly in $\alpha \in [0, 1]$, it is easily seen that there exists a bounded open subset $\mathcal{W} \times \mathcal{V} \subset U_1 \times U_2$, independent of $\alpha \in [0, 1]$, such that $(w, v) \in \mathcal{W} \times \mathcal{V}$ if $(w, v) \in P_{U_1} \times P_{U_2}$ solves (7.63) for some $\alpha \in [0, 1]$.

Subsequently, we choose a sufficiently large $e \geq 0$ such that

$$\sigma_0[\mathfrak{L}_i + e, \mathfrak{B}_i, \Omega] > 1, \qquad i = 1, 2, \tag{7.64}$$

and, for every $\alpha \in [0, 1]$, $w \in \mathcal{W}$, and $v \in \mathcal{V}$,

$$\begin{matrix} \lambda - a\varepsilon w - \alpha b \frac{v}{1+mw} + e > 0, \\ \mu - dv + \alpha \varepsilon c \frac{w}{1+mw} + e > 0, \end{matrix} \qquad \text{in } \bar{\Omega}. \tag{7.65}$$

Then, thanks to (7.64) and (7.65), the map

$$\mathcal{H} : [0, 1] \times \mathcal{W} \times \mathcal{V} \to U_1 \times U_2$$

defined by

$$\mathcal{H}(\alpha,w,v)=\begin{pmatrix} (\mathfrak{L}_1+e)^{-1}[(\lambda-\varepsilon aw-\alpha b\frac{v}{1+mw}+e)w] \\ (\mathfrak{L}_2+e)^{-1}[(\mu-dv+\alpha\varepsilon c\frac{w}{1+mw}+e)v] \end{pmatrix},$$

is a compact order preserving operator whose non-negative fixed points are the solutions of (7.63) in $P_{U_1}\times P_{U_2}$. Adapting the analysis of Steps i)-v) of the proof of [120, Th. 4.1], or Lemmas 5.6-5.9 of [70], one can find out the fixed point indices of the non-negative solutions of (7.7) as fixed points of $\mathcal{H}(1,\cdot,\cdot)$. It turns out that

$$i_{P_{U_1}\times P_{U_2}}(\mathcal{H}(1,\cdot,\cdot),\mathcal{W}\times\mathcal{V})=1, \tag{7.66}$$

whereas

$$i_{P_{U_1}\times P_{U_2}}(\mathcal{H}(1,\cdot,\cdot),(0,0))=0 \quad \text{if } \lambda>\sigma_{0,1} \text{ or } \mu>\sigma_{0,2}. \tag{7.67}$$

Moreover,

$$\begin{cases} i_{P_{U_1}\times P_{U_2}}\left(\mathcal{H}(1,\cdot,\cdot),(\theta_{[\mathfrak{L}_1,\lambda,a]},0)\right)=0 & \text{if } \mu>\Psi_\varepsilon(\lambda), \\ i_{P_{U_1}\times P_{U_2}}\left(\mathcal{H}(1,\cdot,\cdot),(0,\theta_{[\mathfrak{L}_2,\mu,d]})\right)=1 & \text{if } \lambda<\Phi(\mu). \end{cases} \tag{7.68}$$

Thus, for every $\lambda\in(\sigma_{0,1},\Phi(\mu))$ and $\mu>\sigma_{0,2}$,

$$\begin{aligned} 1 &= i_{P_{U_1}\times P_{U_2}}(\mathcal{H}(1,\cdot,\cdot),\mathcal{W}\times\mathcal{V}) = i_{P_{U_1}\times P_{U_2}}(\mathcal{H}(1,\cdot,\cdot),(0,0)) \\ &\quad + i_{P_{U_1}\times P_{U_2}}\left(\mathcal{H}(1,\cdot,\cdot),(\theta_{[\mathfrak{L}_1,\lambda,a]},0)\right)+i_{P_{U_1}\times P_{U_2}}\left(\mathcal{H}(1,\cdot,\cdot),(0,\theta_{[\mathfrak{L}_2,\mu,d]})\right). \end{aligned}$$

Consequently, the global index of the coexistence states, as fixed points of $\mathcal{H}(1,\cdot,\cdot)$, equals zero and, since (7.62) entails

$$i_{P_{U_1}\times P_{U_2}}(\mathcal{H}(1,\cdot,\cdot),\mathcal{O}_\lambda)=-1 \quad \text{for all } \lambda\in[\lambda_0,\lambda_1],$$

the existence of a second coexistence state follows for every $\lambda\in[\lambda_0,\lambda_1]$. Taking into account that $\lambda_0<\lambda^*$ and that λ_1 can be chosen arbitrarily close to $\Phi(\mu)$, the multiplicity result of Theorem 7.3.1(b) readily follows.

Remark 7.3.3. The multiplicity result of Theorem 7.3.1(b) holds as soon as $\lambda'(\varepsilon)<0$, which occurs for $\varepsilon\in[0,\varepsilon^*)$, where $\lambda'(\varepsilon^*)=0$. It remains an open problem to ascertain whether, or not, (7.7) can admit a coexistence state for some $\lambda\in(\varphi_\varepsilon(\mu),\lambda_T(\varepsilon))$. This might depend on the nature of the spatial heterogeneities of the several coefficients involved in the setting of (7.7).

7.4 A simple illustrative example

This section considers (7.7) in the special case when:

- $c_1 = c_2 = 0$ in Ω.
- $\Gamma_1 = \partial\Omega$ (i.e., $\Gamma_0 = \emptyset$), and $\beta_1 = \beta_2 = 0$ on $\partial\Omega$.
- a, b, c and d are positive constants, and $m = 1$ in Ω.

Then, since $\mathfrak{B}_k = \frac{\partial}{\partial\nu_k} \equiv \partial_{\nu_k}$ for $k = 1, 2$, it turns out that we are imposing non-flux boundary conditions on $\partial\Omega$. Thus,

$$\sigma_{0,k} := \sigma_0[\mathfrak{L}_k, \partial_{\nu_k}, \Omega] = 0, \qquad k = 1, 2.$$

Consequently, throughout this section we assume that $\lambda > 0$ and fix $\mu > 0$. As in the preceding sections, $\lambda > 0$ is regarded as a bifurcation parameter.

By the special nature of (7.7) under these conditions, any component-wise positive solution (w, v) of the algebraic system

$$\begin{cases} \lambda - \varepsilon a w - b v \frac{1}{1+w} = 0, \\ \mu - d v + \varepsilon c \frac{w}{1+w} = 0, \end{cases} \tag{7.69}$$

provides us with a coexistence state of (7.7). By the uniqueness of Theorem 6.1.3, it follows that $\theta_{[\mathfrak{L}_2,\mu,d]} = \frac{\mu}{d}$. So,

$$\Phi(\mu) = \sigma_0\left[\mathfrak{L}_1 + b\theta_{[\mathfrak{L}_2,\mu,d]}, \partial_{\nu_1}, \Omega\right] = b\frac{\mu}{d}. \tag{7.70}$$

Eliminating v from the first equation of (7.69), we obtain that

$$v = \frac{1}{b}(1+w)(\lambda - \varepsilon a w), \tag{7.71}$$

and, substituting (7.71) into the second equation of (7.69), yields to

$$\begin{aligned} P(w,\lambda) \equiv P(w) := w^3 + \left(2 - \frac{\lambda}{\varepsilon a}\right) w^2 \\ + \left(1 + \frac{bc}{ad} + \frac{b\mu - 2d\lambda}{\varepsilon a d}\right) w + \frac{b\mu - d\lambda}{\varepsilon a d} = 0. \end{aligned} \tag{7.72}$$

Therefore, (w, v) is component-wise positive solution of the system (7.69) if, and only if, w is a positive root of $P(w)$ with

$$\lambda - \varepsilon a w > 0. \tag{7.73}$$

Thus, to find out the coexistence states of (7.7) for this prototype, one should first ascertain the positive roots of $P(w)$. In this section, we are going to accomplish this task for $\lambda > \Phi(\mu)$ sufficiently close to $\Phi(\mu)$. Note that, according to the analysis of the previous sections, we already know that $(\lambda, w, v) = \left(\Phi(\mu), 0, \theta_{[\mathfrak{L}_2,\mu,d]}\right)$ is a bifurcation point to a component of coexistence states of (7.7).

Suppose $\lambda > \Phi(\mu)$. Then, by (7.70), $\lambda > b\frac{\mu}{d}$. Thus,

$$P(0) = \frac{b\mu - d\lambda}{\varepsilon a d} < 0,$$

and hence, since $\lim_{w\uparrow+\infty} P(w) = +\infty$, $P(w)$ admits, at least, a positive real root. Similarly, the polynomial

$$P'(w) = 3w^2 + 2\left(2 - \frac{\lambda}{\varepsilon a}\right) w + 1 + \frac{bc}{ad} + \frac{b\mu - 2d\lambda}{\varepsilon a d}$$

satisfies

$$P'(0) = 1 + \frac{bc}{ad} + \frac{b\mu - 2d\lambda}{\varepsilon a d} < 0$$

if, and only if,

$$0 < \varepsilon < \varepsilon^*(\lambda) \equiv \frac{2d\lambda - b\mu}{bc + ad}. \tag{7.74}$$

So, since $\lim_{w\uparrow+\infty} P'(w) = +\infty$, also $P'(w)$ possesses, at least, one positive root for every $\varepsilon \in (0, \varepsilon^*)$. Finally, since

$$P''(w) = 6w + 2\left(2 - \frac{\lambda}{\varepsilon a}\right),$$

it is obvious that $w_c \equiv \frac{1}{3}\left(\frac{\lambda}{\varepsilon a} - 2\right)$ is the unique root of P''. Suppose that

$$\varepsilon < \min\left\{\frac{\lambda}{2a}, \varepsilon^*(\lambda)\right\}. \tag{7.75}$$

Then $w_c > 0$, $P''(w) < 0$ if $w \in [0, w_c)$, and $P''(w) > 0$ if $w > w_c$. Thus, $P'(w)$ is decreasing in $(0, w_c)$ and increasing in $(w_c, +\infty)$. Moreover, by (7.74), $P'(0) < 0$, because $\varepsilon < \varepsilon^*(\lambda)$. Consequently, there exists $w^* > 0$ such that $P' < 0$ in $[0, w^*)$, $P'(w^*) = 0$, and $P'(w) > 0$ for all $w > w^*$. Therefore, $P(w)$ is decreasing in $(0, w^*)$ and increasing in $(w^*, +\infty)$, and, since $P(0) < 0$ and $P'(0) < 0$, it becomes apparent that, under condition (7.75), $P(w)$ has a unique positive root, say $w_r > w^* > 0$. Finally, since

$$
\begin{aligned}
P\left(\frac{\lambda}{\varepsilon a}\right) &= \left(\frac{\lambda}{\varepsilon a}\right)^3 + \left(2-\frac{\lambda}{\varepsilon a}\right)\left(\frac{\lambda}{\varepsilon a}\right)^2 + \left(1+\frac{bc}{ad}+\frac{b\mu-2d\lambda}{\varepsilon ad}\right)\frac{\lambda}{\varepsilon a} + \frac{b\mu - d\lambda}{\varepsilon ad} \\
&= 2\left(\frac{\lambda}{\varepsilon a}\right)^2 + \left(1+\frac{bc}{ad}+\frac{b\mu-2d\lambda}{\varepsilon ad}\right)\frac{\lambda}{\varepsilon a} + \frac{b\mu - d\lambda}{\varepsilon ad} \\
&= \frac{1}{\varepsilon^2}\left[2\frac{\lambda^2}{a^2} + \frac{b\mu - 2\lambda d}{a^2 d}\lambda + O(\varepsilon)\right] = \varepsilon^{-2}\left[\frac{\lambda}{a^2}\Phi(\mu) + O(\varepsilon)\right] > 0
\end{aligned}
$$

as $\varepsilon \downarrow 0$, necessarily $w_r < \frac{\lambda}{\varepsilon a}$ for sufficiently small $\varepsilon > 0$ and, in particular, $w = w_r$ satisfies (7.73). Therefore, for sufficiently small $\varepsilon > 0$, (7.69) has a unique coexistence state for every $\lambda > \Phi(\mu)$.

Note that, at $\varepsilon = 0$, (7.69) reduces to

$$
\begin{cases}
\lambda - bv\frac{1}{1+w} = 0, \\
\mu - dv = 0,
\end{cases}
$$

whose unique solution coexistence state is

$$
(w, v) = \left(\frac{b\mu}{d\lambda} - 1, \frac{\mu}{d}\right) \qquad \lambda > 0.
$$

As $\lambda \in (0, \Phi(\mu))$, $w(\lambda) = \frac{b\mu}{d\lambda} - 1$ decays from $+\infty$ to 0, while v remains constant. This is the component $\mathscr{C}_0^+$ studied in Section 4 for this so special example. According to the previous analysis, for sufficiently small $\varepsilon > 0$, the component $\mathscr{C}_0^+$ must perturb into a new component, $\mathscr{C}_\varepsilon^+$, having a unique coexistence state for all $\lambda > \Phi(\mu)$. Thus, $\mathscr{C}_\varepsilon^+$ has a supercritical turning point at some $\lambda_T(\varepsilon)$ such that $\lim_{\varepsilon\downarrow 0} \lambda_T(\varepsilon) = 0$.

However, the uniqueness of the coexistence state for $\lambda > \Phi(\mu)$ can be lost when (7.75) fails and $bc > ad$, giving rise to a S–shaped bifurcation diagram. Indeed, at the critical value $\lambda = \Phi(\mu)$, the cubic polynomial $P(w)$ becomes

$$
\begin{aligned}
P(w) = P(w, \Phi(\mu)) = w^3 &+ \left(2 - \frac{\lambda}{\varepsilon a}\right) w^2 \\
&+ \left(1 + \frac{bc}{ad} - \frac{b\mu}{\varepsilon ad}\right) w = Q(w) w,
\end{aligned}
\tag{7.76}
$$

where

$$
Q(w) := w^2 + \left(2 - \frac{\lambda}{\varepsilon a}\right) w + 1 + \frac{bc}{ad} - \frac{b\mu}{\varepsilon ad}.
$$

Thus, at $\lambda = \Phi(\mu)$, the roots of $P(w)$ are $w = 0$ plus the two roots of $Q(w)$. A direct calculation shows that, as soon as

$$\varepsilon > \frac{b\mu}{bc + ad} = \varepsilon^*,$$

the polynomial $P(w)$ satisfies

$$P(0) = 0, \quad P'(0) = 1 + \frac{bc}{ad} - \frac{b\mu}{\varepsilon ad} > 0.$$

Suppose $\varepsilon > \varepsilon^*$ and $Q(w)$ has two positive roots, $w_+ > w_- > 0$. Then, at $\lambda = \Phi(\mu)$, the polynomial $P(w)$ has three simple roots. Thus, since the coefficients of $P(w, \lambda)$ are analytic functions of the parameter λ, for sufficiently small $\eta > 0$, there are three analytic functions

$$z, w_+, w_- : J_\eta \equiv (\Phi(\mu) - \eta, \Phi(\mu) + \eta) \to \mathbb{R},$$

such that

$$\lim_{\lambda \to \Phi(\mu)} z(\lambda) = 0, \qquad \lim_{\lambda \to \Phi(\mu)} w_\pm(\lambda) = w_\pm \tag{7.77}$$

and, for every $\lambda \in J_\eta$, $z(\lambda)$ and $w_\pm(\lambda)$ provide us with the three simple roots of $P(w)$. Consequently, since $P(0) = 0$, $P'(0) > 0$ at $\lambda = \Phi(\mu)$, $P(0) < 0$ if $\lambda > \Phi(\mu)$, and $P(0) > 0$ if $\lambda < \Phi(\mu)$, it becomes apparent that, for sufficiently small $\eta > 0$,

$$0 < z(\lambda) < w_-(\lambda) < w_+(\lambda) \quad \text{if } \lambda \in (\Phi(\mu), \Phi(\mu) + \eta),$$

while

$$z(\lambda) < 0 < w_-(\lambda) < w_+(\lambda) \quad \text{if } \lambda \in (\Phi(\mu) - \eta, \Phi(\mu)).$$

Therefore, $P(w, \lambda)$ has three simple positive roots if $\lambda \in (\Phi(\mu), \Phi(\mu) + \eta)$ and two if $\lambda \in (\Phi(\mu) - \eta, \Phi(\mu))$, as illustrated in the first picture of Figure 7.8, where we are plotting the polynomials $P(w, \lambda)$ for $\lambda = \Phi(\mu)$ (using a dashed line) and $\lambda_\pm = \Phi(\mu) \pm \delta_\pm$ for some $\delta_+, \delta_- \in (0, \eta)$ (using continuous lines).

Obviously, the roots of $Q(w)$ are

$$w_\pm := \frac{\lambda}{2\varepsilon a} - 1 \pm \sqrt{\left(\frac{\lambda}{2\varepsilon a} - 1\right)^2 - 1 - \frac{bc}{ad} + \frac{b\mu}{\varepsilon ad}} = \frac{\lambda}{2\varepsilon a} - 1 \pm \frac{1}{\varepsilon a}\sqrt{\lambda^2 - 4\varepsilon^2 \frac{abc}{d}}.$$

Thus, if we further impose that

$$\frac{b\mu}{bc + ad} = \varepsilon^* < \varepsilon < \frac{\lambda}{2a},$$

with ε sufficiently close to ε^*, then $w_+ > w_- > 0$ and, hence, $P(w,\lambda)$ has three simple positive roots if $\lambda \in (\Phi(\mu), \Phi(\mu)+\eta)$ and two if $\lambda \in (\Phi(\mu)-\eta, \Phi(\mu))$, provided $bc > ad$ and $\varepsilon > \varepsilon^*$ is sufficiently close to ε^*. The assumption $bc > ad$ is necessary and sufficient so that $\frac{b\mu}{bc+ad} < \frac{\lambda}{2a}$. Finally, since

$$\lambda - \varepsilon a w_+ = \frac{\lambda}{2} + \varepsilon a - \frac{1}{2}\sqrt{\lambda^2 - 4\varepsilon^2 \frac{abc}{d}} > \varepsilon a > 0 \qquad \text{if } \lambda = \Phi(\mu),$$

by (7.77) and (7.71), it becomes apparent that, if $bc > ad$ and $\varepsilon > \varepsilon^*$ is sufficiently close to ε^*, then (7.69) has three coexistence states if $\lambda \in (\Phi(\mu), \Phi(\mu)+\eta)$ and only two if $\lambda \in (\Phi(\mu)-\eta, \Phi(\mu))$. This phenomenology has been illustrated in Figure 7.8, whose right picture shows a paradigmatic S-shaped component $\mathscr{C}_\varepsilon^+$ for $\varepsilon > \varepsilon^*$, $\varepsilon \sim \varepsilon^*$, when $bc > ad$.

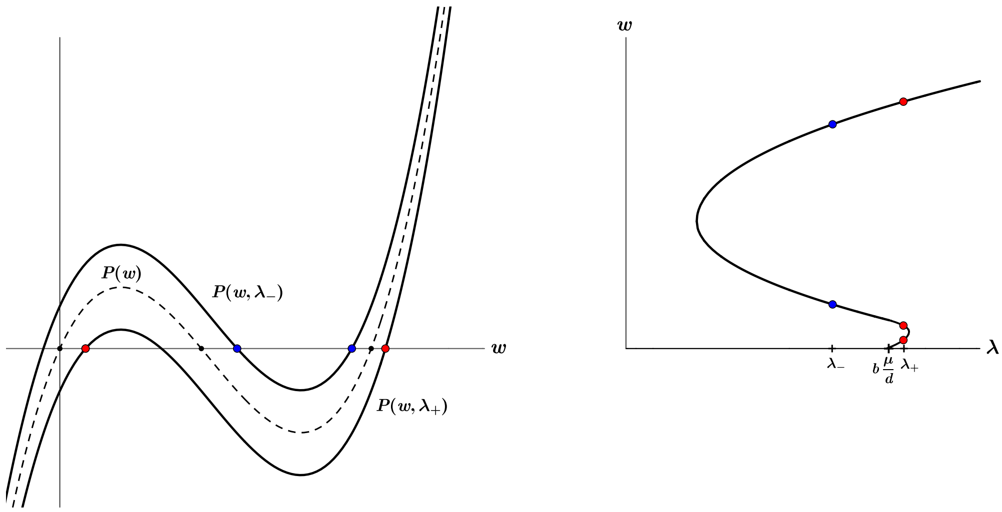

Figure 7.8: The S-shaped component of constant coexistence states

According to (7.72), the coefficients of $P(w,\lambda)$ are decreasing with respect to λ. Thus, in the region $w \geq 0$, the bigger is $\lambda > \Phi(\mu)$, the smaller are the graphs of the polynomials $P(w,\lambda)$ (see the first picture of Figure 7.8). Therefore, there exists $\lambda^* > \Phi(\mu)$ such that $z(\lambda^*) = w_-(\lambda^*)$, which corresponds with the subcritical turning point of the S-shaped component $\mathscr{C}_\varepsilon^+$.

Bibliography

[1] A. Abbondandolo. Sub-harmonics for two-dimensional Hamiltonian systems. *NoDEA Nonlinear Differential Equations Appl.*, 6(4):341–355, 1999.

[2] A. Abbondandolo. *Morse theory for Hamiltonian systems*, volume 425 of *Chapman & Hall/CRC Research Notes in Mathematics*. Chapman & Hall/CRC, Boca Raton, FL, 2001.

[3] R. L. Adler, A. G. Konheim, and M. H. McAndrew. Topological entropy. *Trans. Amer. Math. Soc.*, 114:309–319, 1965.

[4] H. N. Agiza, E. M. ELabbasy, H. EL-Metwally, and A. A. Elsadany. Chaotic dynamics of a discrete prey-predator model with Holling type II. *Nonlinear Anal. Real World Appl.*, 10(1):116–129, 2009.

[5] D. Aleja, I. Antón, and J. López-Gómez. Global structure of the periodic positive solutions for a general class of periodic-parabolic logistic equations with indefinite weights. *J. Math. Anal. Appl.*, 487(1):123961, 23, 2020.

[6] H. Amann. Fixed point equations and nonlinear eigenvalue problems in ordered Banach spaces. *SIAM Rev.*, 18:620–709, 1976.

[7] H. Amann and J. López-Gómez. A priori bounds and multiple solutions for superlinear indefinite elliptic problems. *J. Differential Equations*, 146(2):336–374, 1998.

[8] D. K. Arrowsmith and C. M. Place. *Dynamical systems*. Chapman and Hall Mathematics Series. Chapman & Hall, London, 1992. Differential equations, maps and chaotic behaviour.

[9] B. Aulbach and B. Kieninger. On three definitions of chaos. *Nonlinear Dyn. Syst. Theory*, 1(1):23–37, 2001.

[10] H. Baek and Y. Do. Seasonal effects on a Beddington-DeAngelis type predator-prey system with impulsive perturbations. *Abstr. Appl. Anal.*, pages Art. ID 695121, 19, 2009.

[11] J. L. Begon, M. Harper and C. R. Townsend. *Ecology, Individual, Populations and Communities.* Blackwell Scientific-Publications, Cambridge, Massachusets, 1990.

[12] P. Benevieri and M. Furi. A simple notion of orientability for Fredholm maps of index zero between Banach manifolds and degree theory. *Ann. Sci. Math. Québec*, 22:131–148, 1998.

[13] P. Benevieri and M. Furi. On the concept of orientability for Fredhom maps between real Banach manifolds. *Top. Meth. Nonl. Anal.*, 16:279–306, 2000.

[14] H. Berestycki, L. Nirenberg, and S. R. S. Varadhan. The principal eigenvalue and maximum principle for second-order elliptic operators in general domains. *Comm. Pure Appl. Math.*, 47(1):47–92, 1994.

[15] J. Blat and K. J. Brown. Bifurcation of steady-state solutions in predator-prey and competition systems. *Proc. R. Soc. Edinb., Sect. A, Math.*, 97:21–34, 1984.

[16] J. Blat and K. J. Brown. Global bifurcation of positive solutions in some systems of elliptic equations. *SIAM J. Math. Anal.*, 17:1339–1353, 1986.

[17] A. Boscaggin. Subharmonic solutions of planar Hamiltonian systems: a rotation number approach. *Adv. Nonlinear Stud.*, 11(1):77–103, 2011.

[18] A. Boscaggin, W. Dambrosio, and E. Muñoz-Hernández. A Maupertuis-type principle in relativistic mechanics and applications. *Calc. Var. Partial Differential Equations*, 62(3):95, 2023.

[19] A. Boscaggin and G. Feltrin. Positive periodic solutions to an indefinite Minkowski-curvature equation. *J. Differential Equations*, 269(7):5595–5645, 2020.

[20] A. Boscaggin and M. Garrione. Resonance and rotation numbers for planar Hamiltonian systems: multiplicity results via the Poincaré-Birkhoff theorem. *Nonlinear Anal.*, 74(12):4166–4185, 2011.

[21] A. Boscaggin and E. Muñoz-Hernández. Planar Hamiltonian systems: Index theory and applications to the existence of subharmonics. *Nonlinear Analysis*, 226:113142, 2023.

[22] A. Boscaggin and F. Zanolin. Subharmonic solutions for nonlinear second order equations in presence of lower and upper solutions. *Discrete Contin. Dyn. Syst.*, 33(1):89–110, 2013.

[23] M. Braun. *Differential equations and their applications.* Springer-Verlag, New York-Berlin, 1983. Third edition (short version).

[24] H. W. Broer, V. Naudot, R. Roussarie, and K. Saleh. A predator-prey model with non-monotonic response function. *Regul. Chaotic Dyn.*, 11(2):155–165, 2006.

[25] K. Burns and H. Weiss. A geometric criterion for positive topological entropy. *Comm. Math. Phys.*, 172(1):95–118, 1995.

[26] L. Burra and F. Zanolin. Chaotic dynamics in a simple class of Hamiltonian systems with applications to a pendulum with variable length. *Differential Integral Equations*, 22(9-10):927–948, 2009.

[27] G. J. Butler and H. I. Freedman. Periodic solutions of a predator-prey system with periodic coefficients. *Math. Biosci.*, 55(1-2):27–38, 1981.

[28] S. Cano-Casanova and J. López-Gómez. Properties of the principal eigenvalues of a general class of non-classical mixed boundary value problems. *J. Differential Equations*, 178(1):123–211, 2002.

[29] R. S. Cantrell and C. Cosner. Diffusive logistic equations with indefinite weights: population models in disrupted environments. *Proc. Roy. Soc. Edinburgh Sect. A*, 112(3-4):293–318, 1989.

[30] R. S. Cantrell and C. Cosner. Should a park be an island? *SIAM J. Appl. Math.*, 53(1):219–252, 1993.

[31] R. S. Cantrell and C. Cosner. *Spatial Ecology via Reaction-Diffusion Equations.* Wiley, 2004.

[32] S. E. Cappell, R. Lee, and E. Y. Miller. On the Maslov index. *Comm. Pure Appl. Math.*, 47(2):121–186, 1994.

[33] M. C. Carbinatto, J. Kwapisz, and K. Mischaikow. Horseshoes and the Conley index spectrum. *Ergodic Theory Dynam. Systems*, 20(2):365–377, 2000.

[34] A. Casal, J. C. Eilbeck, and J. López-Gómez. Existence and uniqueness of coexistence states for a predator-prey model with diffusion. *Differential Integral Equations*, 7(2):411–439, 1994.

[35] S. N. Chow and J. K. Hale. *Methods of bifurcation theory*, volume 251 of *Grundlehren der Mathematischen Wissenschaften [Fundamental Principles of Mathematical Sciences].* Springer-Verlag, New York-Berlin, 1982.

[36] C. Conley and E. Zehnder. Subharmonic solutions and Morse theory. *Physica A*, 124:649–657, 1984.

[37] M. G. Crandall and P. H. Rabinowitz. Bifurcation from simple eigenvalues. *J. Functional Analysis*, 8:321–340, 1971.

[38] M. G. Crandall and P. H. Rabinowitz. Bifurcation, perturbation of simple eigenvalues and linearized stability. *Arch. Rational Mech. Anal.*, 52:161–180, 1973.

[39] J. M. Cushing. Periodic time-dependent predator-prey systems. *SIAM J. Appl. Math.*, 32(1):82–95, 1977.

[40] J. M. Cushing. Two species competition in a periodic environment. *J. Mathematical Biology*, 10:385–390, 1980.

[41] F. Dalbono and C. Rebelo. Poincaré-Birkhoff fixed point theorem and periodic solutions of asymptotically linear planar Hamiltonian systems. *Rend. Sem. Mat. Univ. Politec. Torino*, 60(4):233–263, 2002.

[42] E. N. Dancer. On the indices of fixed points of mappings in cones and applications. *J. Math. Anal. Appl.*, 91:131–151, 1983.

[43] E. N. Dancer. On positive solutions of some pairs of differential equations. *Trans. Am. Math. Soc.*, 284:729–743, 1984.

[44] E. N. Dancer. On positive solutions of some pairs of differential equations. II. *J. Differ. Equations*, 60:236–258, 1985.

[45] E. N. Dancer. Bifurcation from simple eigenvalues and eigenvalues of geometric multiplicity one. *Bull. London Math. Soc.*, 34(5):533–538, 2002.

[46] E. N. Dancer, J. López-Gómez, and R. Ortega. On the spectrum of some linear noncooperative elliptic systems with radial symmetry. *Differential Integral Equations*, 8(3):515–523, 1995.

[47] U. D'Ancona. *Dell'influenza della stasi peschereccia del periodo 1914–18 sul patrimonio ittico dell'alto Adriatico*. Venezia: Regio Comitato Talassografico Italiano, Mem. CXXVI, 1926.

[48] U. D'Ancona. Per la miglior conoscenza delle terminazioni nervose nei muscoli somatici dei crostacei decapodi. *Travaux du laboratoire de recherches biologiques de l'Université de Madrid*, 23:393–423, 1926.

[49] U. D'Ancona. *La lotta per l'esistenza.* Torino: Einaudi., 1942.

[50] D. Daners and J. López-Gómez. Global dynamics of generalized logistic equations. *Adv. Nonlinear Stud.*, 18(2):217–236, 2018.

[51] Ch. Darwin. *On the Origin of Species by Means of Natural Selection, or the preservation of favoured races in the struggle of life.* London, John Murray (Sixth edition), 1872.

[52] R. L. Devaney. Subshifts of finite type in linked twist mappings. *Proc. Amer. Math. Soc.*, 71(2):334–338, 1978.

[53] R. L. Devaney. *An introduction to chaotic dynamical systems.* Addison-Wesley Studies in Nonlinearity. Addison-Wesley Publishing Company, Advanced Book Program, Redwood City, CA, second edition, 1989.

[54] R. Dieckerhoff and E. Zehnder. Boundedness of solutions via the twist-theorem. *Ann. Scuola Norm. Sup. Pisa Cl. Sci. (4)*, 14(1):79–95, 1987.

[55] T. Ding and F. Zanolin. Harmonic solutions and subharmonic solutions for periodic Lotka-Volterra systems. In *Dynamical systems (Tianjin, 1990/1991)*, volume 4 of *Nankai Ser. Pure Appl. Math. Theoret. Phys.*, pages 55–65. World Sci. Publ., River Edge, NJ, 1993.

[56] T. Ding and F. Zanolin. Periodic solutions and subharmonic solutions for a class of planar systems of Lotka-Volterra type. In *World Congress of Nonlinear Analysts '92, Vol. I–IV (Tampa, FL, 1992)*, pages 395–406. De Gruyter, Berlin, 1996.

[57] W. Y. Ding. Fixed points of twist mappings and periodic solutions of ordinary differential equations. *Acta Math. Sinica*, 25(2):227–235, 1982.

[58] T. Dondè and F. Zanolin. Multiple periodic solutions for one-sided sublinear systems: a refinement of the Poincaré-Birkhoff approach. *Topol. Methods Nonlinear Anal.*, 55(2):565–581, 2020.

[59] Y. Du and S. B. Hsu. A diffusive predator-prey model in heterogeneous environment. *J. Differential Equations*, 203(2):331–364, 2004.

[60] Y. Du and Y. Lou. Some uniqueness and exact multiplicity results for a predator-prey model. *Trans. Amer. Math. Soc.*, 349(6):2443–2475, 1997.

[61] Y. Du and Y. Lou. S-shaped global bifurcation curve and Hopf bifurcation of positive solutions to a predator-prey model. *J. Differential Equations*, 144(2):390–440, 1998.

[62] Y. Du and Y. Lou. Qualitative behaviour of positive solutions of a predator-prey model: Effects of saturation. *Proc. R. Soc. Edinb., Sect. A, Math.*, 131(2):321–349, 2001.

[63] Y. Du and J. Shi. A diffusive predator-prey model with a protection zone. *J. Differ. Equations*, 229(1):63–91, 2006.

[64] Y. Du and J. Shi. Allee effect and bistability in a spatially heterogeneous predator-prey model. *Trans. Am. Math. Soc.*, 359(9):4557–4593, 2007.

[65] J. Esquinas. Optimal multiplicity in local bifurcation theory, II: General case. *J. Differential Equations*, 75:206–215, 1988.

[66] J. Esquinas and J. López-Gómez. Optimal multiplicity in local bifurcation theory. I. Generalized generic eigenvalues. *J. Differential Equations*, 71(1):72–92, 1988.

[67] G. Feltrin. Positive subharmonic solutions to superlinear ODEs with indefinite weight. *Discrete Contin. Dyn. Syst. Ser. S*, 11(2):257–277, 2018.

[68] X. Feng, Y. Song, and X. An. Dynamic behavior analysis of a prey-predator model with ratio-dependent Monod-Haldane functional response. *Open Math.*, 16:623–635, 2018.

[69] S. Fernández-Rincón and J. López-Gómez. The singular perturbation problem for a class of generalized logistic equations under non-classical mixed boundary conditions. *Adv. Nonlinear Stud.*, 19(1):1–27, 2019.

[70] S. Fernández-Rincón and J. López-Gómez. The Picone identity: a device to get optimal uniqueness results and global dynamics in population dynamics. *Nonlinear Anal., Real World Appl.*, 60:41, 2021.

[71] R. A. Fisher. The wave of advances of advantageous genes. *Ann. Eugen.*, 7:355–369, 1937.

[72] P. M. Fitzpatrick and J. Pejsachowicz. Parity and generalized multiplicity. *Trans. Amer. Math. Soc.*, 326:281–305, 1991.

[73] P. M. Fitzpatrick, J. Pejsachowicz, and P. J. Rabier. Orientability of Fredholm families and topological degree for orientable nonlinear Fredholm mappings. *J. Funct. Anal.*, 124(1):1–39, 1994.

[74] A. Fonda. *Playing around resonance.* Birkhäuser Advanced Texts: Basler Lehrbücher. [Birkhäuser Advanced Texts: Basel Textbooks]. Birkhäuser/Springer, Cham, 2016. An invitation to the search of periodic solutions for second order ordinary differential equations.

[75] A. Fonda and A. C. Lazer. Subharmonic solutions of conservative systems with nonconvex potentials. *Proc. Amer. Math. Soc.*, 115(1):183–190, 1992.

[76] A. Fonda, M. Sabatini, and F. Zanolin. Periodic solutions of perturbed Hamiltonian systems in the plane by the use of the Poincaré-Birkhoff theorem. *Topol. Methods Nonlinear Anal.*, 40(1):29–52, 2012.

[77] A. Fonda and R. Toader. Subharmonic solutions of Hamiltonian systems displaying some kind of sublinear growth. *Adv. Nonlinear Anal.*, 8(1):583–602, 2019.

[78] A. Fonda and A. J. Ureña. A higher dimensional Poincaré-Birkhoff theorem for Hamiltonian flows. *Ann. Inst. H. Poincaré C Anal. Non Linéaire*, 34(3):679–698, 2017.

[79] J. M. Fraile, P. Koch Medina, J. López-Gómez, and S. Merino. Elliptic eigenvalue problems and unbounded continua of positive solutions of a semilinear elliptic equation. *J. Differential Equations*, 127(1):295–319, 1996.

[80] J. Franks. Generalizations of the Poincaré-Birkhoff theorem. *Ann. of Math. (2)*, 128(1):139–151, 1988.

[81] H. I. Freedman. *Deterministic mathematical models in population ecology*, volume 57 of *Monographs and Textbooks in Pure and Applied Mathematics*. Marcel Dekker, Inc., New York, 1980.

[82] M. Garrione, A. Margheri, and C. Rebelo. Nonautonomous nonlinear ODEs: nonresonance conditions and rotation numbers. *J. Math. Anal. Appl.*, 473(1):490–509, 2019.

[83] C. F. Gauss. *Disquisitiones arithmeticae*. Springer-Verlag, New York, 1986.

[84] M. Golubitsky and D. G. Schaeffer. *Singularities and Groups in Bifurcation Theory*. Applied Mathematcial Sciences vol. 51, Springer Verlag, New York University, 1985.

[85] J. Guckenheimer and P. Holmes. *Nonlinear oscillations, dynamical systems, and bifurcations of vector fields*, volume 42 of *Applied Mathematical Sciences*. Springer-Verlag, New York, 1983.

[86] G. Guo and J. Wu. Multiplicity and uniqueness of positive solutions for a predator-prey model with B-D functional response. *Nonlinear Anal., Theory Methods Appl., Ser. A, Theory Methods*, 72(3-4):1632–1646, 2010.

[87] G. Guo and J. Wu. The effect of mutual interference between predators on a predator-prey model with diffusion. *J. Math. Anal. Appl.*, 389(1):179–194, 2012.

[88] A. R. Hausrath. Periodic integral manifolds for periodically forced Volterra-Lotka equations. *J. Math. Anal. Appl.*, 87(2):474–488, 1982.

[89] A. R. Hausrath and R. F. Manásevich. Periodic solutions of a periodically perturbed Lotka-Volterra equation using the Poincaré-Birkhoff theorem. *J. Math. Anal. Appl.*, 157(1):1–9, 1991.

[90] M. Hénon. Numerical study of quadratic area-preserving mappings. *Quart. Appl. Math.*, 27:291–312, 1969.

[91] D. Henry. *Geometric Theory of Parabolic Differential Equations*, volume 840 of *Lectures Notes in Mathematics*. Springer, Berlin, 1981.

[92] P. Hess. *Periodic Parabolic Boundary Value Problems and Positivity*. Longman Scientific and Technical, 1991.

[93] C. S. Holling. The functional response of predators to prey density and its role in mimicry and population regulations. *Mem. Entomol. Soc. Can.*, 45:1–60, 1965.

[94] C. S. Holling. Resilience and stability of ecological systems. *Ann. Rev. of Ecology and Systematics*, 4:1–23, 1973.

[95] S. B. Hsu. On global stability of a predator-prey system. *Math. Biosc.*, 39:1–10, 1978.

[96] S. B. Hsu and T. W. Huang. Global stability for a class of predator-prey systems. *SIAM J. Appl. Math.*, 55(3):763–783, 1995.

[97] V. Hutson, J. López-Gómez, K. Mischaikow, and G. Vickers. Limit behaviour for a competing species problem with diffusion. In *Dynamical systems and applications*, volume 4 of *World Sci. Ser. Appl. Anal.*, pages 343–358. World Sci. Publ., River Edge, NJ, 1995.

[98] G. Israel and A. Millán Gasca. *The biology of numbers. The correspondence of Vito Volterra on mathematical biology*, volume 26 of *Sci. Networks, Hist. Stud.* Basel: Birkhäuser, 2002.

[99] Y. Jia, J. Wu, and H. K. Xu. Spatial pattern in an ecosystem of phytoplankton-nutrient from remote sensing. *J. Math. Anal. Appl.*, 402(1):23–34, 2013.

[100] H. Jiang and L. Wang. Analysis of steady state for variable-territory model with limited self-limitation. *Acta Appl. Math.*, 148(1):103–120, 2017.

[101] J. Kennedy and J. A. Yorke. Topological horseshoes. *Trans. Amer. Math. Soc.*, 353(6):2513–2530, 2001.

[102] U. Kirchgraber and D. Stoffer. On the definition of chaos. *Z. Angew. Math. Mech.*, 69(7):175–185, 1989.

[103] W. Ko and K. Ryu. Qualitative analysis of a predator-prey model with Holling type II functional response incorporating a prey refuge. *J. Differ. Equations*, 231(2):534–550, 2006.

[104] W. Ko and K. Ryu. Coexistence states of a predator-prey system with non-monotonic functional response. *Nonlinear Anal., Real World Appl.*, 8(3):769–786, 2007.

[105] W. Ko and K. Ryu. A qualitative study on general Gause-type predator-prey models with constant diffusion rates. *J. Math. Anal. Appl.*, 344(1):217–230, 2008.

[106] A. N. Kolmogorov. Sulla teoria di Volterra della lotta per l'esistenza. *G. Ist. Ital. Attuari*, 7:74–80, 1936.

[107] A. N. Kolmogorov, I. G. Petrovski, and N. S. Piskunov. Étude de l'équation de la diffusion avec croissance de la quantite de matière et son application à un problème biologique, 1937.

[108] M. A. Krasnosel'skii. *Topological methods in the theory of nonlinear integral equations*. A Pergamon Press Book. The Macmillan Company, New York, 1964. Translated by A. H. Armstrong; translation edited by J. Burlak.

[109] Y. A. Kuznetsov, S. Muratori, and S. Rinaldi. Bifurcations and chaos in a periodic predator-prey model. *Internat. J. Bifur. Chaos Appl. Sci. Engrg.*, 2(1):117–128, 1992.

[110] I. S. Labouriau and E. Sovrano. Chaos in periodically forced reversible vector fields. *J. Singul.*, 22:227–240, 2020.

[111] S. Laederich and M. Levi. Invariant curves and time-dependent potentials. *Ergodic Theory Dynam. Systems*, 11(2):365–378, 1991.

[112] M. Levi. Quasiperiodic motions in superquadratic time-periodic potentials. *Comm. Math. Phys.*, 143(1):43–83, 1991.

[113] S. Li, J. Wu, and Y. Dong. Effects of a degeneracy in a diffusive predator-prey model with Holling II functional response. *Nonlinear Anal., Real World Appl.*, 43:78–95, 2018.

[114] S. Li, J. Wu, and Y. Dong. Effects of degeneracy and response function in a diffusion predator-prey model. *Nonlinearity*, 31(4):1461–1483, 2018.

[115] T. Y. Li and J. A. Yorke. Period three implies chaos. *Amer. Math. Monthly*, 82(10):985–992, 1975.

[116] D. Liberzon. *Switching in systems and control*. Systems & Control: Foundations & Applications. Birkhäuser Boston, Inc., Boston, MA, 2003.

[117] B. Liu. The stability of harmonic solutions of Lotka-Volterra systems. *J. Math. Anal. Appl.*, 194(3):727–740, 1995.

[118] N. G. Lloyd. *Degree theory*. Cambridge Tracts in Mathematics, No. 73. Cambridge University Press, Cambridge-New York-Melbourne, 1978.

[119] Y. Long. *Index theory for symplectic paths with applications*, volume 207 of *Progress in Mathematics*. Birkhäuser Verlag, Basel, 2002.

[120] J. López-Gómez. Positive periodic solutions of Lotka–Volterra reaction-diffusion systems. *Differential and Integral Equations*, 5(1):55–72, 1992.

[121] J. López-Gómez. Nonlinear eigenvalues and global bifurcation application to the search of positive solutions for general Lotka-Volterra reaction diffusion systems with two species. *Differential Integral Equations*, 7(5-6):1427–1452, 1994.

[122] J. López-Gómez. Permanence under strong competition. *World Scientific Series in Applied Analysis*, 4(4):473–488, 1995.

[123] J. López-Gómez. A bridge between operator theory and mathematical biology. In *Operator theory and its applications (Winnipeg, MB, 1998)*, volume 25 of *Fields Inst. Commun.*, pages 383–397. Amer. Math. Soc., Providence, RI, 2000.

[124] J. López-Gómez. *Spectral theory and nonlinear functional analysis*, volume 426 of *Chapman & Hall/CRC Research Notes in Mathematics*. Chapman & Hall/CRC, Boca Raton, FL, 2001.

[125] J. López-Gómez. Classifying smooth supersolutions for a general class of elliptic boundary value problems. *Adv. Differential Equations*, 8(9):1025–1042, 2003.

[126] J. López-Gómez. *Linear second order elliptic operators*. World Scientific Publishing Co. Pte. Ltd., Hackensack, NJ, 2013.

[127] J. López-Gómez. *Metasolutions of Parabolic Equations in Population Dynamics*. CRC Press, Boca Raton, 2015.

[128] J. López-Gómez. Global bifurcation for Fredholm operators. *Rend. Istit. Mat. Univ. Trieste*, 48:539–564, 2016.

[129] J. López-Gómez and M. Molina-Meyer. The maximum principle for cooperative weakly coupled elliptic systems and some applications. *Differential Integral Equations*, 7(2):383–398, 1994.

[130] J. López-Gómez and M. Molina-Meyer. The competitive exclusion principle versus biodiversity through segregation and further adaptation to spatial heterogeneities. *Theoretical Population Biology*, 69:94–109, 2006.

[131] J. López-Gómez and M. Molina-Meyer. Superlinear indefinite systems: beyond Lotka-Volterra models. *J. Differ. Equations*, 221(2):343–411, 2006.

[132] J. López-Gómez and C. Mora-Corral. Counting zeroes of C^1 Fredholm maps of index 1. *Bull. London Math. Soc.*, 37:778–792, 2005.

[133] J. López-Gómez and C. Mora-Corral. *Algebraic multiplicity of eigenvalues of linear operators*, volume 177 of *Operator Theory: Advances and Applications*. Birkhäuser Verlag, Basel, 2007.

[134] J. López-Gómez and E. Muñoz-Hernández. Global structure of subharmonics in a class of periodic predator-prey models. *Nonlinearity*, 33(1):34–71, 2020.

[135] J. López-Gómez and E. Muñoz-Hernández. A spatially heterogeneous predator-prey model. *Discrete Contin. Dyn. Syst. Ser. B*, 26(4):2085–2113, 2021.

[136] J. López-Gómez and E. Muñoz-Hernández. A robust multiplicity result in a generalized diffusive predator-prey model. *Submitted*, 2023.

[137] J. López-Gómez, E. Muñoz-Hernández, and F. Zanolin. On the applicability of the Poincaré-Birkhoff twist theorem to a class of planar periodic predator-prey models. *Discrete Contin. Dyn. Syst.*, 40(4):2393–2419, 2020.

[138] J. López-Gómez, E. Muñoz-Hernández, and F. Zanolin. The Poincaré-Birkhoff theorem for a class of degenerate planar Hamiltonian systems. *Adv. Nonlinear Stud.*, 21(3):489–499, 2021.

[139] J. López-Gómez, E. Muñoz-Hernández, and F. Zanolin. Rich dynamics in planar systems with heterogeneous nonnegative weights. *Communications on Pure and Applied Analysis*, 2023.

[140] J. López-Gómez, E. Muñoz-Hernández, and F. Zanolin. Subharmonic solutions for a class of predator-prey models with degenerate weights in periodic environments. *Submitted*, 2023.

[141] J. López-Gómez, R. Ortega, and A. Tineo. The periodic predator-prey Lotka-Volterra model. *Adv. Differential Equations*, 1(3):403–423, 1996.

[142] J. López-Gómez and R. M. Pardo. Coexistence regions in Lotka-Volterra models with diffusion. *Nonlinear Anal.*, 19(1):11–28, 1992.

[143] J. López-Gómez and R. M. Pardo. Existence and uniqueness of coexistence states for the predator-prey model with diffusion: the scalar case. *Differential Integral Equations*, 6(5):1025–1031, 1993.

[144] J. López-Gómez and R. M. Pardo. Invertibility of linear noncooperative elliptic systems. *Nonlinear Anal.*, 31(5-6):687–699, 1998.

[145] J. López-Gómez and P. Rabinowitz. The effects of spatial heterogeneities on some multiplicity results. *Discrete Contin. Dyn. Syst.*, 36(2):941–952, 2016.

[146] A. J. Lotka. *Analytical theory of biological populations.* The Plenum Series on Demographic Methods and Population Analysis. Plenum Press, New York, 1998. Translated from the 1939 French edition and with an introduction by David P. Smith and Hélène Rossert.

[147] Th. R. Malthus. *An Essay on the Principle of Population.* London, St. Paul's Church Yard, 1798.

[148] A. Margheri, C. Rebelo, and F. Zanolin. Maslov index, Poincaré-Birkhoff theorem and periodic solutions of asymptotically linear planar Hamiltonian systems. *J. Differential Equations*, 183(2):342–367, 2002.

[149] A. Margheri, C. Rebelo, and F. Zanolin. Chaos in periodically perturbed planar Hamiltonian systems using linked twist maps. *J. Differential Equations*, 249(12):3233–3257, 2010.

[150] R. M. May. *Stability and Complexity in Model Ecosystems*, volume 1. Princeton University Press, 1974.

[151] R. M. May. Simple mathematical models with very complicated dynamics. *Nature*, 261:459–467, 1976.

[152] A. Medio, M. Pireddu, and F. Zanolin. Chaotic dynamics for maps in one and two dimensions: a geometrical method and applications to economics. *Internat. J. Bifur. Chaos Appl. Sci. Engrg.*, 19(10):3283–3309, 2009.

[153] R. Michalek and G. Tarantello. Subharmonic solutions with prescribed minimal period for nonautonomous Hamiltonian systems. *J. Differential Equations*, 72(1):28–55, 1988.

[154] K. Mischaikow and M. Mrozek. Isolating neighborhoods and chaos. *Japan J. Indust. Appl. Math.*, 12(2):205–236, 1995.

[155] J. Moser. On invariant curves of area-preserving mappings of an annulus. *Nachr. Akad. Wiss. Göttingen Math.-Phys. Kl. II*, 1962:1–20, 1962.

[156] J. Moser. *Stable and random motions in dynamical systems.* Annals of Mathematics Studies, No. 77. Princeton University Press, Princeton, N. J.; University of Tokyo Press, Tokyo, 1973.

[157] J. D. Murray. *Mathematical Biology. I*, volume 17 of *Interdisciplinary Applied Mathematics.* Springer-Verlag, New York, third edition, 2002.

[158] S. Nakaoka, Y. Saito, and Y. Takeuchi. Stability, delay, and chaotic behavior in a Lotka-Volterra predator-prey system. *Math. Biosci. Eng.*, 3(1):173–187, 2006.

[159] W. D. Neumann. Generalizations of the Poincaré Birkhoff fixed point theorem. *Bull. Austral. Math. Soc.*, 17(3):375–389, 1977.

[160] W. M. Ni. *The Mathematics of Diffusion.* SIAM, Philadelphia, 2011. CBMS-NSF Regional Conf. Ser. in Appl. Math., vol. 82.

[161] H. Nie and J. Wu. Multiplicity and stability of a predator-prey model with non-monotonic conversion rate. *Nonlinear Anal., Real World Appl.*, 10(1):154–171, 2009.

[162] L. Nirenberg. *Topics in Nonlinear Functional Analysis.* Courant Institute of Mathematical Sciences, New York University, 1974.

[163] P. Y. H. Pang and M. Wang. Qualitative analysis of a ratio-dependent predator-prey system with diffusion. *Proc. R. Soc. Edinb., Sect. A, Math.*, 133(4):919–942, 2003.

[164] P. Y. H. Pang and M. Wang. Non-constant positive steady states of a predator-prey system with non-monotonic functional response and diffusion. *Proc. Lond. Math. Soc. (3)*, 88(1):135–157, 2004.

[165] D. Papini, G. Villari, and F. Zanolin. Chaotic dynamics in a periodically perturbed Liénard system. *Differential Integral Equations*, 32(11-12):595–614, 2019.

[166] D. Papini and F. Zanolin. Fixed points, periodic points, and coin-tossing sequences for mappings defined on two-dimensional cells. *Fixed Point Theory Appl.*, (2):113–134, 2004.

[167] D. Papini and F. Zanolin. On the periodic boundary value problem and chaotic-like dynamics for nonlinear Hill's equations. *Adv. Nonlinear Stud.*, 4(1):71–91, 2004.

[168] A. Pascoletti, M. Pireddu, and F. Zanolin. Multiple periodic solutions and complex dynamics for second order ODEs via linked twist maps. In *The 8th Colloquium on the Qualitative Theory of Differential Equations*, volume 8 of *Proc. Colloq. Qual. Theory Differ. Equ.*, pages No. 14, 32. Electron. J. Qual. Theory Differ. Equ., Szeged, 2008.

[169] R. Pearl and L. J. Reed. On the rate of growth of the population of the United States since 1790 and its mathematical representation. *Proc. Nat. Acad. Sci.*, 6:275–288, 1920.

[170] R. Peng, M. X. Wang, and W. Y. Chen. Positive steady states of a prey-predator model with diffusion and non-monotone conversion rate. *Acta Math. Sin., Engl. Ser.*, 23(4):749–760, 2007.

[171] M. Pireddu and F. Zanolin. Chaotic dynamics in the Volterra predator-prey model via linked twist maps. *Opuscula Math.*, 28(4):567–592, 2008.

[172] M. Pireddu and F. Zanolin. Fixed points, periodic points and chaotic dynamics for continuous maps with applications to population dynamics. In *Lotka-Volterra and related systems*, volume 2 of *De Gruyter Ser. Math. Life Sci.*, pages 123–233. De Gruyter, Berlin, 2013.

[173] D. Qian and P. J. Torres. Periodic motions of linear impact oscillators via the successor map. *SIAM J. Math. Anal.*, 36(6):1707–1725, 2005.

[174] A. Quetelet. *Sur l'homme et le développement de ses facultés. Essai de physique sociale.* Paris, Bacheller, 1835.

[175] P. H. Rabinowitz. Some global results for nonlinear eigenvalue problems. *J. Functional Analysis*, 7:487–513, 1971.

[176] P. H. Rabinowitz. On bifurcation from infinity. *J. Differ. Equations*, 14:462–475, 1973.

[177] P. H. Rabinowitz. Some aspects of nonlinear eigenvalue problems. *Rocky Mountain J. Math.*, 3:161–202, 1973.

[178] P. H. Rabinowitz. On subharmonic solutions of Hamiltonian systems. *Comm. Pure Appl. Math.*, 33(5):609–633, 1980.

[179] C. Rebelo. A note on the Poincaré-Birkhoff fixed point theorem and periodic solutions of planar systems. *Nonlinear Anal.*, 29(3):291–311, 1997.

[180] S. Rosenblat. Population models in a periodically fluctuating environment. *J. Math. Biol.*, 9(1):23–36, 1980.

[181] F. Rothe. The periods of the Volterra-Lotka system. *J. Reine Angew. Math.*, 355:129–138, 1985.

[182] A. Ruiz-Herrera. Chaos in predator-prey systems with/without impulsive effect. *Nonlinear Anal. Real World Appl.*, 13(2):977–986, 2012.

[183] K. Ryu and I. Ahn. Positive solutions for ratio-dependent predator-prey interaction systems. *J. Differ. Equations*, 218(1):117–135, 2005.

[184] A. Sard. The measure of the critical values of differentiable maps. *Bull. Amer. Math. Soc.*, 48:883–890, 1942.

[185] R. Schaaf. A class of Hamiltonian systems with increasing periods. *J. Reine Angew. Math.*, 363:96–109, 1985.

[186] E. Serra, M. Tarallo, and S. Terracini. Subharmonic solutions to second-order differential equations with periodic nonlinearities. *Nonlinear Anal.*, 41(5-6, Ser. A: Theory Methods):649–667, 2000.

[187] J. Shi and X. Wang. On global bifurcation for quasilinear elliptic system on bounded domains. *J. Differential Equations*, 124:1–39, 1994.

[188] S. Smale. Diffeomorphisms with many periodic points. In *Differential and Combinatorial Topology (A Symposium in Honor of Marston Morse)*, pages 63–80. Princeton Univ. Press, Princeton, N.J., 1965.

[189] S. Smale. Differentiable dynamical systems. *Bull. Amer. Math. Soc.*, 73:747–817, 1967.

[190] S. Smale. Finding a horseshoe on the beaches of Rio. *Math. Intelligencer*, 20(1):39–44, 1998.

[191] E. Sovrano. About chaotic dynamics in the twisted horseshoe map. *Int. J. Bifurcation Chaos Appl. Sci. Eng.*, 26(6):10, 2016.

[192] E. Sovrano. How to construct complex dynamics? A note on a topological approach. *Int. J. Bifurcation Chaos Appl. Sci. Eng.*, 30(2):7, 2020.

[193] R. Srzednicki. A generalization of the Lefschetz fixed point theorem and detection of chaos. *Proc. Amer. Math. Soc.*, 128(4):1231–1239, 2000.

[194] R. Srzednicki and K. Wójcik. A geometric method for detecting chaotic dynamics. *J. Differential Equations*, 135(1):66–82, 1997.

[195] R. Sturman, J. M. Ottino, and S. Wiggins. *The mathematical foundations of mixing*, volume 22 of *Cambridge Monographs on Applied and Computational Mathematics*. Cambridge University Press, Cambridge, 2006.

[196] P. Táboas. Periodic solutions of a forced Lotka-Volterra equation. *J. Math. Anal. Appl.*, 124(1):82–97, 1987.

[197] Y. Takeuchi and N. Adachi. Influence of predation on species coexistence in Volterra models. *Math. Biosci.*, 70(1):65–90, 1984.

[198] Y. Takeuchi, N. H. Du, N. T. Hieu, and K. Sato. Evolution of predator-prey systems described by a Lotka-Volterra equation under random environment. *J. Math. Anal. Appl.*, 323(2):938–957, 2006.

[199] J. T. Tanner. The stability and the intrinsic growth rates of prey and predator populations. *Ecology*, 56(4):855–867, 1975.

[200] J. Vandermeer, L. Stone, and B. Blasius. Categories of chaos and fractal basin boundaries in forced predator-prey models. *Chaos, Solitons & Fractals*, 12(2):265–276, 2001.

[201] P. F. Verhulst. Notice sur la loi que la population suit dans son accroissement. *Corr. Math. Phys.*, 10:113–125, 1838.

[202] V. Volterra. Fluctuations in the abundance of a species considered mathematically. *Nature*, 118:558–560, 1926.

[203] V. Volterra. *Variazioni e fluttuazioni del numero d'individui in specie animali conviventi.* Mem. Acad. Lincei, Società anonima tipografica Leonardo da Vinci, 1926.

[204] V. Volterra. *Variazioni e fluttuazioni del numero d'individui in specie animali conviventi.* Venezia: Regio Comitato Talassografico Italiano, Mem. CXXXI, 1927.

[205] V. Volterra. *Leçons sur la théorie mathématique de la lutte pour la vie.* Les Grands Classiques Gauthier-Villars. [Gauthier-Villars Great Classics]. Éditions Jacques Gabay, Sceaux, 1990. Reprint of the 1931 original.

[206] J. Waldvogel. The period in the Lotka-Volterra system is monotonic. *J. Math. Anal. Appl.*, 114(1):178–184, 1986.

[207] M. Wang and Q. Wu. Positive solutions of a prey-predator model with predator saturation and competition. *J. Math. Anal. Appl.*, 345(2):708–718, 2008.

[208] S. Wang and D. Qian. Subharmonic solutions of indefinite Hamiltonian systems via rotation numbers. *Adv. Nonlinear Stud.*, 21(3):557–578, 2021.

[209] G. T. Whyburn. *Topological analysis*, volume 23 of *Princeton Math. Ser.* Princeton University Press, Princeton, NJ, 1964.

[210] S. Wiggins. *Introduction to applied nonlinear dynamical systems and chaos*, volume 2 of *Texts in Applied Mathematics*. Springer-Verlag, New York, second edition, 2003.

[211] K. Wójcik and P. Zgliczyński. Isolating segments, fixed point index, and symbolic dynamics. *J. Differential Equations*, 161(2):245–288, 2000.

[212] H. Yuan, J. Wu, Y. Jia, and H. Nie. Coexistence states of a predator-prey model with cross-diffusion. *Nonlinear Anal., Real World Appl.*, 41:179–203, 2018.

[213] X. Zeng, W. Zeng, and L. Liu. Effect of the protection zone on coexistence of the species for a ratio-dependent predator-prey model. *J. Math. Anal. Appl.*, 462(2):1605–1626, 2018.

[214] P. Zgliczyński. Fixed point index for iterations of maps, topological horseshoe and chaos. *Topol. Methods Nonlinear Anal.*, 8(1):169–177, 1996.

[215] P. Zgliczyński and M. Gidea. Covering relations for multidimensional dynamical systems. *J. Differential Equations*, 202(1):32–58, 2004.

[216] J. Zhou and C. Mu. Coexistence states of a Holling type-II predator-prey system. *J. Math. Anal. Appl.*, 369(2):555–563, 2010.

[217] J. Zhou and C. Mu. Coexistence of a diffusive predator-prey model with Holling type-II functional response and density dependent mortality. *J. Math. Anal. Appl.*, 385(2):913–927, 2012.

[218] J. Zhou and J. Shi. The existence, bifurcation and stability of positive stationary solutions of a diffusive Leslie-Gower predator-prey model with Holling-type II functional responses. *J. Math. Anal. Appl.*, 405(2):618–630, 2013.